

University of Montana

## ScholarWorks at University of Montana

---

Graduate Student Theses, Dissertations, &  
Professional Papers

Graduate School

---

2006

### Serotonin transporter inhibitor ligands: Synthesis of 2-(2-alkyl-piperazin-1-yl)-6-nitroquinoline analogs as potential positron emission tomography imaging agents

Brian R. Kusche  
*The University of Montana*

Follow this and additional works at: <https://scholarworks.umt.edu/etd>

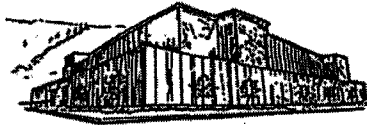
**Let us know how access to this document benefits you.**

---

#### Recommended Citation

Kusche, Brian R., "Serotonin transporter inhibitor ligands: Synthesis of 2-(2-alkyl-piperazin-1-yl)-6-nitroquinoline analogs as potential positron emission tomography imaging agents" (2006). *Graduate Student Theses, Dissertations, & Professional Papers*. 9613.  
<https://scholarworks.umt.edu/etd/9613>

This Dissertation is brought to you for free and open access by the Graduate School at ScholarWorks at University of Montana. It has been accepted for inclusion in Graduate Student Theses, Dissertations, & Professional Papers by an authorized administrator of ScholarWorks at University of Montana. For more information, please contact [scholarworks@mso.umt.edu](mailto:scholarworks@mso.umt.edu).



**Maureen and Mike  
MANSFIELD LIBRARY**

The University of  
**Montana**

---

Permission is granted by the author to reproduce this material in its entirety, provided that this material is used for scholarly purposes and is properly cited in published works and reports.

**\*\*Please check "Yes" or "No" and provide signature\*\***

Yes, I grant permission

No, I do not grant permission

Author's Signature: \_\_\_\_\_

*B. R. [Signature]*

Date: \_\_\_\_\_

*8/3/06*

Any copying for commercial purposes or financial gain may be undertaken only with the author's explicit consent.

---



SEROTONIN TRANSPORTER INHIBITOR LIGANDS: SYNTHESIS OF  
2-(2-ALKYL-PIPERAZIN-1-YL)-6-NITROQUINOLINE ANALOGS AS  
POTENTIAL POSITRON EMISSION TOMOGRAPHY IMAGING AGENTS

by

Brian R. Kusche

B.S. Chemistry, Central Washington University, 2001

B.A. Biology, Central Washington University, 2001

presented in partial fulfillment of the requirements

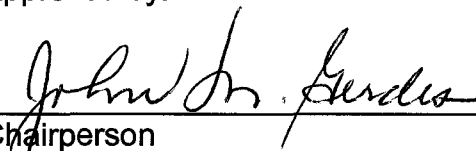
for the degree of

Doctor of Philosophy

The University of Montana

July 2006

Approved by:

  
Chairperson

  
Dean, Graduate School

8-4-06  
Date

UMI Number: 3238375

Copyright 2007 by  
Kusche, Brian R.

All rights reserved.

### INFORMATION TO USERS

The quality of this reproduction is dependent upon the quality of the copy submitted. Broken or indistinct print, colored or poor quality illustrations and photographs, print bleed-through, substandard margins, and improper alignment can adversely affect reproduction.

In the unlikely event that the author did not send a complete manuscript and there are missing pages, these will be noted. Also, if unauthorized copyright material had to be removed, a note will indicate the deletion.

**UMI**<sup>®</sup>

---


UMI Microform 3238375

Copyright 2007 by ProQuest Information and Learning Company.

All rights reserved. This microform edition is protected against unauthorized copying under Title 17, United States Code.

ProQuest Information and Learning Company  
300 North Zeeb Road  
P.O. Box 1346  
Ann Arbor, MI 48106-1346

Serotonin Transporter Inhibitor Ligands: Synthesis of 2-(2-alkyl-piperazin-1-yl)-6-nitroquinoline Analogs as Potential Positron Emission Tomography Imaging Agents

Chairperson: John M. Gerdes 

The pre-synaptic serotonin transporter (SERT) membrane protein is responsible for the clearance of the endogenous neurotransmitter serotonin (5-HT) from the synaptic cleft. The SERT protein is an established target for serotonin selective reuptake inhibitor (SSRI) therapeutic drugs. Alterations in SERT population densities and/or function have been implicated in a number of mental health disorders, including depression, anxiety, schizophrenia, and Parkinson's disease. Efforts to assess SERT changes in living brain utilizing positron emission tomography (PET) have been limited based on the availability of efficacious (as a function of in vivo kinetics and nonspecific binding), potent and selective SERT PET imaging radioligands. To satisfy the demand for new PET SERT imaging agents, investigations have encompassed the interpretation of a SERT pharmacophore model of the SSRI binding domain to identify new lead ligands. The novel SERT inhibitor 2-(2-methyl-piperazin-1-yl)-6-nitroquinoline has been used to design new SERT inhibitors 2-(2-(methoxymethyl)-piperazin-1-yl)-6-nitroquinoline and 2-(2-(3-fluoropropyl)-piperazin-1-yl)-6-nitroquinoline, among others. The syntheses of these new SERT inhibitors were designed to allow for late stage introduction of carbon-11 and fluorine-18 radionuclides. The analogs of 2-(2-methyl-piperazin-1-yl)-6-nitroquinoline have been found to be highly potent (rSERT  $K_i = 2-100$  pM, [ $^3$ H]Paroxetine), and selective (relative to dopamine and norepinephrine transporters) for SERT. Additionally, specific enantiomers of 2-(2-methyl-piperazin-1-yl)-6-nitroquinoline and inhibitors 2-(2-(methoxymethyl)-piperazin-1-yl)-6-nitroquinoline are more potent than their respective opposing enantiomeric forms. These results provide two new non-radioactive ligands that are considered as plausible carbon-11 and fluorine-18 PET SERT imaging agents.

## **Dedication**

I dedicate this thesis to my loving wife Rebecca A. Kusche, my daughter Anika L. Kusche and my parents Paul and Teena Kusche. Without their love and support I could have never achieved so much.

## Acknowledgments

I wish to express my sincere gratitude towards Dr. John Gerdes for the opportunities he has provided during the course of my graduate work at The University of Montana. Dr. John Gerdes has been an excellent mentor, colleague and friend.

I have to thank the members of the Gerdes group (past and present) for their help and encouragement. In particular I thank Melodie Weller for her pharmacological efforts. Most importantly, I have to thank and acknowledge my good friend and colleague Dr. David Bolstad. Life in lab and Missoula would not have been the same with out him and his encouragement, I could not have asked for a better friend and lab partner.

Thank you to Dr. Jim O'Neil at the Lawrence Berkeley National Laboratories for giving me the opportunity to experience radiosynthesis first hand. The work in this thesis would not be complete if not for all the radiochemistry completed with and by Dr. O'Neil.

I would like to express my gratitude to my committee members, Dr. Ed Waali, Dr. Keith Parker, Dr. Ed Rosenberg, and Dr. Sean Esslinger, for their advice and support through my graduate work at The University of Montana.

Thank you to my family and friends for their love and support throughout my college career. I have to thank my parents Paul and Teena for their continued encouragement and for providing me the values that have allowed me succeed in the career path I have chosen.



Most importantly I have to thank my wife Becky for her love and support throughout life and my graduate work. Her faith in my abilities has provided me with the strength to achieve the goals I have set for myself. Of course I have to thank my daughter Anika for all of her help during the writing of this thesis, she made the late nights easier.

## Table of Contents

<b>Chapter 1 Introduction and Background</b> .....	<b>1</b>
1.1 Introduction. ....	1
1.2 The Neurotransmitter Serotonin.....	2
1.3 Serotonin Neurotransmission at the Synapse.....	4
1.4 Serotonin Reuptake Transporter (SERT).....	5
1.5 Functional Brain Imaging (FBI). ....	8
1.6 Criteria for SERT PET Tracers.....	9
1.7 SSRIs as Potential PET Imaging Agents.....	10
1.8 Current SERT Imaging Agents.....	11
1.9 6-Nitroquipazines as SERT Inhibitor Tracers.....	14
1.10 Pharmacophore Development. ....	15
1.11 Me-NQP <b>28</b> and ( <b>±</b> )- <b>30</b> , Implications to the Pharmacophore.....	18
1.12 MOM-NQP ( <b>±</b> )- <b>31</b> .....	21
1.13 R- and S-Me-NQP ( <b>R</b> )- <b>30</b> and ( <b>S</b> )- <b>30</b> .....	24
1.14 Proposed Work. ....	25
<b>Chapter 2 Synthesis of Racemic Targets</b> .....	<b>26</b>
2.1 Introduction and Goals. ....	26
2.2 Synthesis of [ <sup>11</sup> C]MOM-NQP <b>31</b> . ....	26
2.3 Synthesis of PROM-NQP ( <b>±</b> )- <b>51</b> .....	31
2.4 Synthesis of the Radiolabeling Precursor N-formyl-ProTos-NQP <b>63</b> . ....	43
2.5 Nonradioactive Fluorinations of N-formyl-ProTos-NQP <b>63</b> .....	48
2.6 Radiofluorination of N-formyl-ProTos-NQP <b>63</b> .....	49
2.7 Synthesis of the Precursor N-Boc-ProTos-NQP <b>69</b> .....	50
2.8 Radiofluorination Attempts of N-Boc-ProTos-NQP <b>69</b> .....	54
2.9 Radiofluorination Attempts with K <sup>222</sup> , KHCO <sub>3</sub> and Ag <sup>18</sup> F.....	55
2.10 TBA <sup>18</sup> F Radiofluorination Attempts.....	57
2.11 Fluorination Control Reactions.....	62
2.12 Synthesis Pent-NQP ( <b>±</b> )- <b>83</b> and PentF-NQP <b>88</b> .....	66
2.13 Synthesis of BuM-NQP <b>96</b> . ....	70
2.14 Summary and Conclusion.....	72
<b>Chapter 3 Synthesis of Asymmetric Targets</b> .....	<b>74</b>
3.1 Chiral Nitroquipazine Ligand Studies.....	74
3.2 Chiral Piperazine Syntheses.....	76
3.3 Synthesis of Chiral MOM-NQP <b>31</b> . ....	78

3.3.1	Synthesis of N-Boc-N-Bn-glycine. ....	78
3.3.2	Synthesis of 1-Benzyl-3-(hydroxymethyl)piperazine <b>113</b> . ....	79
3.3.3	Synthesis of Chiral MOM-NQP <b>31</b> . ....	81
3.4	Application of the Chiral Synthesis, Chiral PROM-NQP <b>51</b> . ....	82
3.5	Alternate Synthesis of Chiral PROM-NQP. ....	88
3.6	Synthesis of Chiral Pent-NQP <b>83</b> . ....	91
3.7	Synthesis of Chiral BuM-NQP <b>96</b> . ....	94
3.8	Summary and Conclusions. ....	95
<b>Chapter 4 Pharmacology</b> .....		<b>97</b>
4.1	Introduction. ....	97
4.2	Competitive Inhibition, SERT Pharmacology [ <sup>3</sup> H]paroxetine. ....	98
4.2.1	Discussion of Pharmacology. ....	100
4.3	Synthesis of n-PROP-NQP <b>52</b> and [ <sup>3</sup> H]n-PROP-NQP. ....	104
4.4	In Vitro SERT Binding Studies [ <sup>3</sup> H]-n-PROP-NQP <b>52</b> . ....	107
4.5	Determination of the Apparent Equilibrium Dissociation Constant (K <sub>D</sub> ) and Receptor Density (B <sub>max</sub> ). ....	111
4.6	SERT Selectivity of [ <sup>3</sup> H]-n-PROP-NQP <b>52</b> . ....	112
4.7	Summary. ....	114
<b>Chapter 5 Conclusions and Future Work</b> .....		<b>116</b>
<b>Chapter 6 Experimental Section</b> .....		<b>119</b>
6.1	General Experimental. ....	119
6.2	Racemic Propyl Series. ....	120
6.3	Chiral Propyl N-formyl Series. ....	138
6.4	Chiral Propyl N-Boc Series. ....	150
6.5	Racemic n-PROP-NQP Synthesis. ....	158
6.6	Racemic Pent-NQP Series. ....	162
6.7	Chiral Pent-NQP Series. ....	173
6.8	Racemic BuM-NQP Series. ....	187
6.9	Chiral BuM-NQP Series. ....	195
<b>Appendix</b> .....		<b>199</b>
<b>Bibliography</b> .....		<b>207</b>

## List of Figures

Figure 1-1: Biosynthesis and degradation pathway for serotonin in the CNS. ....	4
Figure 1-2: Signals from the pre-synaptic neurons to the post-synaptic neurons of the serotonergic system are linked by the neurotransmitter serotonin (5-HT). Release of 5-HT from the vesicles and subsequent binding with the postsynaptic receptors induces a response in the postsynaptic neuron and propagates the nerve impulse. ....	5
Figure 1-3: Typical SSRIs and related SERT inhibitors. ....	7
Figure 1-4: Commercial SSRI analogs developed as potential SERT PET imaging agents. ....	11
Figure 1-5: Radiolabelled derivatives of the potent and selective SSRI MCN5652. ....	12
Figure 1-6: The Diarylsulfide SERT inhibitor 403U76 <b>15</b> and the potential SERT SPECT analogs IDAM <b>16</b> and ADAM <b>17</b> . ....	13
Figure 1-7: Second generation SERT PET agents. ....	14
Figure 1-8: SSRI 6-nitroquipazine. ....	14
Figure 1-9: SERT pharmacophore training set SSRIs. ....	16
Figure 1-10: Superposition of the SERT pharmacophore training set SSRIs (Figure 1-9), and key SERT binding features. ....	18
Figure 1-11: Structural qualities of <b>22</b> related to the SERT pharmacophore features. ....	18
Figure 1-12: Alignment of ( <i>S</i> )-Me-NQP <b>30</b> with the pharmacophore ligand superposition. ....	21
Figure 1-13: Alignment of MOM-NQP <b>31</b> with the pharmacophore ligand superposition. ....	22
Figure 2-1: Desired fluorine-18 radiolabelled ligand [ <sup>18</sup> F]MeF-NQP <b>42</b> , tosylate precursor <b>43</b> and the cold fluorinated agent, MeF-NQP <b>42</b> . ....	30
Figure 2-4: Chelating potential of piperazine and related chelator ethylenediamine. ....	40
Figure 2-5: N-protected proposed fluorinating precursor. ....	44
Figure 2-6: Explanation for the production of the bromide side product formed during BBr <sub>3</sub> cleavage of the methyl ether. ....	45
Figure 2-7: Radioactive TLC analysis after initial fluorination and silica purification of the K222 radiofluorination trial, showing two possible Boc protected fluorinated products. ....	57
Figure 2-8: Radioactive TLC analysis of the N-Boc-PROF-NQP <b>70</b> , co-spotted with radiation at the baseline, front and on the product spot to allow for direct comparison to the radiofluorination attempt. ....	61
Figure 2-9: Radioactive TLC analysis of the fluorination of <b>69</b> after silica gel purification. Two products are visible with the smaller eluting at the same <i>R<sub>f</sub></i> as <b>70</b> . ....	62
Figure 3-1: Example commercial drugs sold as a racemic mixture. ....	75
Figure 3-2: Sedative ( <i>R</i> )-(+)-Thalidomide <b>101</b> found to cause birth defects. ....	76
Figure 3-3: Potential chiral piperazine syntheses utilizing amino acid building blocks. ....	77
Figure 3-4: Potential amino acid starting materials for the chiral PROM-NQP <b>51</b> synthesis. ....	83
Figure 3-5: Potential amino acid building block for the synthesis of chiral Pent-NQP <b>83</b> . ....	91

Figure 4-1: Example single site competition assay plot of %bound radioligand versus the Log of inhibitor concentration (M).....	100
Figure 4-2: Structure and CLogP comparison of <i>n</i> -PROP-NQP <b>52</b> and PROF-NQP <b>58</b> .....	105
Figure 4-3: Time course association plots of [ <sup>3</sup> H]- <i>n</i> -PROP-NQP <b>52</b> at 21 °C.....	108
Figure 4-4: Time course dissociation plots of [ <sup>3</sup> H]- <i>n</i> -PROP-NQP <b>52</b> at 21 °C.....	109
Figure 4-5: Saturation binding isotherm of [ <sup>3</sup> H]- <i>n</i> -PROP-NQP <b>52</b> binding with rSERT at 21 °C.	112

## List of Schemes

Scheme 1-1: Synthesis of <b>28</b> and ( <b>±</b> )- <b>30</b> , the 2- and 3-alkyl derivatives of 6-NQP <b>22</b> .	19
Scheme 1-2: Synthesis of 2-(2-(methoxymethyl)piperazin-1-yl)-6-nitroquinoline, MOM-NQP ( <b>±</b> )- <b>31</b> .	23
Scheme 1-3: Chiral synthesis of ( <i>R</i> )- and ( <i>S</i> )-Me-NQP <b>30</b> .	24
Scheme 2-1: Synthesis of the radiolabeling precursor N-trityl-HOM-NQP <b>39</b> .	27
Scheme 2-2: Preparation of the radiolabeling precursor, N-Boc-HOM-NQP <b>40</b> .	27
Scheme 2-3: Simulated reaction sequence for the production of the desired radiotracer [ <sup>11</sup> C]MOM-NQP ( <b>±</b> )- <b>31</b> .	28
Scheme 2-4: Radiosynthesis of [ <sup>11</sup> C]MOM-NQP <b>31</b> .	30
Scheme 2-5: Initial synthetic route to the α,β-unsaturated ethyl ester <b>45</b> .	32
Scheme 2-6: Titration reagent for determining the concentration of organometallic reagents.	33
Scheme 2-7: Initial synthesis of the coupling precursor 3-(3-methoxypropyl)-1-tritylpiperazine <b>49</b> .	33
Scheme 2-8: Coupling and nitration to give the desired compound PROM-NQP ( <b>±</b> )- <b>51</b> .	34
Scheme 2-9: Modified synthesis of the key intermediate <b>45</b> for the synthesis of PROM-NQP ( <b>±</b> )- <b>51</b> .	38
Scheme 2-10: Proposed mechanism for the production of the <i>n</i> -allyl side product that would lead to the <i>n</i> -PROP-NQP <b>52</b> product after completing the synthetic steps outlined in Schemes 2-7 and 2-8.	39
Scheme 2-11: Example of a selective reduction of a conjugated system utilizing Mg <sup>0</sup> .	39
Scheme 2-12: Attempted selective reduction of the conjugated alkene of <b>45</b> .	41
Scheme 2-13: Overall synthesis of PROM-NQP ( <b>±</b> )- <b>51</b> .	43
Scheme 2-14: Proposed fluorinated analog <b>58</b> , to be prepared from PROM-NQP ( <b>±</b> )- <b>51</b> .	44
Scheme 2-15: N-formyl protection of PROM-NQP ( <b>±</b> )- <b>51</b> .	46
Scheme 2-16: Cleavage of the methyl ether of N-formyl-PROM-NQP ( <b>±</b> )- <b>51</b> .	47
Scheme 2-17: Synthesis of N-formyl-ProTos-NQP <b>63</b> .	47
Scheme 2-18: Fluorination sequence to prepare PROF-NQP <b>58</b> .	48
Scheme 2-19: Initial radiofluorination trial using N-formyl-ProTos-NQP <b>63</b> to give [ <sup>18</sup> F]PROF-NQP <b>58</b> .	49
Scheme 2-20: BBr <sub>3</sub> methyl ether cleavage of PROM-NQP and subsequent protection as the N-Boc to give N-Boc-HOP-NQP <b>66</b> .	51
Scheme 2-21: Selective cleavage of the undesired Boc carbonate <b>68</b> .	52
Scheme 2-22: Tosylation of N-Boc-HOP-NQP to give the fluorination precursor N-Boc-ProTos-NQP <b>69</b> .	52
Scheme 2-23: Trial fluorination of <b>69</b> with TBAF Boc group deprotection to give PROF-NQP <b>58</b> .	53

Scheme 2-24: Radiofluorination sequence utilizing K222, KHCO <sub>3</sub> , and Ag <sup>18</sup> F with the precursor N-Boc-ProTos-NQP <b>69</b> .	55
Scheme 2-25: Radiofluorination sequence utilizing TBAF.	59
Scheme 2-26: Trail nucleophilic fluorine substitution of N-Boc- <i>n</i> -PROP-NQP <b>71</b> .	63
Scheme 2-27: Trial nucleophilic fluorine substitution with an excess of KF.	64
Scheme 2-28: Trail nucleophilic fluorine substitution using KF as a limiting reagent.	65
Scheme 2-29: Example fluoride aromatic nucleophilic substitution of nitropyridines using TBAF.	66
Scheme 2-30: Overall synthesis of Pent-NQP ( <b>±</b> )- <b>83</b> .	68
Scheme 2-31: Synthesis of PentF-NQP <b>88</b> .	69
Scheme 2-32: Overall synthesis of BuM-NQP <b>96</b> .	71
Scheme 2-33: Synthesis of N-Boc-BuOH-NQP <b>97</b> .	72
Scheme 3-1: Synthesis of N-Boc-N-Benzyl-glycine <b>111</b> .	79
Scheme 3-2: Synthesis of the key synthetic intermediate ( <b>S</b> )- <b>113</b> .	80
Scheme 3-3: Overall synthesis of chiral MOM-NQP ( <b>S</b> )- <b>31</b> .	82
Scheme 3-4: Potential oxidation of the methyl alcohol according Naylor et al. <sup>93</sup>	83
Scheme 3-5: Retrosynthetic analysis for the formation of ( <b>R</b> )- <b>126</b> .	84
Scheme 3-6: Synthesis of 5-hydroxynorvaline from glutamic acid.	84
Scheme 3-7: Potential synthesis of the piperazinedione ring utilizing the lactone ( <b>R</b> )- <b>126</b> .	85
Scheme 3-8: Example peptide coupling using a cyclic lactone derived from 5-hydroxynorvaline <b>121</b> .	86
Scheme 3-9: Overall synthesis of ( <i>R</i> )-PROM-NQP <b>51</b> , the ( <i>S</i> )-enantiomer is afforded according to the same synthetic sequence starting from <b>L-132</b> .	88
Scheme 3-10: Protection of the 2° amine with Boc <sub>2</sub> O.	89
Scheme 3-11: Attempted deprotection of the Boc carbonate ( <b>R</b> )- <b>139</b> .	89
Scheme 3-12: Alternate synthesis of ( <b>R</b> )- <b>51</b> utilizing the N-Boc protected piperazine ( <b>R</b> )- <b>140</b> .	90
Scheme 3-13: Protection of ( <b>R</b> )- <b>134</b> with benzyl bromide (BnBr).	92
Scheme 3-14: Overall synthesis of ( <i>R</i> )-Pent-NQP <b>83</b> , the ( <i>S</i> )-enantiomer was similarly prepared from ( <b>S</b> )- <b>145</b> .	93
Scheme 3-15: Initial synthesis of the BuM-NQP precursor ( <b>R</b> )- <b>92</b> , by Wittig olefination technology.	94
Scheme 3-16: Proposed synthesis of chiral BuM-NQP <b>96</b> from the synthetic intermediate ( <b>R</b> )- <b>92</b> .	95
Scheme 4-1: Synthesis of 2-(2-propylpiperazin-1-yl)-6-nitroquinoline <b>52</b> ( <i>n</i> -PROP-NQP).	106
Scheme 4-2: Radiosynthesis of [ <sup>3</sup> H]-2-(2-propylpiperazin-1-yl)-6-nitroquinoline <b>52</b> ([ <sup>3</sup> H]- <i>n</i> -PROP-NQP).	106

## List of Tables

Table 1-1: <sup>10</sup> The different 5-HT receptor families their subtypes and associated therapeutic potential.....	3
Table 1-2: Structures of the current 5-halo-6-nitroquipazines and their respective SERT imaging radioligands.....	15
Table 1-3: SERT binding affinities of the first generation of 6-nitro-alkylpiperazin-1-ylquinolines.	20
Table 2-1: 2-alkylpiperzin-1-yl-6-nitroquinoline products from the initial PROM-NQP synthesis...	37
Table 4-1: Racemic 2-(2-alkyl-piperazin-1-yl)-6-nitroquiolines, compound name and R-group are given as well as their associated binding inhibition constant ( $K_i$ ), and CLogP(o/w) value.....	101
Table 4-2: Chiral 2-(2-alkyl-piperazin-1-yl)-6-nitroquiolines, compound name and R-group are given as well as their associated binding inhibition constant ( $K_i$ ), and CLogP(o/w) value.....	103
Table 4-3: Comparison of the kinetically derived dissociation constants ( $K_D$ ), the rate constants of association ( $k_{on}$ ) and dissociation ( $k_{off}$ ) for [ $^3H$ ]- <i>n-PROP-NQP 52</i> and select SSRIs at 21 °C. ....	110
Table 4-4: Inhibition constants ( $K_i$ ) for select CNS agents inhibiting the binding of [ $^3H$ ]- <i>n-PROP-NQP 52</i> with rSERT. ....	113



## List of Abbreviations

<b>(COCl)<sub>2</sub></b>	oxalyl chloride
<b>5-HT</b>	5-hydroxytryptamine/serotonin
<b>5-HTT</b>	5-hydroxytryptamine transporter
<b>6-NQP</b>	6-nitroquipazine
<b>9-BBN</b>	9-Borabicyclo[3.3.1]nonane
<b>Ac<sub>2</sub>O</b>	acetic anhydride
<b>ACE-Cl</b>	1-chloroethyl chloroformate
<b>ACN</b>	acetonitrile
<b>AcOH</b>	acetic acid
<b>AgBr</b>	silver bromide
<b>AgF</b>	silver fluoride
<b>AgOTs</b>	silver tosylate
<b>Ar</b>	aromatic group
<b>BBB</b>	blood brain barrier
<b>BBr<sub>3</sub></b>	boron tribromide
<b>bm</b>	broad multiplet
<b>B<sub>max</sub></b>	binding site density
<b>Bn</b>	benzyl group
<b>Boc</b>	<i>tert</i> -butoxycarbonyl
<b>Boc<sub>2</sub>O</b>	di- <i>tert</i> -butyl dicarbonate
<b>bs</b>	broad singlet
<b>BuM-NQP</b>	2-(2-(4-methoxybutyl)piperazin-1-yl)-6-nitroquinoline
<b>calcd</b>	calculated
<b>CH<sub>2</sub>Cl<sub>2</sub></b>	dichloromethane
<b>CH<sub>3</sub>I</b>	iodomethane
<b>CHCl<sub>3</sub></b>	chloroform
<b>CNS</b>	central nervous system
<b>d</b>	doublet
<b>δ</b>	chemical shifts in parts per million
<b>DAST</b>	(diethylamino)sulfur trifluoride
<b>DAT</b>	dopamine transporter
<b>DCE</b>	1,2-dichloroethane
<b>DCM</b>	dichloromethane
<b>dd</b>	doublet of doublets
<b>DIBAL</b>	diisobutylaluminium hydride
<b>DMF</b>	N,N-dimethylformamide
<b>DMSO</b>	dimethylsulfoxide
<b>DRI</b>	dopamine reuptake inhibitor
<b>dt</b>	doublet of triplets
<b>E.O.B.</b>	end of bombardment
<b>EDC HCl</b>	<i>N</i> -ethyl- <i>N</i> -(3-dimethylaminopropyl)carbodiimide hydrochloride
<b>ee</b>	enantiomeric excess
<b>EI</b>	electron impact
<b>equiv</b>	equivalent

<b>ESI</b>	electrospray ionization
<b>Et</b>	ethyl
<b>Et<sub>2</sub>O</b>	diethyl ether
<b>Et<sub>3</sub>N</b>	triethylamine
<b>EtOAc</b>	ethyl acetate
<b>EtOH</b>	ethyl alcohol
<b>FBI</b>	functional brain imaging
<b>g</b>	gram
<b>h</b>	hour(s)
<b>H<sub>2</sub></b>	hydrogen gas
<b>H<sub>2</sub>O<sub>2</sub></b>	hydrogen peroxide
<b>H<sub>2</sub>SO<sub>4</sub></b>	sulfuric acid
<b>HCl</b>	hydrochloric acid
<b>HNO<sub>3</sub></b>	nitric acid
<b>HOM-NQP</b>	2-(2-(hydroxymethyl)piperazin-1-yl)-6-nitroquinoline
<b>HOP-NQP</b>	2-(2-(hydroxypropyl)piperazin-1-yl)-6-nitroquinoline
<b>HPLC</b>	high performance liquid chromatography
<b>HRMS</b>	high resolution mass spectrum
<b>hSERT</b>	human serotonin reuptake transporter
<b>Hz</b>	hertz
<b>IC<sub>50</sub></b>	concentration of a drug that inhibits 50% of a protein (receptor or enzyme)
<b>IPOH</b>	isopropyl alcohol
<b>J</b>	coupling constant (NMR) in hertz
<b>K222</b>	Kryptofix, 4,7,13,16,21,24-Hexaoxa-1,10-diazabicyclo[8.8.8]hexacosane
<b>K<sub>2</sub>CO<sub>3</sub></b>	potassium carbonate
<b>K<sub>A</sub></b>	association constant
<b>KCl</b>	potassium chloride
<b>K<sub>D</sub></b>	dissociation constant
<b>KF</b>	potassium fluoride
<b>K<sub>i</sub></b>	inhibition constant
<b>k<sub>off</sub></b>	dissociation rate constant
<b>k<sub>on</sub></b>	association rate constant
<b>LBNL</b>	Lawrence Livermore National Laboratories
<b>LiAlH<sub>4</sub></b>	lithium aluminum hydride
<b>LogP</b>	octanol/water partition coefficient
<b>M</b>	molarity (moles per liter)
<b>m</b>	multiplet
<b>MAO</b>	monoamine oxidase
<b>Me</b>	methyl
<b>MeF-NQP</b>	2-(2-fluoromethyl-piperazin-1-yl)-6-nitroquinoline
<b>Me-NQP</b>	2-(2-methyl-piperazin-1-yl)-6-nitroquinoline
<b>MeOH</b>	methyl alcohol
<b>mg</b>	milligram
<b>Mg</b>	magnesium metal
<b>MHz</b>	megahertz
<b>min</b>	minute(s)

<b>mL</b>	milliliter
<b>mM</b>	millimolar
<b>μM</b>	micromolar
<b>mmol</b>	millimole
<b>mol%</b>	percent of reagent used (100 mol% = 1 equiv)
<b>MOM-NQP</b>	2-(2-(methoxymethyl)piperazin-1-yl)-6-nitroquinoline
<b>NaCl</b>	sodium chloride
<b>NaH</b>	sodium hydride
<b>NaHCO<sub>3</sub></b>	sodium bicarbonate
<b>NaNO<sub>2</sub></b>	sodium nitrite
<b>NaOH</b>	sodium hydroxide
<b><i>n</i>-BuLi</b>	<i>n</i> -butyl lithium
<b>NET</b>	norepinephrine transporter
<b>NH<sub>4</sub>CO<sub>2</sub>H</b>	ammonium formate
<b>NMR</b>	nuclear magnetic resonance
<b><i>n</i>-PROP-NQP</b>	2-(2-propylpiperazin-1-yl)-6-nitroquinoline
<b>NQP</b>	6-nitroquipazine
<b>NRI</b>	norepinephrine reuptake inhibitor
<b>PCC</b>	Pyridinium chlorochromate
<b>Pd/C</b>	palladium on carbon
<b>PDC</b>	Pyridinium dichromate
<b>PentF-NQP</b>	2-(2-(5-fluoropentyl)piperazin-1-yl)-6-nitroquinoline
<b>Pent-NQP</b>	2-(2-(5-methoxypentyl)piperazin-1-yl)-6-nitroquinoline
<b>PET</b>	positron emission tomography
<b>PG</b>	protecting group
<b>pM</b>	picomolar
<b>ppm</b>	parts per million
<b>PROF-NQP</b>	2-(2-(3-fluoropropyl)piperazin-1-yl)-6-nitroquinoline
<b>PROM-NQP</b>	2-(2-(3-methoxypropyl)-piperazin-1-yl)-6-nitroquinoline
<b>q</b>	quartet
<b>rac</b>	racemic
<b><i>R<sub>f</sub></i></b>	retention factor
<b>rSERT</b>	rat serotonin reuptake transporter
<b>RT °C</b>	room temperature
<b>s</b>	singlet
<b>SAR</b>	structure activity relationship
<b>SepPak</b>	solid phase extraction cartridge
<b>SERT</b>	serotonin reuptake transporter
<b>SOCl<sub>2</sub></b>	thionyl chloride
<b>SPECT</b>	single photon emission computed tomography
<b>SSRI</b>	selective serotonin reuptake inhibitor
<b><i>t</i><sub>1/2</sub></b>	half life
<b>TBAF</b>	tetrabutylammonium fluoride
<b>TBOH</b>	tetrabutylammonium hydroxide
<b>TEA</b>	triethylamine
<b>TFA</b>	trifluoroacetic acid

<b>THF</b>	tetrahydrofuran
<b>TLC</b>	thin layer chromatography
<b>TOF-MS</b>	time of flight mass spectroscopy
<b>tosylate</b>	p-toluenesulfonyl
<b>Tris-HCl</b>	Tris(hydroxymethyl)aminomethane hydrochloride
<b>trit</b>	triphenylmethane
<b>Tryl</b>	triphenylmethane
<b>V<sub>2</sub></b>	measure of nonspecific binding
<b>V<sub>3</sub>"</b>	specific-to-nonspecific equilibrium partition coefficient

## Chapter 1

### Introduction and Background

#### 1.1 Introduction.

Alterations in serotonergic function within the central nervous system (CNS) are believed to be associated with a number of neurological and mental health disorders, including depression, schizophrenia, anxiety and Parkinson's syndrome.<sup>1,2</sup> The serotonin reuptake transporter (SERT) is located on the presynaptic neuron cell surface and is responsible for the clearance of serotonin (5-HT, **3**) from the synaptic cleft after neuronal firing. Presynaptic cell surface densities of SERT may be an excellent marker for measuring the integrity of the 5-HT terminals and 5-HT neurotransmission in relation to neurological and mood disorders.<sup>3</sup> Visualization and quantification of SERT densities in living tissue can be accomplished by positron emission tomography (PET) functional brain imaging (FBI) techniques, allowing for the determination of serotonergic system integrity. Considering SERT cell densities vary depending on the cerebral region, it is important for the understanding of the role of 5-HT **3** and SERT in a disease state to be able to image SERT density in high to low regions. There is currently a need for new PET imaging probes for the measurement of the brain regions with low (e.g. cerebellum) to medium (e.g. limbic system, particularly the hippocampus and amygdala) SERT densities.

We are interested in developing new SERT PET imaging agents with appropriate properties for the imaging of brain regions implicated in SERT related disorders. A desirable imaging agent should have high SERT affinity and

selectivity, good in vivo kinetics ( $K_D$ ,  $k_{on}$  and  $k_{off}$ ), low nonspecific binding and high target to cerebellum ratios ( $>2$ , important for imaging low SERT density regions). The objective of the Gerdes research group has been to develop new PET imaging agents for the in vivo imaging of SERT receptor densities of select brain regions.

## 1.2 The Neurotransmitter Serotonin.

5-hydroxytryptamine (serotonin, 5-HT, **3**) is an endogenous neurotransmitter of the central nervous system (CNS) in addition to peripheral tissues. Serotonin **3** was initially described as a substance present in clotting blood that acted as a vasoconstrictor (constriction of blood vessels).<sup>4</sup> Serotonin **3** was isolated from beef serum and purified by Rapport et al. in 1948.<sup>5</sup> They proposed that **3** contained an indole moiety and was likely related in structure to tryptophan **1** or tryptamine (not shown).<sup>5</sup> In 1951 5-hydroxytryptamine **3** was independently synthesized and compared to the vasoconstrictive substance (**3**) isolated by Rapport and was found to possess vasoconstrictive properties and to be structurally identical to **3**.<sup>6</sup> It was later determined that serotonin was involved in neurotransmission among other peripheral tissue functions.<sup>7</sup> Furthermore, the presence of 5-HT receptors was presented by Gaddum and Picarelli in 1957.<sup>8</sup> The existence of two separate 5-HT receptors was shown by Peroutka and Snyder in 1979.<sup>9</sup> They were able to demonstrate the presence of separate receptors utilizing the radioligands [<sup>3</sup>H]5-HT **3** and [<sup>3</sup>H]spiperone (not shown) to label the different receptor sites termed 5-HT<sub>1</sub> and 5-HT<sub>2</sub> respectively.<sup>9</sup>

Continuing research on the serotonergic system has identified fourteen known 5-HT receptors and the 5-HT transporter (5-HTT, known as SERT). Outlined in Table 1-1 are the known 5-HT receptors and transporter located peripherally and centrally, along with their associated therapeutic potential.<sup>10</sup>

**Table 1-1:**<sup>10</sup> The different 5-HT receptor families their subtypes and associated therapeutic potential.

Receptor Family	Subtype	Receptor Type	Therapeutic Potential
5-HT <sub>1</sub>	5-HT <sub>1A</sub>	G-protein Coupled	Anxiety
	5-HT <sub>1B</sub>		Migraine, Excessive Aggression
	5-HT <sub>1C</sub>		
	5-HT <sub>1D</sub>		Migraine
	5-HT <sub>1E</sub>		Unknown
	5-HT <sub>1F</sub>		Migraine
5-HT <sub>2</sub>	5-HT <sub>2A</sub>		Schizophrenia
	5-HT <sub>2B</sub>		Migraine
	5-HT <sub>2C</sub>		Anxiety, Depression, Obesity
5-HT <sub>4</sub>			Irritable bowel syndrome
5-HT <sub>5</sub>			Unknown
5-HT <sub>6</sub>			Bipolar, Parkinson's
5-HT <sub>7</sub>			Sleep disorders, Depression
5-HT <sub>3</sub>			Ligand-gated ion channel
SERT		Transporter (Reuptake)	Depression

In the CNS the biosynthesis (Figure 1-1) of 5-HT **3** is accomplished in the serotonergic neurons from the amino acid tryptophan **1**. Tryptophan **1** is hydroxylated by the enzyme tryptophan hydroxylase to give 5-hydroxytryptophan **2**. Decarboxylation of **2** by aromatic-L-amino-acid decarboxylase gives 5-HT **3**. The biosynthesis of **3** is dependent upon the transport of tryptophan **1** across the blood brain barrier (BBB). Serotonin **3** is degraded by deamination to 5-hydroxyindoleacetic (5-HIAA, **4**) by the enzyme monoamine oxidase (MAO), and **4** is then excreted by the urinary tract (Figure 1-1).

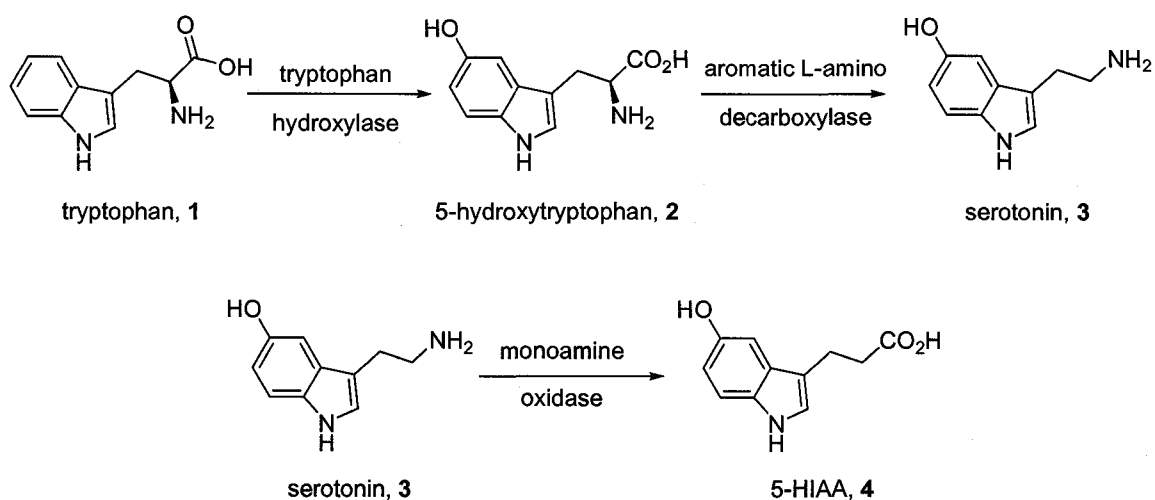


**Figure 1-1:** Biosynthesis and degradation pathway for serotonin in the CNS.

### 1.3 Serotonin Neurotransmission at the Synapse.

The signaling processes of the body and the brain are propagated through neuronal circuitry by electrical action potentials and chemical synaptic potentials. The nerve impulse is carried through the axon to the nerve terminus, for the nerve impulse to be carried from one neuron to the next the signal must be transferred across the synaptic cleft (the junction between the presynaptic and postsynaptic cell). The electrical impulse is not simply transferred from cell to cell. The process occurring at the nerve terminal is summarized in Figure 1-2. As the nerve impulse reaches the nerve terminal there is an influx of calcium ions through voltage gated ion channels. The influx of calcium ions causes the vesicles to fuse with the presynaptic neuron membrane and release stored serotonin **3** neurotransmitters. The neurotransmitters rapidly diffuse across the synapse by a concentration gradient where they are bound to receptors on the post synaptic terminal. Binding of the neurotransmitters propagates the nerve impulse by inducing a change in the membrane potential of the postsynaptic



neuron through a ligand gated ion channel. This can also occur via G-protein coupled receptors that activate a second messenger system within the postsynaptic neuron to propagate the nerve impulse. Following release the neurotransmitters are removed from the synaptic cleft by the serotonin reuptake transporter (SERT) located on the presynaptic nerve terminal and then packaged again into vesicles to await the next nerve impulse.

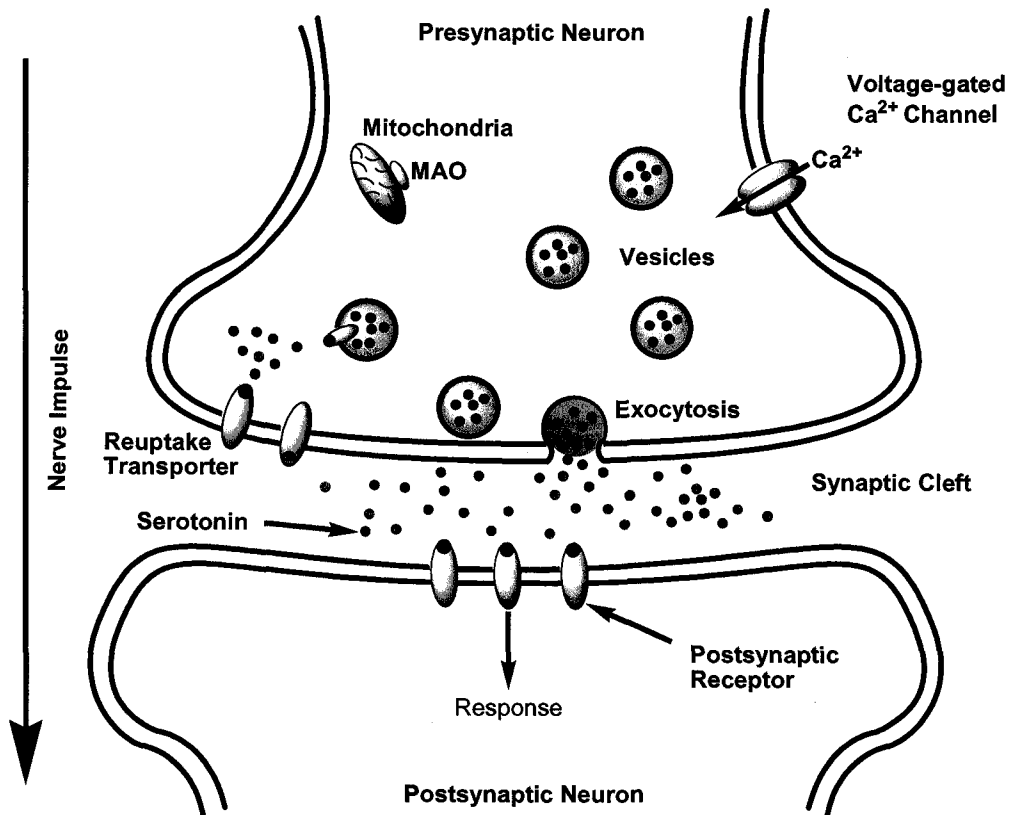


**Figure 1-2:** Signals from the pre-synaptic neurons to the post-synaptic neurons of the serotonergic system are linked by the neurotransmitter serotonin (5-HT). Release of 5-HT from the vesicles and subsequent binding with the postsynaptic receptors induces a response in the postsynaptic neuron and propagates the nerve impulse.

#### 1.4 Serotonin Reuptake Transporter (SERT).

The SERT protein is an integral membrane protein and consists of 12 transmembrane regions with the amino and carboxyl terminals located

intracellularly.<sup>11</sup> The SERT protein is a member of the subfamily monoamine transporters (which includes, noradrenaline (norepinephrine) and dopamine transporters) of the Na<sup>+</sup>/Cl<sup>-</sup> neurotransmitter transporter family.<sup>12</sup> After neuronal firing, the reuptake transporter is responsible for the termination of neurotransmission by uptake of serotonin from the synaptic cleft for later packaging into vesicles for use in subsequent neuronal firing events (Figure 1-2). The SERT protein actively transports 5-HT from the synaptic cleft with the cotransportation of 1 Na<sup>+</sup> and 1 Cl<sup>-</sup>, with the counter ion transport of K<sup>+</sup> (the transport of 5-HT is dependent on the presence of K<sup>+</sup> on the cytoplasmic side of the membrane).<sup>11</sup> The SERT protein is important for the regulation of the levels of 5-HT in the synaptic cleft.<sup>13</sup> The rat and human SERT proteins are of identical length (630 amino acids) and possess 92% amino acid identity.<sup>14</sup> The SERT protein is a well known target for selective serotonin reuptake inhibitors (SSRIs) for the treatment of depression among other disorders (Figure 1-3). By blocking SERT uptake of 5-HT, extracellular levels of 5-HT are increased activating 5-HT neurotransmission.<sup>11</sup>

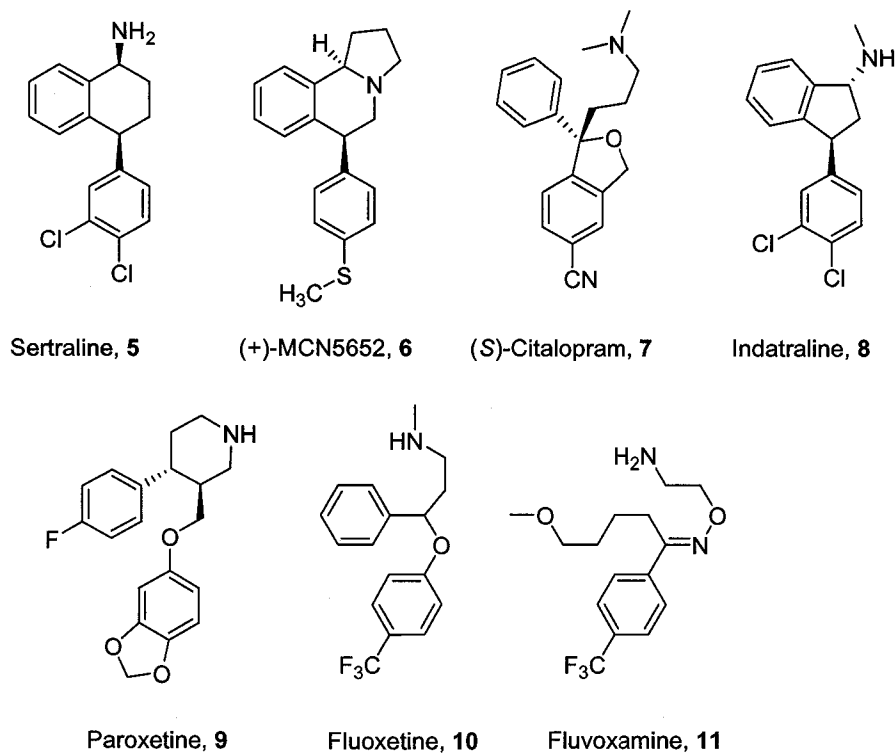


**Figure 1-3:** Typical SSRIs and related SERT inhibitors.

High SERT density is found in the raphe nuclei, substantia nigra, thalamus, hypothalamus and striatum.<sup>15-19</sup> Medium SERT densities are associated with the limbic and paralimbic structures, including the hippocampus, amygdala, and the cingulate cortex.<sup>16,18,20</sup> Low to negligible levels of SERT are found in the neocortex (occipital, and orbital frontal) and the cerebellum.<sup>15,18</sup> The cerebellum is used as a reference region for cerebral comparison of non-specific binding and for calculation of target-to-cerebellum ratios. Alterations in SERT density and function have been attributed to a variety of neuropsychiatric disorders, including depression<sup>21-23</sup> anxiety,<sup>22,24</sup> suicide,<sup>20,25,26</sup> schizophrenia,<sup>27-30</sup> and eating disorders,<sup>31,32</sup> among others. Studies of the distribution of the SERT protein in postmortem human brain samples suggest that the structures of the limbic system (including the amygdala, hippocampus, and hypothalamus) are

connected to the pathology of depression.<sup>33-36</sup> To better understand the pathology of the diseases related to SERT density changes, in vivo imaging studies of SERT densities would be beneficial for diagnosis and monitoring therapies of mental health disorders.

### **1.5 Functional Brain Imaging (FBI).**

Non-invasive in vivo analysis of CNS receptor and transporter densities can be accomplished by positron emission tomography (PET) and single photon emission computed tomography (SPECT).<sup>37,38</sup> In vivo imaging techniques refer to the use of radioligand tracers containing relatively short lived radionuclides ( $^{11}\text{C}$ ,  $^{18}\text{F}$ ,  $^{76}\text{Br}$  and  $^{123}\text{I}$ ,  $t_{1/2} = 20 - 960$  minutes), that are selective for the receptor, transporter or enzyme of interest. The PET and SPECT imaging techniques can measure receptor protein concentrations in the nanomolar (nM) to picomolar (pM) concentration range. These techniques are superior over magnetic resonance imaging measures that detect compounds in the micromolar ( $\mu\text{M}$ ) range.<sup>39</sup> One benefit of the PET or SPECT imaging technique is that the radioligand is used in small amounts reducing the possibility of adverse side effects.<sup>39</sup> The disadvantages to PET and SPECT imaging is the number of tracer exposures for the subject is limited due to radiation exposure (dosimetry) restrictions, availability of the radioligand, and in the case of the short lived radionuclide ( $^{11}\text{C}$  and  $^{18}\text{F}$ ) the proximity of the imaging scanner to the source of the radioligand production facility.

## 1.6 Criteria for SERT PET Tracers.

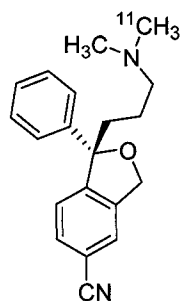
Radioligand selection criteria for PET and SPECT imaging studies are a major hurdle to overcome before any imaging analysis can be accomplished. A number of criteria have been delineated in the literature for the selection of the appropriate ligand and radioisotope to be used, these include: i) the ligand should be selective for the protein of interest, ii) the ligand should have high affinity ( $K_D < 1$  nM), iii) appropriate ligand lipophilicity (LogP 1.5-4, able to cross the blood brain barrier (BBB), but is not so lipophilic the agent suffers from nonspecific binding), iv) radioactive metabolites should not be active in the CNS, and v) the ligand should be non-toxic.<sup>3,13,39</sup> For low density target protein measurement a higher affinity agent is required. According to Laruelle et al., a ligand with a binding affinity in the range of 1 and 0.01 nM is considered sufficient.<sup>39</sup> However, the measurement of the ratio of specific-to-nonspecific binding may truly define a ligand's potential as an imaging agent.<sup>39</sup>

At equilibrium the ratio of specific-to-nonspecific tracer binding is equal to  $V_3''$  ( $V_3''$  is defined as the specific-to-nonspecific equilibrium partition coefficient). A  $V_3''$  value of 0.5 in the region of interest is desirable.<sup>3</sup> The partition coefficient  $V_3''$  is equal  $B_{max}/V_2K_D$ , where  $B_{max}$  is the density of the binding site,  $V_2$  is a measure of nonspecific binding and  $K_D$  (equilibrium dissociation constant) is the affinity of the ligand for the binding site.<sup>39,40</sup> The greater the nonspecific binding of the radioligand the lower the value of  $V_3''$  (less desirable). Also as the binding site density increases ( $B_{max}$ ) and the ligand's affinity increases (smaller  $K_D$ ) so does  $V_3''$  (more desirable). Comparison of  $V_3''$  values allows for direct

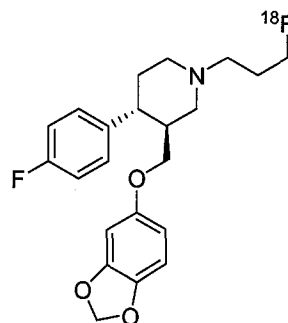
comparison of potential radioligands. Where the greater the ligands associated  $V_3$  value corresponds to a lower nonspecific binding ( $V_2$ ) and a better signal-to-noise ratio. The signal-to-noise ratio is especially important when attempting to measure the density of the tracer binding site in regions of medium density, i.e. SERT density in the limbic and paralimbic system implicated as the regions related to 5-HT and SERT disorders.

### 1.7 SSRIs as Potential PET Imaging Agents.

The use of the SSRIs citalopram **7** and paroxetine **9** was investigated as potential SERT radiotracers based upon their respective SERT affinities and selectivity for SERT. The more biologically active enantiomer (*S*)-citalopram **7** has high affinity and selectivity for SERT and a relatively low lipophilicity.<sup>41</sup> The N-methyl carbon-11 analog [<sup>11</sup>C]**7** was prepared from norcitalopram (not shown) and evaluated for its efficacy as a SERT PET imaging agent.<sup>42</sup> Ex vivo studies of [<sup>11</sup>C]**7** showed low target-to-background ratios and very low specific signal in human volunteers in PET studies.<sup>42,43</sup> A derivative of the SSRI paroxetine **9** (Paxil) was prepared [<sup>18</sup>F]fluoropropylparoxetine **12**, by treatment of **9** with [<sup>18</sup>F]fluoropropyltosylate.<sup>44</sup> However, the functionalized radiotracer [<sup>18</sup>F]**12** suffered from reduced affinity for SERT (3 orders of magnitude) and brain distribution studies showed no distinct localization in SERT rich regions of the brain.



(S)-[<sup>11</sup>C]Citalopram, 7



N-(3-[<sup>18</sup>F]Fluoropropyl)paroxetine, 12

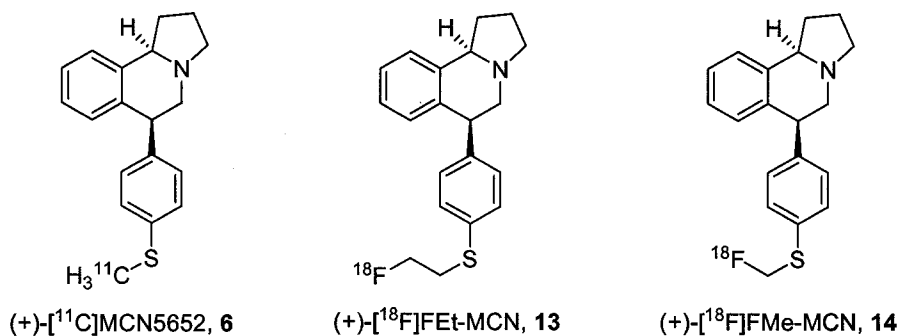
**Figure 1-4:** Commercial SSRI analogs developed as potential SERT PET imaging agents.

### 1.8 Current SERT Imaging Agents.

Initially, imaging the SERT protein was difficult due to the lack of a specific radioligand with suitable in vivo binding kinetics.<sup>38</sup> Attempts at utilizing known radiolabelled SSRIs (Figure 1-4) have been unsuccessful. The first useful radiotracer for SERT imaging in primates was (+)-[<sup>11</sup>C]MCN5652 **6** (Figure 1-5).<sup>38,45,46</sup> Subsequently (+)-[<sup>11</sup>C]**6** became a standard for comparison to determine the efficacy of new radiolabeled agents for PET SERT imaging.<sup>3,18,19</sup> Unfortunately, the in vivo kinetics of (+)-[<sup>11</sup>C]**6** were too slow for the carbon-11 radionuclide to be useful (carbon-11,  $t_{1/2} = 20.4$  min).<sup>19</sup> Additionally, nonspecific binding was too high for quantification of SERT in low density regions of interest (ROI) within the brain, particularly the limbic system.<sup>3</sup>

Attempts to prepare a radiotracer with a longer half life have been made. Suehiro et al. prepared [<sup>18</sup>F]FET-MCN **13** (Figure 1-5), where the fluorine-18 radioisotope with a longer half-life might prove to have better in vivo characteristics allowing for a longer analysis time.<sup>47</sup> However, [<sup>18</sup>F]**13** did not improve upon the lead [<sup>11</sup>C]**6**. It actually showed less favorable properties due to

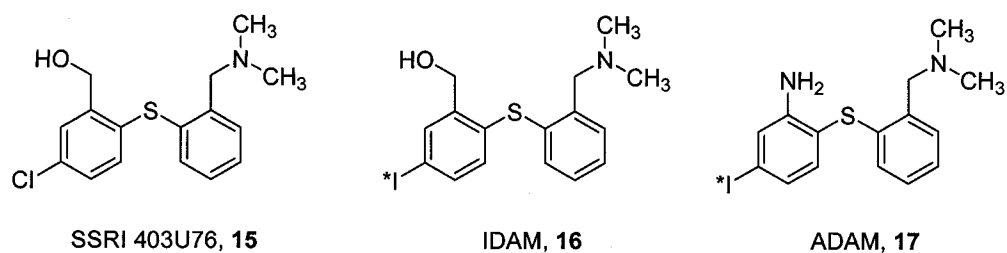
reduced BBB penetrating abilities. Additionally, [ $^{18}\text{F}$ ]FET-MCN showed a lower tissue to cerebellum ratios than the lead [ $^{11}\text{C}$ ]6.<sup>19,47</sup> The fluoromethyl analog [ $^{18}\text{F}$ ]14 (Figure 1-5) was also investigated and showed faster kinetics than the lead [ $^{11}\text{C}$ ]6 and higher specific binding in porcine brain, which is suggestive of its potential in humans.<sup>19,34</sup>



**Figure 1-5:** Radiolabelled derivatives of the potent and selective SSRI MCN5652.

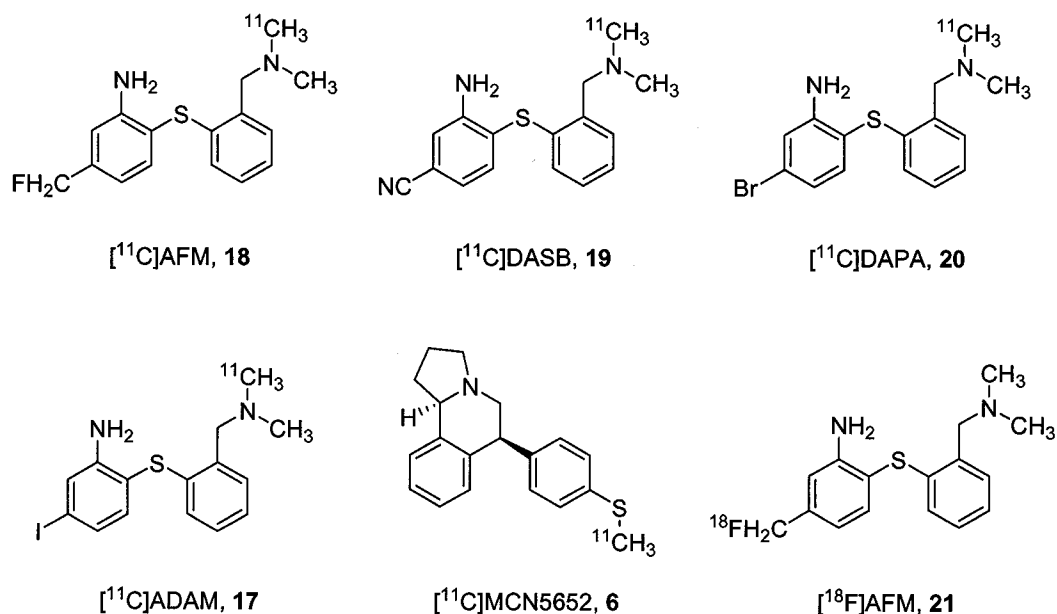
The second generation SERT imaging agents have been based upon the general structure of the diarylsulfide SSRI 403U76 **15** (Figure 1-7). The first tracer introduced for use as a SERT SPECT imaging agent was [ $^{123}\text{I}$ ]IDAM **16**.<sup>48,49</sup> The tracer [ $^{123}\text{I}$ ]IDAM **16** had very good SERT selectivity compared to the norepinephrine reuptake transporter (NET) and the dopamine reuptake transporter (DAT). The SPECT images had similar distribution compared to [ $^{11}\text{C}$ ]6.<sup>49</sup> Following IDAM **16**, the iodinated congener of [ $^{125}\text{I}$ ]ADAM **17** was prepared and found to have superior in vivo profile compared to **16**. The [ $^{123}\text{I}$ ]ADAM **17** is expected to be an excellent SPECT imaging tracer.<sup>2,50</sup>





**Figure 1-6:** The Diarylsulfide SERT inhibitor 403U76 **15** and the potential SERT SPECT analogs IDAM **16** and ADAM **17**.

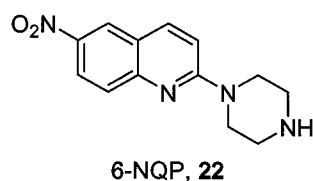
For PET imaging a series of carbon-11 diarylsulfide class of compounds have been evaluated and compared to [<sup>11</sup>C]**6** (Figure 1-7). The diarylsulfide ligands (Figure 1-1) have been shown to be selective for rSERT and have the appropriate regional distribution in rat brain for SERT.<sup>3</sup> Of the four diarylsulfides, [<sup>11</sup>C]DAPA **20** and [<sup>11</sup>C]ADAM **17** showed no benefit over [<sup>11</sup>C]**6**. However, [<sup>11</sup>C]DASB **19** and [<sup>11</sup>C]AFM **18** were demonstrated to outperform [<sup>11</sup>C]**6**. The radioligand [<sup>11</sup>C]AFM **18** with a significantly higher  $V_3$  value than the other tracer has the potential to be an excellent imaging agent for low to medium SERT density regions.<sup>3</sup> The excellent profile of [<sup>11</sup>C]AFM **18**, lead to the development of [<sup>18</sup>F]AFM **21**, where the inclusion of the fluorine-18 atom has the advantage of increased scanning time compared to carbon-11 and a fluorine-18 tracer can be transported to off-site imaging facilities if needed.<sup>3</sup> Biodistribution studies in rat of [<sup>18</sup>F]**21**, showed high brain uptake and high SERT binding affinity and selectivity. Based upon the current in vivo rat studies, [<sup>18</sup>F]**21** has been proposed to be an excellent SERT imaging agent.<sup>51</sup> It remains to be seen whether the benzyl fluoride moiety of [<sup>18</sup>F]**21** will provide suitable imaging performance qualities in primates.



**Figure 1-7:** Second generation SERT PET agents.

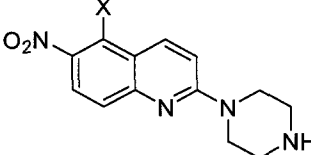
### 1.9 6-Nitroquipazines as SERT Inhibitor Tracers.

The lead structure 6-nitroquipazine **22** (6-NQP, 6-nitro-2-piperazin-1-ylquinoline, DU-24565) (Figure 1-8) is known to be one of the more potent and selective agents for SERT.<sup>1,52,53</sup> It seems plausible that analogs of 6-NQP **22** would lead to an efficacious SPECT or PET agent. The current functional brain imaging (FBI) analogs of 6-NQP are outlined in Table 1-1, including: [<sup>123</sup>I]5-iodo-6-nitroquipazine (INQP) **23**,<sup>54,55</sup> [<sup>76</sup>Br]5-bromo-6-nitroquipazine **24**,<sup>56</sup> [<sup>18</sup>F]5-fluoro-6-nitroquipazine **25**,<sup>57</sup> and [<sup>11</sup>C]5-methyl-6-nitroquipazine **26** (Table 1).<sup>58,59</sup>



**Figure 1-8:** SSRI 6-nitroquipazine.

**Table 1-2:** Structures of the current 5-halo-6-nitroquipazines and their respective SERT imaging radioligands.

	X	X*	
	<b>23</b>	I	<sup>123</sup> I
	<b>24</b>	Br	<sup>76</sup> Br
	<b>25</b>	F	<sup>18</sup> F
	<b>26</b>	CH <sub>3</sub>	<sup>11</sup> CH <sub>3</sub>

However, the metabolic dehalogenation fate of INQP **23** in primate brain, led to the presence of free [<sup>123</sup>I] that ultimately obscures the SPECT images. Additionally, the BrNQP **24** suffers from high non-specific binding.<sup>59</sup> The [<sup>18</sup>F]5-fluoro-6-nitroquipazine tracer **25**, showed lack of selectivity (readily displaced by maprotiline (not shown) a norepinephrine re-uptake inhibitor) and lack of binding affinity (readily displaced by citalopram **7**).<sup>57</sup> The [<sup>11</sup>C]5-methyl-6-nitroquipazine radioligand **26**, was also shown to be a plausible agent for PET imaging. However, the carbon-11 analog suffered from slow binding kinetics,<sup>58</sup> where the short half life of carbon-11 did not allow the tracer to reach apparent equilibrium of binding.

### 1.10 Pharmacophore Development.

Many of the radiolabeled versions of the SSRIs (Figure 1-1), have lipophilic qualities that may interfere with the PET or SPECT imaging through non-specific binding. It is our hypothesis that a portion of the non-specific binding may be related to SSRIs (and their labeled forms) acting as steroid mimics, perhaps interacting at neuroendocrine receptors in the brain.<sup>60</sup> Analysis of the structural similarities of the various SSRIs currently in the literature (Figure

1-3),<sup>61</sup> shows that each SSRI possess dual aromatic ring moieties connected by a central connecting carbon.

It is well known that SSRI treatment can lead to sexual dysfunction, a side effect that has profound implication on a patients willingness to stay on the treatment course.<sup>62</sup> A comparison of the SSRIs in Figure 1-3, shows that fluvoxamine **11** is the only SSRI shown to be devoid of a second aromatic moiety. Additionally, **11** has a marked attenuated difference in its respective side affects.<sup>63,64</sup> We believe the presence of the dual aromatic ring structure may lead to the side effects observed during SSRI treatment. Recently, SSRIs have been shown to be actively involved in the modulation of the neuroendocrine system.<sup>60</sup> It is our hypothesis that in the absence of a second aromatic ring the ability of an SSRI to interact with the neuroendocrine system is diminished, resulting in decreased side effects and prospectively reduced non-specific binding.

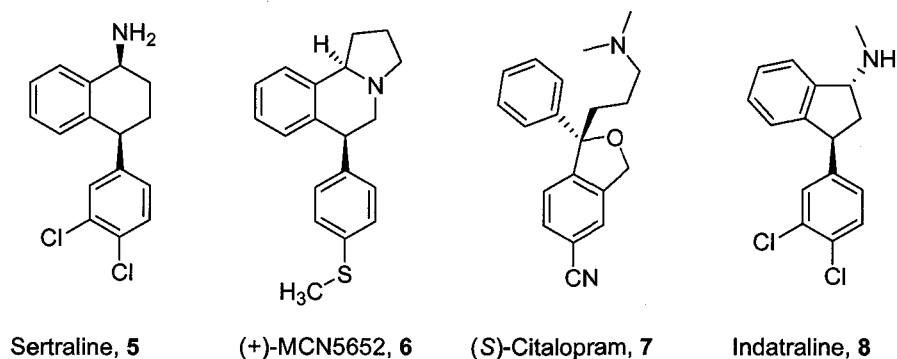


**Figure 1-9:** SERT pharmacophore training set SSRIs.

Therefore, we have developed a pharmacophore model constructed from a superposition of four semi-rigid SSRI ligands (Figure 1-9), in an effort to elucidate key structural features for an efficacious SERT PET tracer.<sup>65,66</sup> Examination of our model suggests there are a number of distinct features

necessary for SERT binding: i) an electronegative region (X group), ii) two aromatic regions (Ar1, and Ar2) iii) a heteroatom moiety and iv) a terminal amine group. It is our belief, based upon the structural diversity of known SERT inhibitor ligands all of the pharmacophore points need not be activated in order to maintain high SERT affinity. Our effort has been to develop ligands devoid of the Ar2 aromatic moiety which may play a key role in eliminating activity as a steroid mimic while maintaining the other structural characteristics of the pharmacophore (Figure 1-10).

Of particular interest to us was the SSRI 6-nitroquipazine **22** that has been shown to be potent and highly selective for SERT. The most interesting feature of **22** is the structural qualities compared to other SSRIs (Figure 1-1). The structure of **22** is composed of one aromatic ring moiety (Ar1), an X-group (Ar-NO<sub>2</sub>), a heteroatom moiety (3° piperazine nitrogen or quinoline nitrogen), terminal amine (2° piperazine nitrogen), but is devoid of a second aromatic ring moiety (Ar2). We then proposed that alkyl-substitution of **22** at the 2- or 3-position of the piperazine ring would likely probe the Ar2 binding pocket of our model.

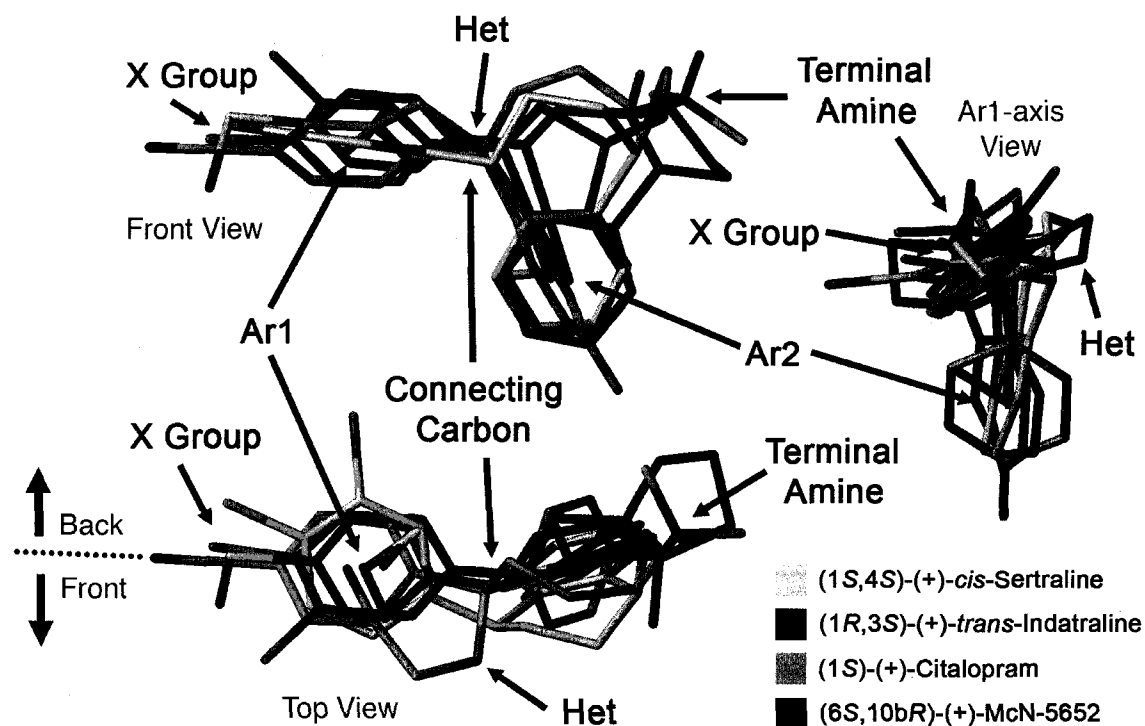


**Figure 1-10:** Superposition of the SERT pharmacophore training set SSRIs (Figure 1-9), and key SERT binding features.

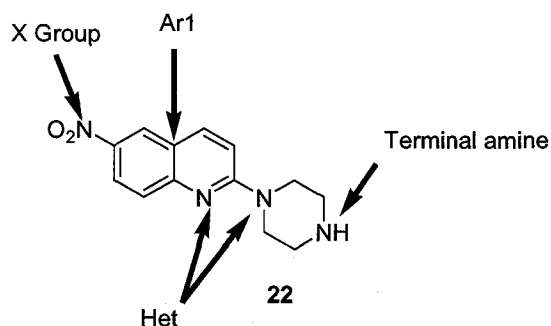
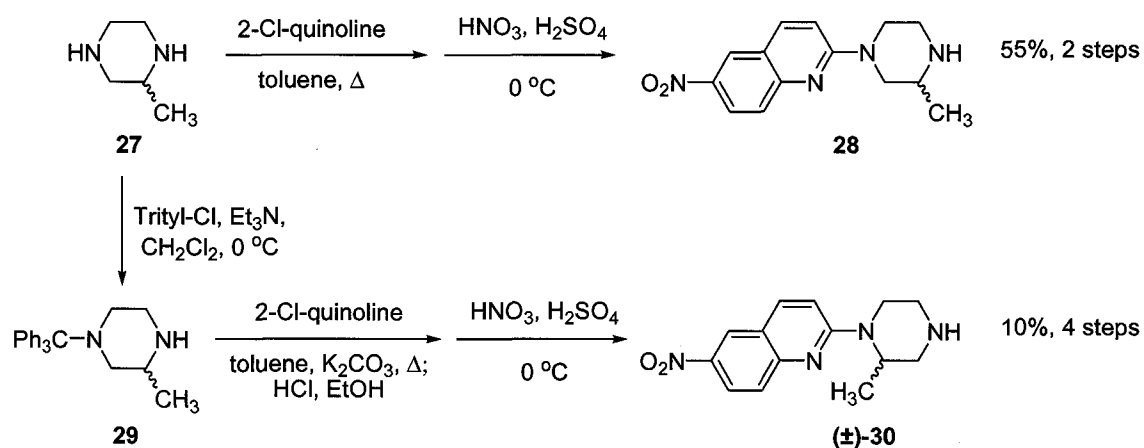


**Figure 1-11:** Structural qualities of **22** related to the SERT pharmacophore features.

### 1.11 Me-NQP 28 and (±)-30, Implications to the Pharmacophore.

We became interested in developing new PET imaging radioligands for SERT based upon the lead selective and potent SSRI 6-NQP **22**. The current 6-NQP FBI agents described above (Figure 1-8) have been shown in vitro to be highly selective for SERT. However, due to variety of factors i.e. dehalogenation,

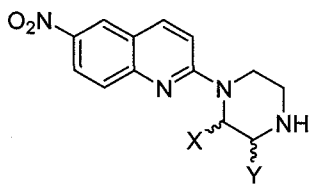
low ROI-cerebellum ratios and low synthetic yields of the desired agent. The aromatic halogenated analogs of **22** have failed to be useful for imaging studies. We believe that functionalizing 6-NQP **22** at the piperazine ring with alkyl groups that are amenable to late stage introduction of a radioisotope will likely show enhanced SERT binding by mimicking the interaction of the Ar2 moiety described in the pharmacophore model.



**Scheme 1-1:** Synthesis of **28** and **(±)-30**, the 2- and 3-alkyl derivatives of 6-NQP **22**.

To initially determine if alkyl substitution on the piperazine ring of the lead structure 6-NQP **22** would increase SERT binding affinity, the racemic forms of 2- and 3-substituted 2-piperazinyl-6-nitroquinoline **(±)-30** and **28** were prepared (Scheme 1-1) and evaluated for SERT binding against the standard [<sup>3</sup>H]paroxetine (Table 1-3).<sup>67</sup>

**Table 1-3:** SERT binding affinities of the first generation of 6-nitro-alkylpiperazin-1-ylquinolines.

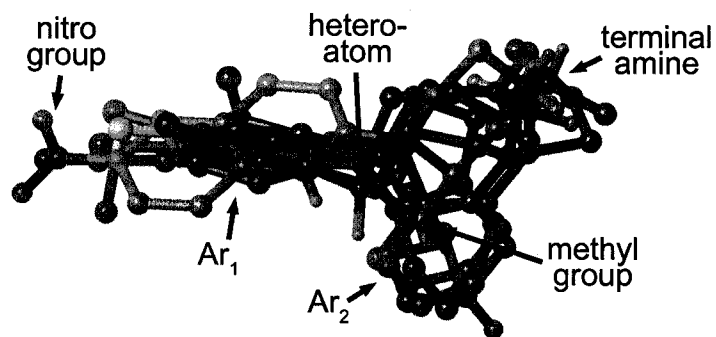


Cmpd #	X	Y	Ki (nM) <sup>a,b</sup>
<b>22</b>	H	H	0.163 ± 0.053
<b>(±)-30</b>	CH <sub>3</sub>	H	0.081 ± 0.061
<b>28</b>	H	CH <sub>3</sub>	4.56 ± 2.4
<b>(±)-31</b>	CH <sub>2</sub> OCH <sub>3</sub>	H	2.48 ± 0.28 (pM)

<sup>a</sup>Gerdes, 2002. <sup>b</sup>Data determined from competition assay utilizing rat cortical membrane suspensions labeled with [3H]paroxetine, method is discussed in Chapter 4.

From this study we were able to determine that substitution at the 2-position of the piperazine ring is 56 times more potent for SERT than the 3-substituted analog. Additionally, **(±)-30** is 2 times more potent than **22**, suggesting that the alkyl substituent at the 2-position has added beneficial interaction for SERT binding compared to the lead **22**. Also, we can deduce from the binding data that the 3-position involves negative interaction at the binding site leading to its decreased affinity for SERT. As shown in Figure 1-12, an overlay of the enantiomer ((S)-2-(2-methylpiperazin-1-yl)-6-nitroquinoline ((S)-MeNQP **30**) with the SERT pharmacophore shows the methyl group positioned for interaction within the Ar2 pocket. This led us to investigate the synthesis of an extended alkyl chain version of MOM-NQP **(±)-31** that could interact deeper within the Ar2 binding region. We also investigated the production of a potential radiolabeling precursor by substitution of the piperazine ring at the 2-position, with a substituent that can be later converted to its radiolabeled equivalent.



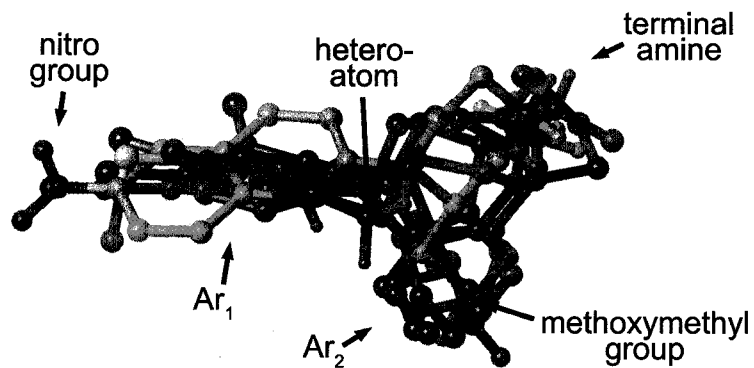


■ S-Citalopram, Indatraline, MCN-5652, Sertraline

**Figure 1-12:** Alignment of (S)-Me-NQP **30** with the pharmacophore ligand superposition.

### 1.12 MOM-NQP ( $\pm$ )-**31**.

In an effort to extend the 2-alkyl-piperazine substituent into the Ar2 binding pocket, as well as to generate a precursor for the development of a FBI agent for SERT, we investigated the synthesis of 2-(2-methoxymethylpiperazin-1-yl)-6-nitroquinoline (MOM-NQP) ( $\pm$ )-**31**. Computational analysis and superposition of ( $\pm$ )-**31** suggests an excellent fit of the methoxymethyl side chain into the region we have defined as Ar2, likely serving as a highly potent SERT inhibitor.

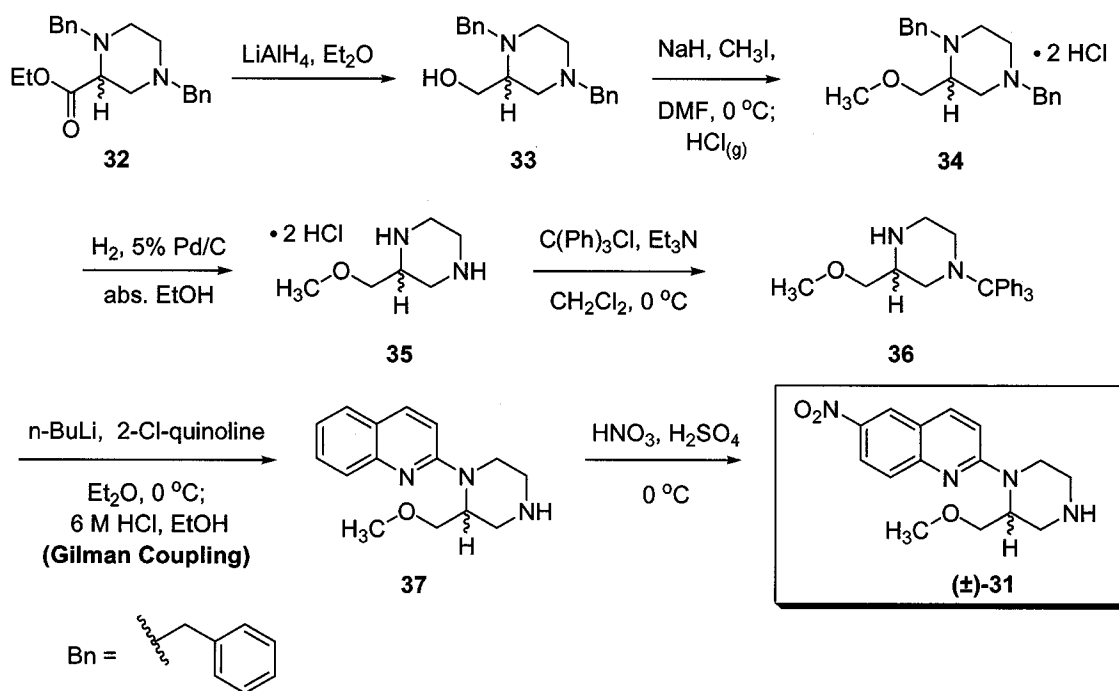


■ S-Citalopram, Indatraline, MCN-5652, Sertraline

**Figure 1-13:** Alignment of MOM-NQP **31** with the pharmacophore ligand superposition.

The synthesis of MOM-NQP ( $\pm$ )-**31** was accomplished from the starting material ethyl 1,4-dibenzylpiperazine-2-carboxylate **32** in six synthetic steps (Scheme 1-2).<sup>68-70</sup> The key step of the synthesis was the utilization of the Gilman coupling method.<sup>71</sup> We have found that the Gilman method is particularly sensitive to the ratio of the reagents used. For successful Gilman coupling the ratio of reagents must be strictly adhered to (150 mol% of the amine, 150 mol% of *n*-BuLi, and 100 mol% of 2-chloroquinoline). Use of the lithium amide of piperazine **36** according to Gilman procedure proved to be a more facile method for the preparation of 2-alkylpiperazin-1-yl-quinolines. The method is far superior to previous methods of amine 2-chloroquinoline couplings that required heating the two components for extended amounts of time resulting in low yields (~22%) of the desired product (Scheme 1-2).<sup>67</sup> The Gilman method allowed us to couple

the 2-substituted N-trityl-protected piperazine **36** with 2-chloroquinoline in the consistent range of 80-95% yield, as per Scheme 1-2.<sup>69,72,73</sup>

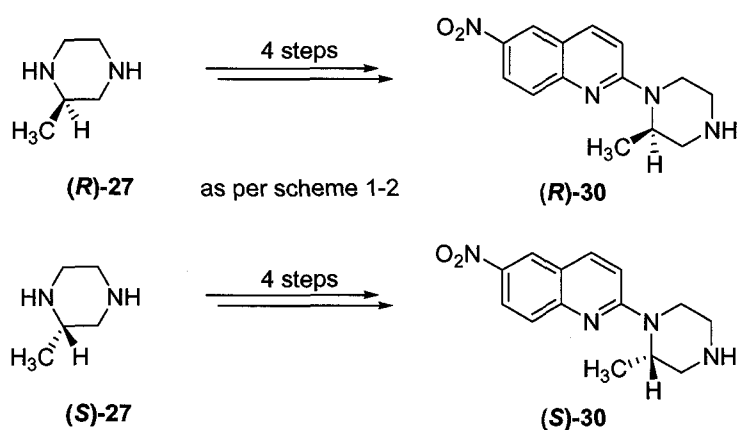


**Scheme 1-2:** Synthesis of 2-(2-(methoxymethyl)piperazin-1-yl)-6-nitroquinoline, MOM-NQP ( $\pm$ )-**31**.

The synthesis of MOM-NQP ( $\pm$ )-**31** not only expanded our knowledge of coupling piperazines to 2-chloroquinoline but also further exemplified our study of the SAR of the 2-(2-alkyl-piperazin-1-yl)-6-nitroquinoline series. Synthesis of MOM-NQP ( $\pm$ )-**31** gave us another ligand to further establish that our computational model is predictive. Extension of the 2-alkyl-piperazine group into the Ar2 region improves the ligands affinity. Table 1-1 shows the binding affinity of ( $\pm$ )-**31** is 33 times more potent than our lead ( $\pm$ )-Me-NQP **30** and 66 times more potent than the initial lead 6-NQP **22**.

### 1.13 R- and S-Me-NQP ((*R*)-30 and (*S*)-30).

Based upon the success found with the methyl (Me-NQP ( $\pm$ )-30) and the methoxymethyl (MOM-NQP ( $\pm$ )-31) analogs of 6-NQP **22** we began to investigate the synthesis and subsequent in vitro pharmacological evaluation of the enantiomers of ( $\pm$ )-30. The synthesis of (*S*)-30 and (*R*)-30 was accomplished utilizing the enantiomeric forms of 2-methyl piperazine available from Sigma-Aldrich. Each piperazine enantiomer was prepared according to the methods described in the MOM-NQP ( $\pm$ )-30 (Scheme 1-2). Briefly, the desired enantiomer of **27** was protected as the N-trityl and coupled to 2-chloroquinoline using the Gilman method. Deprotection of the trityl group and selective nitration at the quinoline 6-position gave the enantiomers (*R*)-30 ( $[\alpha]_D^{20}$  -62° (EtOH)) and (*S*)-30 ( $[\alpha]_D^{20}$  = +65° (EtOH)) in 51% and 49% yields, respectively, over four steps (Scheme 1-3).



**Scheme 1-3:** Chiral synthesis of (*R*)- and (*S*)-Me-NQP **30**.

#### 1.14 Proposed Work.

The goal of this work has been to utilize our SERT pharmacophore model to develop new more selective and potent agents for the SSRI SERT binding domain. In particular, we were interested in developing ligands devoid of a second aromatic ring moiety (Ar2) in the hopes that SERT ligands with only one aromatic moiety would show less nonspecific binding. In doing this we wanted to expand our SAR knowledge of the SSRI SERT binding domain by synthesizing new 2-(2-alkyl-piperazin-1-yl)-6-nitroquinolines to probe the area defined as Ar2. We have shown that functionalizing the 2-position of the piperazine ring with a methyl ( $\pm$ )-**30** and methoxymethyl group ( $\pm$ )-**31** greatly enhances SERT binding affinity. In addition to expanding the SAR study of the 2-(2-alkyl-piperazin-1-yl)-6-nitroquinolines, we were interested in preparing potential radiolabeling precursors for incorporation of carbon-11 and fluorine-18 radioisotopes to explore the development of new PET imaging agents for SERT. We also hoped to show that our 2-(2-alkyl-piperazin-1-yl)-6-nitroquinolines are selective for the SERT and have appropriate vitro binding kinetics for PET imaging studies of low to medium SERT density regions through a kinetic binding study.

## Chapter 2

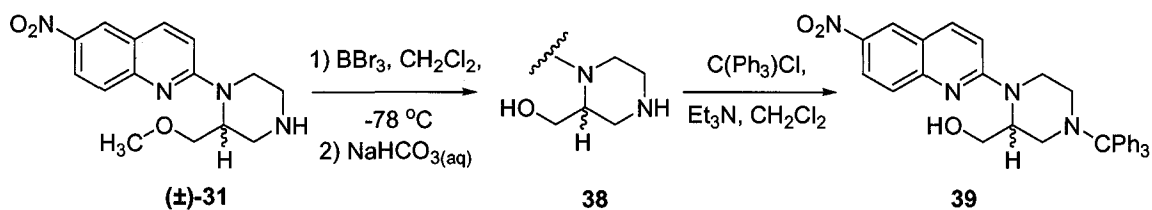
### Synthesis of Racemic Targets

#### 2.1 Introduction and Goals.

The initial SAR study, encompassing synthesis and biological evaluation of the racemic and chiral 2-(2-alkyl-piperazin-1-yl)-6-nitroquinolines (Me-NQP ( $\pm$ )-**30** and MOM-NQP ( $\pm$ )-**31**), has shown that structural alteration of the lead 6-NQP **22** at the piperazine 2-position increases SERT binding affinity of the ligand. This chapter describes the synthesis of six new SERT ligands to expand our knowledge of the SAR of the SERT binding domain. This work has also prompted us to develop new racemic radiolabeled (carbon-11 and fluorine-18) analogs of our lead ( $\pm$ )-**31**. Outlined in this chapter are the syntheses of the new potential radiotracers [ $^{11}\text{C}$ ]MOM-NQP **31** and [ $^{18}\text{F}$ ]PROF-NQP **58**.

#### 2.2 Synthesis of [ $^{11}\text{C}$ ]MOM-NQP **31**.

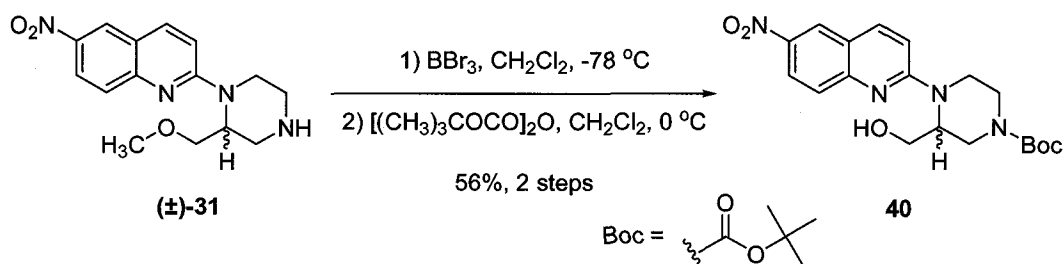
Preliminary work in our group attempted the synthesis of the radiolabeling precursor N-trityl-HOM-NQP **39** according to Scheme 2-1. The synthesis began by demethylation of MOM-NQP ( $\pm$ )-**31** with boron tribromide to give the methyl alcohol HOM-NQP **38**. Once the alcohol **38** was made, our initial thought was that protection of the terminal amine with a trityl group would be the simplest protecting group for us to use giving the N-trityl protected HOM-NQP **39**.



**Scheme 2-1:** Synthesis of the radiolabeling precursor N-trityl-HOM-NQP **39**.

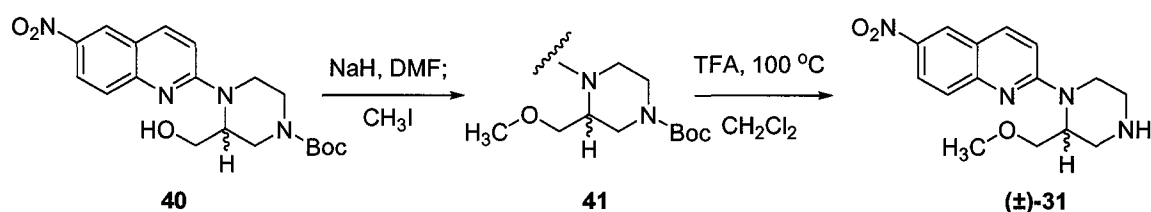
The synthesis of the **39** from HOM-NQP **38** proved to be more challenging than expected. Unfortunately, the mono-N-protected species **39** was difficult to prepare due to the formation of the undesired di-protected (terminal amine and alcohol) HOM-NQP (not shown). Multiple attempts to selectively protect the nitrogen of **39** were performed at varying temperatures;  $-78\text{ }^{\circ}\text{C}$ ,  $0\text{ }^{\circ}\text{C}$  and ambient temperature.<sup>74</sup>

Due to the difficulties of the trityl protecting group, we decided that protection of the free amine of HOM-NQP **38** as the *t*-butyl carbamate (N-Boc) may be a viable alternative radiolabeling precursor. We again began by demethylation of ( $\pm$ )-**31** with  $\text{BBr}_3$  to give **38**. The boron tribromide demethylation was followed by Boc protection of the amine using an excess of di-*tert*-butyl dicarbonate in dichloromethane (DCM) to give the carbon-11 radiolabeling precursor **40** (Scheme 2-2).



**Scheme 2-2:** Preparation of the radiolabeling precursor, N-Boc-HOM-NQP **40**.

To determine the feasibility of the radiolabeling precursor **40**, we ran control methylation and deprotection reactions that were designed to simulate the conditions that would be used during the radiolabeling synthesis (Scheme 2-3). Compound **40** was deprotonated in dimethyl formamide (DMF) with sodium hydride (NaH) at ambient temperature to give the alkoxide as a bright red solution. The alkoxide was quenched with the addition of methyl iodide (CH<sub>3</sub>I) to give the nonradioactive (cold) agent N-Boc-MOM-NQP **41**. The cold agent was isolated by aqueous workup and extraction with DCM, the resulting dried (K<sub>2</sub>CO<sub>3</sub>) DCM solution was treated with trifluoroacetic acid at ambient temperature. The crude reaction mixture was made basic (pH 12) and the deprotected product ( $\pm$ )-**31** was extracted with DCM, followed by purification by reversed phase HPLC utilizing a C-18 column eluting with 50:30:20:0.2 (methanol/acetonitrile/water/triethylamine).

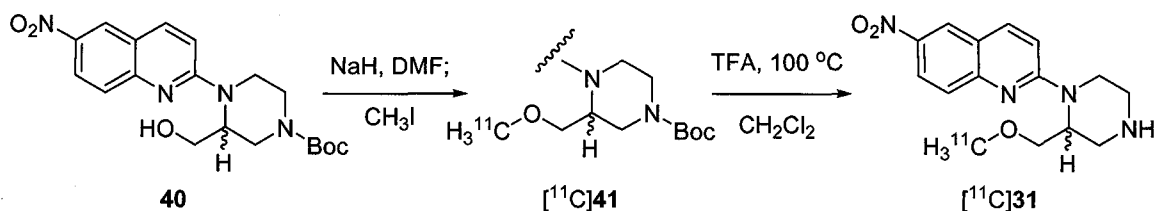


**Scheme 2-3:** Simulated reaction sequence for the production of the desired radiotracer [<sup>11</sup>C]MOM-NQP ( $\pm$ )-**31**.

Upon completion of the nonradioactive synthesis of ( $\pm$ )-**31**, the radiolabeling precursor N-Boc-HOM-NQP **40** was shipped to our collaborators at Lawrence Berkeley National Laboratory (LBNL), Berkeley California to attempt carbon-11 methylation of the alcohol with [<sup>11</sup>C]methyl iodide and subsequent N-



Boc deprotection to give the desired radiolabelled ligand [ $^{11}\text{C}$ ]**31**. Initial experiments performed by our collaborator Dr. James P. O'Neil resulted in a 5% decay corrected, end of bombardment (EOB) purified yield of [ $^{11}\text{C}$ ]**31**. The radiosynthesis encompassed the methylation and N-Boc deprotection of [ $^{11}\text{C}$ ]**31** using trifluoroacetic acid, according to Scheme 2-4.<sup>75</sup> The N-Boc protected HOM-NQP **40** was deprotonated by NaH as a solution in DMF and added to a solution of [ $^{11}\text{C}$ ]methyl iodide. The reaction was sealed and heated at 100 °C for 2-3 minutes. The crude product was isolated by C-18 Sep-Pak eluting with DCM. Trifluoroacetic acid (TFA) as a 1:9 mixture in DCM was added to the N-Boc protected intermediate [ $^{11}\text{C}$ ]**41** and the reaction mixture was concentrated in vacuo at 100 °C to give the crude product [ $^{11}\text{C}$ ]**31**. The crude labelled product was purified by reverse phase semipreparative HPLC, eluting w/ 50:30:20:0.2 (methanol/acetonitrile/water/triethylamine) to provide [ $^{11}\text{C}$ ]**31** in a 2-5% end of bombardment (EOB) decay corrected yield. The [ $^{11}\text{C}$ ]CH<sub>3</sub>I used in the synthesis was generated from  $^{14}\text{N}$  gas using the LBNL onsite cyclotron. Carbon-11 was generated by irradiation of nitrogen-14 in a  $^{14}\text{N}(p,\alpha)^{11}\text{C}$  nuclear reaction in the presence of oxygen giving [ $^{11}\text{C}$ ]CO<sub>2</sub>. The reduction of [ $^{11}\text{C}$ ]CO<sub>2</sub> over a nickel catalyst in the presence of H<sub>2</sub> gave [ $^{11}\text{C}$ ]CH<sub>4</sub> and the [ $^{11}\text{C}$ ]CH<sub>4</sub> is halogenated with I<sub>2</sub> to give [ $^{11}\text{C}$ ]CH<sub>3</sub>I.



**Scheme 2-4:** Radiosynthesis of [ $^{11}\text{C}$ ]MOM-NQP **31**.

Later during the investigation it was proposed that due to the binding kinetics of a related agent [ $^3\text{H}$ ]n-Prop-NQP **52** (preparation and pharmacology are discussed in Chapter 4), the time needed to reach apparent binding equilibrium with SERT was greater than 100 min which exceeded four carbon-11 half lives (20.4 min), precluding the effective use of [ $^{11}\text{C}$ ]**31** for PET imaging. A similar finding has been described for the SERT PET agent [ $^{11}\text{C}$ ](+)McN5652 **6**.<sup>19</sup> Marjamaki et al. proposed that incorporation of the fluorine-18 radionuclide ( $t_{1/2} = 109.8$  min) would allow for increased time need to reach apparent binding equilibrium.<sup>19</sup> We were interested in the preparation of MeF-NQP **42** of a fluorinated version of ( $\pm$ )-**31** (Figure 2-1). The inclusion of the fluorine-18 radionuclide would allow us to reach apparent equilibrium of binding by increasing the time the radiolabelled agent would be useful for imaging..

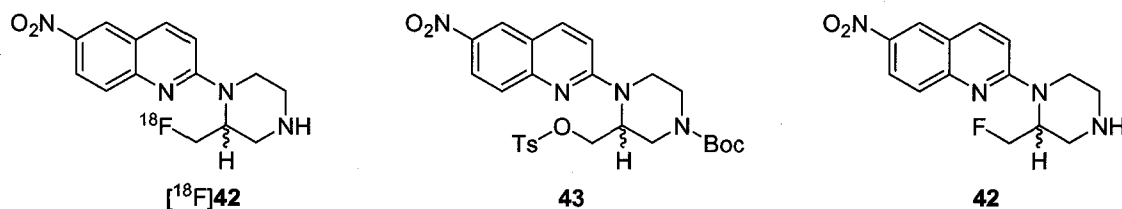


**Figure 2-1:** Desired fluorine-18 radiolabelled ligand [ $^{18}\text{F}$ ]MeF-NQP **42**, tosylate precursor **43** and the cold fluorinated agent, MeF-NQP **42**.

This led us to try to synthesize the cold agent of [ $^{18}\text{F}$ ]MeF-NQP **42** (Figure 2-1). Initial efforts looked into the preparation of MeF-NQP **42** from the precursor

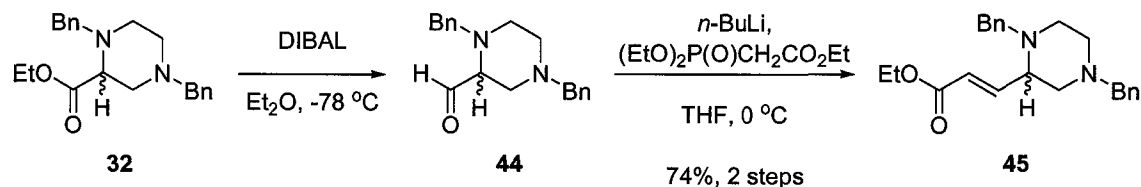
N-Boc-HOM-NQP **41** by preparing the O-tosylate **43**. The O-tosyl moiety is a useful leaving group for radiofluorination. Additionally, our collaborators had an efficient process for the generation of [ $^{18}\text{F}$ ] fluoride that could be used for non-aqueous nucleophilic fluoride ion substitution reactions. However, all efforts in our lab could not produce the desired tosylate product **43**. Furthermore, a number of attempts to synthesize the cold 2-(2-(fluoromethyl)piperazin-1-yl)-6-nitroquinoline **42** via other methods, i.e. (diethylamino)sulfur trifluoride (DAST), resulted in only the formation of undesired side products.<sup>74</sup> With these results, we decided that lengthening the carbon side chain by two carbons may increase the possibility of making a viable tosylate radiolabeling precursor with reduced chances of any side reactions occurring.

### 2.3 Synthesis of PROM-NQP ( $\pm$ )-51.

Described in this section is the overall synthesis of 2-[2-(3-methoxypropyl)-piperazin-1-yl]-6-nitroquinoline (PROM-NQP, ( $\pm$ )-**51**). With the information gained from the one carbon series, efforts in our lab were focused on the production of the three carbon 2-(2-alkyl-piperazin-1-yl)-6-nitroquinoline precursor **59** that we believed would be better suited for late stage introduction of a fluorine-18 atom. In order to accomplish this task we decided to lengthen the piperazine alkyl chain at an early stage in the 2-(2-alkyl-piperazin-1-yl)-6-nitroquinoline synthesis, versus the alternate strategy of a later carbon chain extension post piperazine framework formation. The complete synthesis of PROM-NQP ( $\pm$ )-**51** is shown in Scheme 2-13. This synthesis was afforded in 11

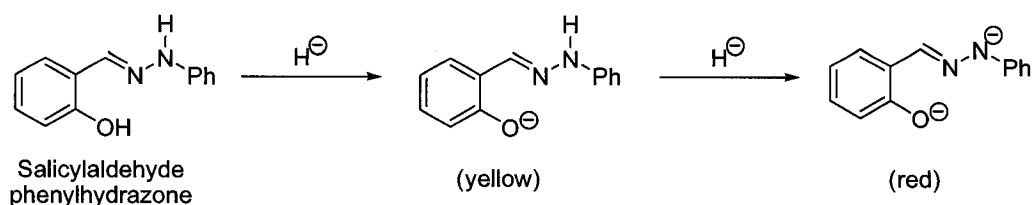
steps with an overall yield of 19%. The following describes the work leading up to the optimized synthesis of ( $\pm$ )-**51**.

As shown in Scheme 2-5, initial experiments were focused on the controlled reduction of ethyl 1,4-dibenzylpiperazine-2-carboxylate **32** to its corresponding aldehyde **44** using diisobutylaluminum hydride (DIBAL). Following reduction the aldehyde **44** would be used in a Horner-Emmons<sup>76</sup> type olefination reaction to extend the length of the chain by two carbons giving the desired piperazine fragment with a three carbon chain length. The ester **32** was reduced with DIBAL to the corresponding aldehyde **44** at -78 °C. The resulting intermediate was converted to the corresponding  $\alpha,\beta$ -unsaturated ethyl ester **45** (74%, 2 steps) using triethyl phosphonoacetate as the Horner-Emmons reagent and *n*-BuLi as the base (Scheme 2-5).



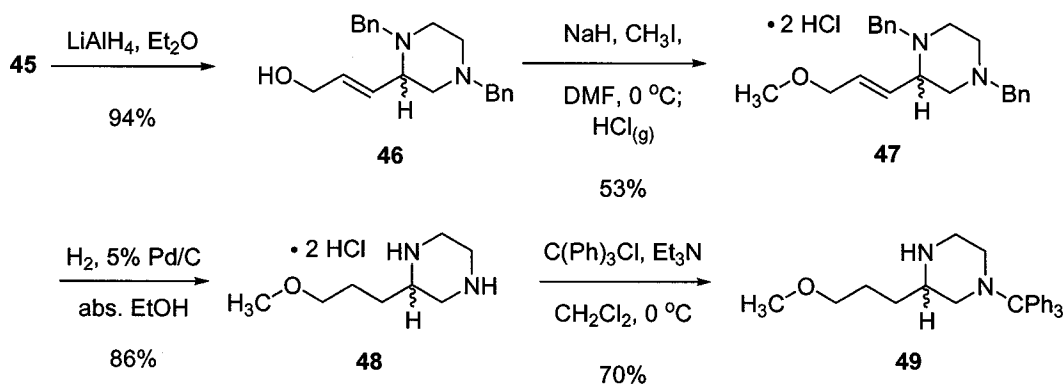
**Scheme 2-5:** Initial synthetic route to the  $\alpha,\beta$ -unsaturated ethyl ester **45**.

However, we found it difficult to drive the DIBAL reduction of **32** to **44**, leaving a portion (10-25 mol%) of the starting material ester **32** remaining. Attempts to improve the reduction by titration of the DIBAL reagent before the reduction with salicylaldehyde phenylhydrazone did not improve the yield (Scheme 2-6).



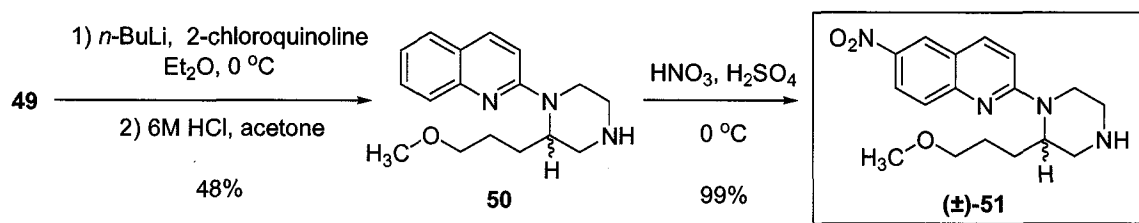
**Scheme 2-6:** Titration reagent for determining the concentration of organometallic reagents.

After the Horner-Emmons homologation we also found that the resulting  $\alpha,\beta$ -unsaturated ethyl ester **45** was difficult to isolate from the starting material **32** by column chromatography. The successfully purified fraction of the unsaturated ester **45** was reduced to the unsaturated alcohol **46** (94%) utilizing lithium aluminum hydride ( $LiAlH_4$ ), followed by methylation of **46**, forming **47** in a 53% yield (Scheme 2-7). Subsequent catalytic reduction of the alkene and hydrogenolysis of the benzyl groups of **47** gave 2-(3-Methoxy-propyl)-piperazine **48** (86%). The least hindered nitrogen of **48** was protected with triphenylmethane chloride (trityl,  $CPh_3$ ) in DCM giving **49** in a 70% yield. For this reaction an excess of  $Et_3N$  was used in situ to give the free base form of the starting material, as well as to act as an acid scavenger for the HCl generated in the reaction.



**Scheme 2-7:** Initial synthesis of the coupling precursor 3-(3-methoxypropyl)-1-tritylpiperazine **49**.

The protected trityl piperazine **49** was coupled to 2-chloroquinoline using the Gilman method (discussed in Chapter 1) and purified by column chromatography to give the N-trityl-PROM-QP (not shown, 75%). The purified coupled product N-trityl-PROM-QP was deprotected by dissolving the material in a minimal amount of acetone and treating with 6 M HCl. The deprotected 2-(3-methoxypropyl-piperazin-1-yl)quinoline was easily isolated from any non-nitrogenous side products (quinoline and trityl alcohol) by diluting the reaction mixture with 1 M HCl and extracting with DCM. The resulting aqueous layer is then brought to basic pH and the 2-(3-methoxypropyl-piperazin-1-yl)quinoline was extracted from the aqueous layer with DCM. The extracted product was found to be of sufficient purity to continue with the nitration step without further purification. Compound **50** was selectively nitrated at the 6-position of the quinoline ring using HNO<sub>3</sub> in H<sub>2</sub>SO<sub>4</sub> at 0 °C to give the 2-[2-(3-methoxypropyl)-piperazin-1-yl]-6-nitroquinoline (**±**)-**51**.



**Scheme 2-8:** Coupling and nitration to give the desired compound PROM-NQP (**±**)-**51**.

The NMR spectra of the final product PROM-NQP (**±**)-**51** (Figure 2-2) when compared to a MOM-NQP (**±**)-**31** NMR (Figure 2-3) (our standard for 2-(2-alkyl-piperazin-1-yl)-6-nitroquinolines) looked promising. We were intrigued by the

doubling of the peak at 7.00 (Figure 2-2). We initially attributed the splitting pattern to the presence of the longer piperazine side chain. The extend alkyl chain was thought to be interacting with and changing the inherent environment of the hydrogen at the quinoline 3-position thus affecting its splitting pattern, possibly through a rotational barrier. Similar splitting patterns have occurred with N-formyl-6-nitroquinoline compounds. Protection as the N-formyl results in splitting of the quinoline signals in the proton spectrum due to amide rotamers where the peak (quinoline 3-position) at 7.00 ppm is typically the most influenced by the amide rotamer.

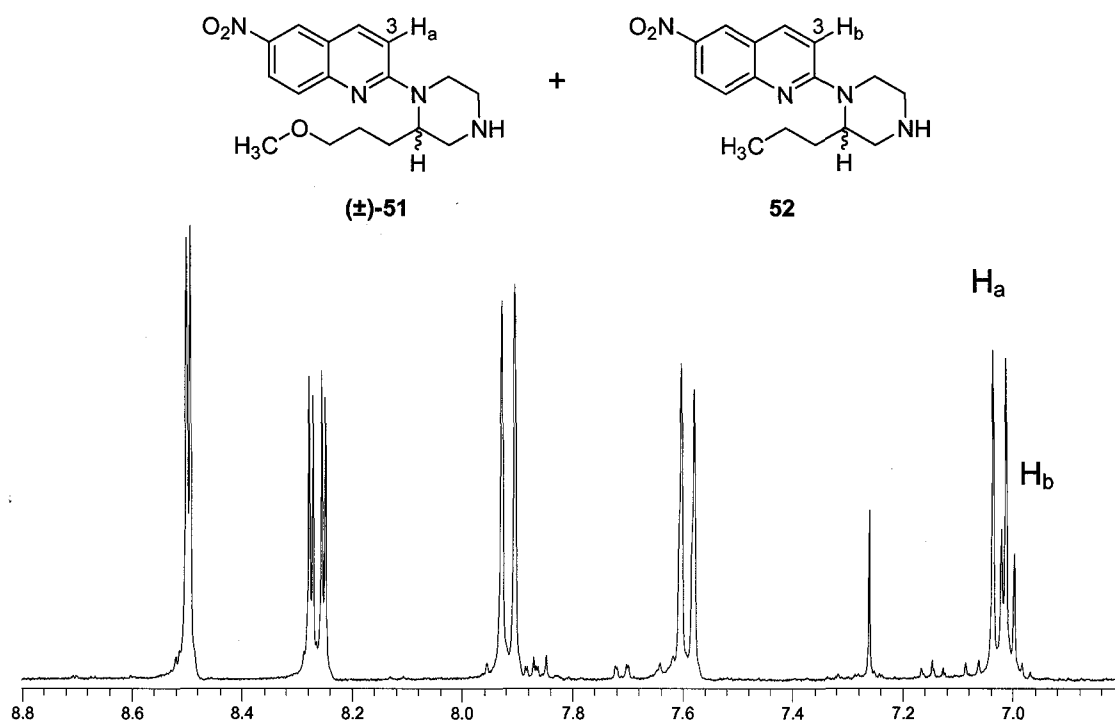


**Figure 2-2:** NMR of the Aromatic region of PROM-NQP (±)-51, showing the splitting of the C-3 quinoline hydrogen.

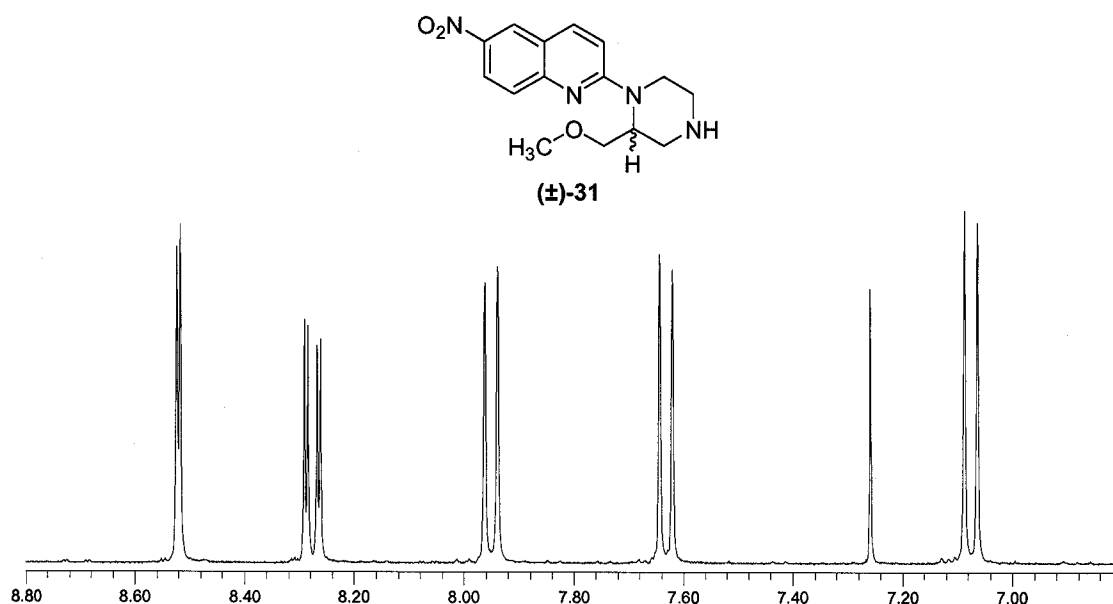


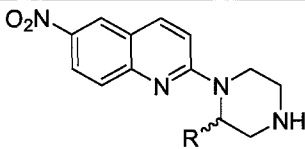
**Figure 2-3:** NMR of the Aromatic region of MOM-NQP ( $\pm$ )-31 as a comparison to the PROM-NQP ( $\pm$ )-51 NMR.

However, analysis of the crude reaction mixture before N-trityl deprotection (Scheme 2-8) by thin layer chromatography (TLC) (1:9 EtOAc/hexanes) showed the presence of three distinct coupled products. Suggesting that at some point during the initial reaction sequence (Scheme 2-5, Scheme 2-7 and Scheme 2-8) two side products had formed in addition to the desired compound ( $\pm$ )-51.

We were able to isolate each coupled product as their respective N-trityl protected species from the crude reaction by column chromatography. Subsequent deprotection of each purified product (6 M HCl, EtOH), followed by NMR and mass spec analysis determined that the three products were *n*-PROP-NQP 52, MOM-NQP ( $\pm$ )-31 and the desired product PROM-NQP ( $\pm$ )-51 (Table 2-1).

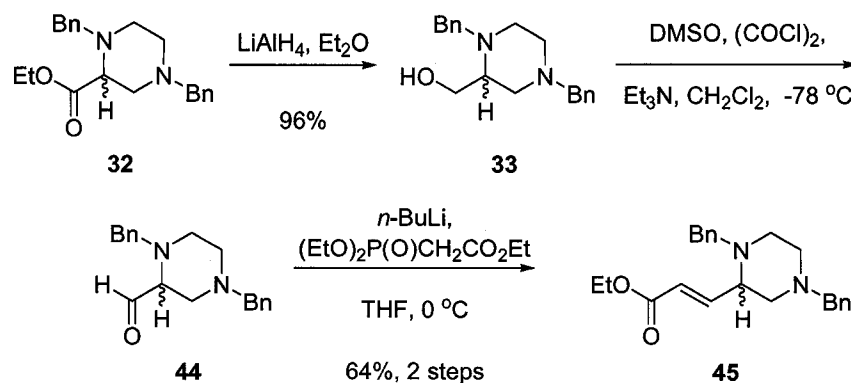


**Table 2-1:** 2-alkylpiperzin-1-yl-6-nitroquinoline products from the initial PROM-NQP synthesis.

	R	Cmpd
	CH <sub>2</sub> OCH <sub>3</sub>	(±)- <b>31</b>
CH <sub>2</sub> CH <sub>2</sub> CH <sub>3</sub>	<b>52</b>	
CH <sub>2</sub> CH <sub>2</sub> CH <sub>3</sub> OCH <sub>3</sub>	(±)- <b>51</b>	

The methoxymethyl product was determined to be carry over of the starting material ethyl ester piperazine **32** due to the incomplete reduction with DIBAL. To eliminate the carry over of **32**, other methods of preparing the aldehyde **44** were investigated; i.e., PCC, PDC, and Swern. We decided that a more efficient method of preparing the aldehyde **44** was to fully reduce the ethyl ester **32** to the alcohol **33** in a similar manner to a literature procedure,<sup>68,70</sup> followed by oxidation of the methyl alcohol **33** to the desired aldehyde **44**.

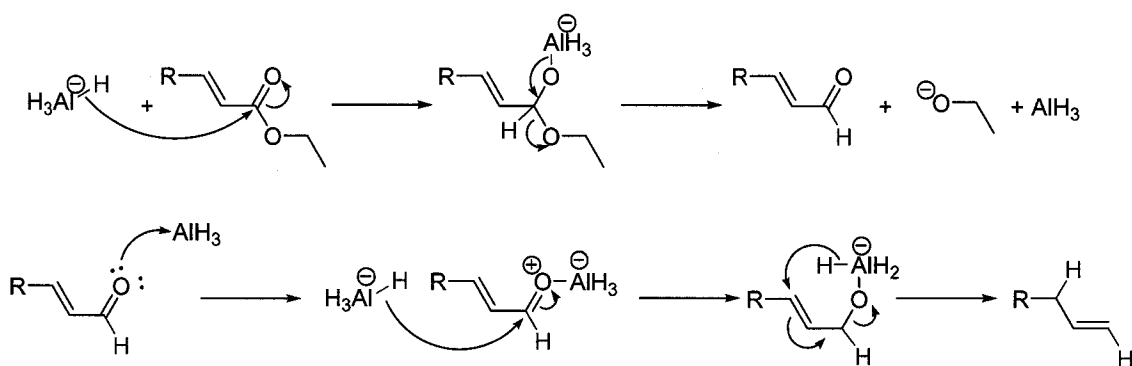
Outlined in Scheme 2-9 is the modified synthesis of the key intermediate **45** for the preparation of PROM-NQP (±)-**51**. The ethyl ester **32** was reduced to its corresponding alcohol **33** via LiAlH<sub>4</sub> reduction at room temperature in Et<sub>2</sub>O to give the alcohol **33** in a 96% yield. This reaction proceeds smoothly in less than one hour to give the alcohol, which after quenching the reaction and isolation from the inorganic salts was of sufficient purity to continue with the next transformation. When necessary, the alcohol can be purified by column chromatography over silica gel eluting with 3:2 EtOAc/hexanes. The aldehyde **44** was generated by Swern oxidation<sup>77-79</sup> (DMSO, COCl<sub>2</sub> and Et<sub>3</sub>N), according to the previous synthesis (Scheme 2-5) the aldehyde **44** was used immediately in the Horner-Emmons olefination to give the unsaturated ester **45** in a 64% yield over two steps (Scheme 2-9).



**Scheme 2-9:** Modified synthesis of the key intermediate **45** for the synthesis of PROM-NQP ( $\pm$ )-**51**.

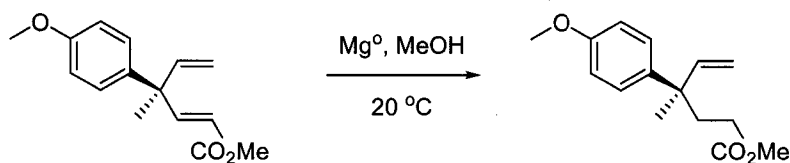
The reaction sequence outlined in Scheme 2-9 proved more facile for the preparation of **45** than the previous controlled reduction of the ester with DIBAL and subsequent Horner-Emmons homologation. Additionally, the purification of the resulting  $\alpha,\beta$ -unsaturated ethyl ester **45** proved to be much easier, considering both the  $\text{LiAlH}_4$  reduction and Swern oxidation go to completion. This eliminated the carryover of any of the starting material ester **32** and the presence of MOM-NQP ( $\pm$ )-**31** after coupling was no longer detected.

This left us to determine where the *n*-propyl side product **52** was being generated. We proposed that the *n*-propyl side product **52** may be the result of a 1,4 addition of the hydride to the  $\alpha,\beta$ -unsaturated system of **45** during the  $\text{LiAlH}_4$  reduction of ester to the propenyl alcohol **46**. A proposed mechanism for the 1,4 hydride addition is detailed in Scheme 2-10. To possibly further support this mechanism similar conditions of the reaction (Scheme 2-5, Scheme 2-7 and Scheme 2-8) could be run using lithium aluminum deuteride ( $\text{LiAlD}_4$ ). The resulting reaction mixture could be analyzed for the presence of the deuterio *n*-propyl product at the 1- and 3-position of the propylene side chain.



**Scheme 2-10:** Proposed mechanism for the production of the *n*-allyl side product that would lead to the *n*-PROP-NQP **52** product after completing the synthetic steps outlined in Schemes 2-7 and 2-8.

To eliminate the possibility of the 1,4 hydride addition, saturation of the alkyl chain of **45** was necessary before  $\text{LiAlH}_4$  reduction. If this was to be accomplished using catalytic hydrogenation, it would be necessary to reduce the alkene selectively and avoid hydrogenolysis of the N-benzyl groups of **45**. To avoid the possibility of cleaving the N-benzyl protecting groups we looked into the reduction of the alkene by a non-catalytic hydrogenation technique. A literature search for the reduction of  $\alpha,\beta$ -unsaturated esters found that the use of magnesium metal in methanol reduced unsaturated esters in good yields (65-99%).<sup>80,81</sup> For example, Fadel, et al. were able to selectively reduce an  $\alpha,\beta$ -unsaturated ester in the presence of a non-conjugated alkene by treatment with Grignard grade magnesium metal in dry methanol (Scheme 2-11).<sup>80</sup>



**Scheme 2-11:** Example of a selective reduction of a conjugated system utilizing  $\text{Mg}^0$ .

According to the literature this was a simple process of reacting the unsaturated ester with magnesium turnings in methanol, quenching with acid to consume any remaining magnesium metal, and isolation of the product by aqueous extraction. This is a useful reaction when there are non-conjugated alkenes present (as above) as well as other catalytic hydrogenation sensitive groups, i.e. cyano and nitrile. The reaction did seem to progress well giving the saturated methyl ester **53**, although the yields were not as expected, ranging in the 26-32% yield (Scheme 2-12). During the reaction progress a large amount of baseline material by TLC material was formed, which has been proposed to be due to chelation of  $Mg^{2+}$  by the piperazine nitrogen atoms. This is likely, considering piperazine is a cyclic version of ethylenediamine, a well known metal chelating agent (Figure 2-4).<sup>82</sup>

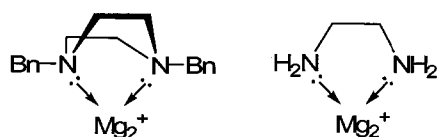
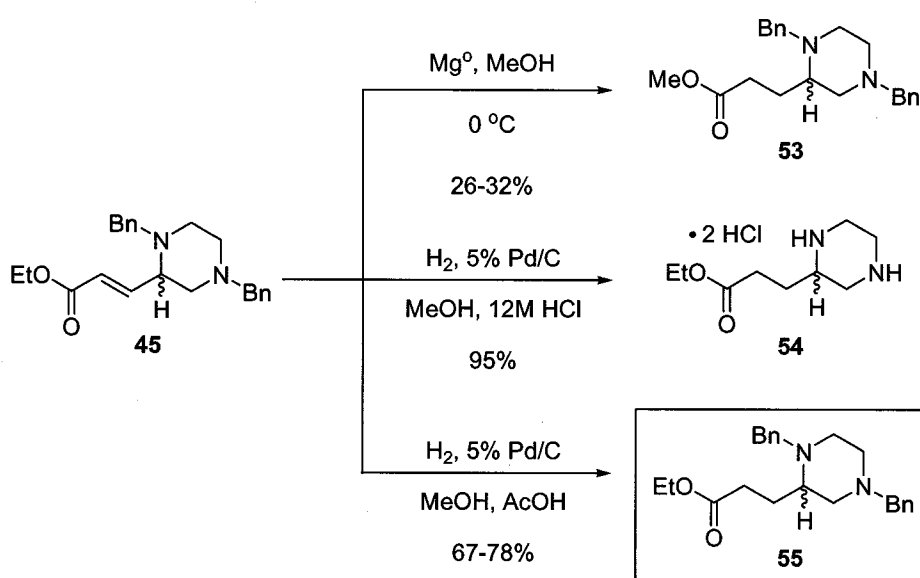


**Figure 2-4:** Chelating potential of piperazine and related chelator ethylenediamine.

In light of the failed  $Mg^0$  reduction we attempted a “gentle” hydrogenation of **45** using 5% Pd/C and  $H_2$  at atmospheric pressure and hydrochloric acid (12 M). When using 12 M HCl the alkene was easily reduced. Unfortunately the cleavage of the benzyl groups also occurred, giving compound **54** in a 95% yield (Scheme 2-12). This was both a positive and negative result, we now knew that a pressure of 50 psi and 50 °C was not necessary to cleave the benzyl groups, a standard method in our group. However, selective reduction of the alkene in the

presence of the benzyl groups was still elusive. We decided to attempt the hydrogenation using acetic acid instead of the typical 12 M HCl. A solution of the dibenzyl  $\alpha,\beta$ -unsaturated ethyl ester **45** was treated with excess of acetic acid and a catalytic amount of 5% Pd/C. The reaction was sealed with a septum and hydrogen was bubbled through the solution. The reduction in the presence of acetic acid allowed us to selectively reduce the alkene leaving the benzyl groups intact, thereby giving the saturated ethyl ester **55** in a 78% yield (Scheme 2-12).

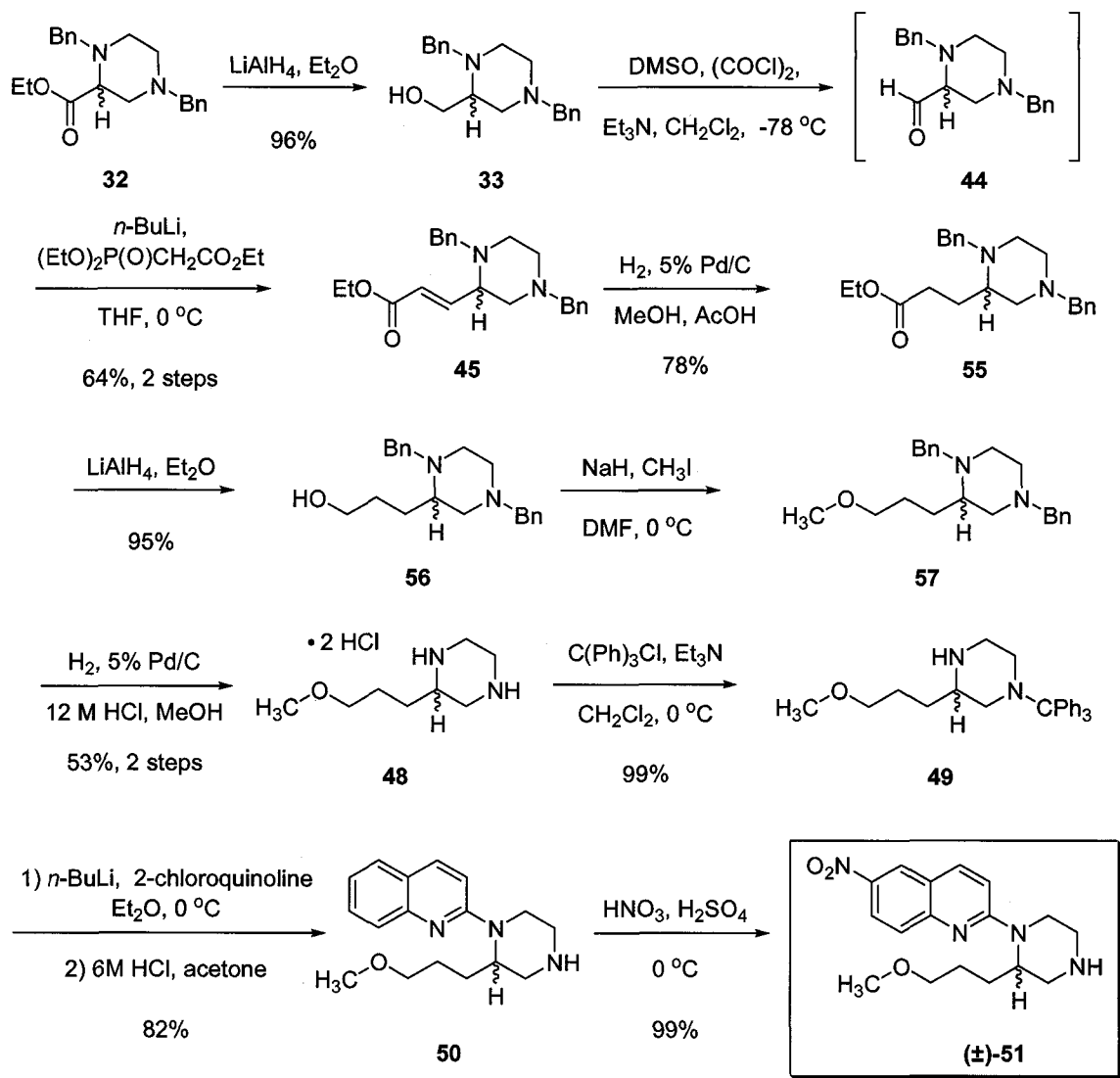


**Scheme 2-12:** Attempted selective reduction of the conjugated alkene of **45**.

The saturated propyl ester **55** was reduced to the propyl alcohol **56** with  $\text{LiAlH}_4$  in  $\text{Et}_2\text{O}$  (95%, Scheme 2-13) in a similar manner to the one carbon side chain case (Scheme 1-2). The propyl alkoxide was generated in DMF using  $\text{NaH}$ , and then methylated by the addition of  $\text{CH}_3\text{I}$  to give **57**. The benzyl groups of the free-base form of methoxypropyl **57** were cleaved at atmospheric pressure and ambient room temperature hydrogenolysis conditions, as a solution

in MeOH and an excess of 12 M HCl, to give the dihydrochloride salt of the piperazine **48** (53%, 2 steps).

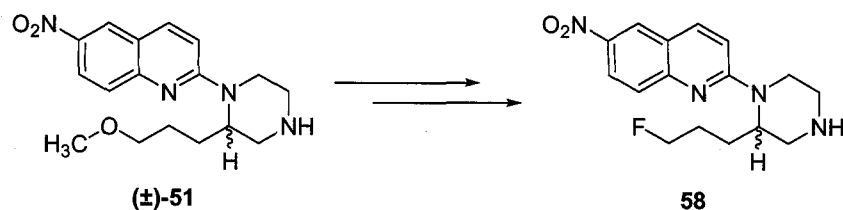
The more accessible nitrogen atom was selectively protected with trityl-chloride to give the N-trityl-piperazine **49** in a 99% yield. Then **49** was coupled to 2-chloroquinoline utilizing the Gilman coupling conditions and the resulting crude material was purified by column chromatography (1:9 EtOAc/hexanes). The N-trityl protected product (not shown) was deprotected in acetone with 6 M HCl, aqueous workup afforded the desired compound **50** in an 82% yield over two steps. Selective nitration at the quinoline six position gave the desired 2-(2-alkyl-piperazin-1-yl)-6-nitroquinoline ( $\pm$ )-**51** (99%). The overall synthesis is shown in Scheme 2-13 and was accomplished in 11 steps with an overall yield of 19%.



Scheme 2-13: Overall synthesis of PROM-NQP ( $\pm$ )-51.

## 2.4 Synthesis of the Radiolabeling Precursor N-formyl-ProTos-NQP 63.

Upon completion of the synthesis of ( $\pm$ )-51, the focus was turned towards generating a fluorinated analog with the intent of preparing a radiolabeling precursor for the introduction of a fluorine-18 atom (Scheme 2-14). The goal



**Scheme 2-14:** Proposed fluorinated analog **58**, to be prepared from PROM-NQP (**±**)-**51**.

was to prepare a stable fluorination precursor that was amenable to late stage incorporation of the fluorine atom by  $S_N2$  displacement technology. We set out to generate an N-protected-propyl-O-tosylate **59** (Figure 2-5) of compound HOP-NQP **146** (not shown).

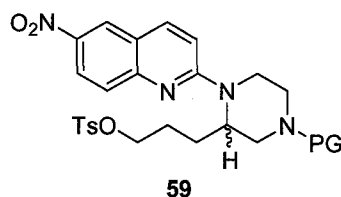


**Figure 2-5:** N-protected proposed fluorinating precursor.

Our specific approach encompassed the nucleophilic displacement of the proposed tosylate **59** by  $F^-$  and subsequent nitrogen deprotection would give the desired radiolabelled compound **58**. To prepare the O-tosyl precursor, PROM-NQP (**±**)-**51** needed to be demethylated and the  $2^\circ$  nitrogen atom had to be protected. Earlier work within the MOM-NQP (**±**)-**31** series found that the MOM group could be easily deprotected using boron tribromide in good to moderate yields (Scheme 2-1). Furthermore the nitrogen could be protected with a BOC group as part of the purification procedure after demethylation. What remained unknown was whether the propyl version could undergo tosylation reaction, this would be in contrast to the one carbon side chain version that failed to tosylate.



Our prediction was that by extension of the carbon chain by two additional carbons would make the oxygen more available for reaction with tosyl chloride.

When PROM-NQP ( $\pm$ )-**51** was treated with boron tribromide under similar conditions to the MOM-NQP demethylation procedure (Scheme 2-2), we found that the desired alcohol **146** was generated; additionally a second more non-polar product was also formed. Mass spectra analysis showed that the side product was the corresponding alkyl-bromide **62**. The mechanism shown in Figure 2-6 below provides a rationale for the formation of the two products under the  $\text{BBr}_3$  conditions. Unfortunately, due to the high polarity of the 6-NQP analogs the bromide could not be easily separated from the desired product by silica gel chromatography. It was necessary to use a high percentage of methanol in DCM to elute the products and the resulting separation was poor.

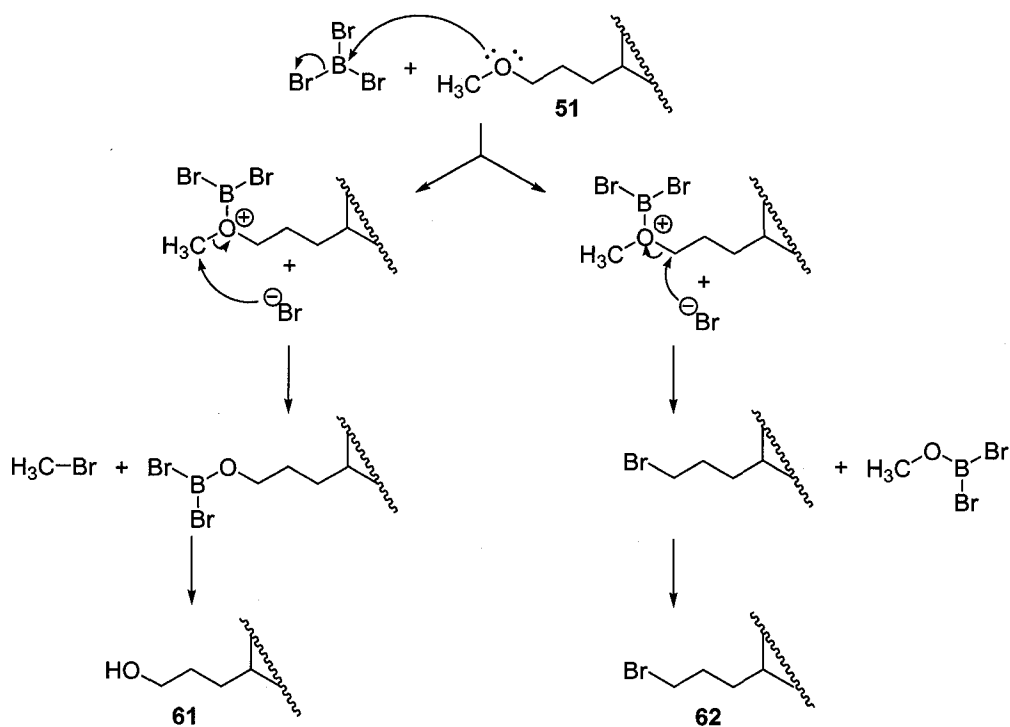
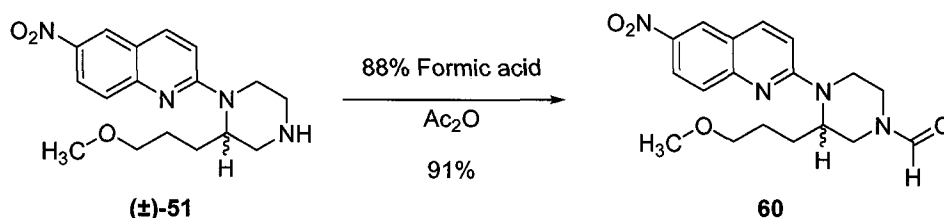


**Figure 2-6:** Explanation for the production of the bromide side product formed during  $\text{BBr}_3$  cleavage of the methyl ether.

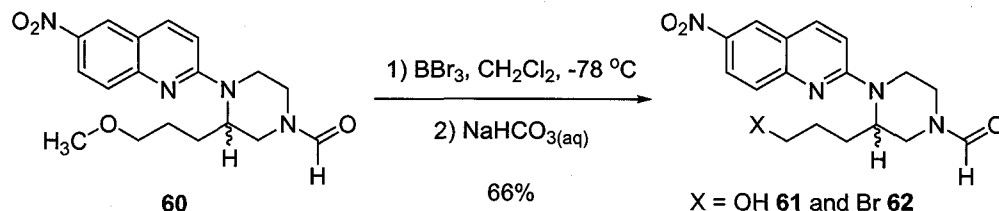
In order to simplify the purification of the  $\text{BBr}_3$  reaction we decided that protection of the terminal amine with a group that is stable to  $\text{BBr}_3$  conditions would be beneficial. Therefore, the free amine of PROM-NQP ( $\pm$ )-**51** was protected as the N-formyl according to Scheme 2-15. Treatment of ( $\pm$ )-**51** with acetic anhydride ( $\text{Ac}_2\text{O}$ ) as a solution in 88% formic acid gave the desired N-formyl-PROM-NQP **60** in a 91% yield.<sup>83</sup> Protection of the amine as the N-formyl group made the purification simple and the use of column solvents that contained a high percent of MeOH were avoided. The resultant N-formyl-2-(3-methoxypropyl-piperazin-1-yl)-6-nitorquinoline was purified using silica gel eluting with 0.01:5 MeOH/ $\text{CHCl}_3$ .



**Scheme 2-15:** N-formyl protection of PROM-NQP ( $\pm$ )-**51**.

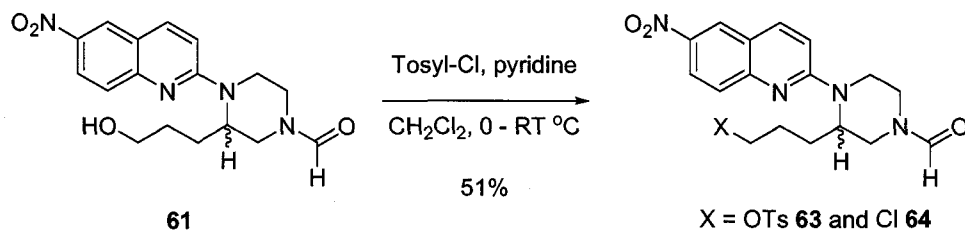
The N-formyl-PROM-NQP **60** was treated with  $\text{BBr}_3$  according to the procedure developed in the MOM-NQP synthesis (Scheme 2-2). In brief a solution of N-formyl-piperazine in DCM at  $-78\text{ }^\circ\text{C}$  was treated with a solution of  $\text{BBr}_3$  (500 mol%) then allowed to warm to room temperature, the reaction was quenched by the addition of a saturated solution of  $\text{NaHCO}_3$ , and the organic portions were extracted with DCM. We found the N-formyl protecting group to be stable to the  $\text{BBr}_3$  reaction conditions. Importantly, by having the terminal amine tied up as the N-formyl allowed for easy separation of the desired alcohol product

from any unreacted starting material **60** or bromide side product **62**. We found that the  $\text{BBr}_3$  demethylation of PROM-NQP ( $\pm$ )-**51** as the N-formyl amide gave consistent results where the product alcohol **61** was easily isolated from any side products by column chromatography with silica gel (66%).



**Scheme 2-16:** Cleavage of the methyl ether of N-formyl-PROM-NQP ( $\pm$ )-**51**.

The N-formyl-HOP-NQP **61** was then treated with tosyl chloride in the presence of pyridine in DCM at 0 °C for 24 hours to give the O-tosylate **63** in a 53% yield. However, we found that the resulting O-tosylate **63** was very reactive to nucleophiles present in the reaction mixture. For example, chloride ion that was generated during the reaction quickly converted **63** to the alkyl chloride **64**.



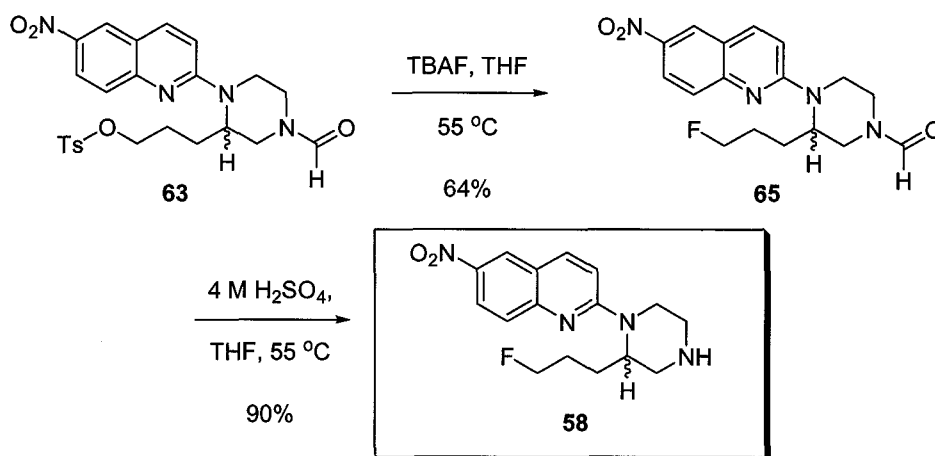
**Scheme 2-17:** Synthesis of N-formyl-ProTos-NQP **63**.

This result was not surprising considering the mixture of products formed during demethylation with  $\text{BBr}_3$ . With NMR analysis it was determined that the reaction gave a 1:1 mixture of tosylate **63** to chloride **64**. The two products could be carefully separated by column chromatography (1:1 EtOAc/ $\text{CHCl}_3$ ). However,

the mixture was typically carried forward to the fluorination step (Scheme 2-17), and extensive purification was undertaken only when the precursor was to be shipped to LBNL for radiofluorination.

## 2.5 Nonradioactive Fluorinations of N-formyl-ProTos-NQP 63.

To investigate the usefulness of **63** as a radiolabeling precursor, trifluoroborate ion substitutions (tetrabutylammonium fluoride, TBAF) and subsequent deprotections (4 M H<sub>2</sub>SO<sub>4</sub>) were performed. We found that N-formyl-ProTos-NQP **63** was readily fluorinated with TBAF in THF at 60 °C. The crude reaction was subsequently concentrated *in vacuo* and then quickly purified by flushing through a silica plug. The N-formyl group was removed using 4 M H<sub>2</sub>SO<sub>4</sub>, at 50 °C, to give the desired fluorinated product PROF-NQP **58** in a 58% yield over 2 steps (Scheme 2-18).

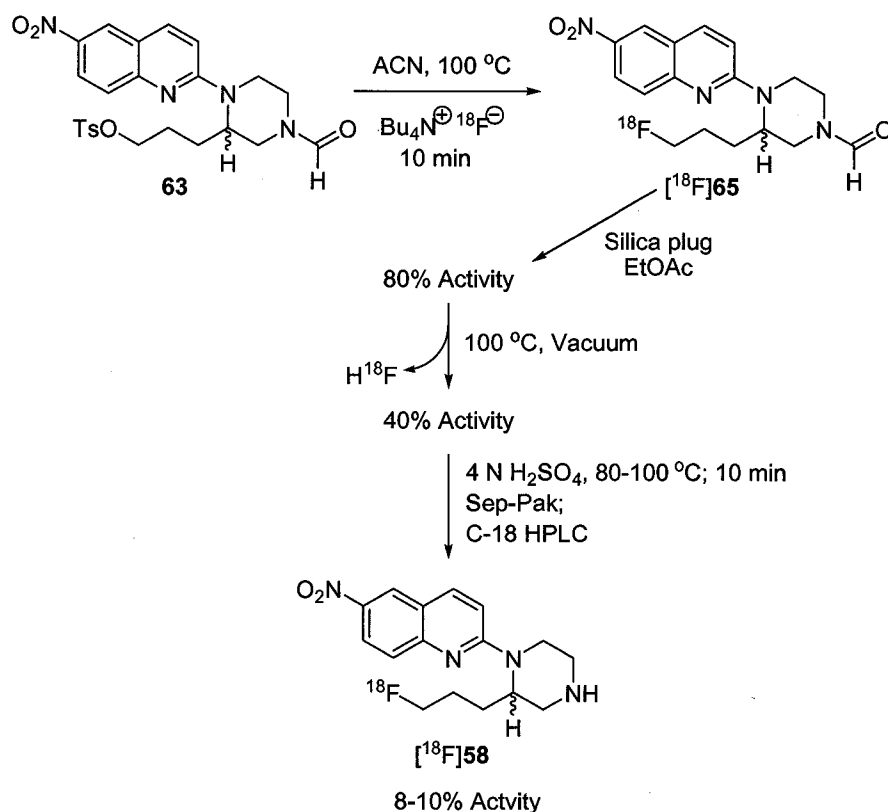


**Scheme 2-18:** Fluorination sequence to prepare PROF-NQP **58**.

With the fluorination and deprotection steps accomplished the tosylate precursor **63** was purified and shipped to our collaborator Dr. O'Neil at LBNL for trial radiofluorination and deprotection.

## 2.6 Radiofluorination of N-formyl-ProTos-NQP **63**.

Based upon successful non-radioactive fluorination of the O-tosylate **63**, the precursor was shipped to LBNL for radiofluorination trials. Outlined in Scheme 2-19, is an overview of the radiofluorination attempts to give [ $^{18}\text{F}$ ]**58**. The synthesis of [ $^{18}\text{F}$ ]**58** was accomplished in 2 synthetic steps from the N-Boc-tosylate precursor **63**.



**Scheme 2-19:** Initial radiofluorination trial using N-formyl-ProTos-NQP **63** to give [ $^{18}\text{F}$ ]**58**.

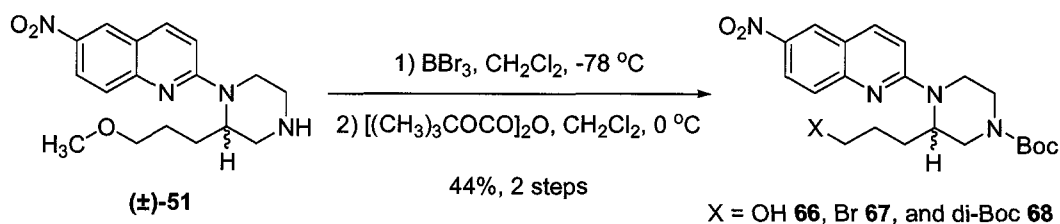
Displacement of the O-tosylate with [ $^{18}\text{F}$ ] is afforded utilizing tetrabutyl ammonium [ $^{18}\text{F}$ ]fluoride ( $\text{TBA}^{18}\text{F}$ ) in acetonitrile (ACN) at 100 °C (80-90% incorporation). After heating the reaction mixture was purified from any inorganic material by elution through a silica plug with ACN, radioactive survey showed 80% activity. Concentration of the eluent under vacuum at 100 °C and subsequent survey showed 40% activity and a 40% loss in activity. The loss of activity was attributed to defluorination of the fluoroalkyl to give  $\text{H}^{18}\text{F}$ . The crude material containing [ $^{18}\text{F}$ ]65 was deprotected with 4 N  $\text{H}_2\text{SO}_4$  at 100 °C, quenched with  $\text{NaOH}(\text{aq})$  and initially purified using a C-18 Sep-Pak, eluting the desired fraction containing [ $^{18}\text{F}$ ]58 with MeOH. Purification of the eluent by semipreparative HPLC (65:35:0.2 MeOH/ $\text{H}_2\text{O}$ / $\text{Et}_3\text{N}$ ) isolated the desired radioactive fraction containing [ $^{18}\text{F}$ ]58 in a 8-10% EOB decay corrected yield.

We were concerned with the large loss in radioactivity when the silica plug eluent was concentrated and during the deprotection of the N-formyl protecting group. It seemed that at high temperatures (80-100 °C) a large amount of  $\text{H}^{18}\text{F}$  was produced. Attempts to circumvent high temperature deprotection conditions (4 N  $\text{H}_2\text{SO}_4$  and 16 M  $\text{H}_2\text{SO}_4$  at ambient temperature, as well as basic deprotection with  $\text{NaOH}$ ) resulted only in incomplete deprotection of [ $^{18}\text{F}$ ]65 to give the desired product [ $^{18}\text{F}$ ]58.

## **2.7 Synthesis of the Precursor N-Boc-ProTos-NQP 69.**

The losses of activity during heating cycles and during deprotection of the N-formyl group lead us to investigate the preparation of a similar precursor with a protecting group that would be removed under more facile conditions. The

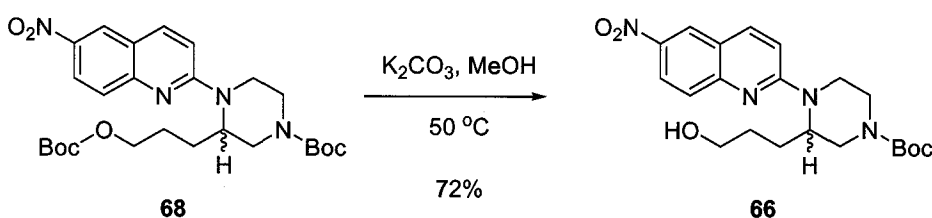
nitrogen protecting group *tert*-butyl carbamate (N-Boc) was used with relative ease in our laboratory as a tool for purifying polar compounds, i.e. HOM-NQP **38** and MOM-NQP ( $\pm$ )-**31**. For example, we had found that deprotection of N-Boc compounds with H<sub>2</sub>SO<sub>4</sub> routinely gave the desired amine product in excellent purity in 5 minutes or less. Using the same BBr<sub>3</sub> procedures as already outlined for MOM-NQP ( $\pm$ )-**31** and N-formyl-PROM-NQP **60** (Scheme 2-16), PROM-NQP ( $\pm$ )-**51** was treated with BBr<sub>3</sub> accordingly and the reaction was quenched and the product was extracted with DCM. The DCM portion was dried, filtered and concentrated to a 5-10 ml volume and an excess of di-*tert*-butyl-dicarbonate was added (Scheme 2-20).



**Scheme 2-20:** BBr<sub>3</sub> methyl ether cleavage of PROM-NQP and subsequent protection as the N-Boc to give N-Boc-HOP-NQP **66**.

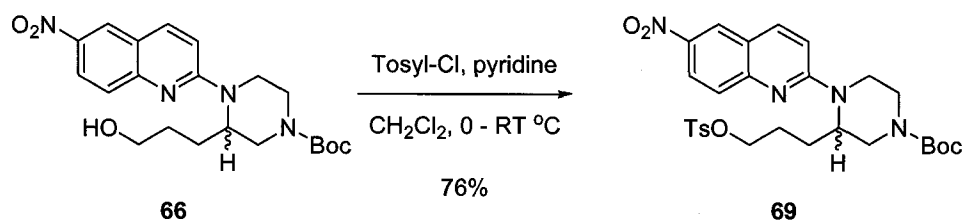
Examination of the crude reaction by TLC after treatment with Boc<sub>2</sub>O showed the expected N-Boc protected alcohol **66** and bromide **67**. However, upon concentrating in vacuo any excess unreacted Boc<sub>2</sub>O reacted with the alcohol group forming the respective carbonate product **68**. Thus, with this reaction workup three products were formed, including the mono-Boc-HOP-NQP **66**, the di-Boc-HOP-NQP **68** and Boc-bromo-NQP **67**. In other experimental attempts when there was a large excess of Boc<sub>2</sub>O used all of the alcohol was protected as the carbonate giving di-Boc-HOP-NQP **68** and the Boc-bromo **67**

in the workup mixture. The presence of the N-Boc made purification of these quipazines very easy (silica gel), where the three products could be separated by column chromatography eluting with a mixture of EtOAc/hexanes. The carbonate group of **68** could then be selectively deprotected over the carbamate moiety by heating to 50 °C in MeOH with an excess of powdered  $K_2CO_3$ , to give the desired N-Boc-HOP-NQP **66** in a 72% yield (Scheme 2-21).



**Scheme 2-21:** Selective cleavage of the undesired Boc carbonate **68**.

The N-Boc protected HOP-NQP **66** could then be tosylated in a similar fashion to the N-formyl case, giving N-Boc-ProTos-NQP **69** in a 76% yield (Scheme 2-22). However, the reaction conditions were improved to limit the amount of propyl chloride side product formed, by simply increasing the amount of pyridine to 600 mol% and tosyl chloride to 420 mol%.



**Scheme 2-22:** Tosylation of N-Boc-HOP-NQP to give the fluorination precursor N-Boc-ProTos-NQP **69**.



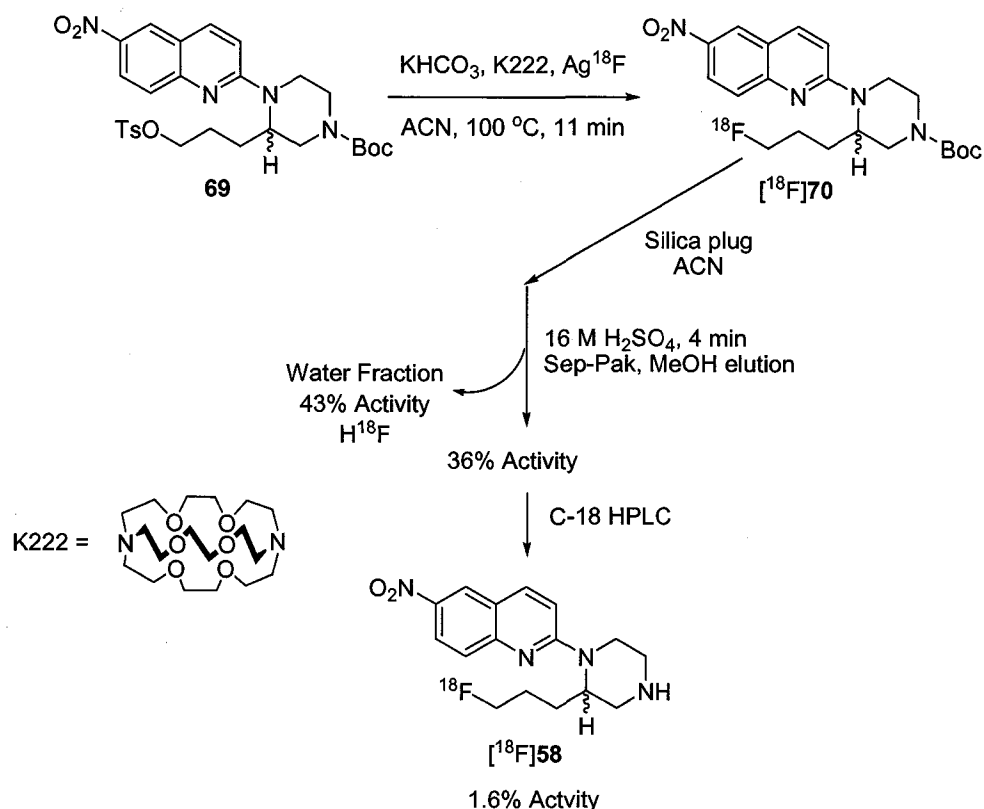


alkene. However, the polar side product to date has not been formally isolated to determine its identity.

## **2.8 Radiofluorination Attempts of N-Boc-ProTos-NQP 69.**

After the successful preparation of nonradioactive PROF-NQP **58** by utilizing the nitrogen protecting group Boc, we shipped the tosylated precursor **69** to LBNL for further [ $^{18}\text{F}$ ] fluorination attempts. Two separate fluorination methods were attempted. The first trial, as outlined in Scheme 2-24, used Kryptofix 222 (K222),  $\text{KHCO}_3$ ,  $\text{Ag}^{18}\text{F}$  in ACN at 100 °C, followed by Boc deprotection ( $\text{H}_2\text{SO}_4$ ) and purification. The second trial outlined in Scheme 2-25 was attempted according to the N-formyl case (Scheme 2-19) utilizing  $\text{TBA}^{18}\text{F}$  in ACN at 100 °C, and similarly deprotected.

## 2.9 Radiofluorination Attempts with K222, KHCO<sub>3</sub> and Ag<sup>18</sup>F.

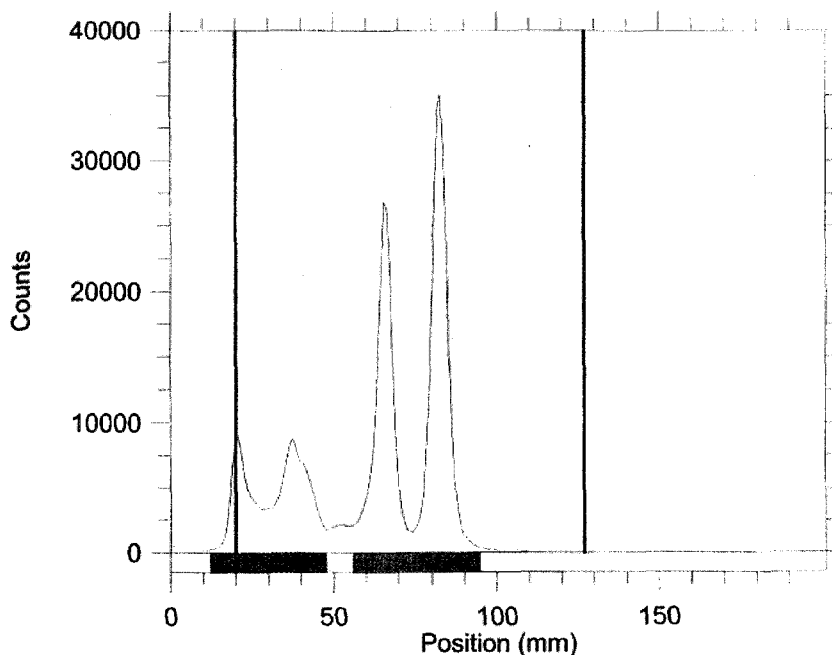


**Scheme 2-24:** Radiofluorination sequence utilizing K222, KHCO<sub>3</sub>, and Ag<sup>18</sup>F with the precursor N-Boc-ProTos-NQP **69**.

As outlined in Scheme 2-24, a dry solution of K222, KHCO<sub>3</sub>, and Ag<sup>18</sup>F in ACN was prepared in a 4 mL vial and transferred to a vial containing a solution of tosylate **69** in ACN. The reaction mixture was heated at 100 °C for 11 min and then cooled on ice. The cooled reaction mixture was treated directly with H<sub>2</sub>SO<sub>4</sub> (16 M) to deprotect [<sup>18</sup>F]**70**, after 4 min the deprotection was quenched by adding to a dilute solution of NaOH (1%), and loaded onto a C-18 SepPak. The SepPak was washed with water and radioactive survey showed 43% activity in the wash. The desired fraction eluted from the SepPak with methanol afforded the fraction containing [<sup>18</sup>F]**58** with 36% activity. Further purification of the SepPak eluent by semi-preparative reverse phase HPLC (65:35:0.2 MeOH/Water/TEA) gave the

desired fraction (eluting at 7.6-9.5 min) containing [ $^{18}\text{F}$ ]58, radioactive survey showed 1.6% activity. Analytical HPLC (70:30 MeOH/0.17 M  $\text{NH}_4\text{CO}_2\text{H}$ , 0.5% AcOH) confirmed the product eluting at 4.6 min. The synthesis was successful in generating the desired radiolabelled product [ $^{18}\text{F}$ ]58 in a 1.6% EOB decay corrected yield. However, the yield was considerably lower than earlier trials using the N-formyl protecting group (8-10% EOB decay corrected yield, Scheme 2-19).

A second fluorination attempt was made using the same procedure outlined above (Scheme 2-24). However, TLC analysis of the initial fluorination was performed to determine if incorporation of the radionuclide was giving the expected product [ $^{18}\text{F}$ ]70. As before, a dry solution of K222,  $\text{KHCO}_3$ , and  $\text{Ag}^{18}\text{F}$  in ACN was prepared in a 4 mL vial, treated with a solution of tosylate 69 in ACN, heated at 100 °C for 11 min and then cooled. The crude mixture was purified by elution through a silica plug with ACN. Radioactive TLC analysis showed the presence of two radioactive products eluting close to the expected product [ $^{18}\text{F}$ ]70  $R_f$ ; product one,  $R_f = 0.422$  and product two,  $R_f = 0.584$  (2:3 EtOAc/hexanes) (Figure 2-7). We were concerned with the presence of two radioactive products and decided that returning to the original conditions (TBA $^{18}\text{F}$ ) attempted with the N-formyl case (Scheme 2-19) would be beneficial.



### Region Analysis

Definition: Table

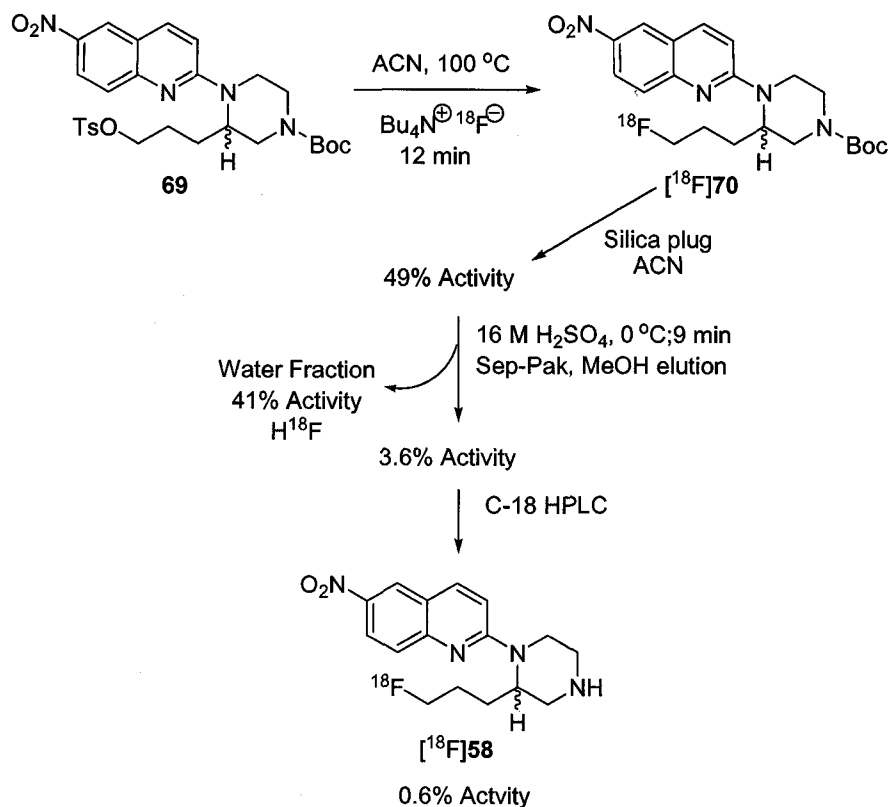
Reg	(mm) Start	(mm) Stop	(mm) Centroid	RF	Region Counts	Region CPM	% of Total	% of ROI
Rgn 1	12.2	29.6	22.2	0.020	75911.0	15182.2	11.63	11.95
Rgn 2	28.7	47.9	37.8	0.167	114717.0	22943.4	17.58	18.06
Rgn 3	55.7	74.0	65.1	0.422	194335.0	38867.0	29.78	30.59
Rgn 4	73.2	94.9	82.5	0.584	250245.0	50049.0	38.35	39.40
4 Peaks					635208.0	127041.6	97.33	100.00

**Figure 2-7:** Radioactive TLC analysis after initial fluorination and silica purification of the K222 radiofluorination trial, showing two possible Boc protected fluorinated products.

### 2.10 TBA<sup>18</sup>F Radiofluorination Attempts.

As outlined in Scheme 2-25, a solution of the tosylate **69** in ACN was treated with a solution of TBA<sup>18</sup>F in dry ACN and the reaction was heated at 100

°C for 12 min. The reaction was cooled and flushed through a silica plug with acetonitrile, with the desired fraction having 49% activity by radioactive survey. Analysis of the silica plug eluent by radioactive TLC (3:2 EtOAc/hexanes) showed one major spot ( $R_f = 0.59$ ) and one minor spot ( $R_f = 0.48$ )(Figure 2-9). The eluent was treated with  $H_2SO_4$  (16 M) at 0 °C for 9 min, quenched by dilution into 1% NaOH (30 mL), and loaded onto a C-18 SepPak. The water flush contained 41% of the radioactivity, and elution of the SepPak, to isolate the product fraction, contained 3.6% of the original radioactivity. At this point we were already at a lower possible yield of [ $^{18}F$ ]**58** than the N-formyl trials utilizing TBA $^{18}F$  or the K222 trial with the N-Boc-ProTos-NQP **69** precursor (Scheme 2-24). Purification of the SepPak methanol eluent by HPLC gave the desired peak [ $^{18}F$ ]**58** eluting at 8.5-9 min with 0.6% EOB decay corrected yield.



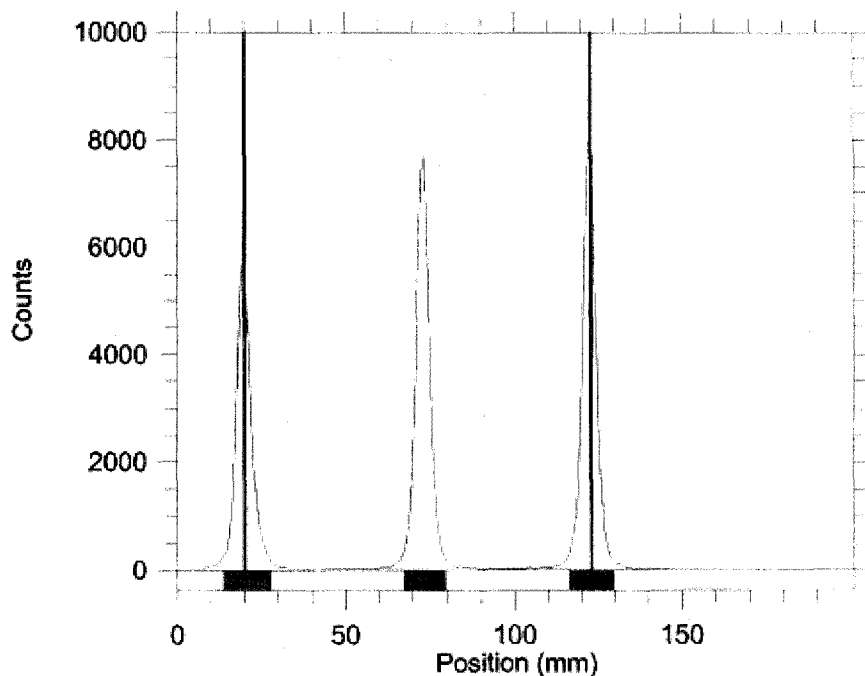
**Scheme 2-25:** Radiofluorination sequence utilizing TBAF.

A second trial was performed and the reaction process was stopped after silica gel purification of the fluorination mixture (Scheme 2-25). Again we analyzed the purified reaction mixture by radioactive TLC. Included on the TLC plate was a lane for the nonradioactive standard **70** and a lane for the silica gel eluent expected to contain [ $^{18}\text{F}$ ]70. This allowed us a direct comparison of [ $^{19}\text{F}$ ]58 and [ $^{18}\text{F}$ ]58 and any other radiofluorinated Boc protected compounds. To enable direct comparison, the solvent front, baseline and UV active spot corresponding to [ $^{19}\text{F}$ ]58 were spotted with a sample of radiation to enable the use of the radioactive TLC analyzer. The TLC analysis of the nonradioactive standard [ $^{19}\text{F}$ ]70 is shown in Figure 2-8. From the nonradioactive lane we determined that the desired product [ $^{18}\text{F}$ ]70 should have an  $R_f = 0.516$ . Figure

2-9 shows the second lane containing the silica gel plug ACN eluent. Comparison of the two TLC lanes shows the desired product is only 20% of the mixture. The other TLC spot was 54% of the mixture ( $R_f = 0.631$ ), could be a second fluorination product with a similar elution profile as the desired product.

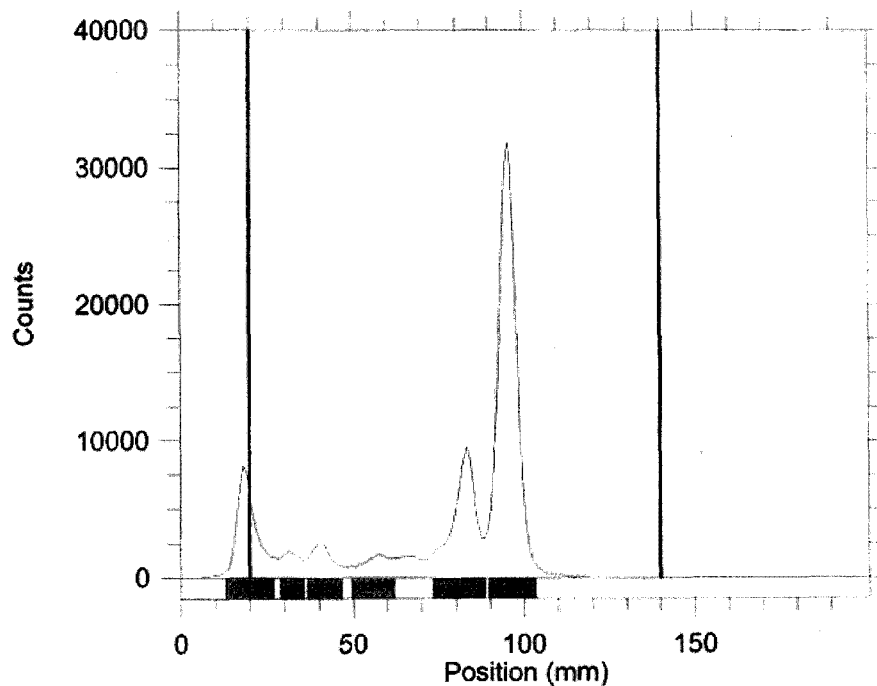
Producing only 20% of the desired product [ $^{18}\text{F}$ ]70 during the fluorination attempt, helps to explain why we were only able to produce 0.6% of the desired labelled compound in the first TBA  $^{18}\text{F}$  trial. Additionally if the compound is labile to acidic conditions as we saw in the N-formyl case, then treatment of the ACN eluent from the silica gel plug would likely cause a further decrease in the yield of [ $^{18}\text{F}$ ]58.





Reg	(mm) Start	(mm) Stop	(mm) Centroid	RF	Region Counts	Region CPM	% of Total	% of ROI
Rgn 1	13.9	27.8	20.0	0.000	34897.0	34897.0	27.27	28.68
Rgn 2	67.1	79.3	72.7	0.512	42461.0	42461.0	33.19	34.90
Rgn 3	116.7	129.8	122.7	0.997	44307.0	44307.0	34.63	36.42
3 Peaks					121665.0	121665.0	95.09	100.00

**Figure 2-8:** Radioactive TLC analysis of the N-Boc-PROF-NQP 70, co-spotted with radiation at the baseline, front and on the product spot to allow for direct comparison to the radiofluorination attempt.



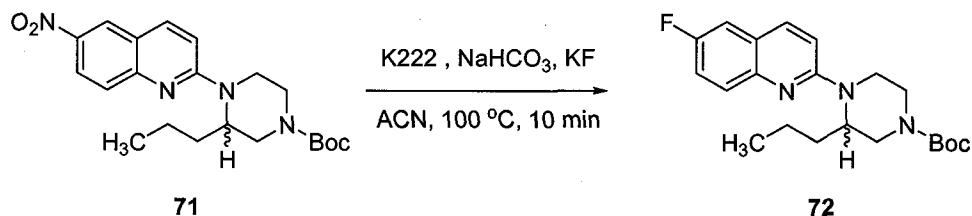
Reg	(mm) Start	(mm) Stop	(mm) Centroid	RF	Region Counts	Region CPM	% of Total	% of ROI
Rgn 1	13.0	27.0	19.5	-0.004	57689.0	11537.8	12.58	13.62
Rgn 2	28.7	35.7	31.7	0.098	13149.0	2629.8	2.87	3.10
Rgn 3	36.6	47.0	40.9	0.174	21546.0	4309.2	4.70	5.09
Rgn 4	49.6	61.8	56.0	0.300	17967.0	3593.4	3.92	4.24
Rgn 5	73.2	88.8	81.9	0.516	84204.0	16840.8	18.37	19.88
Rgn 6	89.7	103.7	95.7	0.631	229100.0	45820.0	49.97	54.08
6 Peaks					423655.0	84731.0	92.40	100.00

**Figure 2-9:** Radioactive TLC analysis of the fluorination of **69** after silica gel purification. Two products are visible with the smaller eluting at the same  $R_f$  as **70**.

### 2.11 Fluorination Control Reactions.

To explain the second fluorinated product observed in the K222 and TBA<sup>18</sup>F radiofluorination attempts we set out to attempt to reproduce the results in our lab. It was hypothesized that at the high temperature of the fluorination reaction that nucleophilic aromatic substitution ( $S_NAr$ ) could occur. To determine

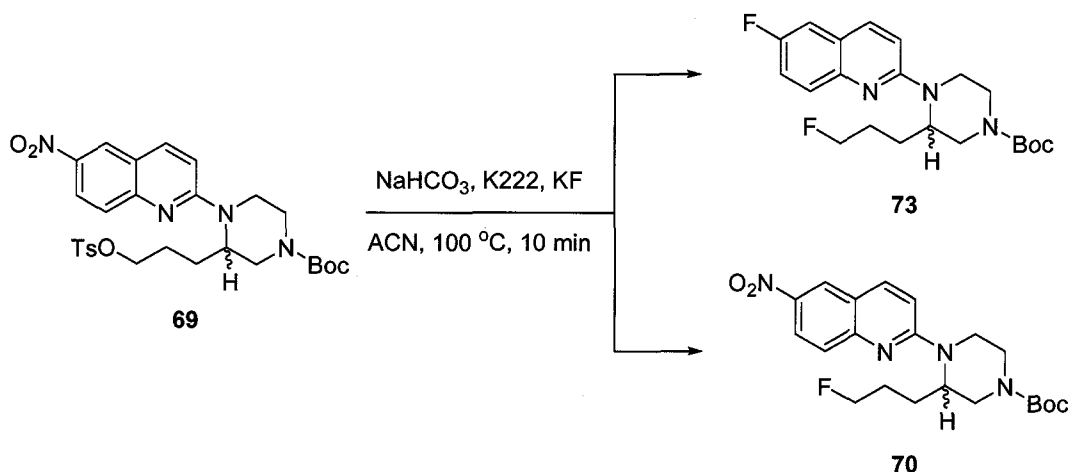
if the aromatic system of the 2-(2-alkyl-piperazin-1-yl)-6-nitroquinolines was susceptible to fluoride attack, N-Boc-*n*-PROP-NQP **71** was used as a test ligand. Outlined in Scheme 2-26 is the nonradioactive control reaction with **71**. Treatment of **71** with NaHCO<sub>3</sub> (600 mol%), K222 (1000 mol%) and KF (800 mol%) and heating at 100 °C for 10 min produced a new spot by TLC ( $R_f = 0.44$ , 3:2 EtOAc/hexanes), purification by silica gel pipette column (2:3 EtOAc/hexanes) the fluoride substitution product **72** was isolated in a 25% yield. Proton NMR of the new product shows a distinct change in the aromatic system that is consistent with substitution at the quinoline 6-position.



**Scheme 2-26:** Trail nucleophilic fluorine substitution of N-Boc-*n*-PROP-NQP **71**.

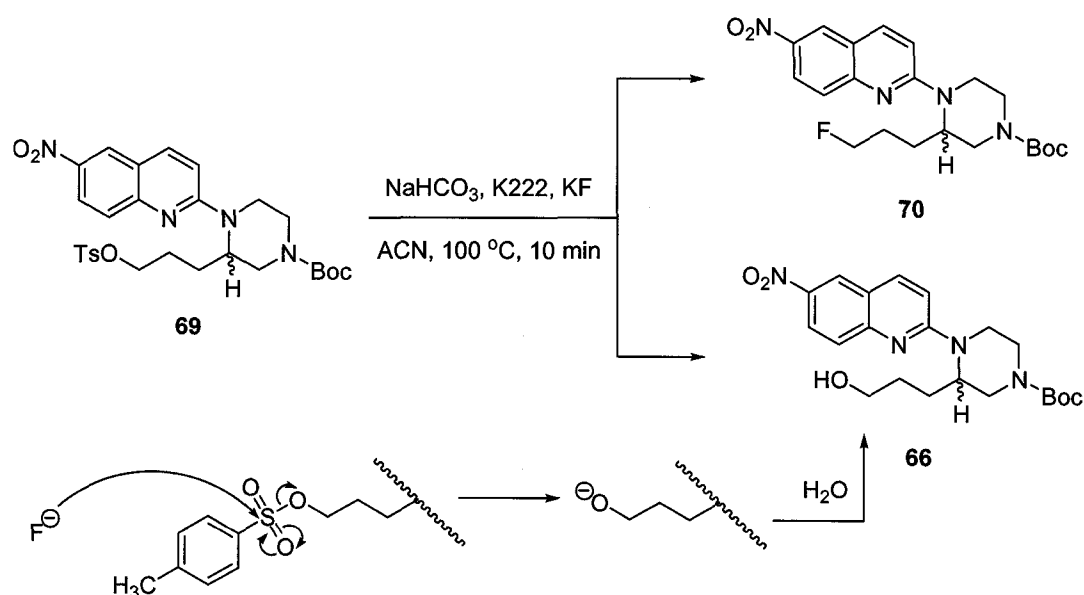
With successful incorporation of a fluoride atom onto the 2-(2-alkyl-piperazinyl)-6-nitroquinoline system we looked to repeat the results using the radiolabeling precursor **69** in two separate control reactions. Scheme 2-27 describes the fluorination control reaction according to the procedure used with the N-Boc-*n*-PROP-NQP **71** control reaction. Accordingly, **69** was heated as a solution in ACN at 100 °C for 10 min with K222 (1000 mol%), NaHCO<sub>3</sub> (600 mol%), and KF (1000 mol%). This gave two products by TLC analysis and separation of the products was afforded using silica gel chromatography (2:3 EtOAc/hexanes). NMR analysis of the more nonpolar product ( $R_f = 0.5$ , 3:2 EtOAc/hexanes) suggests the product is the result of nucleophilic fluoride

substitution of the tosylate in addition to the aromatic substitution to give **73**. The more polar product ( $R_f = 0.4$ , 3:2 EtOAc/hexanes) by NMR comparison to standards is the expected fluorination product N-Boc-PROF-NQP **70**.



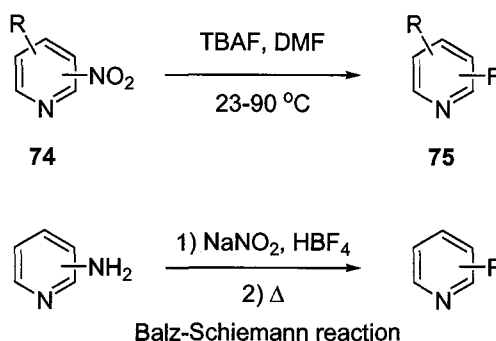
**Scheme 2-27:** Trial nucleophilic fluorine substitution with an excess of KF.

We were then interested as to what a control reaction would give using the ratios resembling the radiolabeling protocol (K222 (1000 mol%), NaHCO<sub>3</sub> (600 mol%), but KF (50 mol%)) was used as a limiting reagent (Scheme 2-28). Using the same procedures outlined above tosylate **69** was heated at 100 °C for 10 min, giving two products by TLC analysis of the crude reaction. The products were purified by silica gel pipette column (1:3 EtOAc/hexanes to elute **70**, and 3:2 EtOAc/hexanes to elute **66**) and analyzed by NMR. The product with an  $R_f$  of 0.55 was N-Boc-PROF-NQP **70**, the more polar product ( $R_f = 0.2$ ) is the result of nucleophilic fluoride attack at the sulfur of the tosyl group to give the alcohol **66**.



**Scheme 2-28:** Trail nucleophilic fluorine substitution using KF as a limiting reagent.

Based upon the fluorination control reactions it seems likely that the difluoro species **73** is the anomalous radiofluorinated product observed during the  $\text{TBA}^{18}\text{F}$  and  $\text{Ag}^{18}\text{F}$  radiofluorinations. As shown in Scheme 2-29, TBAF has been used with successfully to displace aromatic nitro groups in the preparation of fluoro-substituted pyridines **75** from 2, 3, and 4 nitropyridines **74**, and as an alternative for the Balz-Schiemann reaction (Scheme 2-29).<sup>84</sup> Additionally, the use of KF has been also been shown to give aromatic substitution by fluorodenitration of nitropyridines.<sup>85</sup> In order to determine if the difluoro **73** is the unknown product of radiofluorination a standard sample would need to be sent to LBNL, the radiofluorination attempted again and isolation of the side product for HPLC comparison completed.



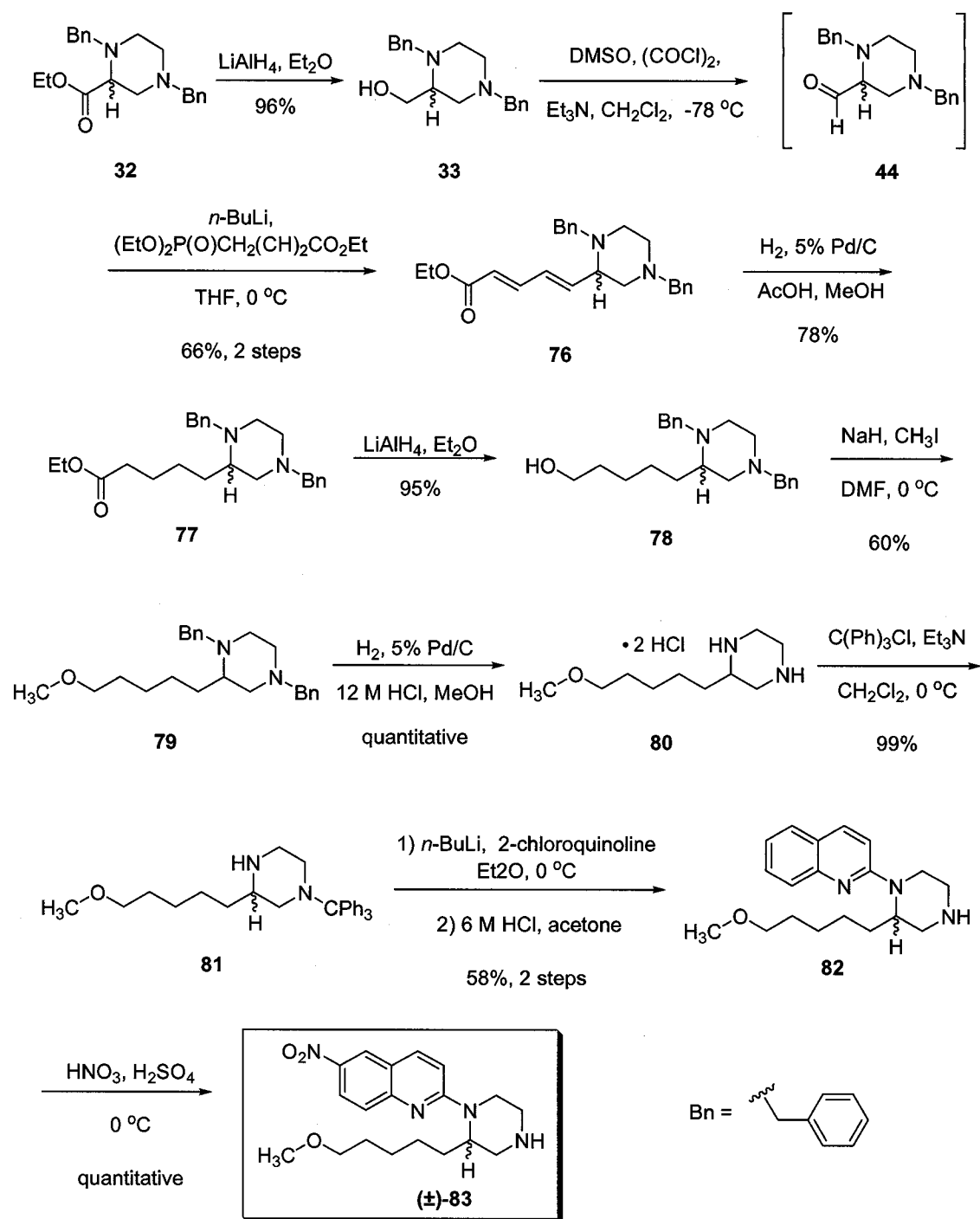
**Scheme 2-29:** Example fluoride aromatic nucleophilic substitution of nitropyridines using TBAF.

Based upon the three trial radiofluorinations, it is likely that the N-formyl precursor **63** would be more suited for the preparation of the radioligand PROF-NQP **58**. The N-formyl case resulted in a much higher yield (8-10% EOB decay corrected yield) of [ $^{18}\text{F}$ ]**58** compared to either fluorinations using the Boc precursor **69**. In addition to a better radiofluorination yield the preparation of the N-formyl tosylate precursor **63** is far more facile to produce, especially considering the nitrogen protecting group (N-CHO) is in place before borontribromide cleavage of the ether. Also,  $\text{BBr}_3$  demethylation of the N-formyl-PROM-NQP **60** is more consistent than the Boc series (Scheme 2-22). With the improvements of the tosylation conditions the likelihood of generating the chloride side product **64** (Scheme 2-17) is diminished, thus improving the tosylate yield and eliminating the need for cautious purification of **63**.

## 2.12 Synthesis Pent-NQP ( $\pm$ )-**83** and PentF-NQP **88**.

As shown in Scheme 2-30 the universal starting material ester **32** for our quipazine syntheses was reduced by  $\text{LiAlH}_4$  to give the alcohol **33** in 96% yield. Swern oxidation of the alcohol followed Horner-Emmons olefination furnished the

unsaturated ester **76** in a 66% over 2 steps. Catalytic hydrogenation at atmospheric pressure with 5% Pd/C in MeOH and acetic acid gave the saturated ester **77** in 78% yield. The ester was reduced with LiAlH<sub>4</sub> to give the pentyl alcohol **78** (95%). Subsequently, the alkoxide was generated with NaH in DMF and alkylated with iodomethane to give **79** in a 60% yield. Hydrogenolysis of the benzyl groups utilizing 5% Pd/C in MeOH and HCl gave the pentyl piperazine dihydrochloride **80** (quantitative yield), which was protected at the least hindered amine with trityl chloride to give the N-trityl piperazine **81** (99%). The protected piperazine was coupled to 2-chloroquinoline using the typical Gilman coupling and subsequent deprotection with 6 M HCl in acetone gave the pentyl quipazine **82** (58%, 2 steps). Selective nitration with HNO<sub>3</sub> in sulphuric acid gave the desired 2-pentyl-nitroquipazine (**±**)-**83** (quantitative yield). Together, (**±**)-**83** was afforded in 11 steps in an overall yield of 16%.

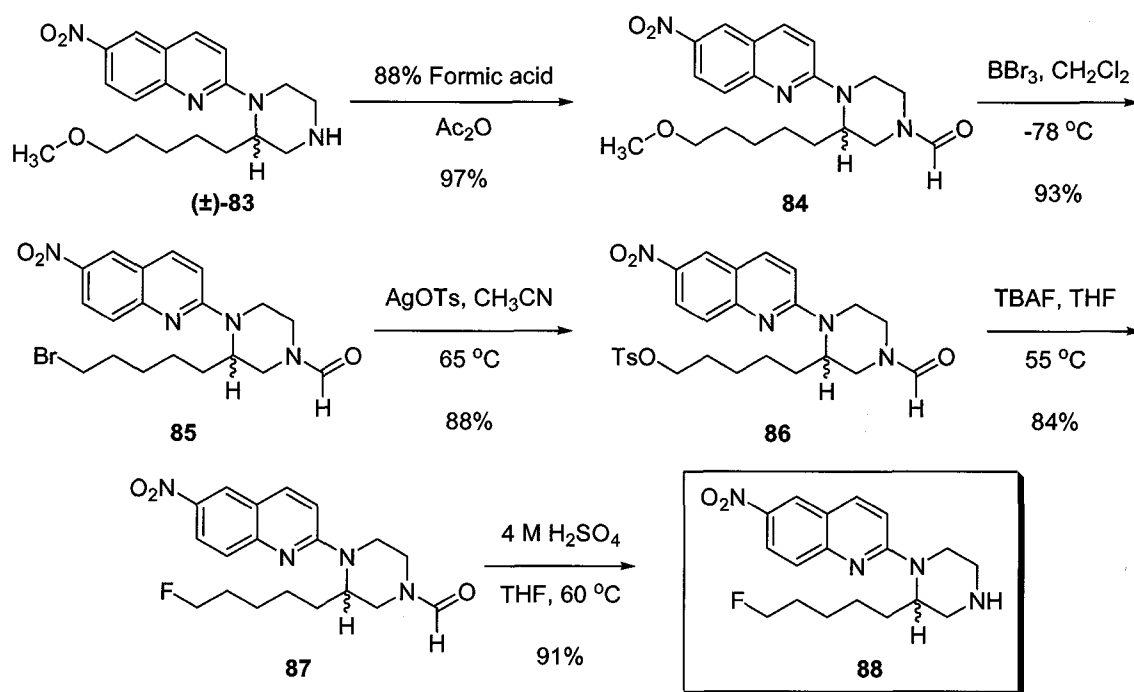


**Scheme 2-30:** Overall synthesis of Pent-NQP ( $\pm$ )-83.

The free amine of Pent-NQP ( $\pm$ )-83 was protected as the N-formyl according to the procedures described in the propyl synthesis (Scheme 2-31) to give **84** in a 97% yield. Treatment with  $\text{BBr}_3$  to generate the desired alcohol for



subsequent tosylation, only gave the bromide product **85** in a 93% yield. To generate the tosylate from the bromide a new technique was used. We found that the pentyl bromide could be transformed to the tosylate **86** by treatment with silver tosylate (AgOTs),<sup>86</sup> in a Finkelstein-like reaction. For this reaction, the nucleophilic O-tosylate group displaces the bromide affording the AgBr solid. Treatment of N-formyl-PentBr-NQP **85** with an excess of AgOTs at 50-60 °C gave the desired tosylate **86** in a 88% yield. Fluoride ion displacement of tosylate **86** was accomplished using TBAF conditions developed for the propyl series to give **87** in a 84% yield. Subsequent N-formyl deprotection with 4 M H<sub>2</sub>SO<sub>4</sub> at 50 °C gave **88** (91%). To date, no further work has been attempted to examine radiofluorination of **86**.

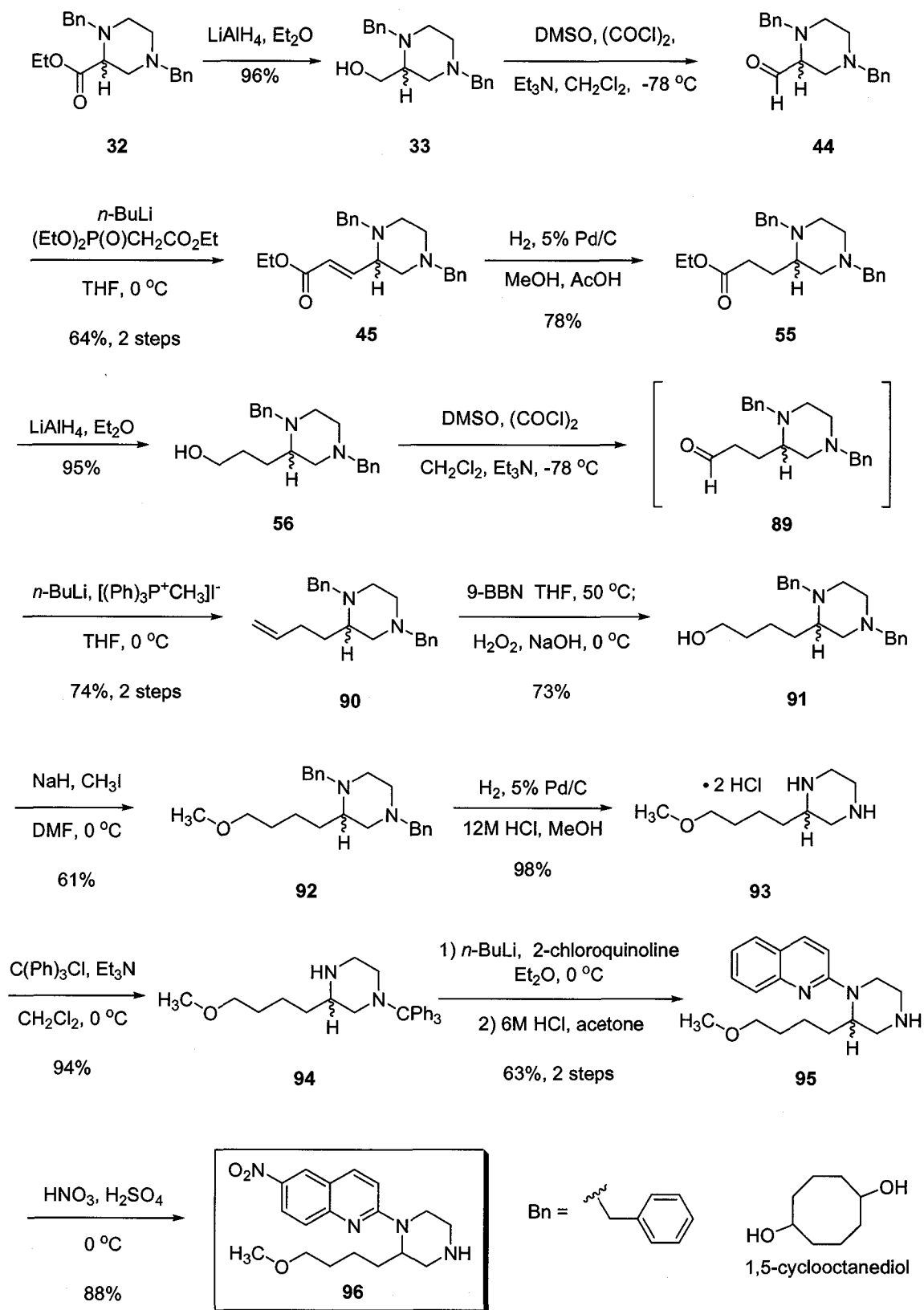


**Scheme 2-31:** Synthesis of PentF-NQP **88**.

### 2.13 Synthesis of BuM-NQP 96.

The BuM-NQP analog **96** was synthesized from the common dibenzyl starting material **32** according to Scheme 2-32. The dibenzyl alcohol **33** was oxidized by Swern oxidation, followed by Horner-Emmons olefination (64%, 2 steps) to give the  $\alpha,\beta$ -unsaturated ester **45**. The alkene of **45** was reduced with  $H_2$  and 5% Pd/C (78%), then the ester **55** was reduced with  $LiAlH_4$  to provide the propyl alcohol **56** (95%). Swern oxidation of **56** gave the aldehyde **89** and subsequent Wittig olefination with ethyltriphenylphosphonium bromide gave the butylene **90** in 74% yield over 2 steps. The butyl alcohol **91** was prepared by hydroboration of **90** with 9-BBN followed by oxidation gave **91** in a 73% yield. *At this stage we found that careful purification of the dibenzyl alcohol away from any 1,5-cyclooctanediol (see inset) that is generated after quenching of the borane reagent was necessary.* If **91** is not carefully purified by chromatography, the following methylation reaction results in a much lower yield (6-10%). We found that monitoring the column chromatography of the alcohol product by TLC and staining with vanillin aided in determining the presence of the 1,5-cyclooctanediol.

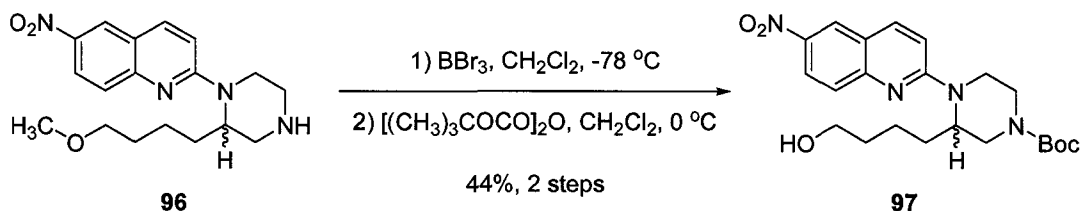
After purification, the alcohol **90** was methylated with iodomethane (DMF, NaH, 61%). The benzyl groups were cleaved catalytically with  $H_2$  and 5% Pd/C to give the desired piperazine hydrochloride **93** in 98% yield. The least hindered amine of the piperazine was protected as the N-trityl and the protected piperazine **94** (94%).



**Scheme 2-32:** Overall synthesis of BuM-NQP **96**.

The trityl piperazine was coupled to 2-chloroquinoline according to the method of Gilman. Deprotection gave **95** in a 63% yield (2 steps). Selective nitration at the 6-position of the quinoline ring gave the desired methoxybutyl piperazine **96** in 88% yield. The BUM-NQP target ligand was prepared from the dibenzyl ester **32** in 14 steps in an overall 7.7% yield.

The Boc protected alcohol N-Boc-BuOH-NQP **97** was prepared from BuM-NQP **96** by treatment with  $\text{BBr}_3$ , treatment of the crude workup mixture with di-*tert*-butyl-dicarbonate gave **97** in a 44% overall 2 step yield (Scheme 2-33). The N-Boc-BuOH-NQP intermediate is ready for tosylation and subsequent fluorination when needed.



**Scheme 2-33:** Synthesis of N-Boc-BuOH-NQP **97**.

## 2.14 Summary and Conclusion.

The syntheses of new 2-(2-alkyl-piperazin-1-yl)-6-nitroquinolines have been described, including PROM-NQP ( $\pm$ )-**51**, PROF-NQP **58**, Pent-NQP ( $\pm$ )-**83**, PentF-NQP **88**, and BuM-NQP **96**. The syntheses of these analogs has furthered our SERT SAR study by expanding upon the lead compound 6-NQP **22**. We are interested how the 2-alkyl-piperazine substitutions affect SERT binding affinity, particularly to probe the Ar2 binding domain described by the pharmacophore model. The in vitro competitive binding studies of a select group

of the ligands prepared here is described in Chapter 4. Furthermore, the PROM-NQP ( $\pm$ )-51 ligand was useful in the preparation of two radiofluorination precursor N-formyl-ProTos-NQP **63** and N-Boc-ProTos-NQP **69**. The synthesis of the precursors **63** and **69**, along with the initial nonradioactive and radioactive fluorinations were used as foundational synthetic sequences and radiofluorination experiments for the analogous radioligand MePROF-NQP **148**.<sup>74</sup> The initial radiofluorination results with the N-formyl-ProTos-NQP **63** suggests that [<sup>18</sup>F]PROF-NQP **58** is a plausible PET radioligand. The radiosynthesis using **63** should be revisited now that we have more knowledge from the N-Boc-ProTos-NQP **69** radiolabeling trials. There is more work to be accomplished in understanding the major side product formation from the N-Boc-ProTos-NQP **69** radiolabelling trials. It would be very intriguing to determine if fluoride substitution of the aromatic nitro group is really occurring. If indeed there is aromatic fluoride substitution occurring, perhaps a second generation of our compounds could be prepared that possesses a dual fluorine-18 label.

## Chapter 3

### Synthesis of Asymmetric Targets

#### 3.1 Chiral Nitroquipazine Ligand Studies.

Described in this chapter are the chiral syntheses of 6-NQP SERT analogs previously prepared in racemic form, including, MOM-NQP ( $\pm$ )-**31**, PROM-NQP ( $\pm$ )-**51** and Pent-NQP ( $\pm$ )-**83**. The chiral syntheses utilize the amino acids glycine, serine and glutamate to form the piperazine ring structures. The use of the optically pure forms of serine and glutamate eliminates the need for later separation of a racemic mixture by HPLC or diastereomeric salt formation. Chiral pharmaceuticals are commonplace in the drug industry. A number of commonly used drugs are sold as the racemic mixture, including ibuprofen (Advil), citalopram HBr ( $\pm$ )-**7** (Celexa), cetirizine HCl **99** (Zyrtec), methylphenidate **100** (Ritalin), and fluoxetine HCl **10** (Prozac) (Figure 3-1). The application of chiral drug development as well as “chiral switches”<sup>87</sup> (the development of chiral drugs from their racemic mixture) has become a major focus to industry as more studies show the importance of stereoisomer distinction within many pharmacological therapies.<sup>88,89</sup> Of the racemates mentioned above (**98**, ( $\pm$ )-**7**, **99**, **100**) all except fluoxetine **10** are currently licensed to be sold as their more potent or preferred enantiomeric form under new brand names. The benefits of producing enantiomerically pure forms of a racemic drug include diminished side effects, reduction in dose, among other features. For example, the active form of

ibuprofen, (S)-ibuprofen has a markedly faster onset of action than the racemic form and is currently licensed in Austria and Switzerland.

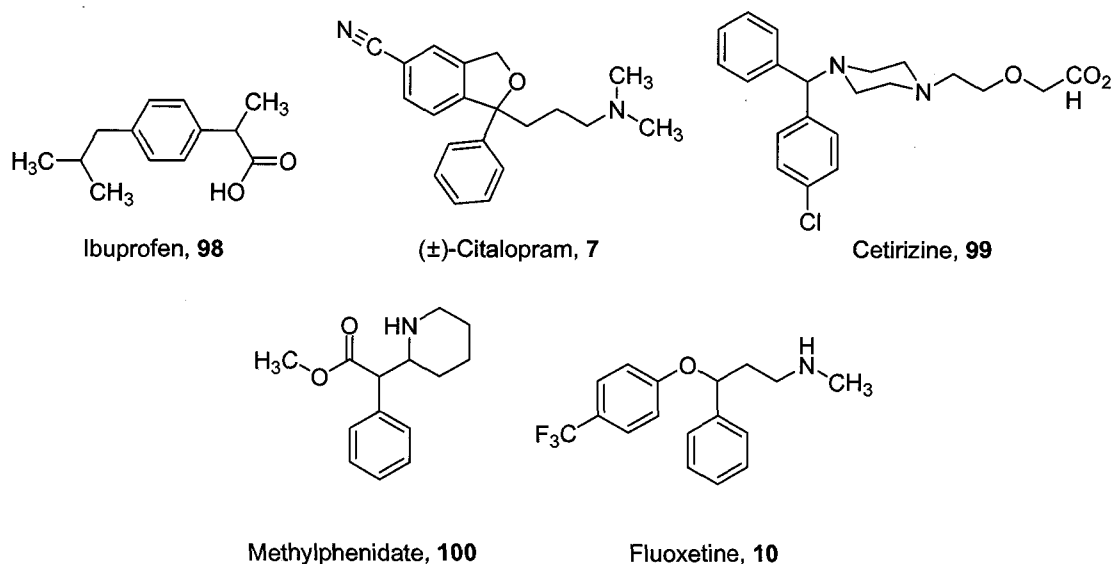
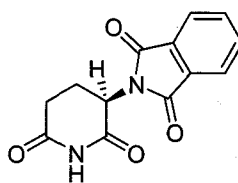


**Figure 3-1:** Example commercial drugs sold as a racemic mixture.

One of the most historically noteworthy examples on the differences between enantiomeric drug forms is that of thalidomide. In the early 1960's the racemic form of thalidomide was given to pregnant mothers during their first trimester of pregnancy as a sedative. Sadly, it was later determined that thalidomide resulted in the birth of 'thalidomide babies' that were characterized by incomplete or missing arms and legs. The discovery of thalidomide birth defects lead to the removal of the drug from use. It was later proposed that the teratogenic properties of thalidomide were attributed only to the (*R*)-(+)-thalidomide enantiomer **101** (Figure 3-2).



(*R*)-(+)-Thalidomide, **101**

**Figure 3-2:** Sedative (*R*)-(+)-Thalidomide **101** found to cause birth defects.

The work with the chiral forms of fluoxetine **10** and citalopram **7** are especially interesting for our research. The difference in binding potency to the SERT target for their enantiomers suggests that the synthesis of chiral analogs of our 2-(2-alkyl-piperazin-1-yl)-6-nitroquinolines may result in more potent and selective agents. Each enantiomer of fluoxetine **10** have progressed through phase II clinical development for their separate pharmacological actions; (*R*)-fluoxetine **10** for its antidepressant qualities and associated fast tissue washout and (*S*)-fluoxetine **10** for the prevention of migraines. Particularly interesting is the enantiomer (*S*)-citalopram **7** (escitalopram) that is ~150 times more potent than the enantiomer (*R*)-citalopram **7** for rat SERT (rSERT)<sup>90</sup> and ~30 times more potent for human SERT (hSERT).<sup>90,91</sup>

### 3.2 Chiral Piperazine Syntheses.

As in many pharmacologically active agents, including the 2-(2-alkyl-piperazin-1-yl)-6-nitroquinolines we have prepared, the racemic qualities of the ligand is due to alkyl-substitutions of the piperazine ring. The piperazine ring system is an integral part of a number of biologically active ligands, that include:  $\sigma$ -receptor agents,<sup>92</sup>  $\kappa$ -opioid receptor antagonists,<sup>93</sup> farnesyltransferase inhibitor,<sup>94</sup> and an H1-receptor antagonist.<sup>95</sup> Considering the selectivity of



receptors for specific piperazine ring ligand enantiomers, the synthesis of enantiomerically pure piperazine ring structures is important.

A brief review of the literature found multiple articles focusing on the preparation of chiral piperazine rings for a number of pharmacological ligands. The literature includes diastereomeric salt formation,<sup>96,97</sup> the use of chiral building blocks i.e. amino acids,<sup>92-94,98</sup> diastereoselective hydrogenation,<sup>99</sup> and kinetic resolutions with bacterial cells and enzymes.<sup>100,101</sup> Of particular interest to our group was the preparation of chiral piperazines utilizing amino acids as the chiral building blocks (Figure 3-3).<sup>93,94,98</sup>

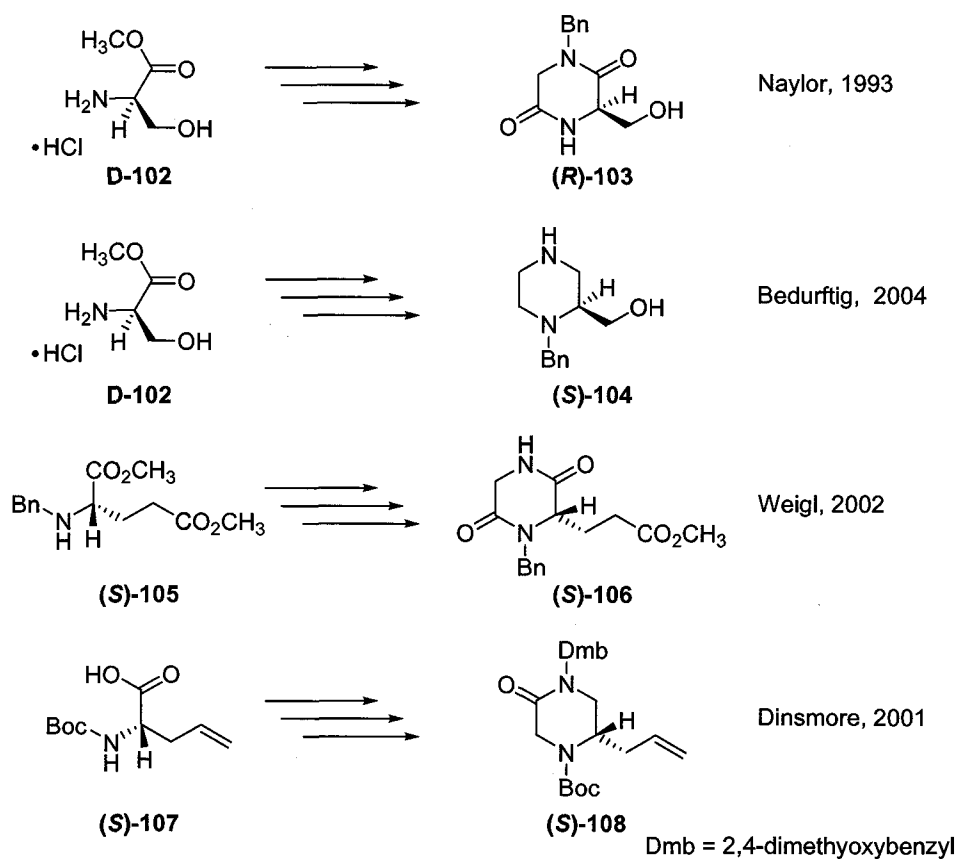


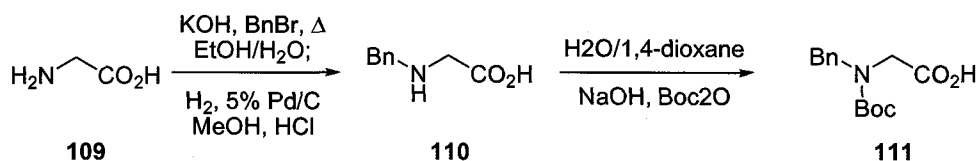
**Figure 3-3:** Potential chiral piperazine syntheses utilizing amino acid building blocks.

### 3.3 Synthesis of Chiral MOM-NQP 31.

The rSERT binding potency ( $K_i$ ) of the racemic forms of Me-NQP ( $\pm$ )-30, MOM-NQP ( $\pm$ )-31, and PROM-NQP ( $\pm$ )-51, and also the evidence of preferred transporter binding site selectivity for enantiomerically pure ligands (escitalopram (**S**)-10) led us to investigate the synthesis and biological potencies of the related enantiomers for our ligand series. The synthesis of (**R**)-30 and (**S**)-30 were accomplished utilizing the commercially available (*R*)- and (*S*)-2-methylpiperazine hydrochloride salts (Sigma Aldrich), according to procedures used in the Gerdes laboratory (Scheme 1-3).<sup>72</sup> Attempts at preparing the (*R*)- and (*S*)-2-methoxymethyl-piperazine diastereomeric salts using D- and L-tartaric acid according to the procedure of Kawachi et al. failed.<sup>96</sup> Following their procedure our efforts to generate the diastereomeric salts resulted in the formation of oils. The diastereomeric salt formation method of producing analogs of (*R*)- and (*S*)-2-methoxymethyl-piperazine was abandoned. However, we opted to utilize the method of Naylor et al. (Scheme 3-3) to synthesize the piperazine ring structure using amino acids as chiral building blocks. The synthesis of chiral MOM-NQP 31 outlined in Scheme 3-3 is adapted from a synthesis of 2-hydroxymethyl-4-benzylpiperazine (**S**)-113 according the procedure developed by Naylor et al. as described below.<sup>93</sup>

#### 3.3.1 Synthesis of N-Boc-N-Bn-glycine.

To begin the synthesis of chiral MOM-NQP, we needed to prepare the starting material N-Boc-N-Bn-glycine 111 from glycine 109 (Scheme 3-1).<sup>102,103</sup>



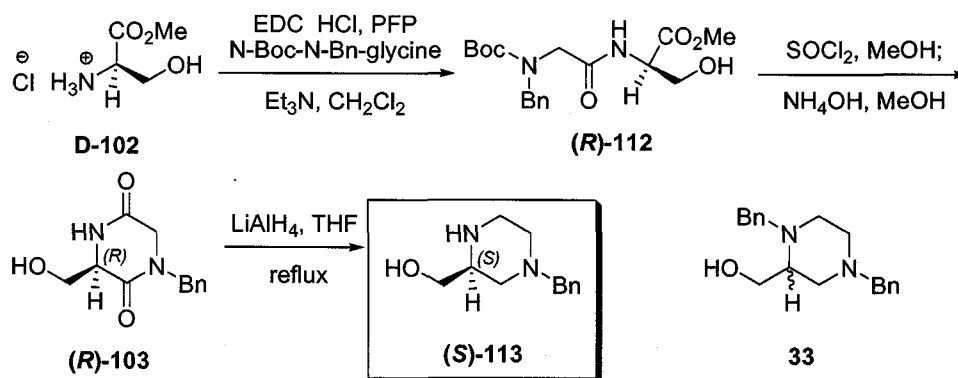
**Scheme 3-1:** Synthesis of N-Boc-N-Benzyl-glycine **111**.

A warm solution of glycine **109** in 1:1 EtOH/H<sub>2</sub>O is treated with potassium hydroxide (KOH) and benzyl-bromide (BnBr), then heated to reflux for 2 hours. The crude solution is concentrated by 20%, then the reduced solution is boiled while acetic acid (AcOH) is added, to give the free acid of dibenzyl-glycine (not shown) as a white precipitate (79%).<sup>102</sup> Dibenzyl-glycine is converted to mono-benzyl-glycine **110** by catalytic hydrogenolysis with a Parr hydrogenator (5% Pd/C in methanol (MeOH) and 12 M HCl) at an initial pressure of 50 psi.<sup>102</sup> The catalyst is removed by filtration and the reaction mixture is concentrated giving the mono-benzyl-glycine HCl **110** in a 98% yield. Product **110** was converted to N-Boc-N-Bn-glycine **111** by treatment with Boc<sub>2</sub>O as a basic solution in 1:1 H<sub>2</sub>O/1,4-dioxane gave **111** in a 66% yield according to the method of Bail et al.<sup>103</sup>

### 3.3.2 Synthesis of 1-Benzyl-3-(hydroxymethyl)piperazine **113**.

The preparation of the chiral piperazine (**S**)-**113** from D-serine hydrochloride is shown in Scheme 3-2; the (**R**)-**113** enantiomer is prepared in a similar procedure from L-serine hydrochloride.<sup>93</sup> The methyl ester of D-serine **D-102** is coupled to the pentafluorophenol activated ester of N-Boc-N-Bn-glycine **111** (EDC hydrochloride and pentafluorophenol (PFP)).<sup>93</sup> The dipeptide is easily

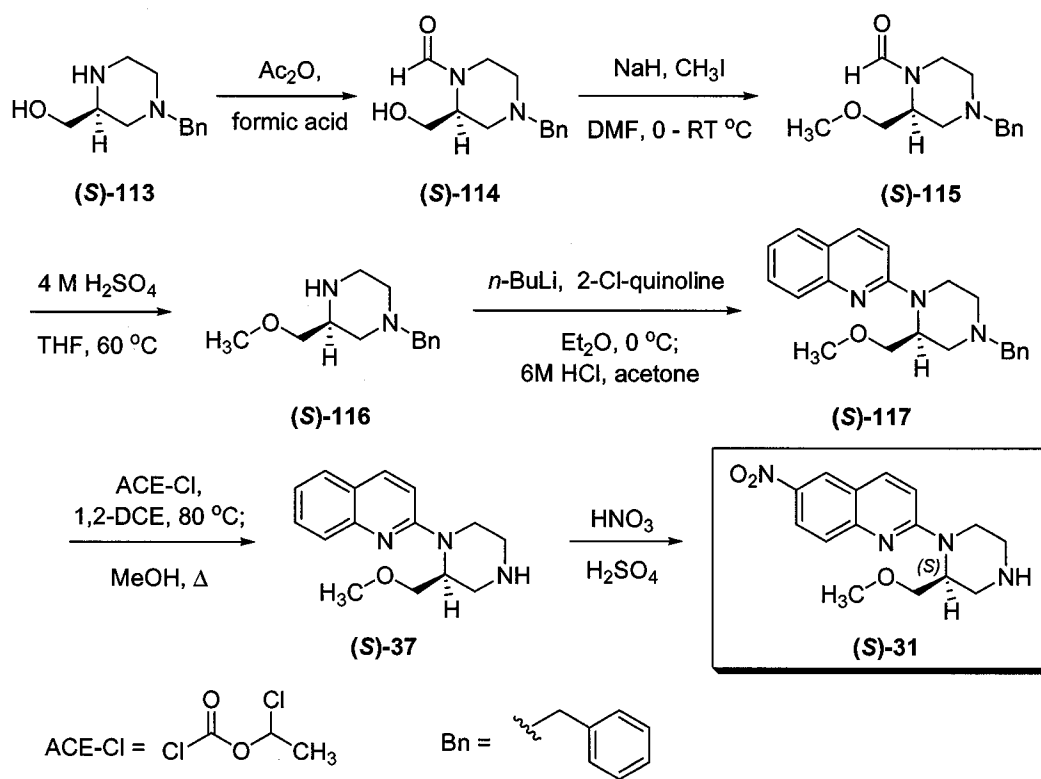
purified by column chromatography eluting with 3:2 EtOAc/hexanes, to give (*R*)-N-Boc-N-Benzyl-glycyl-D-serine methyl ester (**(R)**-112 in a 96% yield. The Boc group of the dipeptide is removed by treatment with SOCl<sub>2</sub> in MeOH and concentration in vacuo, and then triturated with Et<sub>2</sub>O to give the corresponding HCl salt (not shown). The N-Boc deprotected dipeptide is dissolved in MeOH and treated with NH<sub>4</sub>OH, aqueous workup and extraction with 4:1 IPOH/CHCl<sub>3</sub> gives the cyclized piperazinedione (**(R)**-103. Reduction of (**(R)**-103 with LiAlH<sub>4</sub> in refluxing THF affords the desired 2-hydroxymethyl-4-benzylpiperazine (**(S)**-103 (note the stereochemistry switch from R to S after reduction). We considered (*S*)-2-hydroxymethyl-4-benzylpiperazine to be a chiral structural equivalent to the racemic 1,4-dibenzyl-2-hydroxymethyl-piperazine **33**, requiring only protection of the 2° nitrogen and the alcohol group for Gilman coupling to 2-chloroquinoline according to the racemic syntheses (Scheme 1-2 and Scheme 2-13).



**Scheme 3-2:** Synthesis of the key synthetic intermediate (**(S)**-113.

### 3.3.3 Synthesis of Chiral MOM-NQP 31.

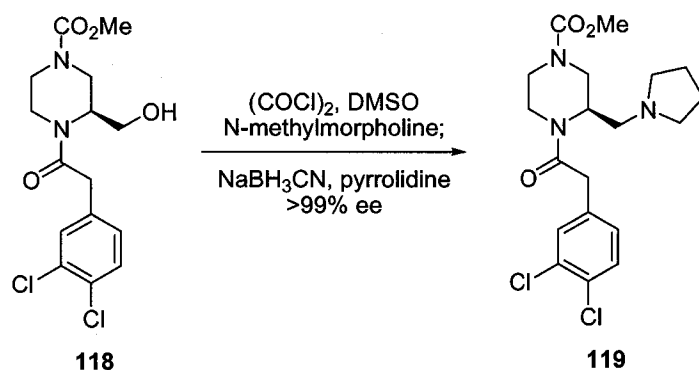
After completion of the synthesis of chiral 2-hydroxymethyl-4-benzylpiperazine (**R**)-113 and (**S**)-113, we extended the methodology of the racemic synthesis of ( $\pm$ )-31 to the chiral synthesis of (**R**)-31 and (**S**)-31 (Scheme 3-3).<sup>74</sup> The N-formylation of the free amine (**S**)-113, using acetic anhydride in formic acid, gave the N-formyl-monobenzyl-HOM (**S**)-114. Treatment of (**S**)-114 with NaH (300 mol%) in DMF gave the alkoxide, which was subsequently methylated with methyl iodide (CH<sub>3</sub>I) gave (**S**)-115. The N-formyl group was deprotected with 4 M H<sub>2</sub>SO<sub>4</sub> at 60 °C. The resulting piperazine (**S**)-116 was coupled to 2-chloroquinoline according to the standard Gilman procedure, to give the N-benzyl-MOM-QP (**S**)-117. Deprotection of the benzyl group was performed by heating (**S**)-117 with 1-chloroethyl chloroformate (ACE-Cl) in 1,2-dichloroethane at 80 °C, with cleavage of the intermediate carbamate (structure not shown) by heating in methanol, thereby affording the debenzylated product MOM-QP (**S**)-31. Nitration of (**S**)-31 at the 6-position of the quinoline ring gave the desired product (**S**)-31 typically with a 40% yield overall in seven steps. Repeating the synthesis using L-serine gives the alternate enantiomer (**R**)-MOM-NQP (**R**)-31 also in 40% overall yield.<sup>74</sup>



**Scheme 3-3:** Overall synthesis of chiral MOM-NQP (**S**)-31.

### 3.4 Application of the Chiral Synthesis, Chiral PROM-NQP 51.

With the success of the chiral MOM-NQP synthesis we turned our focus to using the technology developed for the production of (*R*)- and (*S*)-PROM-NQP ((*R*)-51 and (*S*)-51, respectively). Naylor et al. were successful in using a Swern oxidation of **118** to generate the corresponding aldehyde (not shown).<sup>93</sup> To minimize racemization during the oxidation, N-methylmorpholine was used by Naylor, instead of employing Et<sub>3</sub>N amine as a base. After oxidation, Naylor was successful in using the aldehyde in a reductive amination with pyrrolidine to give **119**. According to Naylor et al. they were able to accomplish the oxidation and reductive amination with minimal racemization giving the desired compound **119** in a >99% ee (HPLC).<sup>93</sup>



**Scheme 3-4:** Potential oxidation of the methyl alcohol according Naylor et al.<sup>93</sup>

We examined the possibility of using the Naylor method to oxidize a N-protected version of (**S**)-**113** followed by a Horner-Emmons olefination according to the racemic PROM-NQP ( $\pm$ )-**51** synthesis (Scheme 2-13). However, we thought that it would be more beneficial to investigate the use of other amino acids with the appropriate piperazine side chain all ready in place as the amino acids side chain (R) group. We were particularly interested in the methyl esters of D- and L-glutamate **120**, as well as the D- and L- forms of 5-hydroxynorvaline **121** (an equivalent to serine for the three carbon case) for the synthesis of (**R**)-**51** and (**S**)-**51**.

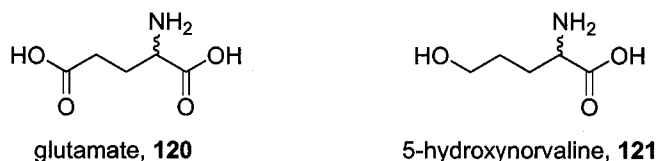
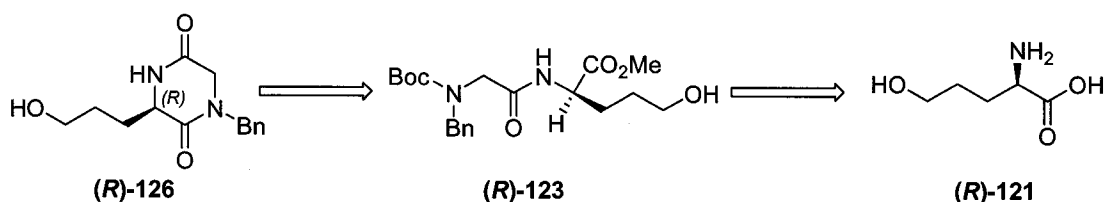


**Figure 3-4:** Potential amino acid starting materials for the chiral PROM-NQP **51** synthesis.

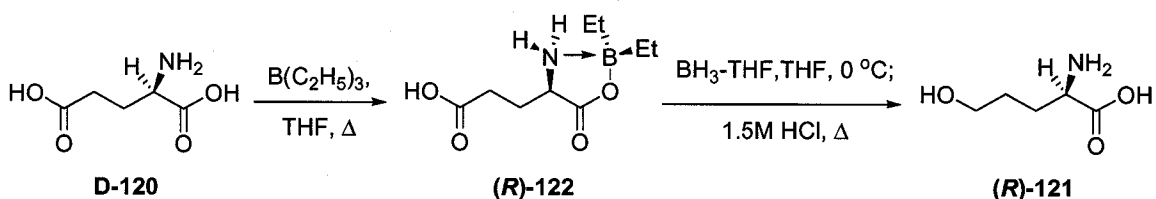
If 5-hydroxynorvaline **121** could be readily prepared in our lab, we could utilize all the procedures developed with the earlier chiral MOM-NQP ( $\pm$ )-**31**

synthesis. Scheme 3-5 shows the retrosynthetic strategy for the synthesis of the propyl (*R*)-**126** equivalent to the methyl hydroxy (*R*)-**103**.



**Scheme 3-5:** Retrosynthetic analysis for the formation of (*R*)-**126**.

A search of the literature found that **121** could be synthesized from D- or L-glutamic acid **120** by selective protection of the  $\alpha$ -carboxylate as the boroxazolidone and reduction of the terminal carboxylate, according to Scheme 3-6. The  $\alpha$ -carboxylic acid of glutamic acid **120** is protected as the boroxazolidone according to the procedures of Nefkens and Gong.<sup>104,105</sup> The  $\delta$ -carboxylate was selectively reduced with borohydride-THF complex ( $\text{BH}_3\text{-THF}$ ) to give the alcohol and the boroxazolidone was cleaved by refluxing in 1.5M HCl, purified by ion exchange to give 5-hydroxynorvaline (*R*)-**121** according to the procedure of Garcia.<sup>106</sup>

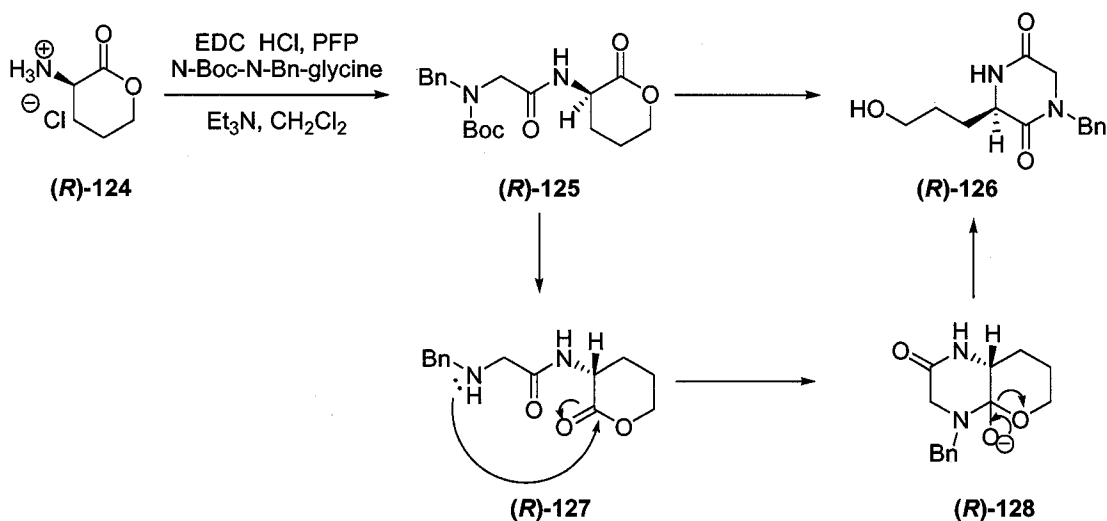


**Scheme 3-6:** Synthesis of 5-hydroxynorvaline from glutamic acid.

Attempts to generate the methyl ester of 5-hydroxynorvaline (*R*)-**121** resulted in the formation of the cyclized lactone (*R*)-**124** according to Scheme 3-7. The lactone (*R*)-**124** was posed as a possible substrate for the peptide coupling to give compound (*R*)-**126**, where the lactone of dipeptide (*R*)-**125**

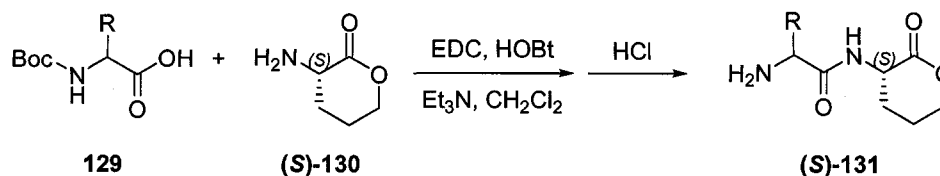


would act as the methyl ester of (**R**)-**112** for the cyclization to the piperazine ring in the chiral MOM-NQP synthesis (Scheme 3-2).



**Scheme 3-7:** Potential synthesis of the piperazinedione ring utilizing the lactone (**R**)-**126**.

As shown in Scheme 3-8 the lactone form of 5-hydroxynorvaline (**S**)-**130** has been prepared and similarly used in a dipeptide coupling with N-Boc protected amino acids, including alanine, glycine among others to give the peptide (**S**)-**131** after deprotection of the N-Boc group.<sup>94,107</sup> While only the (**S**)-enantiomer of the lactone (prepared from L-glutamic acid) was used in the preparation of the dipeptide, the (**R**)-lactone can be afforded using the same procedure.<sup>105</sup> The missing experiment in our research would be to attempt a cyclization to the piperazine (**R**)-**126** as solution in MeOH and NH<sub>4</sub>OH according to Scheme 3-8. However, due to the expense and labor intensive process of preparing large quantities (>10 g) of 5-hydroxynorvaline **121** and its associated lactone **124**, we decided on using a more economical route.

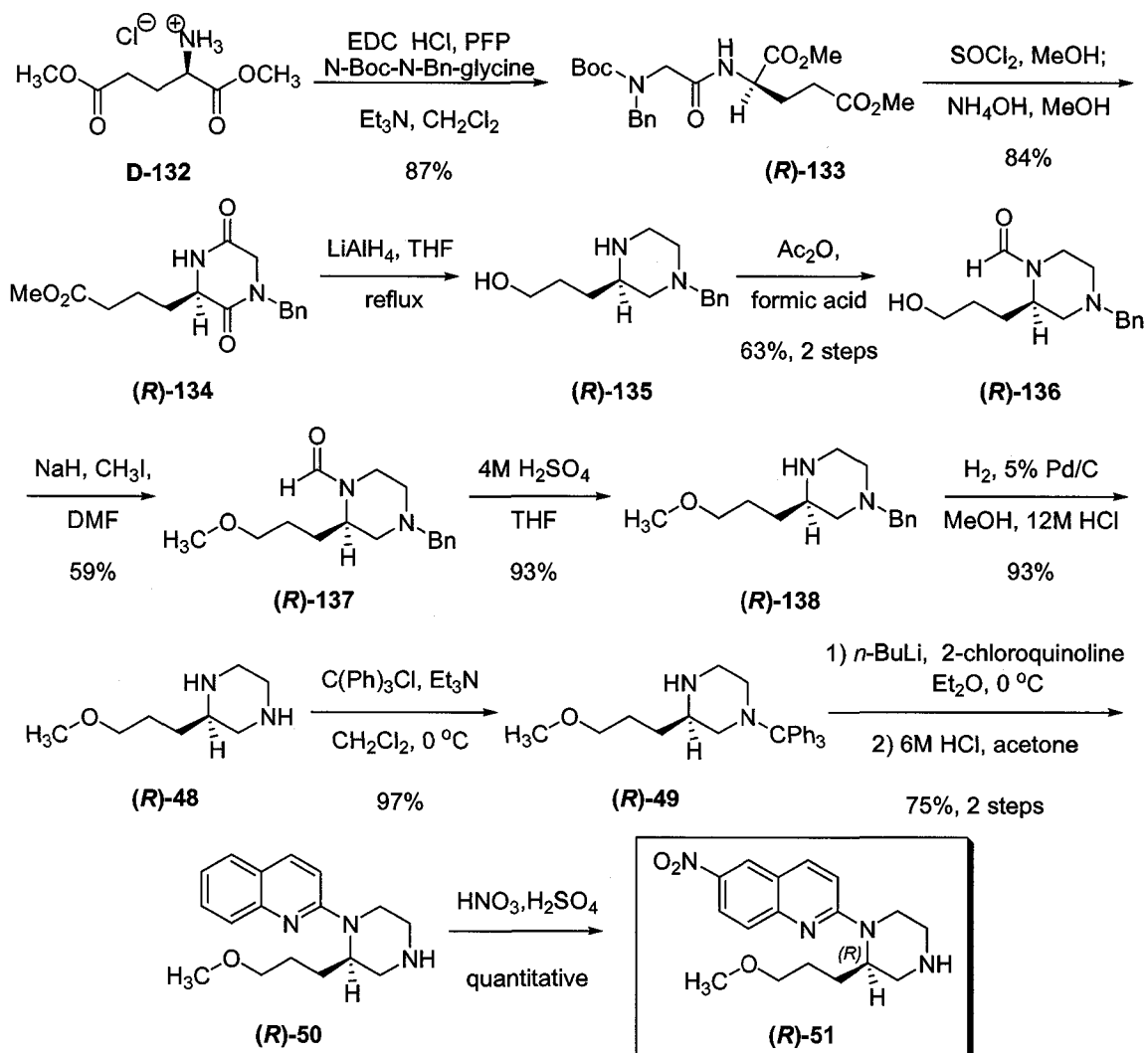


**Scheme 3-8:** Example peptide coupling using a cyclic lactone derived from 5-hydroxynorvaline **121**.

As shown in Scheme 3-9, the dimethyl ester of D-glutamic acid **D-132** easily couples with N-Boc-N-Bn-glycine **111**, according to the chiral MOM-NQP **31** synthesis (Scheme 3-2), to give the dipeptide **(R)-133** in an 87% yield. Dipeptide **(R)-133** was deprotected ( $\text{SOCl}_2$ , MeOH) and cyclized to give compound **(R)-134** in an 84% yield. The cyclization required stirring overnight at room temperature to achieve complete conversion. This is in contrast to the MOM-NQP synthesis where 2-3 hours were required to complete the cyclization, suggesting the kinetic differences for the reactions is a function of side chain length or substitution, i.e. alcohol vs. ester. The cyclized piperazinedione **(R)-134** was reduced with  $\text{LiAlH}_4$  and the crude material was treated with acetic anhydride in formic acid to give the N-formyl-piperazine **(R)-136** in a 63% yield over 2 steps. The N-formyl-piperazine **(R)-136** was treated with NaH (300 mol%) as a solution in DMF to generate the alkoxide that was quenched by the addition of  $\text{CH}_3\text{I}$  to give compound **(R)-137** in a 59% yield. Deprotection of the N-formyl protecting group of **(R)-137** was afforded by treatment with 4 M  $\text{H}_2\text{SO}_4$  as a solution in THF to give **(R)-138**.

Importantly, the mono-benzyl propyl ester **(R)-138** was not coupled to 2-chloroquinoline as in the chiral MOM-NQP **31** synthesis (Scheme 3-3), due to difficulties at that time to get consistent benzyl group deprotection results.<sup>74</sup>

Instead, we opted to remove the benzyl group of **(R)-138** by catalytic hydrogenolysis conditions at atmospheric pressure, to give PROM-piperazine dihydrochloride **(R)-48** in a 93% yield. The least hindered nitrogen was protected with trityl-chloride (97%) and the resulting protected piperazine **(R)-49** was coupled to 2-chloroquinoline by the standard Gilman conditions and according to the earlier racemic PROM-NQP ( $\pm$ )-**51** synthesis (Scheme 2-13). The coupled product was purified accordingly and deprotected to give PROM-NQP **(R)-50** in a 75% yield. Nitration at the 6-position gave the desired chiral agent (*R*)-PROM-NQP **(R)-51** in a quantitative yield. The *R*- and *S*-enantiomers of PROM-NQP were prepared from D- and L-glutamic acid dimethyl esters, respectively in 11 steps in a 17% and 23% overall yield, respectively.

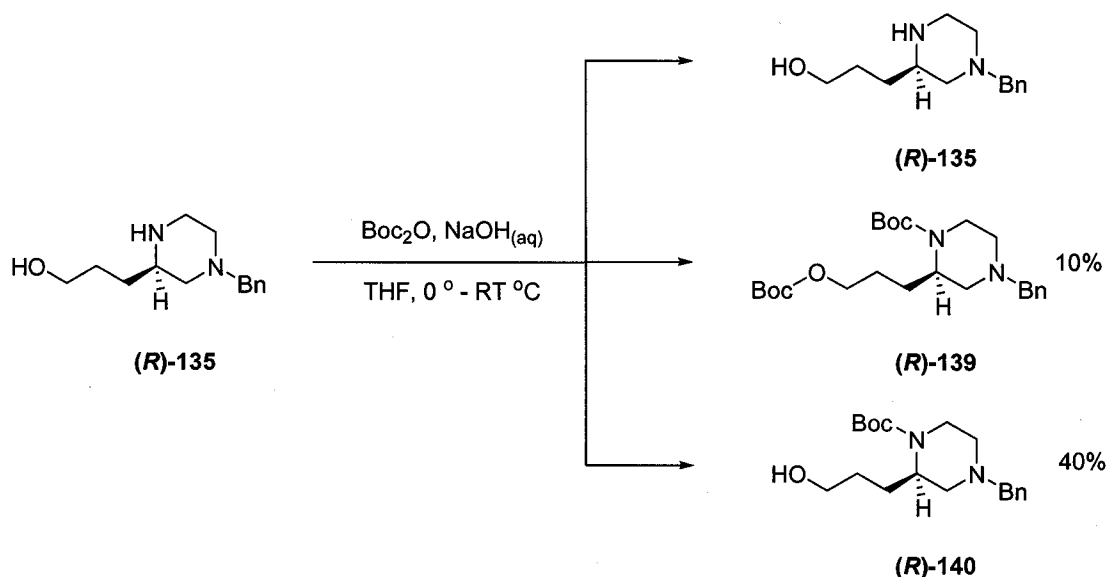


**Scheme 3-9:** Overall synthesis of (R)-PROM-NQP 51, the (S)-enantiomer is afforded according to the same synthetic sequence starting from L-132.

### 3.5 Alternate Synthesis of Chiral PROM-NQP.

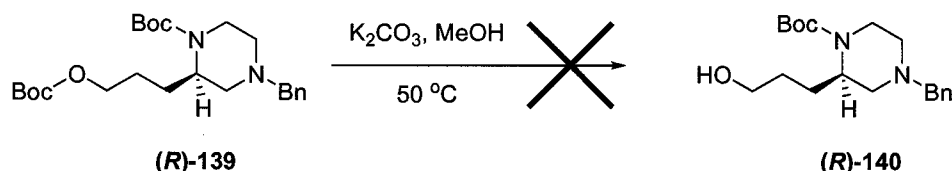
The alternate synthesis of (R)-51 and (S)-51 utilized the nitrogen protecting group Boc for the protection the 2° amine of (R)-135. To accomplish this, the ester and the amides of (R)-134 were reduced with LiAlH<sub>4</sub> in refluxing THF. Attempts to selectively protect the nitrogen of the piperazine with a Boc group were moderate at best (25-40% yield). For example, treatment of (R)-135 with 98 mol% of di-*tert*-butyl dicarbonate (Boc<sub>2</sub>O) according to Scheme 3-10

gave the N-Boc-N-Bn-propylpiperazine (**R**)-**140** in a 40% yield. Unfortunately, the Boc protection of the free amine was not selective and the crude reaction workup gave a mixture with of the unprotected starting material (**R**)-**135**, the desired product (**R**)-**140**, and the diprotected species (**R**)-**139**. These results were not surprising, considering the problems associated with Boc protection of the racemic form of HOP-NQP **146** (Scheme 2-20).



**Scheme 3-10:** Protection of the 2° amine with  $\text{Boc}_2\text{O}$ .

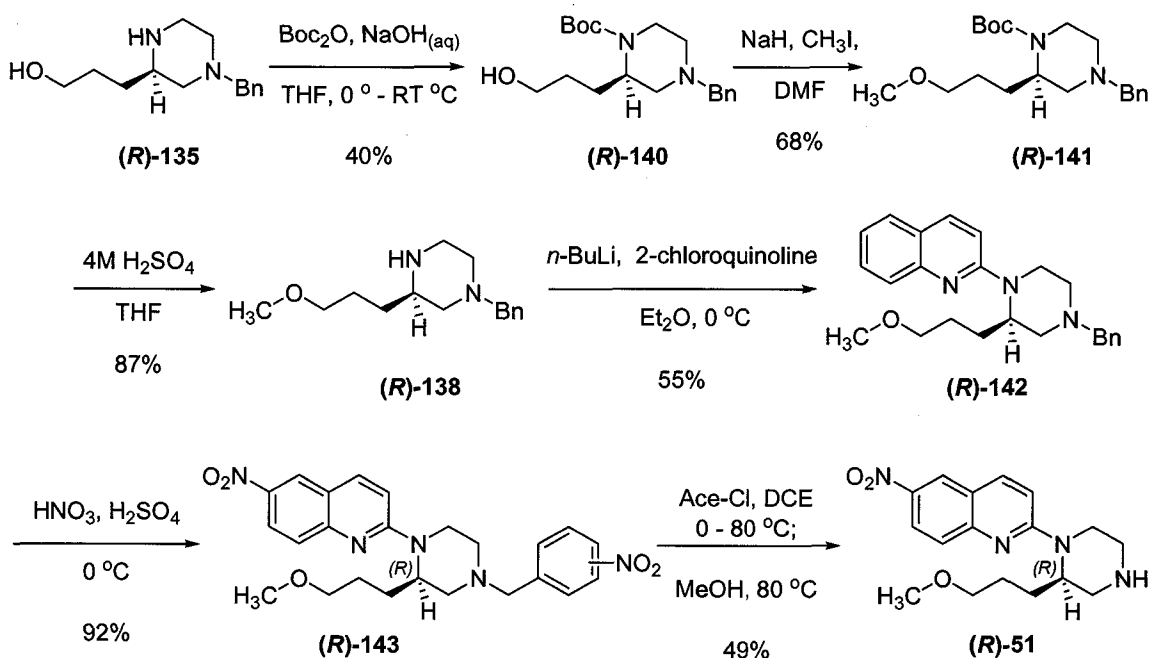
Attempts to selectively deprotect the side chain carbonate according to the racemic synthesis of **66** failed ( $\text{K}_2\text{CO}_3$ , MeOH, Scheme 2-21).



**Scheme 3-11:** Attempted deprotection of the Boc carbonate (**R**)-**139**.

Despite the selectivity problems with Boc protection the chiral synthesis was completed as proof of concept as shown in Scheme 3-12. The Boc

protected piperazine (**R**)-140 was methylated (DMF, NaH and CH<sub>3</sub>I) according to the N-formyl series to give (**R**)-141 in a 68% yield. The Boc group was deprotected (4 M H<sub>2</sub>SO<sub>4</sub>, THF) (87%) and the resulting monobenzyl piperazine (**R**)-138 was coupled to 2-chloroquinoline by the standard Gilman method to give (**R**)-142 in a 55% yield. The coupled product (**R**)-142 was nitrated (H<sub>2</sub>SO<sub>4</sub>, HNO<sub>3</sub>, 0 °C) at the 6-position of the quinoline ring and the 2 and 4 positions of the benzyl group (**R**)-143 giving a mixture of regioisomers of the phenyl ring in a 92% yield. Cleavage of the nitro-benzyl groups with 1-Chloroethyl chloroformate (ACE-Cl) gave the desired enantiomers of **51**, (**R**)-**51** and (**S**)-**51** in 49% and 62% yields, respectively. Scheme 3-12 details the overall synthesis of (**R**)-**51** and (**S**)-**51** from (**R**)-135 in 6 steps and an overall yield of 6% yield for (**R**)-**51** and 11% yield for (**S**)-**51**.



**Scheme 3-12:** Alternate synthesis of (**R**)-**51** utilizing the N-Boc protected piperazine (**R**)-140.

### 3.6 Synthesis of Chiral Pent-NQP 83.

To further explore the application of the chiral synthetic approach, the synthesis of (*R*)- and (*S*)-Pent-MOM 83 were explored. Initially, we looked into using an unnatural amino acid with a carbon chain of the appropriate length that could be used in the peptide coupling and cyclization procedures. A survey of the literature and chemical supplier catalogs found ( $\pm$ )-2-aminoheptanedioic acid (Figure 3-5). However, 144 is only available as the racemate, and a chiral synthesis for the enantiomeric forms 144 was not available.

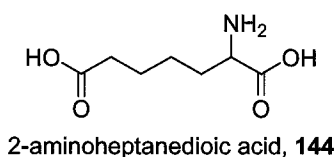
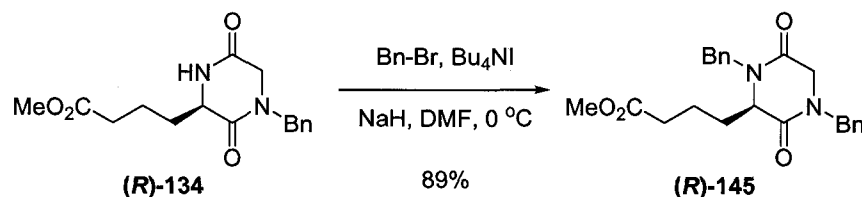


**Figure 3-5:** Potential amino acid building block for the synthesis of chiral Pent-NQP 83.

Our second option was to use an intermediate of the chiral propyl synthesis and perform the carbon extension via Swern oxidation and Horner-Emmons olefination (*R*)-135. In order to accomplish the carbon extension, the free amine of (*R*)-135 needed to be protected with a protecting group stable to the Swern and Horner-Emmons conditions. An examination of protecting groups used routinely in our lab and comparison of their respective stabilities to the reagents utilized in Swern and Horner-Emmons was performed.<sup>108</sup> The ease of the protecting group deprotection procedures was also taken into consideration.<sup>108</sup>

Considering the questionable success of protecting the chiral piperazine (*R*)-135 as the N-Boc (*R*)-140 we decided a benzyl group protection of the piperazinedione (*R*)-134 (Scheme 3-13) would be the preferred route. The N-

benzyl protecting group was also preferred, considering that after reduction of the amides and the ester of (**R**)-**145** we would be afforded a chiral piperazine matching the synthesis of the racemic propyl and pentyl series (compound **33**, Scheme 2-13 and Scheme 2-30). Thus, we would now be able to apply all the technologies developed in those series for the preparation of chiral Pent-NQP **83**. Initial trials of the benzylation reaction using NaH and benzyl bromide in DMF resulted in only moderate yields (54-70%) of product (**R**)-**145**. Supplementing the reaction with a catalytic amount (40 mol%) of tetrabutylammonium iodide (TBAI) improved the yields (89-93%), by changing the leaving group from a bromide to an iodide.<sup>109</sup>

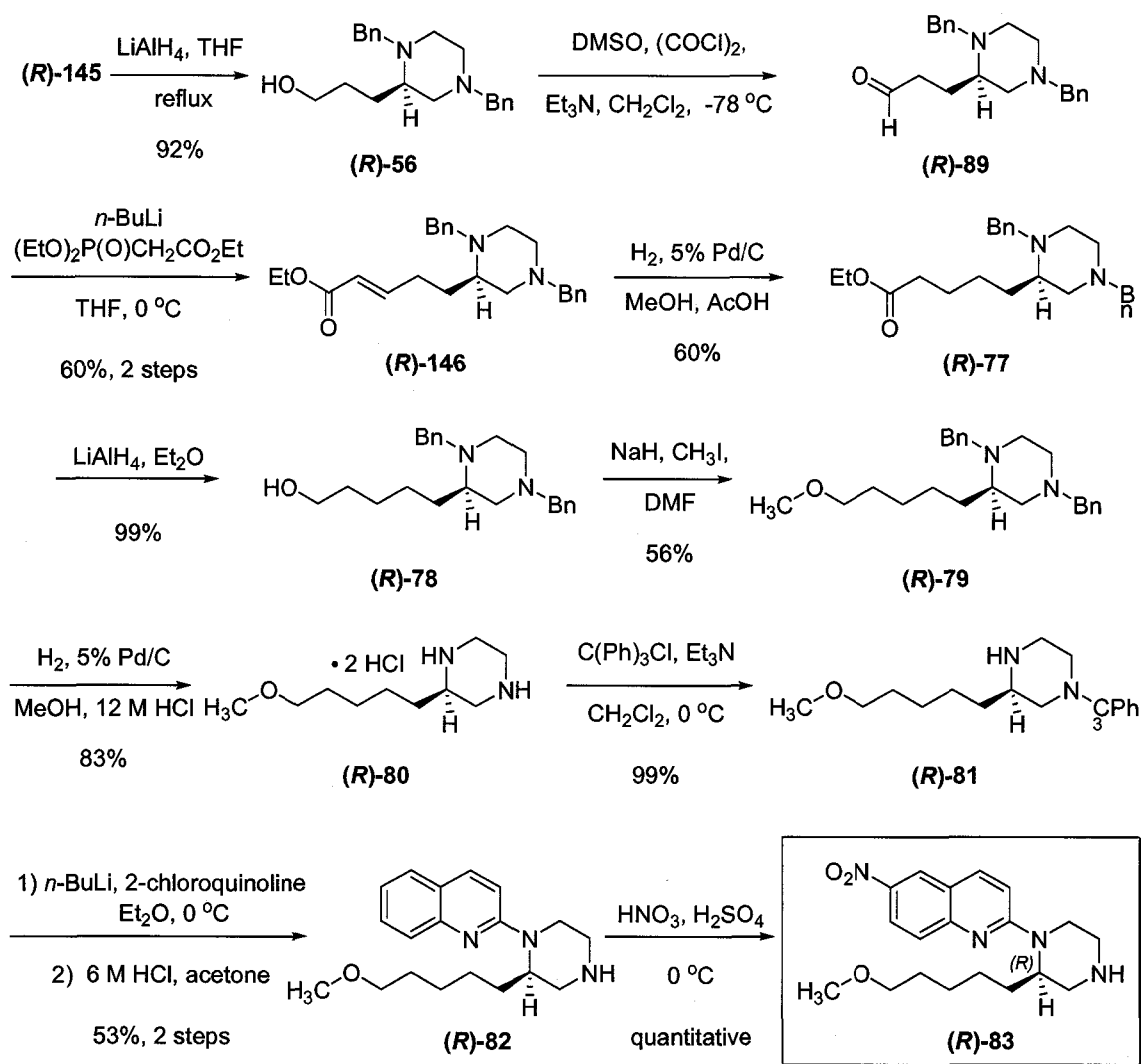


**Scheme 3-13:** Protection of (**R**)-**134** with benzyl bromide (BnBr)

As shown in Scheme 3-14, piperazinedione (**R**)-**145** was reduced with  $\text{LiAlH}_4$  in refluxing THF to give the dibenzyl propyl alcohol (**R**)-**56** (92%). Swern oxidation and Horner-Emmons olefination with triethylphosphonoacetate gave the unsaturated pentyl ester (**R**)-**146** (60%, 2 steps). Subsequent saturation was accomplished by catalytic hydrogenation using 5% Pd/C in MeOH and acetic acid (AcOH) (60%). The saturated ester (**R**)-**77** was reduced with  $\text{LiAlH}_4$  in  $\text{Et}_2\text{O}$  (99%) and the resultant alcohol (**R**)-**78** was methylated as the alkoxide (NaH) in DMF with  $\text{CH}_3\text{I}$  to afford (**R**)-**79** (56%). Hydrogenolysis of the benzyl groups gave the Pent-MOM piperazine dihydrochloride (**R**)-**80** in a 83% yield, which was



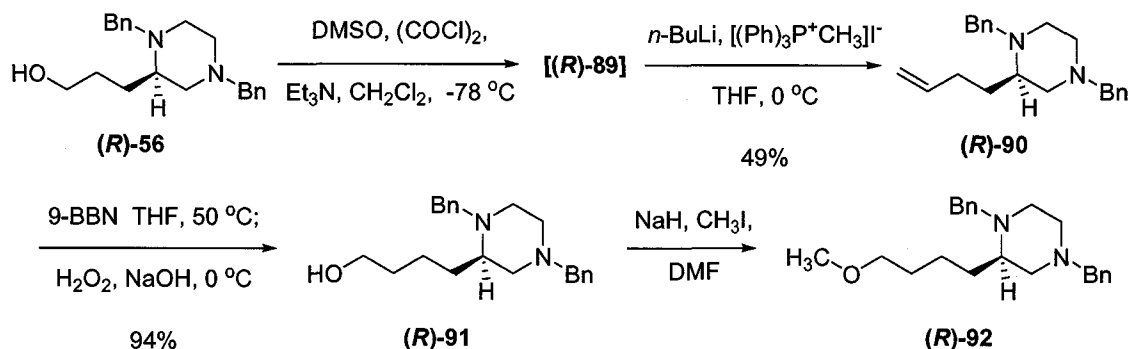
protected using trityl-chloride (99%). The N-trityl-pentyl-piperazine (**R**)-**81** was coupled to 2-chloroquinoline according to the Gilman method, deprotected with 6 M HCl in acetone to give (**R**)-**82** (53%, 2 steps). Nitration at the 6-position of the quinoline ring gave Pent-NQP (**R**)-**83** in a quantitative yield. The synthesis of (**R**)-**83** and (**S**)-**83** were accomplished in 8% and 5% yield, respectively, in 11 steps.



**Scheme 3-14:** Overall synthesis of (**R**)-Pent-NQP **83**, the (**S**)-enantiomer was similarly prepared from (**S**)-**145**.

### 3.7 Synthesis of Chiral BuM-NQP 96.

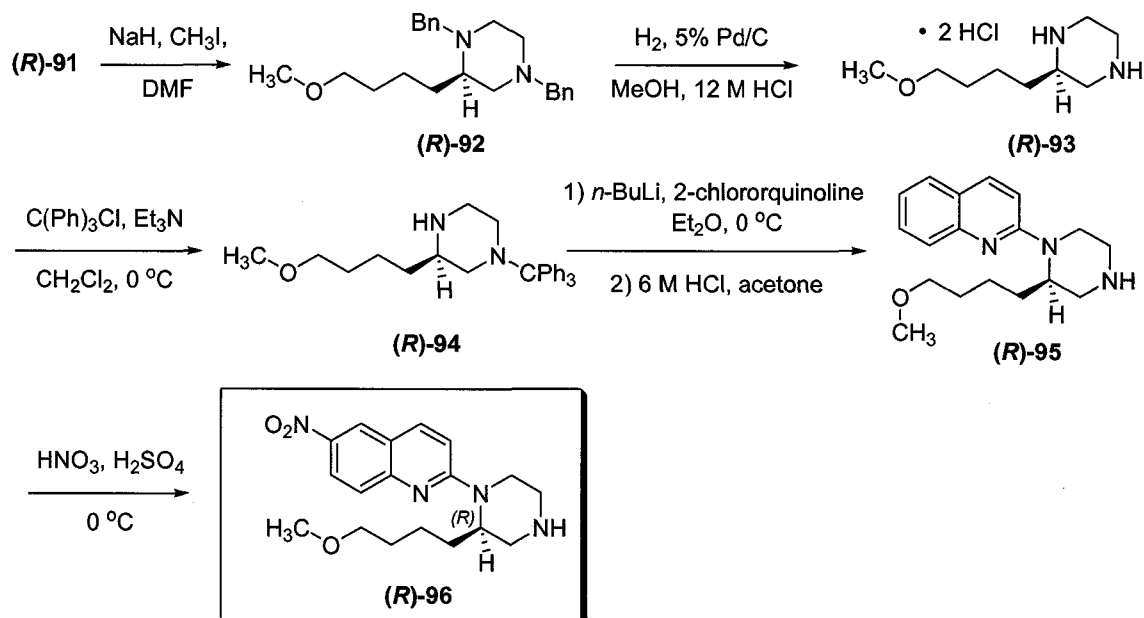
Preliminary accomplishments for the synthesis of the chiral butyl variant (*R*)-**91** have been realized, as shown in Scheme 3-15. However, at the time of this writing this (*R*)- and (*S*)-BuM-NQP **96** have not been prepared. The intermediate chiral dibenzyl-HOP (*R*)-**56** was prepared as described above in the chiral pentyl synthesis from the cyclized piperazinedione (*R*)-**145** (Scheme 3-13). Swern oxidation of alcohol (*R*)-**56** to the aldehyde [*R*]-**89** was followed by Wittig olefination with methyltriphenylphosphonium and *n*-BuLi gave the terminal alkene (*R*)-**90** in a 49% yield over two steps. Hydroboration of (*R*)-**90** with 9-BBN followed by oxidation gave the desired butyl alcohol (*R*)-**91** (94%). For this reaction careful purification was required to remove the side product 1,5-cyclooctanediol by column chromatography, before the subsequent methylation reaction. Attempts to methylate the alcohol (*R*)-**91** after aqueous acid-base workup gave low yields (<10%) of the desired product (*R*)-**92**.



**Scheme 3-15:** Initial synthesis of the BuM-NQP precursor (*R*)-**92**, by Wittig olefination technology.

Completion of the synthesis of (*R*)- and (*S*)-BuM-NQP **96**, can be afforded during the future by repeating the reaction sequence for the preparation of the ( $\pm$ )-BuM-NQP **96** as outlined in Chapter 2. Briefly as per Scheme 3-16, the

alcohol (**R**)-**91** would be methylated and the benzyl groups cleaved. The less hindered nitrogen of the piperazine can be protected as the N-trityl group. The N-trityl piperazine (**R**)-**94** would be coupled to 2-chloroquinoline, then deprotected and nitrated to give the desired (**R**)- and (**S**)-BuM-NQP **96**.



**Scheme 3-16:** Proposed synthesis of chiral BuM-NQP **96** from the synthetic intermediate (**R**)-**92**.

### 3.8 Summary and Conclusions.

Typically, the synthesis of the chiral forms of a SERT agent results in an enantiomer with higher SERT affinity compared to the opposing enantiomer. For, example the synthesis of (**R**) and (**S**)-citalopram **7** resulted in discovering a more potent SSRI in (**S**)-**7**. This chapter summarizes our efforts to prepare the enantiomeric forms of PROM-NQP ( $\pm$ )-**31**, Pent-NQP ( $\pm$ )-**83** and the initial synthesis of BuM-NQP **96**. Further work is required to accomplish the enantiomers of **96**. Chapter 4 discusses the pharmacology of the enantiomers of Me-NQP ( $\pm$ )-**30** and MOM-NQP ( $\pm$ )-**31**, as it has been our goal to further the SAR

of the 6-NQP **22** analogs according to their respective SERT binding affinities. The synthesis of the longer chain derivatives of the 2-(2-alkyl-piperazin-1-yl)-6-nitroquinolines furthers our understanding of the affects of chain length and chirality of the 6-NQP analogs and their selectivity for SERT binding. The synthesis of the radiolabeling precursors and the cold fluorinated analogs **58** and **88** should be accomplished to benefit the SAR studies allowing direct comparison of binding affinities of the enantiomeric forms of the ligands to the racemic forms.

## Chapter 4

### Pharmacology

#### 4.1 Introduction.

The pharmacological evaluation of the prepared 2-(2-alkyl-piperazin-1-yl)-6-nitroquinoline analogs for their respective competitive binding affinities at the serotonin reuptake transporter (SERT) is outlined in Table 4-1 and Table 4-2. Our focus was to develop a more detailed understanding of the structure-activity relationship (SAR) of the 2-(2-alkyl-piperazin-1-yl)-6-nitroquinoline analogs that would afford the most favored SERT ligand binding. By doing so we would be able to describe the pharmacological profile of the proposed PET imaging agents **58** and **148**.

The alkyl side chain groups of the 2-(2-alkyl-piperazin-1-yl)-6-nitroquinoline ligands are designed to probe the area of the binding domain (Ar2) that is shared by the alkyl side chain of the antidepressant fluvoxamine (Figure 1-3). We have also proposed that this binding area is also shared by an aromatic ring of other serotonin selective reuptake inhibitors (SSRIs) that contain two aromatic moieties. It is thought that one of the two aromatic moieties is critical for SERT binding (Chapter 1).<sup>67</sup>

Our research group utilizes a published in vitro competitive ligand binding assay for the determination of the inhibition constant ( $K_i$ ) as a comparative analog SAR measurement.<sup>67,110</sup> Described below is the competitive inhibition pharmacology measures, a summary of the SAR of the 2-(2-alkyl-piperazin-1-yl)-

6-nitroquinoline ligands based upon their respective  $K_i$  values. Additionally the synthesis of [ $^3\text{H}$ ]n-PROP-NQP **52** is provided, as well as the kinetic binding profile of [ $^3\text{H}$ ]52. Kinetic analysis of [ $^3\text{H}$ ]n-PROP-NQP **52** will allow us to gain a better understanding of the rate constants  $k_{\text{on}}$  (association) and  $k_{\text{off}}$  (dissociation) and also kinetic and the related equilibrium dissociation constants ( $K_D$ ).

#### **4.2 Competitive Inhibition, SERT Pharmacology [ $^3\text{H}$ ]paroxetine.**

The in vitro inhibition binding constants ( $K_i$ ) of the ligands outlined in Table 4-1 and Table 4-2 were determined using an established radioligand competition binding assay (rat cortical SERT (rSERT), [ $^3\text{H}$ ]Paroxetine **9**)<sup>67,110</sup> which is a modified method of Habert.<sup>111</sup> The measured  $K_i$  data (mean  $\pm$  s.e.m.,  $n = 3$  or more runs) is summarized in Table 4-1 and Table 4-2, where a lower  $K_i$  value is indicative of higher SERT ligand binding affinity.

The in vitro assays were performed with aliquots of partially purified male rat cortex membrane tissue (Pel-Freeze Biologicals, Inc.). The cerebral cortex was dissected from adult rat brains. The cortex was homogenized using a Polytron tissue homogenizer in Tris-HCl buffer. Centrifugation of the crude homogenate isolated the desired membrane fraction. The pellet material was suspended in assay buffer (50 mM Tris-HCl, pH 7.4, 120 mM NaCl, and 5 mM KCl). The suspensions were incubated with 0.25 nM [ $^3\text{H}$ ]Paroxetine (DuPont-NEN, specific activity of  $\sim 19.5$  Ci/mmol) and decreasing concentrations ( $10^{-6}$  M to  $10^{-11}$  M) of the inhibitors. After 3 hours, the incubations were terminated by dilution with ice-cold buffer and then filtered using S & S glass filter papers

(Schleicher and Schuell #32 glass fiber filter paper) under vacuum (Brandel cell harvester). To minimize nonspecific binding of the radioligand, the filter papers were presoaked in a 0.05% v/v solution of polyethyleneimine. The filter papers were washed rapidly with cold Tris-HCl buffer and transferred to scintillation vials. To the vials was added 10 mL of Ecolume scintillation fluid (ICN, Irvine, CA), the vials were shaken 24 hours and the radioactivity was counted with a Packard scintillation counter.

Specific binding was determined as the binding difference between total binding and non-specific binding. Non-specific binding was defined as the residual binding in the presence of 1  $\mu$ M 6-Nitroquipazine **22** to the incubation media. Total binding is described as the level of radioactivity of the assay medium in the absence of unlabeled competitive inhibitor. Binding data was analyzed using the software program Prism (GraphPad, Inc.) where percent of total specific binding vs. -log molar concentration of inhibitor (six or more data points per curve) were plotted. The inhibitor concentrations ( $IC_{50}$ ) required to obtain 50% inhibition of [ $^3$ H]paroxetine **9** binding were determined.<sup>112</sup> Assay data points were done in triplicate and the experiments were repeated a minimum of three times on different days. The  $K_i$  value was calculated according to the equation:  $K_i = IC_{50}/(1+[L]/K_D)$ , where [L] is the concentration of the unbound [ $^3$ H]paroxetine **9** (0.25 nM), and  $K_D$  is the equilibrium dissociation of paroxetine (0.15 nM).<sup>111,112</sup> An example plot for the binding of **9** is given below (Figure 4-1).

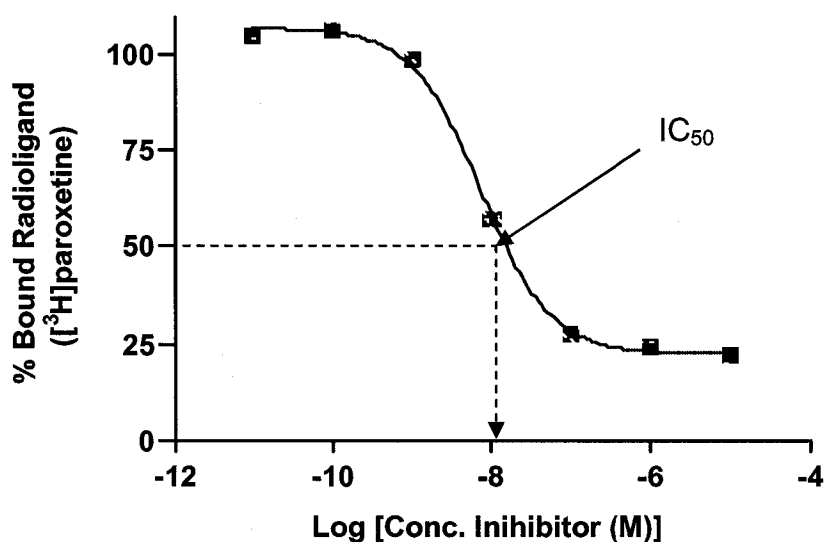


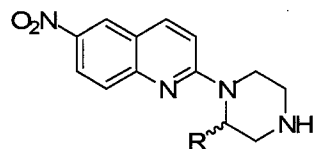
**Figure 4-1:** Example single site competition assay plot of %bound radioligand versus the Log of inhibitor concentration (M).

#### 4.2.1 Discussion of Pharmacology.

Based upon the lead structure 6-nitroquipazine (6-NQP) **22** a number of racemic (Table 4-1) and chiral (Table 4-2) 2-(2-alkyl-piperazin-1-yl)-6-nitroquinolines have been prepared, and their respective binding affinities ( $K_i$ ) for rSERT have been determined. Included in the table are their structural differences from the lead 6-NQP **22** and their calculated lipophilicity values (LogP).<sup>113</sup>



**Table 4-1:** Racemic 2-(2-alkyl-piperazin-1-yl)-6-nitroquinolines, compound name and R-group are given as well as their associated binding inhibition constant ( $K_i$ ), and CLogP(o/w) value.



	Name	R	$K_i$ (pM)	CLogP(o/w)**	Ref
<b>22</b>	NQP	H	160 ± 50	1.9	67
<b>(±)-30</b>	(±)-Me-NQP	CH <sub>3</sub>	81 ± 61	2.42	"
<b>(±)-31</b>	(±)-MOM-NQP	CH <sub>2</sub> OCH <sub>3</sub>	2.48 ± 0.28	1.94	72
<b>38</b>	HOM-NQP	CH <sub>2</sub> OH	12.65 ± 3.00	1.19	74
<b>(±)-51</b>	PROM-NQP	(CH <sub>2</sub> ) <sub>3</sub> OCH <sub>3</sub>	2.12 ± 1.13	2.21	This Work
<b>147</b>	HOP-NQP	(CH <sub>2</sub> ) <sub>3</sub> OH	50.25 ± 35.76	1.5	This Work
<b>58</b>	PROF-NQP	(CH <sub>2</sub> ) <sub>3</sub> F	2.48 ± 0.19	2.75	This Work
<b>52</b>	<i>n</i> -PROP-NQP	CH <sub>2</sub> CH <sub>2</sub> CH <sub>3</sub>	41.48 ± 19.87	3.48	This Work
<b>(±)-83</b>	PentOM-NQP	(CH <sub>2</sub> ) <sub>5</sub> OCH <sub>3</sub>	1.02*	3.26	This Work
<b>148</b>	MePROF-NQP	CH <sub>2</sub> O(CH <sub>2</sub> ) <sub>3</sub> F	3.96 ± 0.88	2.28	74
<b>88</b>	PentF-NQP	(CH <sub>2</sub> ) <sub>5</sub> F	79.6 ± 21.2	3.81	This Work

\*Preliminary Value \*\*Daylight Software (<http://www.daylight.com/daycgi/clogp>)

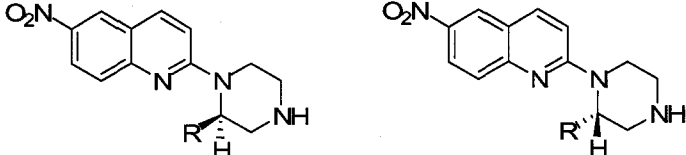
Early work by Gerdes et al. has shown that methyl group substitution of the piperazine ring at the 2-position Me-NQP (**(±)-30**) is 56 times more potent for rSERT than methyl substitution at the 3-position 3-Me-NQP **28**.<sup>67</sup> Additionally binding potency of Me-NQP (**(±)-31**) was 2 times (81 pM) more potent compared to the lead 6-NQP **22** (160 pM). The next generation ligand MOM-NQP (**(±)-31**) was obtained by extending the alkyl chain by two atoms as the methoxymethyl, increased binding affinity to 2.5 pM (64 times more potent than **22**). The increase in binding of (**(±)-31**) suggests that the piperazine substitution is interacting deeper in the Ar2 binding pocket (Figure 1-10). Comparison of (**(±)-MOM-NQP (±)-31**) to the all carbon case *n*-PROP-NQP **52** (similar chain length) shows that in the absence of an oxygen binding potency is decreased ( $K_i = 42$  pM). The addition of an oxygen as the propyl methyl ether PROM-NQP (**(±)-51**),

showed an increase in binding affinity ( $K_i = 2.1 \text{ pM}$ ) that is equivalent to the affinity of ( $\pm$ )-**31**. A similar comparison can be made between PentF-NQP **88** (void of oxygen) and MePROF-NQP **148** (oxygen present). The all carbon case **88** (79.6 pM) has the same potency as ( $\pm$ )-**30** (81 pM). The introduction of an oxygen atom in MePROF-NQP **148** (oxygen location is the same as ( $\pm$ )-**31**) results in an increase in binding affinity that is consistent with the ligands containing an ether functionality ( $\pm$ )-**31** and ( $\pm$ )-**51** ( $K_i = 4.0 \text{ pM}$ ). The increase in binding of the alkyl chains containing an ether functional group is suggestive that the Ar2 binding region may prefer hydrogen bonding acceptors, i.e. oxygen and perhaps fluorine.

When comparing the binding affinities of the all carbon substitutions there is a doubling in potency by increasing the carbon length from one carbon ( $\pm$ )-**30** to three carbons ( $\pm$ )-**52**  $K_i = 81 \text{ pM}$  and  $42 \text{ pM}$ , respectively. The increase in chain length may enhance potency through lipophilic interactions within the Ar2 domain. It is interesting to note that there is relatively no change in potency between PROM-NQP ( $\pm$ )-**51** and ( $\pm$ )-MOM-NQP ( $\pm$ )-**31** ( $K_i = 2.12$  and  $2.48 \text{ pM}$ , respectively), perhaps the presence of a hydrogen bond acceptor far out weighs the chain length. Replacement of a terminal hydrogen of *n*-PROP-NQP **52** with a fluorine atom to give PROF-NQP **58** ( $K_i = 2.5 \text{ pM}$ ) increased potency by 17 times further substantiating the benefit of an H-bonding acceptor. It is interesting to note that the propyl hydroxyl version HOP-NQP **147** shows a ~25 times drop in potency ( $K_i = 50 \text{ pM}$ ) compared to PROM-NQP ( $\pm$ )-**51** and ( $\pm$ )-MOM-NQP ( $\pm$ )-**31**. Additionally the methyl alcohol HOM-NQP **38** showed a 6 fold decrease in

potency compared to MOM-NQP (**±**)-**31**. It seems that the presence of a hydrogen bonding donor is not well tolerated in the Ar2 binding domain. The binding potency of PROF-NQP **58** and MePROF-NQP **148** bode well for their use as potential PET imaging agents.

**Table 4-2:** Chiral 2-(2-alkyl-piperazin-1-yl)-6-nitroquiolines, compound name and R-group are given as well as their associated binding inhibition constant ( $K_i$ ), and CLogP(o/w) value.



	Name	R	$K_i$ (pM)	Ref
<b>(±)-30</b>	(±)-Me-NQP	CH <sub>3</sub>	81 ± 61	67
<b>(R)-30</b>	(R)-(-)-Me-NQP	"	91 ± 16	73
<b>(S)-30</b>	(S)-(+)-Me-NQP	"	68 ± 21	"
<b>(±)-31</b>	(±)-MOM-NQP	CH <sub>2</sub> OCH <sub>3</sub>	2.48 ± 0.28	72
<b>(R)-31</b>	(R)-(+)-MOM-NQP	"	47*	74
<b>(S)-31</b>	(S)-(-)-MOM-NQP	"	1*	"

\*Preliminary Values

To further expand upon our SERT SAR the enantiomeric forms of (±)-Me-NQP **30** and (±)-MOM-NQP **31** were evaluated for their respective SERT binding affinities (Table 4-2). Comparison of the enantiomers (**R**)-**30** and (**S**)-**30** binding affinity at rSERT ( $K_i = 91 \pm 16$  pM and  $68 \pm 21$  pM) shows no significant difference in SERT preference for either enantiomer. Perhaps the methyl group is not long enough to evoke a definite preference at the SSRI binding domain. Initial binding affinity values of the (**R**)-**31** and (**S**)-**31** enantiomers ( $K_i = 47$  pM and 1 pM, respectively) shows a 47 times higher affinity for (**S**)-**31**. This is encouraging; suggesting that in there is a receptor preference for one enantiomer, which is similar to the results seen for citalopram **7** and fluoxetine **10**.

### 4.3 Synthesis of *n*-PROP-NQP 52 and [<sup>3</sup>H]*n*-PROP-NQP.

Our interests in developing a PET imaging agent for SERT lead us to investigate the binding kinetics of our 2-(2-alkyl-piperazin-1-yl)-6-nitroquinoline analogs with the SERT protein. In addition we wanted to assess the selectivity of our ligands for SERT relative to the other biogenic amine transporter targets within the CNS. To accomplish these evaluations we investigated the possibility of generating a tritium labeled compound based upon our 2-(2-alkyl-piperazin-1-yl)-6-nitroquinoline analog series. When examining our library of compounds we decided that *n*-PROP-NQP 52 would be an excellent analog for the preparation of a tritiated [<sup>3</sup>H]2-(2-alkyl-piperazin-1-yl)-6-nitroquinoline. Since 52 was complete with a propyl side chain it could act as a good representative analog compared to the balance of our compound library, particularly 58.

Initially *n*-PROP-NQP 52 was considered a side product of the PROM-NQP (±)-51 synthesis. However, the synthesis of 52 and related binding affinity for SERT was fortuitous. We proposed that 52 could be used as a pharmacological tool for assessing the binding kinetics of our ligand series as well as selectivity of our ligand series for SERT over other monoamine transporters, i.e. DAT and NET. Additionally, 52 is good replacement for PROF-NQP 58 based upon the similarity of the side chain length and lipophilicity between 52 and 58 (Figure 4-2).

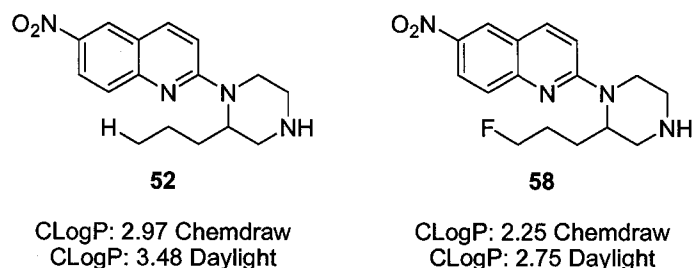
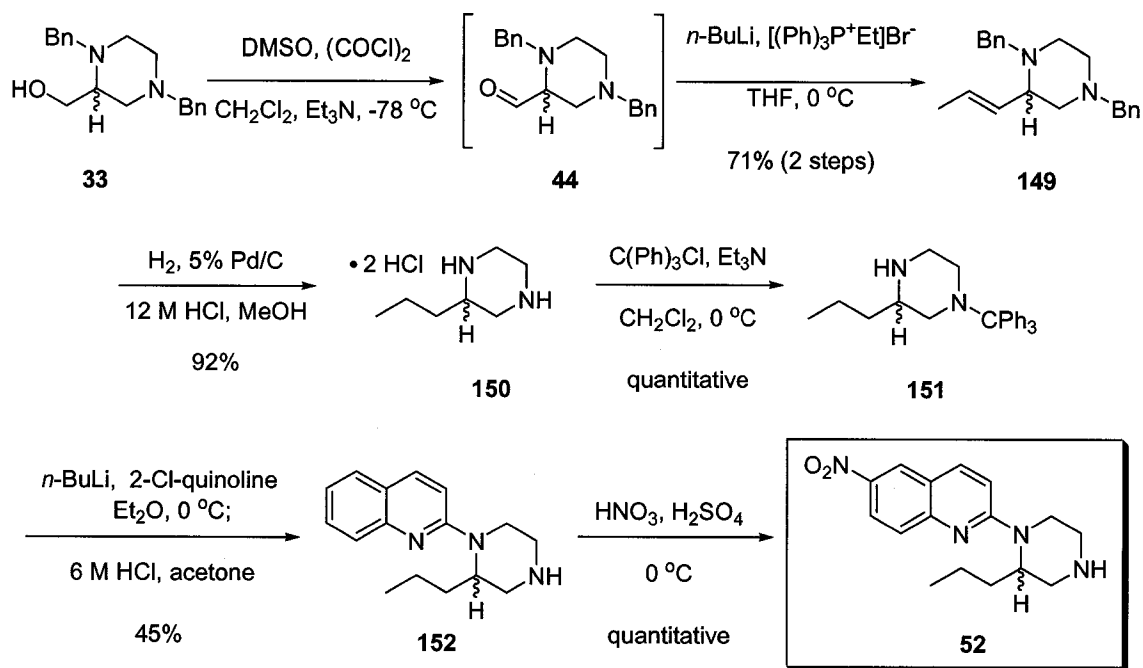


**Figure 4-2:** Structure and CLogP comparison of *n*-PROP-NQP **52** and PROF-NQP **58**.

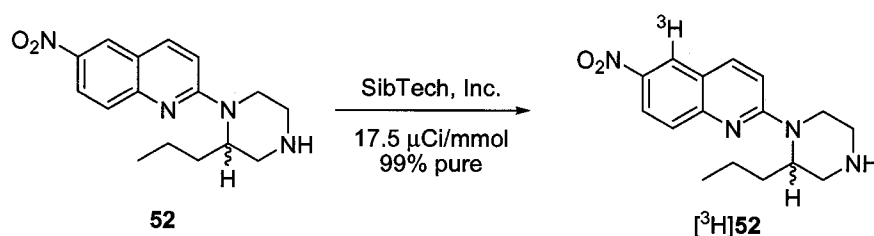
Determination of the in vitro binding kinetics using the [<sup>18</sup>F]PROF-NQP **58** agent would be more desirable,<sup>114</sup> but due to the difficulties of preparing [<sup>18</sup>F]PROF-NQP **58** analog at the time of this study, *n*-PROP-NQP **52** was a more desirable agent.

As shown in Scheme 4-1, the synthesis of the **52** began with the Swern oxidation of dibenzyl alcohol **33** to the aldehyde **44**, followed by Wittig olefination with ethyl-triphenylphosphonium bromide to give **149** (71%, 2 steps). Hydrogenolysis of the benzyl groups and simultaneous hydrogenation of the alkene with 5% Pd/C and HCl in MeOH, (atmospheric pressure) gave the *n*-propyl piperazine dihydrochloride **150** in a 92% yield. The piperazine was protected with triphenylmethane chloride to give **151**, then coupled to 2-chloroquinoline, deprotected (**152**, 45%, 2 steps) and then selectively nitrated at the 6-position to give the desired *n*-PROP-NQP **52** in a quantitative yield. The *n*-PROP-NQP **52** target was synthesized from the common intermediate dibenzyl-alcohol **33** affording 2-(2-propylpiperazin-1-yl)-6-nitroquinoline **52** in 7 steps and a 29% overall yield.



**Scheme 4-1:** Synthesis of 2-(2-propylpiperazin-1-yl)-6-nitroquinoline **52** (*n*-PROP-NQP).

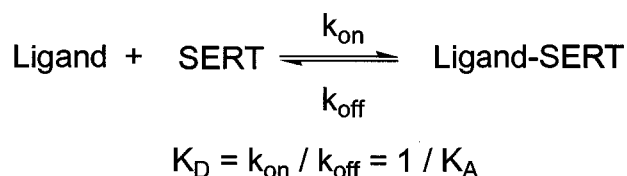
Upon completion of the synthesis of **52**, it was shipped to SibTech, Inc. (Newington, CT) and radiolabeled with tritium. This was accomplished by aromatic halogenation of the quinoline ring, followed by dehalogenation-tritium exchange to give [<sup>3</sup>H]**52**, with a specific activity of 17.5 μCi/mmol, and a chemical purity of 99% (Scheme 4-2).



**Scheme 4-2:** Radiosynthesis of [<sup>3</sup>H]-2-(2-propylpiperazin-1-yl)-6-nitroquinoline **52** ([<sup>3</sup>H]-*n*-PROP-NQP).

#### 4.4 In Vitro SERT Binding Studies [<sup>3</sup>H]-*n*-PROP-NQP 52.

In this study our aim was to examine the in vitro binding characteristics and receptor selectivity of the radiolabeled SERT inhibitor [<sup>3</sup>H]*n*-PROP-NQP 52 prepared according to Schemes 4-1 and 4-2. We were interested in determining the equilibrium dissociation constant ( $K_D$ ), binding site density ( $B_{max}$ ), association and dissociation rate constants ( $k_{on}$  and  $k_{off}$ ), and to assess the selectivity of [<sup>3</sup>H]52 for rSERT. The equilibrium dissociation constant ( $K_D$ ) is useful to describe a ligand's affinity for a given binding domain, considering  $K_D$  is the reciprocal of binding affinity  $K_A$  ( $K_A = 1/K_D$ ).<sup>115</sup> A lower the  $K_D$  value represents higher affinity of the ligand for the receptor and at equilibrium if the  $K_D$  value is small the dissociation of the ligand-protein complex will be slower. The association rate constant ( $k_{on}$ ) is a measure of how fast the ligand-receptor complex is formed. The dissociation rate constant ( $k_{off}$ ) is a measure of how tightly the ligand is bound to the receptor. A low  $K_D$  and a slow dissociation ( $k_{off}$ ) of the ligand-receptor complex are thought to be favorable for a SERT imaging agent. Additionally, fast association is desirable to establish binding equilibrium at the receptor relatively quickly to benefit the imaging experiment. The  $K_D$  values can be determined kinetically from the rate constants  $k_{on}$  and  $k_{off}$  where  $K_D = k_{off}/k_{on}$  and from saturation equilibrium binding studies.



Measurement of the dissociation constants ( $K_D$ ) were performed according to the published procedures.<sup>13,110,111</sup> The association rate constant ( $k_{on}$ ) and the time to reach binding equilibrium was determined by incubation of the radioligand [ $^3H$ ]52 (200 pM) with the rSERT membrane preparation at 21 °C and 37 °C for varying amounts of time (10 minutes – 4 hours). From the plot of association (Figure 4-3), the apparent equilibrium time was determined to be between 2-3 hours. The time to reach apparent equilibrium is in agreement with a structurally related compound [ $^{125}I$ ]5-iodo-6-nitroquipazine **23** as previously reported.<sup>110</sup> The observed association constant ( $k_{obs}$ ) of [ $^3H$ ]52 was determined from the formula  $\ln[B_e / (B_e - B_t)] = k_{obs} \cdot t$ , where  $B_e$  is specific binding at equilibrium, and  $B_t$  is specific binding at time  $t$  (Figure 4-3).

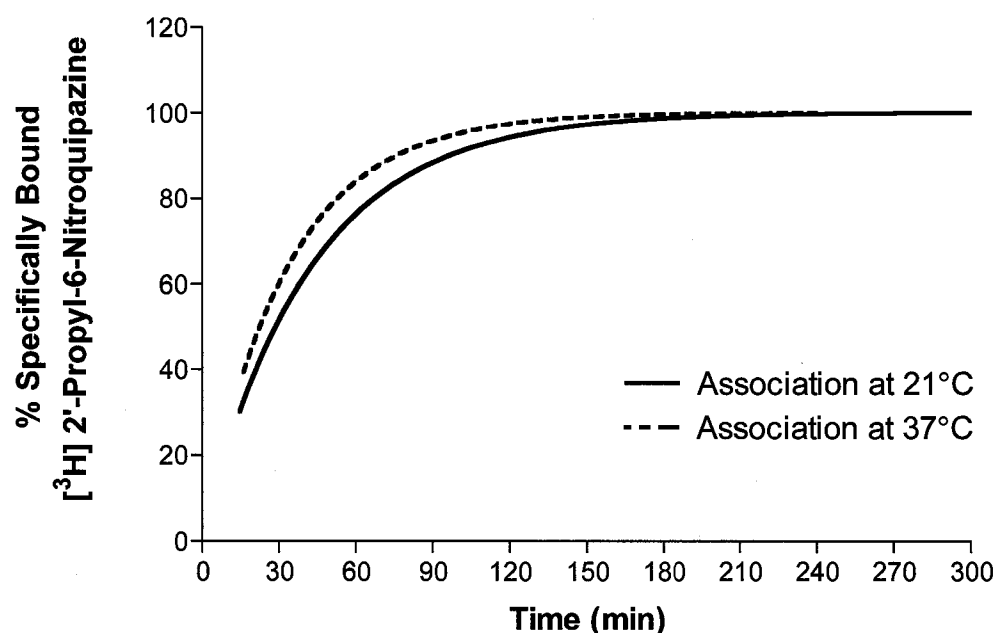
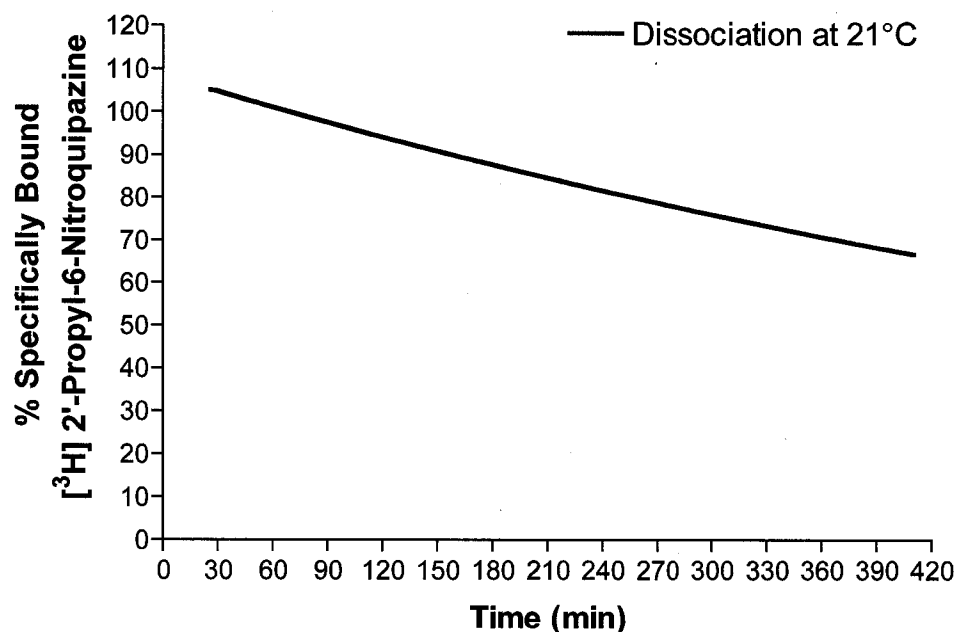


Figure 4-3: Time course association plots of [ $^3H$ ]-*n*-PROP-NQP **52** at 21 °C.



The dissociation rate constant ( $k_{off}$ ) was determined by treatment of the incubation medium with 1.0  $\mu$ M of the non-radioactive form **52**, 3 hours after the addition of [ $^3$ H]**52** (Figure 4-4). The dissociation rate constant ( $k_{off}$ ) was calculated from the formula;  $\ln[B_t / B_e] = -k_{off} \cdot t$  and the results are shown in Figure 4-4.



**Figure 4-4:** Time course dissociation plots of [ $^3$ H]-*n*-PROP-NQP **52** at 21 °C.

The association rate constant was determined from the relationship  $k_{on} = (k_{obs} - k_{off}) / [L]$ , where  $[L]$  is the concentration of unbound **52**. From  $k_{on}$  and  $k_{off}$  the kinetically derived dissociation constant ( $K_D$ ) can be calculated according to  $K_D = (k_{off} / k_{on})$ . The calculated values for  $K_D$ ,  $k_{on}$  and  $k_{off}$  are outlined in Table 4-3 and compared to the SERT selective 6-nitroquinoline analog [ $^{125}$ I]5-iodo-6-nitroquinoline **23** ([ $^{125}$ I]INQP) and the SSRIs (+)-MCN5652 **6** and (S)-citalopram **7**.

**Table 4-3:** Comparison of the kinetically derived dissociation constants ( $K_D$ ), the rate constants of association ( $k_{on}$ ) and dissociation ( $k_{off}$ ) for [ $^3H$ ]-*n*-PROP-NQP **52** and select SSRIs at 21 °C.

°C	Name	$K_D$ (pM)	$k_{on}$ (mol <sup>-1</sup> min <sup>-1</sup> )	$k_{off}$ (min <sup>-1</sup> )	Ref
21°	[ $^3H$ ] <b>52</b> <i>n</i> -PROP-NQP	8.5	$1.1 \times 10^8$	$9.4 \times 10^{-4}$	Weller, 2003
	[ $^{125}I$ ] <b>23</b> INQP	7.9	$4.8 \times 10^8$	$3.8 \times 10^{-4}$	Mathis, 1993
	[ $^3H$ ] <b>6</b> (+)-MCN5652	80	$3.6 \times 10^8$	$3.1 \times 10^{-3}$	Elfving, 2001
	[ $^3H$ ] <b>7</b> (S)-Citalopram	310	$4.9 \times 10^7$	$1.2 \times 10^{-2}$	Elfving, 2001

Comparison of the  $K_D$  value determined for [ $^3H$ ]*n*-PROP-NQP **52** (8.42 pM) to the  $K_D$  values of other SSRIs ([ $^{125}I$ ]INQP **23**, [ $^3H$ ]-(+)-MCN5652 **6**, and [ $^3H$ ]-(*S*)-citalopram) showed [ $^3H$ ]**52** had comparable binding potency to the structurally related quipazine agent INQP **23** (7.9 pM) at 21 °C (Table 4-3). Also, [ $^3H$ ]**52** has a much higher affinity for rSERT (lower  $K_D$ ) compared to the SSRIs MCN5652 **6** and citalopram **7** (21 °C). The rate of association ( $k_{on}$ ) at 21 °C of [ $^3H$ ]**52** is essentially equivalent to that of [ $^{125}I$ ]INQP **23** and [ $^3H$ ]-(+)-MCN5652 **6**, but was an order of magnitude faster than [ $^3H$ ]-(*S*)-citalopram **7**. The dissociation rate ( $k_{off}$ ) of [ $^3H$ ]**52** was slightly faster than [ $^{125}I$ ]INQP **23**, but slower than [ $^3H$ ]-(+)-MCN5652 **6**, and [ $^3H$ ]-(*S*)-citalopram **7** (21°C). The comparison of binding potency ( $K_D$ ), association rate ( $k_{on}$ ) and dissociation rate ( $k_{off}$ ) at 21 °C suggest that the 2-(2-alkyl-piperazin-1-yl)-6-nitroquinoline analogs will have good in vitro binding properties for use as PET imaging agents.<sup>39</sup> The slower dissociation rate of [ $^3H$ ]**52** at 21 °C compared to [ $^3H$ ]-(+)-MCN5652 **6** and [ $^3H$ ]-(*S*)-citalopram **7**, is thought to be important for the imaging of medium to low SERT density regions.

#### **4.5 Determination of the Apparent Equilibrium Dissociation Constant ( $K_D$ ) and Receptor Density ( $B_{max}$ ).**

Determination of the receptor density ( $B_{max}$ ) and the apparent equilibrium dissociation constant ( $K_D$ ) were determined from saturation studies of the crude rat brain membrane preparation with the radiolabeled compound [ $^3H$ ]52, according to the methods of Mathis and Habert.<sup>110,111</sup> In brief, the crude membrane preparations were treated with increasing concentrations of [ $^3H$ ]52 (0.001 – 2.5 nM) in the absence and presence of 1 mM paroxetine (to establish non-specific binding) and incubated for three hours at 21 °C. The samples were filtered and counted as described above. An example plot of the saturation experiments is shown (Figure 4-5). From the saturation binding isotherm we were able to calculate the apparent equilibrium  $K_D = 38$  pM and  $B_{max} = 395$  fmol/mg of protein, using the iterative least squares curve fitting program Prism (Graphpad).

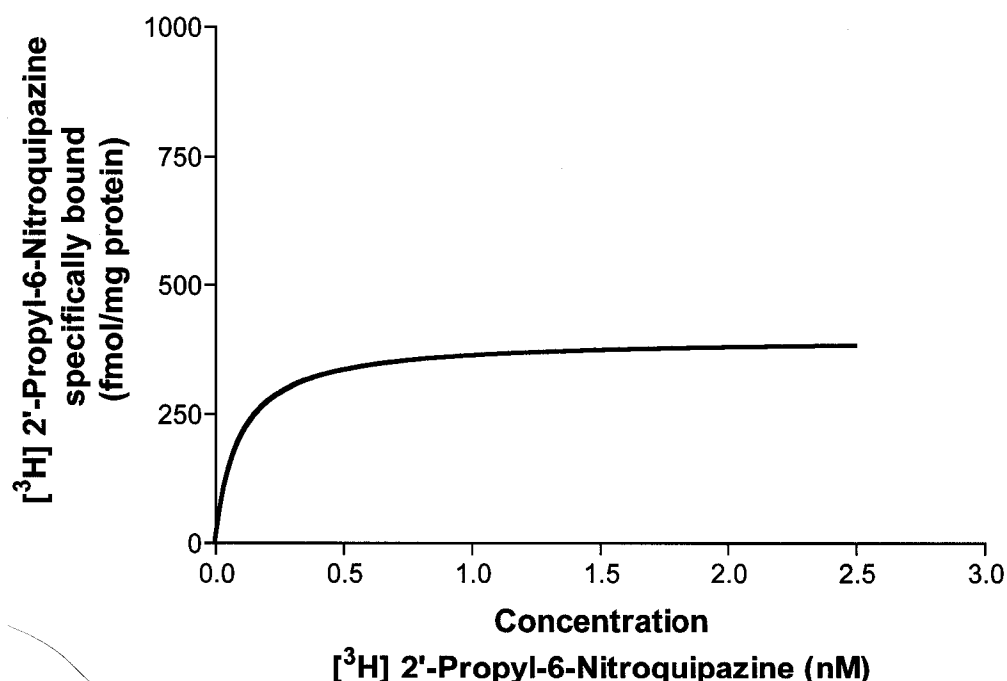


**Figure 4-5:** Saturation binding isotherm of [<sup>3</sup>H]-*n*-PROP-NQP 52 binding with rSERT at 21 °C.

The  $K_D$  (38 pM) determined for [<sup>3</sup>H]52 is similar to the equilibrium derived  $K_D$  determined for the structurally related analog [<sup>125</sup>I]INQP 23 (23 pM) and slightly larger than that of the kinetically derived  $K_D$  for [<sup>3</sup>H]52 (8.5 pM). The  $B_{max}$  value determined in our saturation studies is consistent with other rSERT saturation measures (~400 fmol/mg protein).<sup>13,110</sup>

#### 4.6 SERT Selectivity of [<sup>3</sup>H]-*n*-PROP-NQP 52.

The labeled form of [<sup>3</sup>H]52 was also useful for examining and estimating the selectivity of the 2-(2-alkyl-piperazin-1-yl)-6-nitroquioline ligands for the SERT binding site. The SERT selectivity assays are outlined in Table 4-4, the ligand name, competitive binding affinity ( $K_i$ ) and ligand classification are included. For the selectivity assays we used known selective agents for the

biogenic amine transporters, these are classified as either a serotonin selective reuptake inhibitor (SSRI), dopamine reuptake inhibitor (DRI), norepinephrine reuptake inhibitor (NRI), or SSRI (quipazine). The assays were performed by adding a solution of the unlabelled test agent to the rat membrane preparation containing [<sup>3</sup>H]52 and assay buffer. Total binding was determined by treatment of the membrane preparation with [<sup>3</sup>H]52 in the absence of any competitive ligand. Competitive drugs were screened at varying concentrations (1 μM – 10 pM), the results were plotted and the K<sub>i</sub> values were determined using Prism, utilizing the kinetically derived K<sub>D</sub> of [<sup>3</sup>H]52 at 20 °C (8.42 pM). Non-specific binding was determined in the presence of 1 μM 6-NQP 22. The ligands tested are summarized in Table 4-4 with their associated inhibition constants.

**Table 4-4:** Inhibition constants (K<sub>i</sub>) for select CNS agents inhibiting the binding of [<sup>3</sup>H]-*n*-PROP-NQP 52 with rSERT.

Cmpd #	Name	K <sub>i</sub> (nM)	
6	(+)-MCN5652	0.19 ± 0.04	SSRI
7	(S)-Citalopram	1.96 ± 0.59	SSRI
9	Paroxetine	0.27 ± 0.08	SSRI
153	GBR12935	> 500	DRI
154	Nisoxetine	> 10,000	NRI
58	PROF-NQP	0.0056 ± 0.0002	SSRI (Quipazine)
52	<i>n</i> -PROP-NQP	0.0018 ± 0.0005	SSRI (Quipazine)
(±)-31	MOM-NQP	0.03 ± 0.01	SSRI (Quipazine)

The ligands tested include the SSRIs (+)-MCN5652 6, citalopram 7 and paroxetine 9 the selective DAT inhibitor GBR-12935 (not shown) and the selective NET inhibitor nisoxetine (not shown). Included in this study were a select group of 2-(2-alkyl-piperazin-1-yl)-6-nitroquinolines prepared in our lab, including; PROF-NQP 58, MOM-NQP (±)-31, and PROP-NQP 52. The results shown in Table 4-4 are indicative that [<sup>3</sup>H]52 is binding at the same SERT

binding domain as the known SSRIs, (+)-MCN5652 **6**, citalopram **7** and paroxetine **9**. Additionally, [<sup>3</sup>H]**52** is selective for SERT based upon challenging with known selective DAT and NET inhibitors. Also, based upon the potent inhibition constants (low nanomolar range) of the 2-(2-alkyl-piperazin-1-yl)-6-nitroquinolines (**±**)-**31**, **52** and **58**, it is indicative that those ligands have potent rSERT affinity. The selectivity and binding profiles of the quipazine ligands indicate that these ligands will likely show very good in vivo characteristics for PET imaging of low SERT density regions of the brain.

#### 4.7 Summary.

Competition assay ([<sup>3</sup>H]paroxetine, **9**) of the 2-(2-alkyl-piperazin-1-yl)-6-nitroquinolines (Table 4-1 and Table 4-2) show an overall increase in binding affinity compared to the lead agent 6-NQP **22**. From these studies we can infer that a hydrogen bonding acceptor located in the alkyl chain will benefit binding affinity. For example (**±**)-**31**, (**±**)-**51**, **58**, and (**±**)-**83** all showed affinity for SERT in the 2 pM range. This is a much higher affinity when compared to the all carbon analogs **52**, and (**±**)-**30** whose affinities were >20 times less potent. We can also comfortably say that the presence of a hydrogen bonding donor is detrimental to binding, HOM-NQP **38** and HOP-NQP **147** both show a decrease in binding affinity compared to their respective ether analogs. The in vitro studies of [<sup>3</sup>H]**52** demonstrate the selectivity and binding affinity of [<sup>3</sup>H]**52** for SERT. The in vitro kinetic data ( $K_D$ ,  $k_{on}$  and  $k_{off}$ ) for [<sup>3</sup>H]**52** is representative of the kinetics we expect for our analog series. This data suggests that a fluorine-18 radioligand derivative

of a 2-(2-alkyl-piperazin-1-yl)-6-nitroquoline analog, such as PROF-NQP **58** could prove to be a useful ligand for PET imaging studies; especially considering that **58** exhibits a higher binding affinity (2.5 pM) compared to **52** (42 pM), in addition to its implied SERT selectivity.

## Chapter 5

### Conclusions and Future Work

The syntheses of seven new 2-(2-alkyl-piperazin-1-yl)-6-nitroquinoline racemic analogs of 6-NQP **22** have been completed, including PROM-NQP ( $\pm$ )-**51**, HOP-NQP **147**, PROF-NQP **58**, *n*-PROP-NQP **52**, Pent-NQP ( $\pm$ )-**83**, PentF-NQP **88**, and BuM-NQP **96**. Of these analogs all except BuM-NQP **96** have been evaluated for their in vitro binding affinity for rSERT by radioligand competition assay (rSERT, [ $^3\text{H}$ ]paroxetine **9**) as outlined in Chapter 4. The 2-(2-alkyl-piperazin-1-yl)-6-nitroquinolines ligands tested show higher binding affinity ( $K_i = 1\text{-}80\text{ pM}$ ) for rSERT compared to the lead SSRI 6-NQP **22** ( $K_i = 160\text{ pM}$ ). This initial SAR study of the quipazine ligands prepared during this work suggests that probing of the Ar2 binding domain of our pharmacophore model, with alkyl chain moieties at the piperazine 2-position of the quipazine base structure, is a useful method for preparing new more potent quipazine ligands.

The presence of hydrogen bonding acceptor moieties (methoxy ether and alkylfluoride) in the alkyl chain is beneficial to ligand binding and the inverse is seen for the presence of hydrogen bond donating moieties, i.e. hydroxyl. Overall, the presence of any alkyl chain results with increased binding affinity of the analogs for rSERT. At this time, the SAR indicates that a chain length of 3-5 atoms is acceptable as can be seen in the respective binding affinities of MOM-NQP ( $\pm$ )-**31** and the propyl series ligands ( $\pm$ )-**51**, **52**, **58**, and **147** (Table 4-1). Further assessments of the racemic butyl and pentyl series will extend our knowledge of the chain length limits for SERT binding.



To expand our SAR studies the (*R*)- and (*S*)-enantiomers of MOM-NQP (**±**-31), PROM-NQP (**±**-51) and Pent-NQP (**±**-83) were synthesized. Unfortunately, only the enantiomers of MOM-NQP (*R*-31 and *S*-31) have been evaluated for their associated rSERT affinity at the time of this writing. The initial studies show a difference in potency of (*R*-31 and *S*-31), suggesting that the (*S*)-enantiomer ( $K_i = 1 \text{ pM}$ ) is more potent for SERT than the (*R*)-enantiomer ( $K_i = 47 \text{ pM}$ ). This trend could be further evaluated using the enantiomers of PROM-NQP and Pent-NQP (*R*-51, *S*-51, *R*-83 and *S*-83). The syntheses of the chiral forms of PROF-NQP 58, PentF-NQP 88, BuM-NQP 96 and the related BuF-NQP (not shown) should be accomplished to afford a complete ligand series. As per the experimental section the final compounds of the chiral propyl and pentyl series (*R*-51, *S*-51, *R*-83 and *S*-83) have been analyzed for their optical rotations. The measures are indicative that the final compounds have retained their enantiomeric purity within reasonable experimental error. The final chiral forms of the pentyl series (*R*-83 and *S*-83) require more analysis when larger quantities have been prepared. However, more rigorous determination of enantiomeric purity should be completed by chiral HPLC, gas chromatography (GC) or spectroscopically (Mosher amide). Furthermore, each enantiomer and the untested racemic forms should be analyzed for their respective SERT binding affinities. Completion of the analog series and pharmacological analysis will give a more complete understanding of our SERT ligand SAR studies.

The tritium labelled ligand [ $^3\text{H}$ ]52 was prepared as a representative ligand to assess the *in vitro* binding characteristics and receptor selectivity of our

quipazine ligand family. Ligand [<sup>3</sup>H]52 was shown to have superior in vitro kinetic values ( $K_D$ ,  $k_{on}$  and  $k_{off}$ ) for SERT binding than the SSRIs (+)-MCN5652 **6** and (S)-citalopram **7**. Comparison of [<sup>3</sup>H]52 to the structurally related analog [<sup>125</sup>I]INQP **23** shows a similar equilibrium dissociation constant ( $K_D$ ) value. This suggests that our ligand family will show similar receptor selectivity and the in vitro kinetic data looks promising for in vivo imaging. We believe that a radioligand, i.e. [<sup>18</sup>F]PROF-NQP **58** will show far superior in vivo characteristics based upon the lipophilicity of **58** (LogP ~2.5) and binding affinity for rSERT ( $K_i$  = 2.5 pM).

Furthermore, based on the radiofluorination trials with N-Boc-ProTos-NQP the N-formyl-ProTos-NQP radiolabeling precursor should be reevaluated for its potential to provide the radioligand [<sup>18</sup>F]PROF-NQP **58**. Also, it would be very interesting to determine if the fluoride substitution of the aromatic nitro group is occurring during the radiofluorination. This could be accomplished by synthesizing more of the nonradioactive side product **73** and having it chromatographically tested against the crude mixture from the radiofluorination of N-Boc-ProTos-NQP **69**, under the K222 conditions that gave a 1:1 mixture of the two fluorinated products (based upon radioactive TLC) and with the TBAF conditions that favored the formation of the side product (based upon radioactive TLC).

## Chapter 6

### Experimental Section

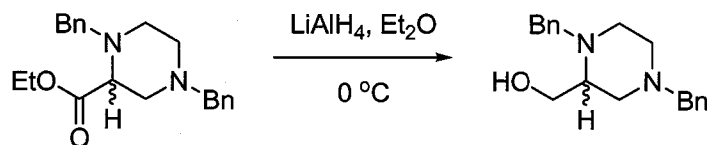
#### 6.1 General Experimental.

Reactions utilizing dry solvents were performed in oven-dried glassware under an atmosphere of argon. Reagent grade chemicals and solvents were purchased from commercial suppliers (Aldrich, Fisher and VWR) and used without further purification or treatment unless otherwise noted. Methyltriphenylphosphonium iodide was prepared according to the method of McCortney, 1990.<sup>116</sup> Tosyl chloride was purified according to Armarego.<sup>117</sup> Dry solvents (ACN, THF, Et<sub>2</sub>O, DMF and CH<sub>2</sub>Cl<sub>2</sub>) were purchased from J.T. Baker, EMD science, and Acros, and used without further treatment. The concentration of *n*-BuLi (Aldrich) was estimated according to the method of Kofron.<sup>118</sup>

NMR spectra <sup>1</sup>H and <sup>13</sup>C were obtained using a Varian-Unity spectrometer operating at 400 MHz and 100 MHz respectively. Chemical shifts were recorded in parts per million (ppm, δ) and were reported relative to the solvent peak of CHCl<sub>3</sub> (7.26 ppm). High resolution mass spectra (HRMS) were obtained using an electrospray ionization (ESI) Micromass LCT connected to a Water 2790 HPLC. Optical rotations were determined at ambient temperature utilizing a Perkin-Elmer 241 polarimeter at the sodium D-line (589 nm) and a 10 cm (1 dm) cell. Specific rotations were calculated using the relationship  $[\alpha]_D^{20} = \alpha / L \cdot c$ ; where α is the observed rotation, L is the path length and c is the concentration in grams solute / solution volume (g/mL). Column chromatography was

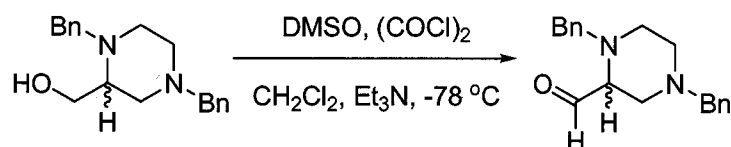
performed using EM Science, Silica gel 60 (230-400 mesh ASTM). Reactions were monitored by TLC using EM Science 20 x 20 cm Silica gel 60 F<sub>254</sub> aluminum backed plates. Compound spots were detected visually by ultraviolet light at 254nm and 365 nm or by staining with ninhydrin (0.3 g ninhydrin, 100 mL EtOH, 3 mL AcOH) or vanillin (15 g vanillin, 250 mL EtOH, 2.5 mL H<sub>2</sub>SO<sub>4</sub>) developed by heating. Reactions were performed at room temperature 21-25 °C (RT °C) unless otherwise specified. All pH determinations were performed using EM ColorpHast pH strips. All organic extractions were dried with K<sub>2</sub>CO<sub>3</sub> and filtered before concentration unless otherwise specified. Biotage purification was carried out on a Biotage Sp1 high-performance flash chromatography system (Biotage, Charlottesville, VA) equipped with a Biotage NH normal phase Flash column (12-M). Elution solvents were; solvent A: hexanes and solvent B: EtOAc. The flash column was pre-equilibrated with 10% B at 10 mL/min.

## 6.2 Racemic Propyl Series



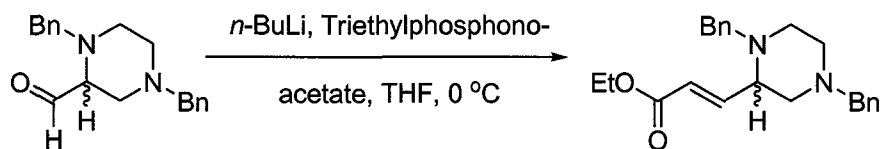
**1,4-Dibenzyl-2-hydroxymethylpiperazine (33).** A suspension of LiAlH<sub>4</sub> (1.53 g, 40.3 mmol) in dry ether (80 mL) was treated with a solution of ethyl 1,4-dibenzylpiperazine-2-carboxylate **32** (11.4 g, 33.6 mmol) in dry ether (30 mL) at 0 °C under argon, maintaining a gentle effervescence. The reaction was stirred for

30 min and the ice bath was removed. Stirring was continued at 25 °C for 1 hour. The reaction was quenched by consecutive addition of H<sub>2</sub>O (1.5 mL), NaOH (3 mL 3 M) and H<sub>2</sub>O (1.5 mL); the inorganic salts were filtered over a pad of Celite, and the pad was rinsed with EtOAc. The filtrate was concentrated *in vacuo* to give **33** as a clear oil (9.45 g, 96%): TLC  $R_f$  = 0.33 (1:9 MeOH/CH<sub>2</sub>Cl<sub>2</sub>); <sup>1</sup>H NMR (CDCl<sub>3</sub>, 400 MHz) δ 2.30-2.73 (3m, 7H), 2.95 (m, 1H), 3.39-3.67 (m, 4H), 3.93-4.14 (m, 2H), 7.20-7.40 (m, 10H); <sup>13</sup>C NMR (CDCl<sub>3</sub>, 100 MHz) δ 49.8, 52.4, 56.0, 58.0, 58.5, 62.1, 63.1, 127.0, 127.2, 128.3, 128.8, 129.1, 137.5, 138.0.



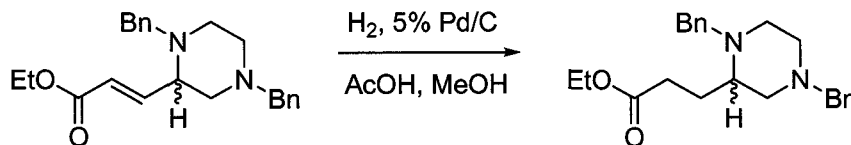
**1,4-Dibenzyl-piperazine-2-carboxaldehyde (44).** DMSO (3.5 g, 44.6 mmol) in dry CH<sub>2</sub>Cl<sub>2</sub> (15 mL) was added dropwise to a solution of oxalyl chloride (2 M in CH<sub>2</sub>Cl<sub>2</sub>, 17.7 mL, 35.4 mmol) in dry CH<sub>2</sub>Cl<sub>2</sub> (80 mL) at -78 °C (dry ice, acetone bath). After 5 min a solution of 1,4-dibenzyl-2-hydroxymethyl-piperazine **33** (9.45 g, 32.14 mmol) in dry CH<sub>2</sub>Cl<sub>2</sub> (30 mL) was added dropwise, the solution was allowed to stir for an additional 20 min. The reaction was treated with Et<sub>3</sub>N (16.3 g, 160.7 mmol), forming a tan precipitate and allowed to stir for 5 min. The mixture was allowed to warm to room temperature and stir for 1 hour. The reaction was quenched by the addition of water (100 mL), the organics were separated and the aqueous phase was extracted with CH<sub>2</sub>Cl<sub>2</sub> (75 mL). The combined organics were washed with saturated NaHCO<sub>3</sub> (50 mL), dried with

$K_2CO_3$  and concentrated *in vacuo*. The aldehyde was used in the next step without further purification: TLC  $R_f = 0.69$  (1:9 MeOH/ $CH_2Cl_2$ ).

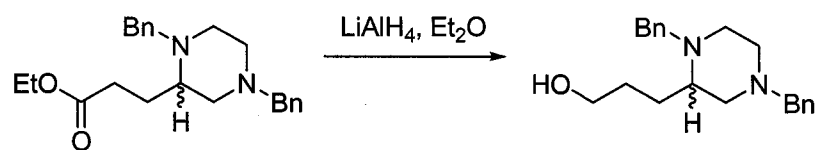


**3-(1,4-Dibenzyl-piperazin-2-yl)-acrylic acid ethyl ester (45).** A stirred solution of  $n\text{-BuLi}$  (17 mL, 2.45 M in hexanes, 40.8 mmol) in dry THF (30 mL) was treated with triethylphosphonoacetate (9.1 g, 40.8 mmol) at  $0\text{ }^\circ\text{C}$  under argon, to give a light yellow solution. After 15 min a solution of 1,4-dibenzyl-piperazine-2-carbaldehyde **44** (6.0 g, 20.4 mmol) in dry THF (10 mL) was added dropwise to the cooled solution. The reaction mixture was allowed to warm to room temperature and to stir for 20 h. The reaction was quenched by the addition of water (25 mL) and concentrated *in vacuo* to remove THF. The aqueous layer was treated with 20 mL of sat.  $\text{NaHCO}_3$  and extracted with  $\text{CH}_2\text{Cl}_2$  (3 x 20 mL). The combined organics were washed with brine (20 mL), dried ( $K_2CO_3$ ) and concentrated *in vacuo*. The crude orange oil was purified by column chromatography over silica gel (80 g) loaded with  $\text{CHCl}_3$  eluted with 1:9 EtOAc/hexanes followed by 1:3 EtOAc/hexanes to elute **45** as a light tan oil (4.6 g, 64% 2 steps): TLC  $R_f = 0.63$  (MeOH: $\text{CH}_2\text{Cl}_2$ , 1:9) or  $R_f = 0.36$  (2:3 EtOAc/hexanes);  $^1\text{H}$  NMR ( $\text{CDCl}_3$ , 400 MHz)  $\delta$  1.29 (t,  $J = 7.1$  Hz, 3H), 2.10-2.30 (2m, 3H), 2.60-2.77 (2m, 3H), 3.12 (m, 1H), 3.50 (dd,  $J = 13.3$  and  $17.5$  Hz, 2H), 3.91 and 3.12 (2d,  $J = 13.6$  Hz, 2H), 4.19 (q,  $J = 7.1$  Hz, 2H), 6.04 (d,  $J = 15.9$  Hz, 1H), 6.98 (dd,  $J = 8.4$  and  $15.9$  Hz, 1H), 7.20-7.35 (m, 10H);  $^{13}\text{C}$  NMR

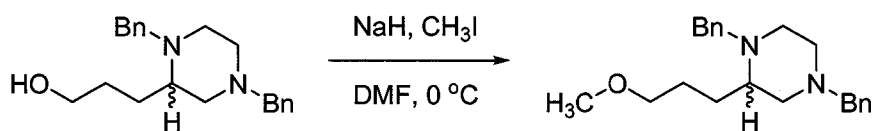
(CDCl<sub>3</sub>, 100 MHz)  $\delta$  50.6, 52.8, 58.0, 59.7, 60.4, 62.8, 123.8, 126.9, 127.1, 128.1, 128.2, 128.9, 129.1, 137.7, 138.3, 148.6, 166.1.



**3-(1,4-Dibenzyl-piperazin-2-yl)-propionic acid ethyl ester (55).** 5% Pd/C (0.9 g) was added to a solution of 3-(1,4-Dibenzyl-piperazin-2-yl)-acrylic acid ethyl ester **45** (4.5 g, 12.4 mmol) in HPLC grade MeOH (60 mL) and acetic acid (3.7 g, 61.8 mmol). The reaction flask was sealed with a septum, fitted with a hydrogen balloon and a bleed needle. One balloon of hydrogen was bubbled through the stirred solution the needle was removed and a second balloon was attached. The reaction was stirred overnight, then filtered over a pad of Celite, rinsing with MeOH and concentrated *in vacuo*. The oil was dissolved in CH<sub>2</sub>Cl<sub>2</sub>, free based with 4M NaOH to pH 12 then buffered to pH 10 with sat. NaHCO<sub>3</sub>. The organics were separated and the aqueous layer was extracted with CH<sub>2</sub>Cl<sub>2</sub> (3 x 20 mL). The organic portions were combined, dried (K<sub>2</sub>CO<sub>3</sub>) and concentrated *in vacuo*. The crude oil was purified by column chromatography over silica gel (44 g) loaded with CHCl<sub>3</sub> and eluted with 1:3 EtOAc/hexanes to give **55** as clear oil (3.5 g, 78%): TLC  $R_f$  = 0.26 (2:3 EtOAc/hexanes) or  $R_f$  = 0.5 (3:2 EtOAc/hexanes); <sup>1</sup>H NMR (CDCl<sub>3</sub>, 400 MHz)  $\delta$  1.23 (t, J = 7.3 Hz, 3H), 1.88-2.8 (5m, 12H), 3.23 and 4.02 (2d, J = 13.2 Hz, 2H), 4.11 (q, J = 7.3 Hz, 3H), 7.20-7.40 (m, 10H); <sup>13</sup>C NMR (CDCl<sub>3</sub>, 100 MHz)  $\delta$  14.2, 24.4, 30.2, 50.3, 52.7, 56.8, 57.5, 58.5, 60.3, 63.0, 126.7, 126.9, 128.1, 128.7, 129.0, 138.1, 139.0, 173.7.



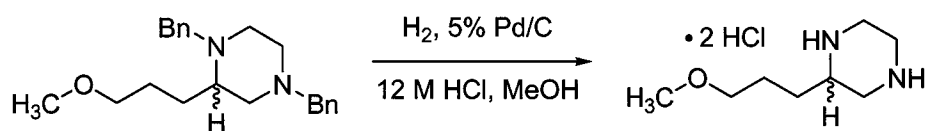
**1,4-Dibenzyl-2-(3-hydroxypropyl)-piperazine (56).** A suspension of  $\text{LiAlH}_4$  (0.41 g, 10.9 mmol) in dry ether (20 mL) was treated with a solution of 3-(1,4-dibenzyl-piperazin-2-yl)-propionic acid ethyl ester **55** (3.3 g, 9.1 mmol) in dry ether (15 mL) at 0 °C under argon, maintaining a gentle effervescence. The reaction was stirred for 5 min and the ice bath was removed. Stirring was continued at 25 °C for 35 min. The reaction was quenched by consecutive addition of  $\text{H}_2\text{O}$  (0.41 mL),  $\text{NaOH}$  (0.82 mL, 4 M) and  $\text{H}_2\text{O}$  (0.41 mL). The inorganic salts were filtered over a pad of Celite and the pad was rinsed with  $\text{EtOAc}$ . The filtrate was concentrated *in vacuo* to give **56** (2.8 g, 95%): TLC  $R_f$  = 0.1 (3:2  $\text{EtOAc}$ /hexanes);  $^1\text{H}$  NMR ( $\text{CDCl}_3$ , 400 MHz)  $\delta$  1.52-1.95 (3m, 4H), 2.12-2.37 (2m, 3H), 2.48-2.80 (3m, 4H), 3.20 and 4.19 (2d,  $J$  = 12.8, 2H), 3.48 (dd,  $J$  = 17.9 and 13.2 Hz), 3.66 (m, 2H), 7.20-7.40 (m, 10H);  $^{13}\text{C}$  NMR ( $\text{CDCl}_3$ , 100 MHz)  $\delta$  27.6, 28.6, 50.5, 52.2, 56.4, 57.8, 59.4, 62.8, 63.0, 126.9, 127.1, 128.1, 128.3, 129.0, 129.3, 137.8, 138.0



**1,4-Dibenzyl-2-(3-methoxypropyl)-piperazine (57).** A cooled (0 °C) stirred solution of 1,4-dibenzyl-2-(3-hydroxypropyl)-piperazine **56** (1.7 g, 5.2 mmol) in dry DMF (15 mL) was treated  $\text{NaH}$  powder (0.38 g, 15.7 mmol) to give a turbid

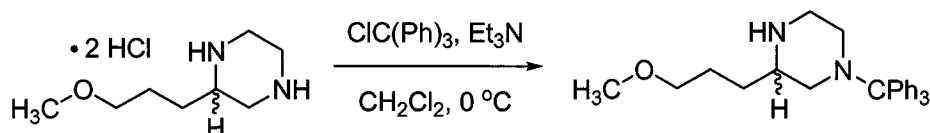


white suspension. The flask was placed under argon and stirring was continued for 20 min. iodomethane (0.78 g, 5.5 mmol) was added dropwise to the cooled solution, the reaction was allowed to stir on ice for 20 min, followed by room temperature for 3.5 h. The reaction was quenched by the addition of water (20 mL) followed by sat. NaHCO<sub>3</sub> (20 mL). The aqueous layer was extracted with Et<sub>2</sub>O (4 x 10 mL), dried (K<sub>2</sub>CO<sub>3</sub>), and concentrated *in vacuo* to give a tan oil. The oil was purified by column chromatography over silica gel (45 g) loaded with CHCl<sub>3</sub> and eluted with 1 column length 1:3 EtOAc/hexanes followed by 2:3 EtOAc/hexanes to give a clear oil **57**. The oil was pumped briefly and used in the next step without further purification: *R<sub>f</sub>* = 0.33 (3:2 EtOAc/hexanes); <sup>1</sup>H NMR (CDCl<sub>3</sub>, 400 MHz) δ 1.44-1.85 (m, 4H), 2.08-2.35 (m, 3H), 2.37-2.87 (3m, 4H), 3.20 and 4.03 (2d, J = 13.2 Hz, 2H), 3.31 (s, 3H), 3.35 (m, 2H), 3.48 (q, J = 13.2 Hz, 2H), 7.18-7.40 (m, 10H); <sup>13</sup>C NMR (CDCl<sub>3</sub>, 100 MHz) δ 25.6, 26.1, 50.7, 52.8, 57.48, 57.53, 58.5, 59.3, 63.1, 72.9, 126.7, 126.9, 128.1, 128.9, 129.0, 138.2, 139.1.

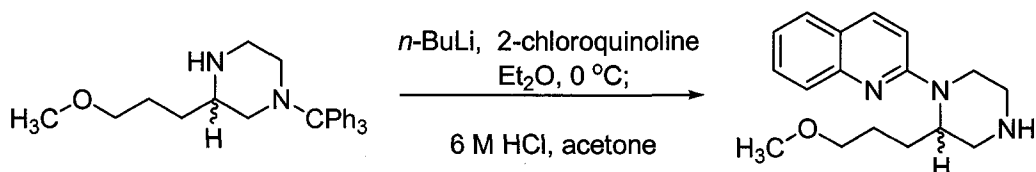


**2-(3-Methoxypropyl)-piperazine dihydrochloride (48).** A solution of 1,4-dibenzyl-2-(3-methoxypropyl)-piperazine **57** in HPLC MeOH (20 mL) and HCl (12 M, 12.4 mmol, 1 mL) was treated with 5% Pd/C (0.21 g). The flask was sealed with a septum and a hydrogen balloon was bubbled through the stirred solution. The reaction mixture was filtered over a pad of Celite rinsing with

MeOH and concentrated *in vacuo* to give a white solid **48** (0.50 g, 53% 2 steps):  $^1\text{H}$  NMR (DMSO, 400 MHz)  $\delta$  1.40-1.85 (m, 4H), 2.92-3.62 (4m, 11H, overlapped singlet 3.21, 3H), 4.14 (bs, 1H), 9.79-10.31 (2bs, 4H);  $^{13}\text{C}$  NMR (DMSO, 100 MHz)  $\delta$  24.3, 26.8, 39.3, 39.9, 43.4, 51.5, 57.9, 71.0.



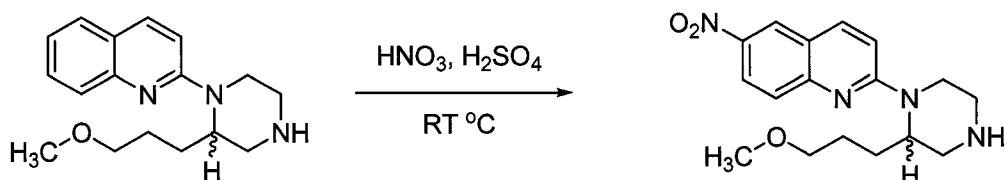
**3-(3-Methoxypropyl)-1-tritylpiperazine (49).** A solution of 2-(3-methoxypropyl)-piperazine dihydrochloride **48** (0.44 g, 1.9 mmol) in dry  $\text{CH}_2\text{Cl}_2$  (16 mL) and dry  $\text{Et}_3\text{N}$  (0.77 g, 1.1 mL, 7.6 mmol) at  $0\text{ }^\circ\text{C}$ , was treated with dropwise addition a solution of trityl chloride (0.53 g, 1.9 mmol) in dry  $\text{CH}_2\text{Cl}_2$  (5 mL). The ice bath was removed and the reaction stirred for 3 h at room temperature. The reaction mixture was transferred to a separatory funnel, diluted to 15 mL with  $\text{CH}_2\text{Cl}_2$ . The organics were washed with saturated  $\text{NaHCO}_3$  (25 mL) and brine (25 mL), dried ( $\text{K}_2\text{CO}_3$ ) and concentrated *in vacuo* to give an amorphous white foam **49** (7.3 g, 99% yield): TLC  $R_f = 0.33$  (1:9 MeOH/ $\text{CH}_2\text{Cl}_2$ ). The product was used without further purification, or characterization.



**2-[2-(3-Methoxypropyl)-piperazin-1-yl]-quinoline (50).** A cooled ( $0\text{ }^\circ\text{C}$ ) solution of 3-(3-methoxypropyl)-1-tritylpiperazine **49** (0.50 g, 1.24 mmol) in dry

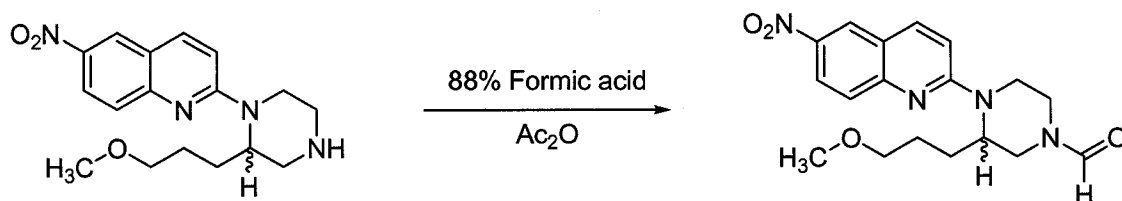
Et<sub>2</sub>O (20 mL) under argon, was treated by a dropwise addition of a solution of *n*-BuLi (0.51 mL, 2.45 M in hexanes, 1.24 mmol), giving a white precipitate. The resulting suspension was allowed to stir for 20 min. A solution of 2-chloroquinoline (0.14 g, 0.83 mmol) in dry Et<sub>2</sub>O (5 mL) was added dropwise to the cooled solution under argon to give a purple solution. The purple solution was allowed to stir for 20 min and the ice bath was removed. The reaction was allowed to stir overnight under argon giving a red-purple solution. The reaction was quenched by the addition of saturated NaHCO<sub>3</sub> (20 mL). The organics were separated and the aqueous phase was extracted 1 x 20 mL with Et<sub>2</sub>O. The organic portions were combined, washed with water (50 mL), brine (50 mL), dried (K<sub>2</sub>CO<sub>3</sub>), and concentrated *in vacuo* to give an amorphous foam. The foam was purified by column chromatography over silica gel (50 g) loaded with CHCl<sub>3</sub> and eluted with 1:3 EtOAc/hexanes to give a clear yellow oil. The trityl protected quipazine (not shown) was dissolved in acetone (3 mL) with stirring. To the stirred solution was added 6 M HCl (1 mL) giving an orange solution that slowly generated a white precipitate, stirring continued for 10 min. The reaction was diluted out to 25 mL with 1 M HCl, the crude aqueous mixture was extracted with CH<sub>2</sub>Cl<sub>2</sub> (4 x 25 mL). The aqueous layer was brought to pH 14 with 4 M NaOH, and buffered to pH 10 with saturated NaHCO<sub>3</sub>. The aqueous layer was then extracted with CH<sub>2</sub>Cl<sub>2</sub> (4 x 30 mL), dried (K<sub>2</sub>CO<sub>3</sub>), filtered, and concentrated *in vacuo*, giving a yellow oil **50** (0.36 g, 82%): TLC *R*<sub>f</sub> = 0.1 (1:9 MeOH/CH<sub>2</sub>Cl<sub>2</sub>); <sup>1</sup>H NMR (CDCl<sub>3</sub>, 400 MHz) δ 1.50-1.70 (m, 2H), 1.72-2.00 (2m, 2H), 2.37 (bs, 1H), 2.88 (dt, J = 3.2 and 12.0 Hz, 1H), 2.95-3.25 (m, 4H), 3.30 (s, 3H), 3.38 (m, 2H),

4.38 (bd, 1H), 4.52 (bs, 1H), 6.94 (d, J = 9.1 Hz, 1H), 7.20 (ddd, J = 1.3 and 7.1 Hz, 1H), 7.52 (ddd, J = 1.7 and 6.8 Hz, 1H), 7.58 (dd, J = 1.3 and 7.8 Hz, 1H), 7.84 (d, J = 8.4 Hz, 1H);  $^{13}\text{C}$  NMR ( $\text{CDCl}_3$ , 100 MHz)  $\delta$  24.7, 26.7, 40.0, 46.0, 47.9, 51.4, 58.6, 72.6, 109.3, 122.0, 122.8, 126.4, 127.1, 129.4, 137.4, 147.9, 157.0.

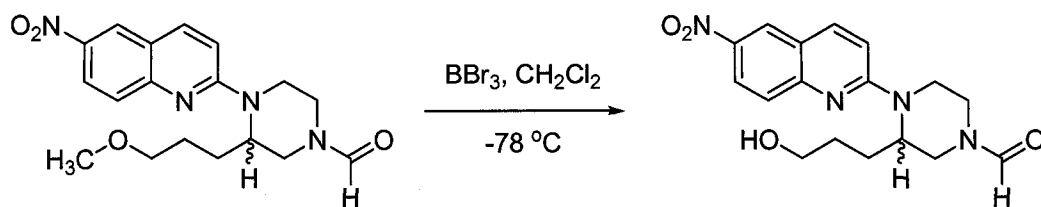


**2-[2-(3-Methoxypropyl)-piperazin-1-yl]-6-nitroquinoline ((±)-51).** A cooled (0 °C) stirred solution of 2-[2-(3-methoxypropyl)-piperazin-1-yl]-quinoline **50** (0.35 g, 1.2 mmol) in  $\text{H}_2\text{SO}_4$  (16 M, 15 mL) was treated with  $\text{HNO}_3$  (15.4 M, 0.32 mL) by dropwise addition. The resultant solution was allowed to stir for 20 min, then quenched by pouring onto ice. The acid was neutralized with 4 M NaOH to give a bright yellow solution. The resulting solution was buffered to pH 10 with sat.  $\text{NaHCO}_3$ . The aqueous solution was extracted with  $\text{CH}_2\text{Cl}_2$  until minimal yellow color persisted in the aqueous layer. The organics were dried ( $\text{K}_2\text{CO}_3$ ), and concentrated *in vacuo* to give a bright yellow oil ((±)-**51**) (0.40 g, 99% yield): TLC  $R_f$  = 0.14 (1:9 MeOH/ $\text{CH}_2\text{Cl}_2$ );  $^1\text{H}$  NMR ( $\text{CDCl}_3$ , 400 MHz)  $\delta$  1.46-1.68 (m, 2H), 1.78-2.00 (m, 2H), 1.92 (bs, 1H), 2.82 (dt, J = 3.6 and 12.0 Hz, 1H), 2.96 (dd, J = 3.9 and 12.3 Hz, 1H), 3.03-3.15 (m, 2H), 3.15-3.26 (m, 1H), 3.29 (s, 3H), 3.38 (m, 2H), 4.45 (bd, 1H), 5.59 (bs, 1H), 7.01 (d, J = 9.4 Hz, 1H), 7.57 (d, J = 9.4 Hz, 1H), 7.87 (d, J = 9.4 Hz, 1H), 8.24 (dd, J = 2.6 and 9.4 Hz, 1H), 8.47 (d, J =

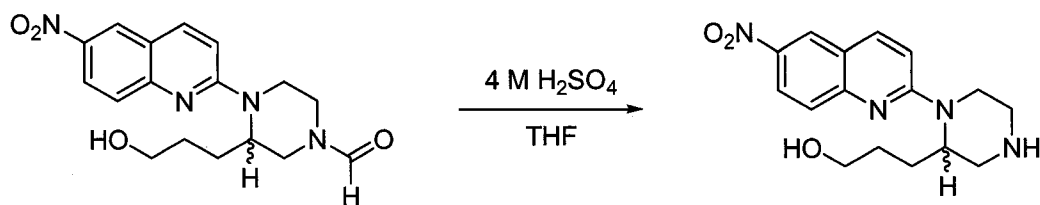
2.6 Hz, 1H);  $^{13}\text{C}$  NMR ( $\text{CDCl}_3$ , 100 MHz)  $\delta$  25.6, 26.7, 40.1, 46.0, 48.1, 51.6, 58.8, 72.7, 111.0, 121.1, 123.8, 124.4, 127.2, 138.8, 141.9, 151.8, 158.6; HRMS (ESI-TOF)  $m/z$  ( $M + H$ ) $^+$  calcd. for  $\text{C}_{17}\text{H}_{23}\text{N}_4\text{O}_3$  331.1770 found 331.1770.



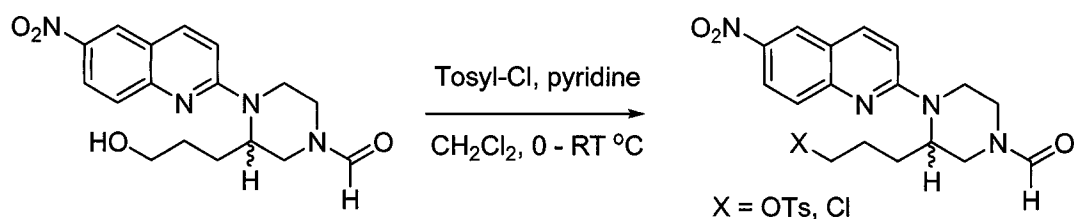
**N-Formyl-3-(3-methoxypropyl)-4-(6-nitroquinolin-2-yl)piperazine (60).** A solution of 2-[2-(3-methoxypropyl)-piperazin-1-yl]-6-nitroquinoline (**±**)-**51** (0.19 g, 0.58 mmol) in 88% formic acid (1.5 mL) was treated with acetic anhydride ( $\text{Ac}_2\text{O}$ ) (0.54 g, 0.5 mL, 5.2 mmol) and the reaction stirred for 30 min. The reaction was quenched by pouring onto ice, then brought to basic pH with 4 M NaOH, buffered to pH 10 with sat.  $\text{NaHCO}_3$ . The basic portion was extracted with  $\text{CH}_2\text{Cl}_2$  (3 x 10 mL). The organic portions were combined, dried ( $\text{K}_2\text{CO}_3$ ), and concentrated *in vacuo* to give **60** as a yellow oil (0.19 g, 91%): TLC  $R_f$  = 0.65 (1:9 MeOH/ $\text{CH}_2\text{Cl}_2$ );  $^1\text{H}$  NMR ( $\text{CDCl}_3$ , 400 MHz) (1:1 mixture of amide rotamers)  $\delta$  1.45-1.90 (m, 4H), 2.9 (dt,  $J$  = 4.2 and 12.6 Hz, 0.5H), 2.98 (dd,  $J$  = 3.9 and 13.3, 0.5H), 3.14-3.43 (m, 7.5H), 3.44-3.51 (m, 0.5H), 3.58 (bd, 0.5H), 3.70 (bd, 0.5H), 4.45 (bt, 1H), 4.74 (bs, 0.5H), 4.91 (bs, 0.5H), 7.70 (dd,  $J$  = 7.4 and 9.1 Hz, 1H), 7.63 (d,  $J$  = 9.1 Hz, 1H), 7.98 (d,  $J$  = 9.4 Hz, 1H), 8.09 (s, 0.5H), 8.2 (s, 0.5H), 8.28 (dd,  $J$  = 2.6 and 9.1 Hz, 1H), 8.51 (d,  $J$  = 2.6 Hz, 1H).



**N-Formyl-3-(3-hydroxypropyl)-4-(6-nitroquinolin-2-yl)piperazine (61).** A solution of N-formyl-3-(3-methoxypropyl)-4-(6-nitroquinolin-2-yl)piperazine **60** (0.19 g, 0.53 mmol) in dry  $\text{CH}_2\text{Cl}_2$  (25 mL) was cooled at  $-78\text{ }^\circ\text{C}$  in a dry ice acetone bath. A solution of  $\text{BBr}_3$  (2.6 mL, 1 M in  $\text{CH}_2\text{Cl}_2$ , 2.6 mmol, Aldrich) was added dropwise under argon giving a dark purple suspension. After 2 h the reaction was warmed to RT  $^\circ\text{C}$  and stirred for 2.5 h giving a yellow-orange suspension. The reaction was quenched by the addition of sat.  $\text{NaHCO}_3$  (20 mL), the organic portion was separated and the aqueous was extracted with  $\text{CH}_2\text{Cl}_2$  (3 x 20 mL). The organic portions were combined, dried ( $\text{K}_2\text{CO}_3$ ), filtered and concentrated *in vacuo*. The crude material was purified by column chromatography over silica gel (8 g) eluting with 4:1 EtOAc/ $\text{CHCl}_3$  to elute the bromide side product **62**, followed by 1:19 MeOH/EtOAc to elute the product, concentration *in vacuo* gave **61** as a yellow foam (0.12 g, 66% yield): TLC  $R_f$  = 0.43 (1:9 MeOH/ $\text{CH}_2\text{Cl}_2$ );  $^1\text{H}$  NMR ( $\text{CDCl}_3$ , 400 MHz) (mixture of amide rotamers)  $\delta$  1.48-1.96 (m, 5H), 2.88-3.08 (m, 1H), 3.24-3.45 (m, 1.5H), 3.50 (dd,  $J$  = 3.9 and 13.6 Hz, 0.5H), 3.61 (bd,  $J$  = 13.3 Hz, 0.5H), 3.66-3.84 (m, 2.5H), 4.24-5.15 (bm, 3H), 7.11 (d,  $J$  = 9.4 Hz, 1H), 7.76 (bs, 1H), 8.04 (d,  $J$  = 9.1 Hz, 1H), 8.12 (s, 0.5H), 8.26 (s, 0.5H), 8.33 (dd,  $J$  = 2.6 and 9.4 Hz, 1H), 8.57 (d,  $J$  = 2.6 Hz, 1H).



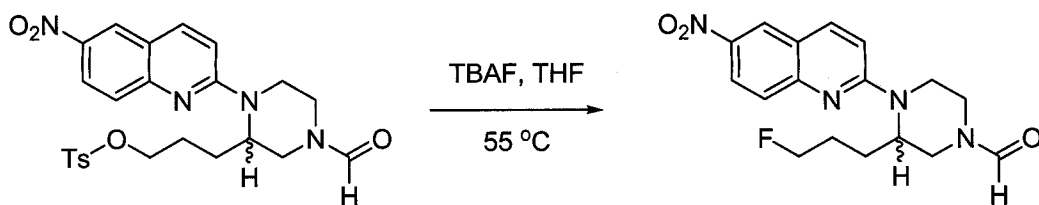
**2-[2-(3-Hydroxypropyl)-piperazin-1-yl]-quinoline (147).** A solution of N-formyl-3-(3-hydroxypropyl)-4-(6-nitroquinolin-2-yl)piperazine **61** (0.029 g, 0.084 mmol) in THF (1 mL) was treated with H<sub>2</sub>SO<sub>4</sub> (4 M, 0.5 mL) and heated at 55 °C for 1 hour. The reaction was quenched by pouring onto ice. The mixture was brought to a basic pH with 4 M NaOH, and buffered to pH 10 with sat. NaHCO<sub>3</sub>. The aqueous layer was extracted with CH<sub>2</sub>Cl<sub>2</sub> (3 x 10 mL), the organic portions were combined, dried (K<sub>2</sub>CO<sub>3</sub>) and concentrated *in vacuo* to give **147** as yellow oil (0.021 g, 90%): <sup>1</sup>H NMR (CDCl<sub>3</sub>, 400 MHz) δ 1.61 (m, 2H), 1.80 (m, 1H), 2.07 (m, 1H), 2.49 (bs, 2H), 2.86 (td, J = 3.6 Hz, 12.3 Hz, 1H), 2.97 (dd, J = 3.9 Hz, 12.3 Hz, 1H), 3.04-3.18 (m, 2H), 3.27 (td, J = 3.6 Hz, 12.6 Hz, 1H), 3.74 (m, 2H), 4.20 (bd, 1H), 4.74 (bs, 1H) 7.04 (d, J = 9.4 Hz, 1H), 7.67 (d, J = 9.4 Hz, 1H), 7.93 (d, J = 9.4 Hz, 1H), 8.26 (dd, J = 2.6 Hz, 9.1 Hz, 1H), 8.49 (d, J = 2.6 Hz, 1H); <sup>13</sup>C NMR (CDCl<sub>3</sub>, 100 MHz) δ 24.7, 28.4, 41.1, 46.1, 47.7, 50.7, 62.4, 111.0, 120.9, 123.8, 124.1, 126.6, 138.7, 141.8, 151.4, 158.3; HRMS (ESI-TOF) *m/z* (M + H)<sup>+</sup> calcd. for C<sub>16</sub>H<sub>21</sub>N<sub>4</sub>O<sub>3</sub> 317.1614 found 317.1604.



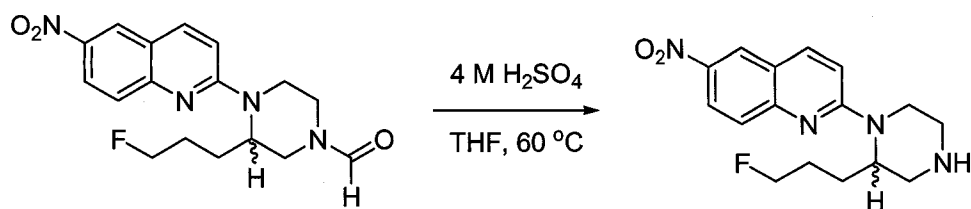
**3-(4-Formyl-1-(6-nitroquinolin-2-yl)piperazin-2-yl)propyl-4-**

**methylbenzenesulfonate (63).** In an 8 mL vial a solution of N-formyl-3-(3-hydroxypropyl)-4-(6-nitroquinolin-2-yl)piperazine **61** (0.081g, 0.24 mmol) in dry  $\text{CH}_2\text{Cl}_2$  (0.5 mL) and dry pyridine (0.029 g, 0.37 mmol) was cooled at 0 °C. To the solution was added tosyl chloride (0.062 g, 0.33 mmol). The vial was flushed with argon and sealed with a cap and Para film. The solution was allowed to stir at RT °C for 3 h. The crude reaction mixture was purified by column chromatography over silica gel (12 g) loaded with  $\text{CHCl}_3$ , eluting with 1:1 EtOAc/hexanes followed by 4:1 EtOAc/ $\text{CHCl}_3$  to give the product **63** as a yellow foam (0.060 g, 51% yield): TLC  $R_f$  = 0.71 (1:9 MeOH/ $\text{CH}_2\text{Cl}_2$ ); Determined by NMR to be a 1:1 mixture of N-formyl-ProTos-NQP **63** and N-formyl-ProCl-NQP **64**.  $^1\text{H}$  NMR ( $\text{CDCl}_3$ , 400 MHz) (mixture of amide rotamers)  $\delta$  1.70-2.02 (m, 8H), 2.44 (s, Ar $\text{CH}_3$ , 3H), 2.90 (dt, J = 4.2 and 12.6, 1H), 3.03 (dd, J = 3.9 and 13.3 Hz), 3.20-3.60 (m, 10H), 3.73 (bd, 1H), 4.30-4.70 (4m, 4H), 4.88 (bs, 1H), 5.10 (bs, 1H), 7.07 (dd, J = 2.9 and 9.1 Hz, 2H), 7.33 (d, J = 7.8 Hz, 2H), 7.66 (dd, J = 4.5 and 9.4 Hz, 2H), 7.78 (d, J = 8.1 Hz, 2H), 8.03 (d, J = 9.4 Hz, 2H), 8.12 (s, 1H), 8.26 (s, 1H), 8.31 (dd, J = 2.6 and 9.4 Hz, 2H), 8.55 (d, J = 2.6 Hz, 2H).

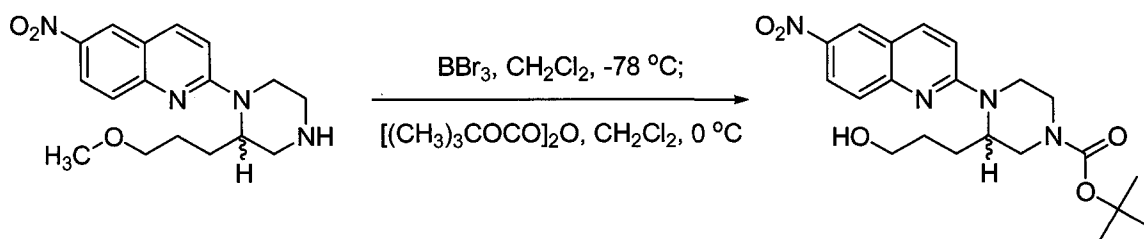




**N-Formyl-3-(3-fluoropropyl)-4-(6-nitroquinolin-2-yl)piperazine (65).** In an 8 mL vial a solution of 3-(4-formyl-1-(6-nitroquinolin-2-yl)piperazin-2-yl)propyl 4-methylbenzenesulfonate **63** (0.056 g, 0.11 mmol) in dry THF (0.30 mL) was treated with a solution of TBAF (0.16 mL, 1 M in THF, 0.16 mmol, Aldrich) to give a dark orange solution. The vial was capped and heated at 55 °C for 2 h. The reaction was concentrated *in vacuo* and then dissolved in  $\text{CHCl}_3$ . The crude material was purified by column chromatography over silica gel (2 g) eluting with 1:1 EtOAc/hexanes followed by 1:19 MeOH/EtOAc and concentrated *in vacuo* to give **65** as a yellow foam (0.025 g, 64%): TLC  $R_f$  = 0.22 (1:19 MeOH/EtOAc);  $^1\text{H}$  NMR ( $\text{CDCl}_3$ , 400 MHz) (mixture of amide rotamers)  $\delta$  1.60-2.00 (m, 4H), 2.90 (dt,  $J$  = 3.6 and 12.3 Hz, 0.5H), 3.00 (dd,  $J$  = 4.2 and 13.3 Hz, 0.5H), 3.20-3.40 (2m, 2H), 3.44-3.62 (m, 1.5H), 3.72 (bd, 0.5H), 4.32-4.60 (m, 3H), 4.83 (bs, 0.5H), 5.07 (bs, 0.5H), 7.07 (dd,  $J$  = 3.2 and 9.4 Hz, 1H), 7.69 (m, 1H), 8.03 (d,  $J$  = 9.1 Hz, 1H), 8.10 (s, 0.5H), 8.25 (s, 0.5H), 8.32 (dd,  $J$  = 2.6 and 9.1 Hz, 1H), 8.56 (d,  $J$  = 2.3 Hz, 1H).

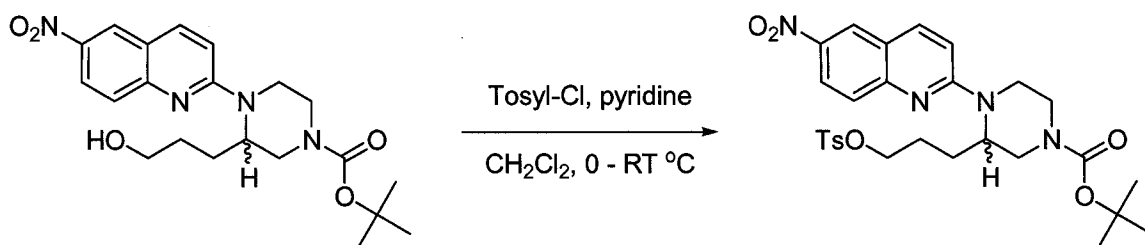


**2-(2-(3-Fluoropropyl)piperazin-1-yl)-6-nitroquinoline (58).** A solution of N-formyl-3-(3-fluoropropyl)-4-(6-nitroquinolin-2-yl)piperazine **65** (0.025 g, 0.072 mmol) in THF (0.5 mL) was treated with H<sub>2</sub>SO<sub>4</sub> (4 M, 0.25 mL) and heated at 60 °C for 1 hour. The reaction was quenched by pouring onto ice. The mixture was brought to a basic pH with 4 M NaOH, and buffered to pH 10 with sat. NaHCO<sub>3</sub>. The aqueous layer was extracted with CH<sub>2</sub>Cl<sub>2</sub> (3 x 10 mL), the organic portions were combined, dried (K<sub>2</sub>CO<sub>3</sub>) and concentrated *in vacuo* to give **58** as yellow oil (0.021 g, 90%): TLC *R<sub>f</sub>* = 0.35 (1:9 MeOH/CH<sub>2</sub>Cl<sub>2</sub>); <sup>1</sup>H NMR (CDCl<sub>3</sub>, 400 MHz) δ 1.56-2.10 (2m, 5H, CH<sub>2</sub>CH<sub>2</sub>CH<sub>2</sub>F and NH), 2.91 (dt, J = 3.3 and 12.3 Hz, 1H), 3.06 (dd, J = 3.9 and 12.3 Hz, 1H), 3.14-3.38 (3m, 3H), 4.40-4.60 (2m, 2H, CH<sub>2</sub>F), 4.81 (bs, 1H), 7.04 (d, J = 9.4 Hz, 1H), 7.64 (d, J = 9.1 Hz, 1H), 7.99 (d, J = 9.4 Hz, 1H), 8.31 (dd, J = 2.6 and 9.4 Hz, 1H), 8.54 (d, J = 2.6 Hz, 1H).



**tert-Butyl-3-(3-hydroxypropyl)-4-(6-nitroquinolin-2-yl)piperazine-1-carboxylate (66).** A solution of 2-[2-(3-methoxypropyl)-piperazin-1-yl]-6-nitroquinoline **50** (0.16g, 0.48 mmol) in dry CH<sub>2</sub>Cl<sub>2</sub> (50 mL) was cooled at -78 °C

in a dry ice acetone bath. A solution of  $\text{BBr}_3$  (2.4 mL, 1M in  $\text{CH}_2\text{Cl}_2$ , 2.4 mmol) was added dropwise under argon giving a dark purple suspension. After 3 h the reaction was warmed to RT °C and stirred for an additional 4 h giving a yellow-orange suspension. The reaction was quenched by the addition of sat.  $\text{NaHCO}_3$  (20 mL). The organic layer was separated and the aqueous layer was extracted 3 x 20 mL  $\text{CH}_2\text{Cl}_2$ . The organic portions were combined, dried ( $\text{K}_2\text{CO}_3$ ), filtered and concentrated *in vacuo*. The yellow semi-solid was transferred to a 50 mL flask with 0.5:9.5 MeOH/ $\text{CH}_2\text{Cl}_2$  and concentrated. The residue was treated with  $\text{CH}_2\text{Cl}_2$  (45 mL) sonicated to suspend all the material, then cooled to 0 °C and treated with di-*tert*-butyl dicarbonate (0.1g, 0.48 mmol). After 2.5 h the reaction was warmed to RT °C and allowed to stir an additional hour. The solution was concentrated *in vacuo* (25 °C) and suspended in  $\text{CHCl}_3$ . The crude material was purified by column chromatography over silica gel (8 g) eluting with 3:2 EtOAc/hexanes, concentrated *in vacuo* to give **66** as a yellow foam (0.088 g, 44% yield, 2 steps): TLC  $R_f$  = 0.29 (6:4 EtOAc/hexanes);  $^1\text{H}$  NMR ( $\text{CDCl}_3$ , 400 MHz)  $\delta$  1.40-1.94 (1s and 2m, 13H), 2.90-3.22 (bm, 2H), 3.24-3.42 (m, 1H), 3.66-3.88 (bs, 2H), 3.94-4.34 (bm, 3H), 4.76 (bs, 1H), 7.04 (d,  $J$  = 9.2 Hz, 1H), 7.67 (d,  $J$  = 9.2 Hz, 1H), 7.95 (d,  $J$  = 9.5 Hz, 1H), 8.25 (dd,  $J$  = 2.6 and 9.5 Hz, 1H), 8.47 (d,  $J$  = 2.6 Hz, 1H);  $^{13}\text{C}$  NMR ( $\text{CDCl}_3$ , 100 MHz) (mixture of amide rotamers)  $\delta$  24.9, 25.2, 28.3, 40.0, 42.7, 43.8, 44.4, 45.5, 50.7, 51.5, 62.2, 80.3, 111.1, 121.1, 123.8, 124.1, 126.7, 139.0, 141.9, 151.1, 154.9, 158.1; HRMS (ESI-TOF)  $m/z$  ( $M + \text{H}$ ) $^+$  calcd. for  $\text{C}_{21}\text{H}_{29}\text{N}_4\text{O}_5$  417.2138 found 417.2132.



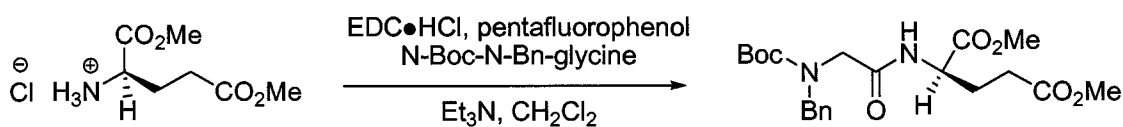
**3-(4-(*tert*-Butoxycarbonyl)-1-(6-nitroquinolin-2-yl)piperazin-2-yl)propyl 4-methylbenzenesulfonate (69).** A solution of *tert*-butyl 3-(3-hydroxypropyl)-4-(6-nitroquinolin-2-yl)piperazine-1-carboxylate **66** (0.040g, 0.097 mmol) in dry CH<sub>2</sub>Cl<sub>2</sub> (1 mL) and dry pyridine (6 drops from 18 gauge needle) in an 8 mL vial, was cooled to 0 °C. To the solution was added tosyl chloride (0.078 g, 0.41 mmol), the vial was flushed with argon and sealed with a cap and Parafilm. The solution was allowed to stir warming to RT °C overnight. The crude reaction mixture was diluted with CH<sub>2</sub>Cl<sub>2</sub> (5 mL), washed with sat. NaHCO<sub>3</sub> (5 mL), dried K<sub>2</sub>CO<sub>3</sub>, filtered and concentrated *in vacuo*. The crude material was purified by column chromatography over silica gel (12 g) loaded with CHCl<sub>3</sub>, eluting with 2:3 EtOAc/hexanes, concentration *in vacuo* gave **69** as a yellow foam (0.042 g, 76% yield): TLC *R<sub>f</sub>* = 0.37 (6:4 EtOAc/hexanes); <sup>1</sup>H NMR (CDCl<sub>3</sub>, 400 MHz) δ 1.47 (s, 9H), 1.60-1.82 (bm, 4H), 2.41 (s, 3H), 2.80-3.30 (2bm, 3H), 3.92-4.44 (bm, 2H), 4.76 (bs, 1H), 7.00 (d, *J* = 9.5 Hz, 1H), 7.29 (d, *J* = 8.1 Hz, 1H), 7.58 (d, *J* = 9.1 Hz, 1H), 7.73 (d, *J* = 8.1 Hz, 1H), 7.96 (d, *J* = 9.5 Hz, 1H), 8.26 (dd, *J* = 2.6 and 9.2 Hz, 1H), 8.50 (d, *J* = 2.6 Hz, 1H); <sup>13</sup>C NMR (CDCl<sub>3</sub>, 100 MHz) (mixture of amide rotamers) δ 21.6, 24.6, 25.5, 28.3, 39.5, 42.7, 43.8, 44.9, 46.1, 50.7, 51.0, 70.0, 80.3, 110.6, 121.0, 123.6, 124.2, 125.8, 127.1, 127.8, 129.8, 132.8, 139.0, 141.9, 144.8, 151.2, 154.8, 158.0; HRMS (ESI-TOF) *m/z* (*M* + *H*)<sup>+</sup> calcd. for C<sub>28</sub>H<sub>35</sub>N<sub>4</sub>O<sub>7</sub>S 571.2226 found 571.2222.



**2-(2-(3-Fluoropropyl)piperazin-1-yl)-6-nitroquinoline (58).** A solution of 3-(4-(*tert*-butoxycarbonyl)-1-(6-nitroquinolin-2-yl)piperazin-2-yl)propyl-4-methylbenzenesulfonate **69** (0.042 g, 0.074 mmol) in dry THF (1 mL) in an 8 mL vial was treated with a solution of TBAF (0.11 mL, 1 M in THF, 0.11 mmol, Aldrich) to give a dark orange solution. The vial was capped and heated at 55 °C for 3 h. The reaction was concentrated *in vacuo* and dissolved in CHCl<sub>3</sub>. The crude material was purified by column chromatography over silica gel (8 g) eluting with 2:3 EtOAc/hexanes to give the product as a yellow foam (0.025 g, 79%). TLC  $R_f$  = 0.49 (3:2 EtOAc/hexanes). A portion (4 mg) of the purified N-Boc-PROF-NQP **70** was treated with H<sub>2</sub>SO<sub>4</sub> (0.5 mL, 16 M) at RT °C and stirred for 4 min. The reaction was quenched by pipetting the mixture onto ice, then rinsing the vial with ice cold water. The aqueous solution was brought to a basic pH (persistent yellow color) with 4 M NaOH at 0 °C then buffered to pH 10 with saturated NaHCO<sub>3</sub>. The aqueous solution was extracted with CH<sub>2</sub>Cl<sub>2</sub> (3 x 5 mL), the organic portions were combined, dried (K<sub>2</sub>CO<sub>3</sub>), filtered, and concentrated *in vacuo*. The crude material was purified over silica gel (1 g) loading with CHCl<sub>3</sub> and eluted with 1:49 MeOH/CHCl<sub>3</sub> followed by 1:9 MeOH/CHCl<sub>3</sub> to give the final amine product **58** as a yellow oil (0.002, 78% yield): TLC  $R_f$  = 0.22 (1:9 MeOH/CH<sub>2</sub>Cl<sub>2</sub>); <sup>1</sup>H NMR (CDCl<sub>3</sub>, 400 MHz) δ 1.56-2.10 (2m, 5H, CH<sub>2</sub>CH<sub>2</sub>CH<sub>2</sub>F

and NH), 2.91 (dt, J = 3.3 and 12.3 Hz, 1H), 3.06 (dd, J = 3.9 and 12.3 Hz, 1H), 3.14-3.38 (3m, 3H), 4.40-4.60 (2m, 2H, CH<sub>2</sub>F), 4.81 (bs, 1H), 7.04 (d, J = 9.4 Hz, 1H), 7.64 (d, J = 9.1 Hz, 1H), 7.99 (d, J = 9.4 Hz, 1H), 8.31 (dd, J = 2.6 and 9.4 Hz, 1H), 8.54 (d, J = 2.6 Hz, 1H).

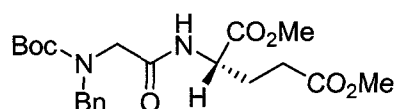
### 6.3 Chiral Propyl N-formyl Series.



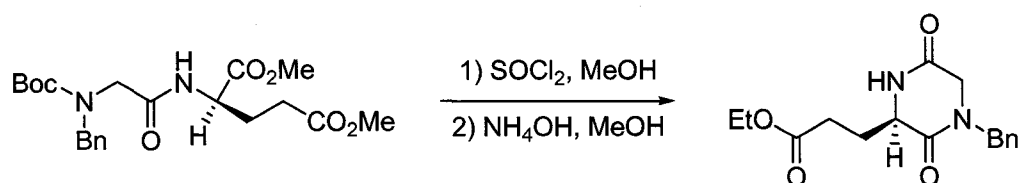
**(R)-N-Boc-N-Benzyl-glycyl-L-glutamate Dimethyl Ester ((R)-133).** N-Ethyl-N'-(3-dimethylaminopropyl)carbodiimide hydrochloride (EDC) (1.4 g, 7.1 mmol) was suspended with stirring in CH<sub>2</sub>Cl<sub>2</sub> (30 mL), to the suspension was added a solution of pentafluorophenol (PFP) (1.75 g, 9.5 mmol) in CH<sub>2</sub>Cl<sub>2</sub> (10 mL) and stirred for 20 min. N-Boc-N-Benzyl glycine (1.6 g, 5.9 mmol) in CH<sub>2</sub>Cl<sub>2</sub> (20 mL) was added to the stirred solution. The mixture was allowed to stir for 1 hour, and Et<sub>3</sub>N (3.0 mL) was added followed by D-glutamate dimethyl ester hydrochloride **D-132** in CH<sub>2</sub>Cl<sub>2</sub> (20 mL). The reaction was allowed to stir for 24 h at 21 °C. The crude reaction mixture was washed with 1 M Na<sub>2</sub>CO<sub>3</sub> (120 mL), 1 M citric acid (120 mL), and water (60 mL). The organic layer was dried (K<sub>2</sub>CO<sub>3</sub>), filtered, and concentrated *in vacuo*. The crude material was purified by column chromatography over silica gel (50 g) loaded with CHCl<sub>3</sub>, eluting with 1:3 EtOAc/hexanes (1 column length) followed by 2:3 EtOAc/hexanes to elute PFP and then 3:2 EtOAc/hexanes, concentration *in vacuo* to elute **(R)-133** as a clear

oil (2.19 g, 87%): TLC  $R_f$  = 0.69 (1:9 MeOH/CH<sub>2</sub>Cl<sub>2</sub>); <sup>1</sup>H NMR (CDCl<sub>3</sub>, 400 MHz) δ 1.48 (s, 9H), 1.87 (bs, 1H), 2.00-2.43 (2bs, 3H), 3.65 (s, 3H), 3.71 (s, 3H), 3.80 (m, 1H), 4.39 (d, J = 15.5 Hz, 1H), 4.48-4.72 (m, 2H), 6.56 and 6.91 (2bs, 1H), 7.12-7.40 (m, 5H); <sup>13</sup>C NMR (CDCl<sub>3</sub>, 100 MHz) δ 50.5, 51.3, 51.7, 52.4, 81.3, 127.6, 128.1, 128.6, 137.1, 169.2, 171.7, 172.9.

The opposing enantiomer was similarly prepared:



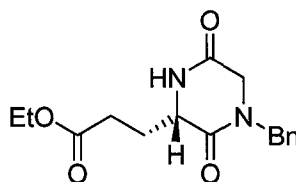
**(S)-N-Boc-N-Benzyl-glycyl-L-glutamate Dimethyl Ester ((S)-133).** Clear oil; (2.28 g, 91%).



**Ethyl 3-((R)-4-benzyl-3,6-dioxopiperazin-2-yl)propanoate ((R)-134).** A cooled (0 °C) stirred solution of (*R*)-N-Boc-N-Benzyl-glycyl-L-glutamate dimethyl ester (**(R)-133**) (2.2 g, 5.2 mmol) in methanol (30 mL, HPLC grade) was treated with thionyl chloride (3.2 g, 27.1 mmol) dropwise, then allowed to stir at 0 °C for 15 min and at RT °C for 2 h. The reaction was concentrated *in vacuo* and then placed under high vacuum for 10 min to give a white foam. The foam was triturated with ether (2 x 30 mL). The resultant white oily semi-solid was placed under high vacuum overnight to give a white foam. The foam was dissolved in

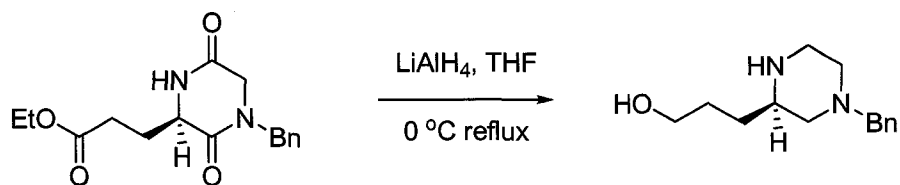
methanol (60 mL, HPLC grade) and stirred. Ammonium hydroxide (12 mL, 177 mmol, 28-30%) was added and the mixture was stirred for 24 h. The crude mixture was concentrated *in vacuo* to give a white solid. The solid was dissolved in sat. NaHCO<sub>3</sub> (50 mL) and 4:1 CHCl<sub>3</sub>/IPOH (50 mL), the organic layer was separated, and the aqueous layer was extracted with 4:1 CHCl<sub>3</sub>/IPOH (3 x 30 mL). The organic portions were combined, dried (K<sub>2</sub>CO<sub>3</sub>), filtered, and concentrated *in vacuo* to give a clear oil (**R**)-**134** (1.25 g, 84% yield), which required no further purification: TLC *R<sub>f</sub>* = 0.39 (1:9 MeOH/CH<sub>2</sub>Cl<sub>2</sub>); <sup>1</sup>H NMR (CDCl<sub>3</sub>, 400 MHz) δ 2.16 (m, 2H), 2.44 (m, 2H), 3.61 (s, 3H), 3.79 (q, J = 6.5 and 17.8 Hz, 2H), 4.1 (bt, 1H), 4.54 (m, 2H), 7.14-7.42 (m, 5H), 7.85 (s, 1H); <sup>13</sup>C NMR (CDCl<sub>3</sub>, 100 MHz) δ 29.0, 29.3, 48.7, 49.5, 51.8, 54.3, 128.0, 128.2, 128.8, 135.0, 165.4, 166.1, 173.1.

The opposing enantiomer was similarly prepared:



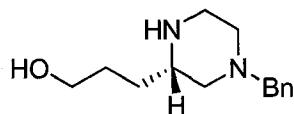
**Ethyl 3-((S)-4-benzyl-3,6-dioxopiperazin-2-yl)propanoate ((S)-134).** Clear oil; (1.30 g, 81%).



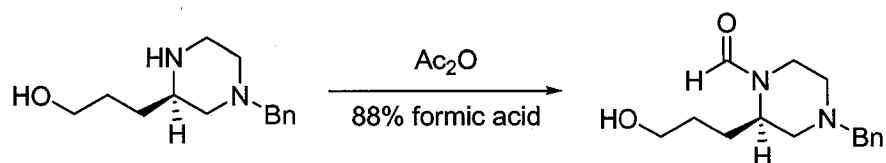


**3-((*R*)-4-Benzylpiperazin-2-yl)propan-1-ol ((*R*)-135).** A stirred and cooled (0 °C) suspension of LiAlH<sub>4</sub> (0.93 g, 24.5 mmol) in dry THF (30 mL) under argon, was treated with a solution of ethyl 3-((*R*)-4-benzyl-3,6-dioxopiperazin-2-yl)propanoate (**(*R*)-134**) (1.42 g, 4.89 mmol) in THF (30 mL) by syringe, maintaining a gentle effervescence. The reaction flask was fitted with a water-cooled condenser and the reaction was heated at reflux for 2 h. The mixture was allowed to cool to room temperature and stir overnight. The reaction was quenched by consecutive addition of water (0.8 mL), NaOH (1.7 mL, 4 M), then water (0.8 mL). The inorganic solids were vacuum filtered (Celite pad) and the rinsed with EtOAc. The filtrate was concentrated *in vacuo*, giving (**(*R*)-135**) as a clear oil (1.16 g, quantitative): TLC  $R_f = 0.06$  (1:9 MeOH/CH<sub>2</sub>Cl<sub>2</sub>). The product was used without further purification, or characterization.

The opposing enantiomer was similarly prepared:

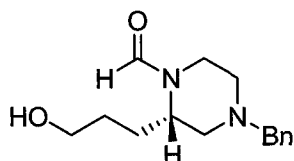


**3-((*S*)-4-Benzylpiperazin-2-yl)propan-1-ol ((*S*)-135).** Clear oil; (1.04 g, 98%).

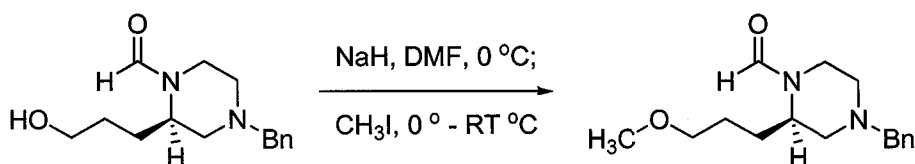


**(R)-4-Benzyl-2-(3-hydroxypropyl)piperazine-1-carbaldehyde ((R)-136).** A cooled (0 °C) solution of 3-((R)-4-benzylpiperazin-2-yl)propan-1-ol (**(R)-135**) (1.16 g, 4.95 mmol) in formic acid (23 M, 12.5 mL) was treated dropwise with acetic anhydride (4.2 mL, 44.6 mmol). The solution was allowed to stir for 5 min at 0 °C, then allowed to warm to room temperature and stir overnight. The reaction was quenched by pouring onto ice, and then basified with 4 M NaOH to pH 12. The resultant mixture was buffered to pH 10 with a saturated solution of NaHCO<sub>3</sub>. The aqueous layer was extracted with CH<sub>2</sub>Cl<sub>2</sub>, the organic portions were combined, dried (K<sub>2</sub>CO<sub>3</sub>), filtered and concentrated *in vacuo*, to give a light brown oil 1.25 g (89% crude yield). The crude material was purified by column chromatography over silica gel (50 g) loaded with CHCl<sub>3</sub> and eluted with 0.3:9.7 MeOH/CH<sub>2</sub>Cl<sub>2</sub> to elute **(R)-136** as a clear oil (0.81 g, 63%): TLC *R<sub>f</sub>* = 0.22 (1:9 MeOH/CH<sub>2</sub>Cl<sub>2</sub>); <sup>1</sup>H NMR (CDCl<sub>3</sub>, 400 MHz) δ 1.25-1.58 (m, 2H), 1.60-1.86 (m, 1H), 1.89-2.27 (m, 3H), 2.65-3.05 (m, 2H), 3.20-3.80 (m, 6H), 4.05-4.55 (2m, 1H), 7.15-7.50 (m, 5H), 8.00 (s, 1H); <sup>13</sup>C NMR (CDCl<sub>3</sub>, 100 MHz) (mixture of amide rotamers) δ 26.0, 26.6, 28.7, 29.1, 36.3, 42.2, 48.1, 52.6, 53.5, 54.7, 55.3, 56.6, 62.0, 62.3, 62.5, 127.2, 128.3, 128.7, 137.7, 161.0, 161.3.

The opposing enantiomer was similarly prepared:



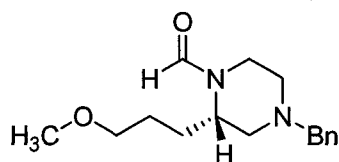
**(S)-4-Benzyl-2-(3-hydroxypropyl)piperazine-1-carbaldehyde ((S)-136).** Clear oil; (0.73 g, 73%).



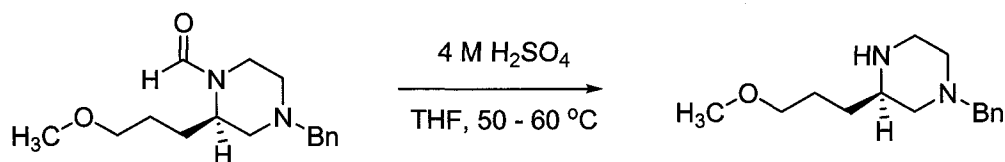
**(R)-4-Benzyl-2-(3-methoxypropyl)piperazine-1-carbaldehyde ((R)-137).** A cooled (0 °C) stirred solution of (*R*)-4-benzyl-2-(3-hydroxypropyl)piperazine-1-carbaldehyde (**(R)-136**) (0.81 g, 3.11 mmol) in dry DMF (50 mL) was treated with NaH powder (0.22 g, 9.3 mmol) in a portion-wise fashion, giving an off-white suspension. The resulting suspension was allowed to stir for 45 min at 0° C. To the suspension was added (dropwise) iodomethane (0.19 mL, 3.11 mmol) with stirring at 0 °C for 5 min and then RT °C for 2.5 h. The reaction was quenched by the addition of water (40 mL). The aqueous solution was extracted with Et<sub>2</sub>O (3 x 30 mL) and EtOAc (15 mL). The organic portions were combined, dried (K<sub>2</sub>CO<sub>3</sub>), and concentrated *in vacuo* to give a tan oil. The crude material was purified by column chromatography over silica gel (30 g) loaded with CHCl<sub>3</sub> eluting with 0.3:9.7 MeOH/CH<sub>2</sub>Cl<sub>2</sub>, concentration *in vacuo* gave (**(R)-137**) as a clear oil (0.51 g, 59%): TLC *R<sub>f</sub>* = 0.5 (1:9 MeOH/CH<sub>2</sub>Cl<sub>2</sub>); <sup>1</sup>H NMR (CDCl<sub>3</sub>, 400 MHz) δ 1.30-1.54 (m, 2H), 1.60-1.75 (m, 1H), 1.86-2.20 (m, 3H), 2.66-2.99 (m,

2.5H), 3.22-3.56 (m, 8.5H, singlet at 3.28, 3H), 4.13 (bd, 0.5H), 4.25 (bs, 0.5H), 7.18-7.40 (m, 5H), 8.00 (s, 1H);  $^{13}\text{C}$  NMR ( $\text{CDCl}_3$ , 100 MHz) mixture of amide rotamers)  $\delta$  25.9, 26.1, 26.9, 36.2, 42.1, 47.9, 52.5, 53.6, 54.6, 55.3, 56.6, 58.3, 58.4, 62.5, 72.1, 127.1, 128.2, 128.6, 137.8, 160.8, 160.9.

The opposing enantiomer was similarly prepared:



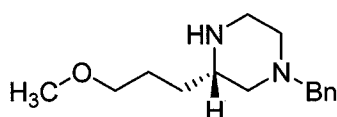
**(S)-4-Benzyl-2-(3-methoxypropyl)piperazine-1-carbaldehyde ((S)-137).** Clear oil; (0.30 g, 72%).



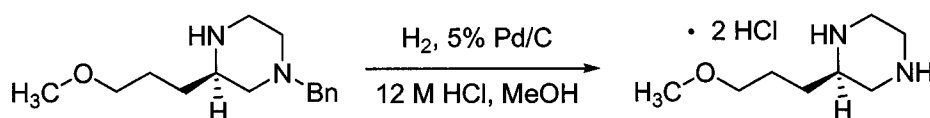
**(R)-1-Benzyl-3-(3-methoxypropyl)piperazine ((R)-138).** A stirred solution of (*R*)-4-benzyl-2-(3-methoxypropyl)piperazine-1-carbaldehyde (**(R)-137**) (0.51 g, 1.8 mmol) in THF (4 mL) was treated with  $\text{H}_2\text{SO}_4$  (4 M, 9 mL). The flask was fitted with a water-cooled condenser and heated to 60° C for 3 h. The reaction was cooled to RT °C and poured into ice cold 4 M NaOH and then buffered to pH 10 with sat.  $\text{NaHCO}_3$ . The aqueous layer was extracted with  $\text{CH}_2\text{Cl}_2$  (4 x 30 mL). The organic portions were combined, dried ( $\text{K}_2\text{CO}_3$ ), filtered and concentrated *in vacuo* giving (**(R)-138**) as a light tan oil (0.42 g, 93%), product was used without further purification: TLC  $R_f$  = 0.05 (1:9 MeOH/ $\text{CH}_2\text{Cl}_2$ );  $^1\text{H}$  NMR ( $\text{CDCl}_3$ , 400

MHz)  $\delta$  1.30-1.47 (m, 2H), 1.50-1.68 (m, 2H), 1.72 (t,  $J = 10.4$  Hz), 1.96 (bs, 1H), 2.03 (dt,  $J = 3.2$  and 11.0 Hz), 2.70-2.84 (m, 3H), 2.84-3.00 (2m, 2H), 3.30 (s, 3H), 3.31-3.39 (m, 2H), 3.49 (dd,  $J = 12.9$  and 15.2 Hz), 7.20-7.35 (m, 5H);  $^{13}\text{C}$  NMR ( $\text{CDCl}_3$ , 100 MHz)  $\delta$  26.0, 31.0, 45.8, 53.8, 54.8, 58.5, 59.8, 63.4, 72.6, 127.0, 128.2, 129.2, 138.0.

The opposing enantiomer was similarly prepared:



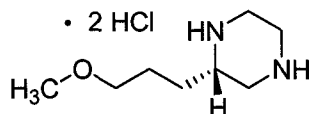
**(S)-1-Benzyl-3-(3-methoxypropyl)piperazine ((S)-138).** Light tan oil; (0.25 g, 92%).



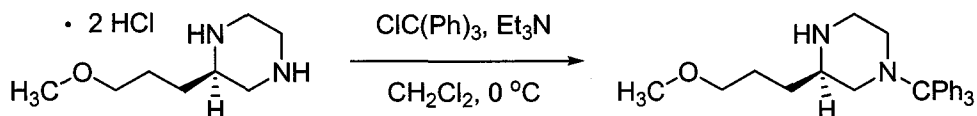
**(R)-2-(3-Methoxypropyl)-piperazine dihydrochloride ((R)-48).** Starting material (*R*)-1-benzyl-3-(3-methoxypropyl)piperazine (**(R)-138**) (0.42 g, 1.7 mmol) was dissolved in MeOH (50 mL, HPLC) with stirring. To the stirred solution was added 12 M HCl (0.28 mL, 3.4 mmol), followed by 5% Pd/C (0.063 g). Flask was sealed with a septum and  $\text{H}_2$  was bubbled through the suspension by balloon. The reaction was filtered over a pad of Celite, rinsing with MeOH. The filtrate was concentrated giving (**R**)-**48** as a white salt (0.36 g, 93%).  $^1\text{H}$  NMR (DMSO, 400 MHz)  $\delta$  1.40-1.85 (m, 4H), 2.92-3.62 (4m, 11H), 3.18 (s, 3H), 4.14 (bs, 1H),

9.79-10.31 (2bs, 4H).  $^{13}\text{C}$  NMR (DMSO, 100 MHz)  $\delta$  24.3, 26.8, 39.3, 39.9, 43.4, 51.5, 57.9, 71.0.

The opposing enantiomer was similarly prepared:

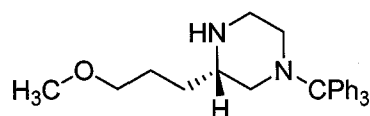


**(S)-2-(3-Methoxypropyl)-piperazine dihydrochloride ((S)-48).** White solid; (0.22 g, 95%).

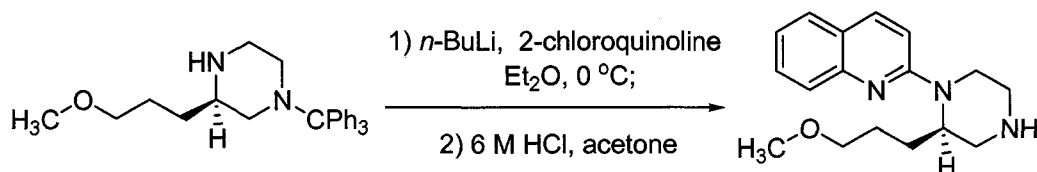


**(R)-3-(3-Methoxypropyl)-1-tritylpiperazine ((R)-49).** A stirred suspension of starting material (*R*)-2-(3-methoxypropyl)-piperazine dihydrochloride (**(R)-48**) (0.36 g, 1.56 mmol) in dry  $\text{CH}_2\text{Cl}_2$  (15 mL) was treated with  $\text{Et}_3\text{N}$  (0.87 mL, 6.25 mmol) under argon, giving a clear solution. The solution was cooled at  $0\text{ }^\circ\text{C}$  and trityl chloride (0.44 g, 1.56 mmol) in  $\text{CH}_2\text{Cl}_2$  (10 mL) was added drop-wise. The reaction was stirred overnight allowing it to slowly warm to  $\text{RT } ^\circ\text{C}$ . The crude reaction mixture was then transferred to a separatory funnel and washed with sat.  $\text{NaHCO}_3$  (1 x 50 mL), water (1 x 30 mL), and then brine (1 x 30 mL). The organic layer was dried ( $\text{K}_2\text{CO}_3$ ), filtered and concentrated *in vacuo*, to give **(R)-49** as a white foam (0.60 g, 97%): TLC  $R_f = 0.33$  (1:9 MeOH/ $\text{CH}_2\text{Cl}_2$ ); The crude product was used directly in the next reaction without further purification or characterization.

The opposing enantiomer was similarly prepared:



**(S)-3-(3-Methoxypropyl)-1-tritylpiperazine ((S)-49).** White foam; (0.37 g, 97%).



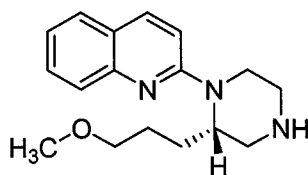
**(R)-2-[2-(3-Methoxypropyl)-piperazin-1-yl]-quinoline ((R)-50).** A stirred and cooled (0 °C) solution of (*R*)-3-(3-methoxypropyl)-1-tritylpiperazine (**(R)-49**) (0.60 g, 1.51 mmol) in dry Et<sub>2</sub>O (25 mL) was treated with *n*-BuLi (0.67 mL, 2.25 M in hexanes, 1.51 mmol) under an atmosphere of argon, giving a cloudy suspension. After 20 min a solution of 2-chloroquinoline (0.17 g, 1.01 mmol) in dry Et<sub>2</sub>O (10 mL) was added drop-wise to give initially a orange solution. The mixture was allowed to stir for 20 min and the ice bath was removed. The solution then darkened to a red wine color over 2 h. The reaction was allowed to stir under argon (4 h), where the solution returned to an orange color. The reaction was quenched by the addition of saturated NaHCO<sub>3</sub> (50 mL). The aqueous phase was separated and the organic layer was washed with brine (30 mL). The organic phase was dried (K<sub>2</sub>CO<sub>3</sub>), and concentrated *in vacuo* to give a yellow amorphous foam. The foam was purified by column chromatography over silica gel (50 g) loaded with CHCl<sub>3</sub> and eluting with 1:3 EtOAc/hexanes to give the

intermediate 2-((R)-2-(3-methoxypropyl)-4-tritylpiperazin-1-yl)quinoline as a clear yellow oil (0.44 g, 83% yield).

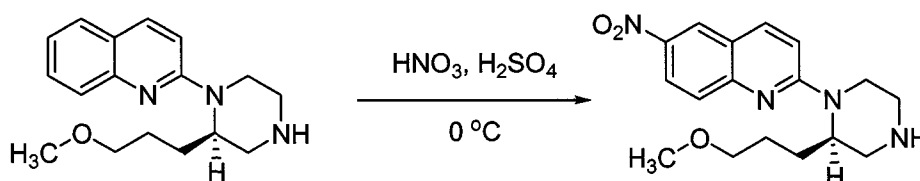
The trityl protected quipazine (0.44 g, 0.55 mmol) was dissolved in acetone (3 mL) with stirring. To the stirred solution was added 6 M HCl (0.7 mL, 4.2 mmol) giving an orange solution that slowly generated a white precipitate, stirring continued for 10 min. The reaction was diluted out in 1 M HCl (50 mL), the crude aqueous mixture was extracted with CH<sub>2</sub>Cl<sub>2</sub> (4 x 25 mL). The aqueous layer was then basified to pH 14 with 4 M NaOH, and then buffered to pH 10 with saturated NaHCO<sub>3</sub>. The aqueous layer was extracted with CH<sub>2</sub>Cl<sub>2</sub> (4 x 30 mL). The organic portions were combined, dried (K<sub>2</sub>CO<sub>3</sub>), filtered, and concentrated *in vacuo*, giving a yellow oil (**R**)-50 (0.22 g, 90%; 75% 2 steps overall): TLC  $R_f$  = 0.1 (1:9 MeOH/CH<sub>2</sub>Cl<sub>2</sub>); <sup>1</sup>H NMR (CDCl<sub>3</sub>, 400 MHz) δ 1.50-1.70 (m, 2H), 1.72-2.00 (2m, 2H), 2.37 (bs, 1H), 2.88 (dt, J = 3.2 and 12.0 Hz, 1H), 2.95-3.25 (m, 4H), 3.30 (s, 3H), 3.38 (m, 2H), 4.38 (bd, 1H), 4.52 (bs, 1H), 6.94 (d, J = 9.1 Hz, 1H), 7.20 (ddd, J = 1.3 and 7.1 Hz, 1H), 7.52 (ddd, J = 1.7 and 6.8 Hz, 1H), 7.58 (dd, J = 1.3 and 7.8 Hz, 1H), 7.84 (d, J = 8.4 Hz, 1H); <sup>13</sup>C NMR (CDCl<sub>3</sub>, 100 MHz) δ 24.7, 26.7, 40.0, 46.0, 47.9, 51.4, 58.6, 72.6, 109.3, 122.0, 122.8, 126.4, 127.1, 129.4, 137.4, 147.9, 157.0.



The opposing enantiomer was similarly prepared:



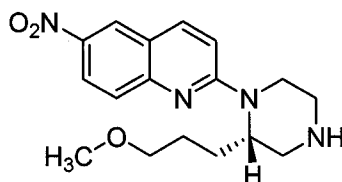
**(S)-2-[2-(3-Methoxypropyl)-piperazin-1-yl]-quinoline ((S)-50).** Yellow oil; (0.13 g, 73% 2 steps).



**(R)-2-[2-(3-Methoxypropyl)-piperazin-1-yl]-6-nitroquinoline ((R)-51).** A cooled (0 °C) stirred solution of (*R*)-2-[2-(3-methoxypropyl)-piperazin-1-yl]-quinoline (**(R)-50**) (0.22 g, 0.76 mmol) in H<sub>2</sub>SO<sub>4</sub> (6 mL, 16 M) was treated dropwise with HNO<sub>3</sub> (0.20 mL, 3.0 mmol, 15.4 M). The reaction was stirred at 0° C for 20 min and quenched by pouring over ice. The solution was brought to pH 14 by the addition of 4 M NaOH giving a bright yellow solution, and then buffered to pH 10 with saturated NaHCO<sub>3</sub> followed by extraction with CH<sub>2</sub>Cl<sub>2</sub>, until no yellow color was brought into the organic layer. The organic portions were combined, dried (K<sub>2</sub>CO<sub>3</sub>), filtered, and concentrated *in vacuo* to give a dark yellow oil (**(R)-51**) (0.25 g, quantitative):  $[\alpha]_D^{20} = -136^\circ$  (*c* = 0.0016, CH<sub>2</sub>Cl<sub>2</sub>); TLC *R<sub>f</sub>* = 0.14 (1:9 MeOH/CH<sub>2</sub>Cl<sub>2</sub>); <sup>1</sup>H NMR (CDCl<sub>3</sub>, 400 MHz)  $\delta$  1.46-1.68 (m, 2H), 1.78-2.00 (m, 2H), 1.92 (bs, 1H), 2.82 (dt, *J* = 3.6 and 12.0 Hz, 1H), 2.96 (dd, *J* = 3.9 and 12.3 Hz, 1H), 3.03-3.15 (m, 2H), 3.15-3.26 (m, 1H), 3.29 (s, 3H), 3.38 (m, 2H), 4.45 (bd, 1H), 5.59 (bs, 1H), 7.01 (d, *J* = 9.4 Hz, 1H), 7.57 (d, *J* = 9.4 Hz, 1H), 7.87 (d,

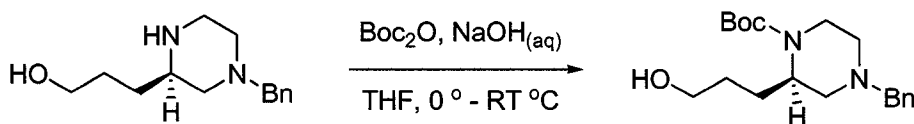
J = 9.4 Hz, 1H), 8.24 (dd, J = 2.6 and 9.4 Hz, 1H), 8.47 (d, J = 2.6 Hz, 1H);  $^{13}\text{C}$  NMR ( $\text{CDCl}_3$ , 100 MHz)  $\delta$  25.6, 26.7, 40.1, 46.0, 48.1, 51.6, 58.8, 72.7, 111.0, 121.1, 123.8, 124.4, 127.2, 138.8, 141.9, 151.8, 158.6.

The opposing enantiomer was similarly prepared:



**(S)-2-[2-(3-Methoxypropyl)-piperazin-1-yl]-6-nitroquinoline ((S)-51).** Dark yellow oil;  $[\alpha]_D^{20} = +132^\circ$  ( $c = 0.0011$ ,  $\text{CH}_2\text{Cl}_2$ ); (0.15 g, 98%).

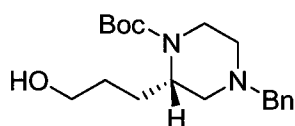
#### 6.4 Chiral Propyl N-Boc Series.



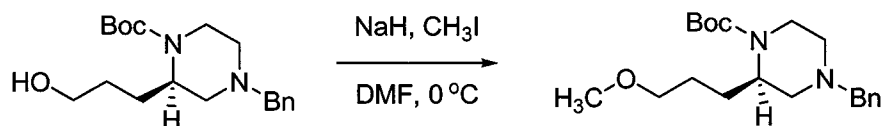
**(R)-tert-Butyl-4-benzyl-2-(3-hydroxypropyl)piperazine-1-carboxylate ((R)-140).** 3-((R)-4-benzylpiperazin-2-yl)propan-1-ol (**(R)-135**) (1.68 g, 6.41 mmol) in NaOH (3 M, 6.4 mL) and THF (2 mL) was treated with di-*tert*-butyl dicarbonate ( $\text{Boc}_2\text{O}$ ) (1.54 g, 7.05 mmol) in THF (6.4 mL) at 0 °C. The reaction was allowed to stir for 15 min then warmed to RT °C and stirred for 2.5 hrs forming a white solid. The reaction was concentrated *in vacuo* to remove the THF. The resulting aqueous layer was extracted with EtOAc, dried ( $\text{Na}_2\text{SO}_4$ ), filtered, and concentrated. The crude material was purified by column chromatography over silica gel (80 g) loaded with  $\text{CHCl}_3$  and then elution using 2:3 EtOAc/hexanes to

remove nonpolar impurities, followed by 3:2 EtOAc/hexanes, then flushed with EtOAc to elute **(R)**-**140** as a clear oil (0.94 g, 40%); TLC  $R_f$  = 0.40 (6:4 EtOAc/hexanes);  $^1\text{H}$  NMR ( $\text{CDCl}_3$ , 400 MHz)  $\delta$  1.43 (bs, 11H), 1.71 (bm, 1H), 1.84-2.14 (3m, 3H), 2.68 (bd,  $J$  = 11.4 Hz, 1H), 2.75 (bd,  $J$  = 11.0 Hz, 1H), 3.06 (bm, 1H), 3.46 (dd,  $J$  = 13.2 and 53.5, 2H,  $\text{CH}_{2\text{-AXAr}}$ ), 3.65 (m, 2H,  $\text{CH}_2\text{OH}$ ), 3.86 (bs, 1H), 4.09 (bs, 1H), 7.18-7.40 (m, 5H);  $^{13}\text{C}$  NMR ( $\text{CDCl}_3$ , 100 MHz)  $\delta$  26.2, 28.4, 29.3, 39.1(broad), 50.6 (broad) 53.4, 55.8, 63.0, 63.1, 79.8, 127.0, 128.2, 128.7, 138.2, 154.8.

The opposing enantiomer was similarly prepared:



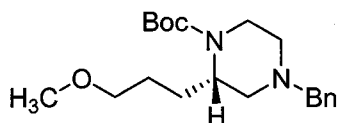
**(S)**-*tert*-Butyl-4-benzyl-2-(3-hydroxypropyl)piperazine-1-carboxylate **((S)**-**140**). Clear oil; (0.87 g, 42%).



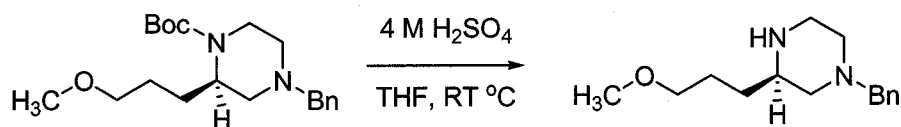
**(R)**-*tert*-Butyl-4-benzyl-2-(3-methoxypropyl)piperazine-1-carboxylate **((R)**-**141**). A stirred solution of **(R)**-*tert*-butyl 4-benzyl-2-(3-hydroxypropyl)piperazine-1-carboxylate **(R)**-**140** (0.89 g, 2.7 mmol) in dry DMF (15 mL) was treated with NaH powder (0.13 g, 5.3 mmol) at 0 °C and stirred for an additional 30 min. The resulting alkoxide intermediate was treated with  $\text{CH}_3\text{I}$  at 0 °C and then allowed to warm to RT °C overnight. The reaction was quenched by the addition of water

(15 mL) followed by the addition of sat. NaHCO<sub>3</sub> (15 mL). The aqueous layer was extracted with Et<sub>2</sub>O, dried (K<sub>2</sub>CO<sub>3</sub>), filtered, and concentrated *in vacuo*. The crude material was purified by column chromatography over silica gel (35 g) loaded with CHCl<sub>3</sub>, eluting with 1:3 EtOAc/hexanes (1 column length) followed by 2:3 EtOAc/hexanes to elute (**R**)-**141** as a clear oil (0.63 g, 68%): TLC *R<sub>f</sub>* = 0.55 (6:4 EtOAc/hexanes); <sup>1</sup>H NMR (CDCl<sub>3</sub>, 400 MHz) δ 1.44 (s, 11H), 1.66 (bm, 1H), 1.80-2.12 (3m, 3H), 2.66 (bd, *J* = 11.4 Hz, 1H), 2.73 (bd, *J* = 10.6 Hz, 1H), 3.04 (bm, 1H), 3.13 (s, 3H), 3.33-3.41 (m, 3H), 3.50 (d, *J* = 13.2 Hz, 1H, CH<sub>2</sub>Ar), 3.87 (bs, 1H), 4.04 (bs, 1H), 7.20-7.36 (m, 5H); <sup>13</sup>C NMR (CDCl<sub>3</sub>, 100 MHz) δ 26.2, 26.3, 28.4, 38.6 (broad), 51.2 (broad), 53.2, 55.7, 58.4, 62.8, 72.5, 79.3, 126.9, 128.1, 128.7, 138.2, 154.7.

The opposing enantiomer was similarly prepared:



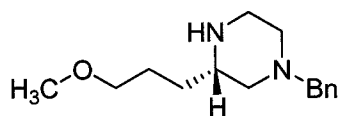
**(S)-tert-Butyl-4-benzyl-2-(3-methoxypropyl)piperazine-1-carboxylate ((S)-141)**. Clear oil; (0.61 g, 70%).



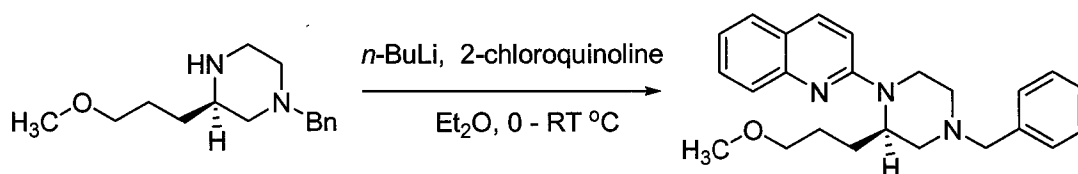
**(R)-1-Benzyl-3-(3-methoxypropyl)piperazine ((R)-138)**. A stirred solution of (*R*)-tert-butyl 4-benzyl-2-(3-methoxypropyl)piperazine-1-carboxylate (**R**)-**141** (0.58 g, 1.67 mmol) in THF (2 mL) was treated with H<sub>2</sub>SO<sub>4</sub> (4 M, 4 mL) and was

allowed to stir at RT °C overnight. The reaction was cooled at 0 °C and treated with NaOH (4 M) then buffered to pH 10 with sat. NaHCO<sub>3</sub>. The aqueous layer was extracted with CH<sub>2</sub>Cl<sub>2</sub> (2 x 10 mL) and 4:1 CHCl<sub>3</sub>/IPOH (15 mL). The organic portions were combined, dried (K<sub>2</sub>CO<sub>3</sub>), filtered and concentrated *in vacuo* to give (*R*)-**138** as a clear oil (0.36 g, 87%): TLC *R<sub>f</sub>* = 0.05 (1:9 MeOH/CH<sub>2</sub>Cl<sub>2</sub>); <sup>1</sup>H NMR (CDCl<sub>3</sub>, 400 MHz) δ 1.24-1.41 (m, 2H), 1.43-1.70 (m, 4H), 1.97 (dt, *J* = 3.7 and 11.0 Hz, 1H), 2.64-2.94 (4m, 5H), 3.26 (s, 3H), 3.31 (m, 2H, CH<sub>2</sub>OCH<sub>3</sub>), 3.44 (dd, *J* = 2.2 and 13.2 Hz, 2H, CH<sub>2-AB</sub>Ar), 7.16-7.30 (m, 5H); <sup>13</sup>C NMR (CDCl<sub>3</sub>, 100 MHz) δ 25.8, 31.0, 45.7, 53.8, 54.6, 58.4, 59.9, 63.3, 72.5, 126.8, 128.0, 129.0, 137.9.

The opposing enantiomer was similarly prepared:



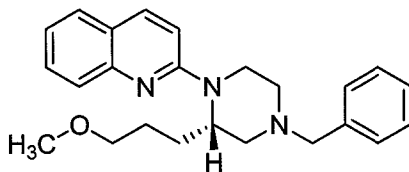
**(S)-1-benzyl-3-(3-methoxypropyl)piperazine ((S)-138).** Clear oil; (0.32 g, 80%).



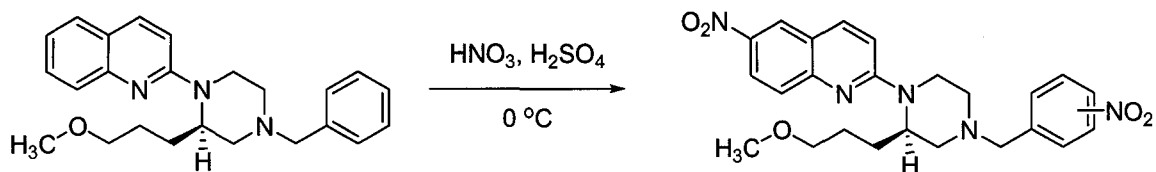
**2-((R)-4-Benzyl-2-(3-methoxypropyl)piperazin-1-yl)quinoline ((R)-142).** A stirred solution of (*R*)-1-benzyl-3-(3-methoxypropyl)piperazine (**R**)-**138** (0.17 g, 0.69 mmol) in dry Et<sub>2</sub>O (20 mL) at 0 °C was treated with *n*-BuLi (0.3 mL, 2.27M in

hexanes, 0.69 mmol) giving a yellow-orange solution. The solution was allowed to stir at 0 °C for 20 min, then treated with a solution of 2-chloroquinoline in Et<sub>2</sub>O (4 mL) to give an orange solution that was allowed to stir for 30 min. The mixture was warmed to RT °C and stirred overnight. The reaction was quenched by the addition water (10 mL). The organic portion was separated and washed with sat. NaHCO<sub>3</sub> (10 mL) and brine (10 mL). The organic layer was dried (K<sub>2</sub>CO<sub>3</sub>), filtered, and concentrated *in vacuo*. The crude material was purified by column chromatography over silica gel (8 g) loaded with CHCl<sub>3</sub>, eluting with 1:9 EtOAc/hexanes (1 column length) followed by 1:3 EtOAc/hexanes, concentration *in vacuo* gave **(R)-142** as a light yellow oil (0.094 g, 55%): TLC *R<sub>f</sub>* = 0.35 (4:6 EtOAc/hexanes); <sup>1</sup>H NMR (CDCl<sub>3</sub>, 400 MHz) δ 1.42-1.62 (m, 2H), 1.74-1.88 (m, 1H), 1.92-2.08 (m, 1H), 2.14-2.32 (m, 2H), 2.82-3.04 (m, 2H), 3.20-3.50 (m, 7H, overlapped singlet at 3.30, 3H), 3.57-3.69 (d, 1H), 4.32-4.62 (bm, 2H), 6.92 (d, J = 9.2 Hz, 1H), 7.15-7.75 (m, 9H), 7.84 (d, J = 9.2 Hz, 1H); <sup>13</sup>C NMR (CDCl<sub>3</sub>, 100 MHz) δ 25.6, 26.6, 39.8, 51.9, 53.4, 55.0, 58.4, 62.8, 72.7, 109.3, 121.8, 122.6, 126.3, 127.0, 128.2, 128.8, 129.3, 137.2, 138.4, 147.9, 156.7.

The opposing enantiomer was similarly prepared:



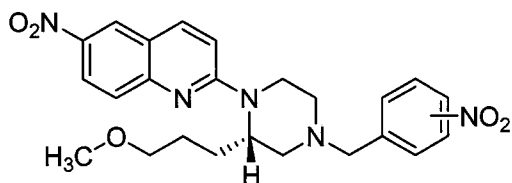
**2-((S)-4-Benzyl-2-(3-methoxypropyl)piperazin-1-yl)quinoline ((S)-142)**. Light yellow oil; (0.26, 80%).



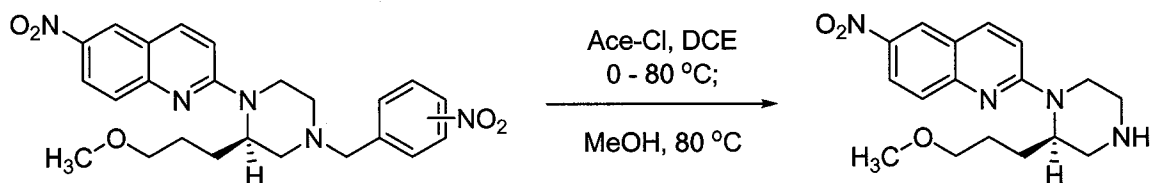
**2-((R)-4-(2-Nitrobenzyl)-2-(3-methoxypropyl)piperazin-1-yl)quinoline and 2-((R)-4-(4-Nitrobenzyl)-2-(3-methoxypropyl)piperazin-1-yl)quinoline mixture ((R)-143).** A cooled (0 °C) stirred solution of 2-((R)-4-benzyl-2-(3-methoxypropyl)piperazin-1-yl)quinoline (**(R)-142**) (0.30 g, 0.80 mmol) in H<sub>2</sub>SO<sub>4</sub> (16 M, 4 mL) was treated (dropwise) with HNO<sub>3</sub> (15.4 M, 0.16 mL). The mixture was allowed to stir for 20 min. The reaction was quenched by pouring onto ice. The acid was neutralized with 4 M NaOH to give a bright yellow solution, and the resulting solution was buffered to pH 10 with sat NaHCO<sub>3</sub> and extracted with CH<sub>2</sub>Cl<sub>2</sub> until minimal yellow color persisted in the aqueous layer. The organics were dried (K<sub>2</sub>CO<sub>3</sub>), and concentrated *in vacuo* to give a bright yellow oil (**(R)-143**) (0.022 g, 84% yield). The crude material was purified by column chromatography over silica gel (3 g) loaded with CHCl<sub>3</sub> and eluting with 1:3 EtOAc/hexanes followed by 2:3 EtOAc/hexanes, concentration *in vacuo* gave **(R)-143** as a yellow oil (0.34 g, 92%)(mixture of regioisomers): TLC 0.21 (4:6 EtOAc/hexanes); <sup>1</sup>H NMR (CDCl<sub>3</sub>, 400 MHz) δ 1.40-1.52 (m, 2H), 1.80-2.08 (m, 2H), 2.20-2.32 (m, 2H), 2.80-3.00 (bm, 2H), 3.29 (s, 3H), 3.32-3.40 (m, 2H), 3.49-3.73 (dd, J = 13.9 and 60.8 Hz, 2H, CH<sub>2-AM</sub>Ar), 4.57 (bd, 2H), 7.03 (d, J = 9.5 Hz, 1H), 7.46-7.64 (m, 2H), 7.70 (d, J = 7.7 Hz, 1H), 7.92 (d, J = 9.2 Hz, 1H), 8.10-8.30 (m, 3H), 8.50 (d, J = 2.9 Hz, 1H); <sup>13</sup>C NMR (CDCl<sub>3</sub>, 100 MHz) (mixture of BnNO<sub>2</sub> regioisomers) δ 26.2, 26.5, 39.8, 51.9, 53.4, 55.1, 58.6, 61.8, 72.5, 110.8,

120.9, 122.3, 123.4, 123.6, 124.2, 127.0, 129.3, 134.7, 138.6, 140.6, 141.7, 148.4, 151.6, 158.2.

The opposing enantiomer was similarly prepared:



**2-((S)-4-(2-Nitrobenzyl)-2-(3-methoxypropyl)piperazin-1-yl)quinoline and 2-((S)-4-(4-Nitrobenzyl)-2-(3-methoxypropyl)piperazin-1-yl)quinoline mixture ((S)-143).** Yellow oil; (0.30 g, 94%).

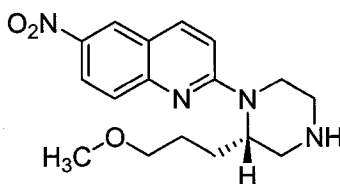


**(R)-2-[2-(3-Methoxypropyl)-piperazin-1-yl]-6-nitroquinoline ((R)-51).** To a cooled (0 °C) stirred solution of 2-((R)-4-(2 and 4-nitrobenzyl)-2-(3-methoxypropyl)piperazin-1-yl)quinoline **(R)-143** (0.25 g, 0.54 mmol) in 1,2-dichloroethane (12 mL) was added dropwise 1-Chloroethyl chloroformate (Ace-Cl) (0.3 g, 2.2 mmol) under argon. After the addition the reaction was stirred at 80 °C for 3 h, then cooled giving a yellow precipitate and concentrated *in vacuo*. The residue was dissolved in MeOH (10 mL) and heated at 70 °C for 3 h. The crude reaction mixture was concentrated *in vacuo* and the residue was taken up in 1 M HCl and then extracted with CH<sub>2</sub>Cl<sub>2</sub> (3 x 10 mL). The resulting aqueous



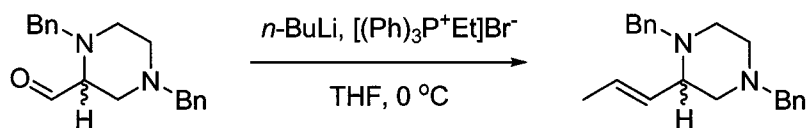
layer was brought to basic pH with 4 M NaOH and then buffered to pH 10 with sat. NaHCO<sub>3</sub>. The basic phase was extracted with CH<sub>2</sub>Cl<sub>2</sub> (3 x 15 mL), the organic portions were combined, dried (K<sub>2</sub>CO<sub>3</sub>), and concentrated *in vacuo*. The crude material was purified by flash chromatography (Biotage). The column was eluted by a 3 segment gradient elution; segment 1: 10% - 25% EtOAc/hexanes over 120 mL, segment 2: 25% - 100% EtOAc/hexanes over 120 mL, segment 3: 100% EtOAc over 120 mL. The fractions containing product were combined and concentrated *in vacuo* to give (**R**)-**51** as a yellow foam (0.087 g, 49%): TLC  $R_f$  = 0.14 (1:9 MeOH/CH<sub>2</sub>Cl<sub>2</sub>); <sup>1</sup>H NMR (CDCl<sub>3</sub>, 400 MHz) δ 1.46-1.68 (m, 2H), 1.78-2.00 (m, 2H), 1.92 (bs, 1H), 2.82 (dt, J = 3.6 and 12.0 Hz, 1H), 2.96 (dd, J = 3.9 and 12.3 Hz, 1H), 3.03-3.15 (m, 2H), 3.15-3.26 (m, 1H), 3.29 (s, 3H), 3.38 (m, 2H), 4.45 (bd, 1H), 5.59 (bs, 1H), 7.01 (d, J = 9.4 Hz, 1H), 7.57 (d, J = 9.4 Hz, 1H), 7.87 (d, J = 9.4 Hz, 1H), 8.24 (dd, J = 2.6 and 9.4 Hz, 1H), 8.47 (d, J = 2.6 Hz, 1H); <sup>13</sup>C NMR (CDCl<sub>3</sub>, 100 MHz) δ 25.6, 26.7, 40.1, 46.0, 48.1, 51.6, 58.8, 72.7, 111.0, 121.1, 123.8, 124.4, 127.2, 138.8, 141.9, 151.8, 158.6.

The opposing enantiomer was similarly prepared:

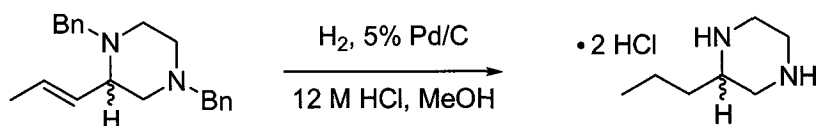


**2-((S)-4-(2 and 4-nitrobenzyl)-2-(3-methoxypropyl)piperazin-1-yl)quinoline ((S)-51)**. Yellow foam; (0.11, 62%).

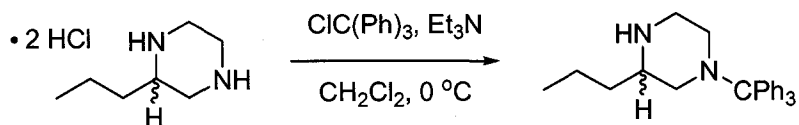
## 6.5 Racemic *n*-PROP-NQP Synthesis.



**1,4-Dibenzyl-2-(prop-1-enyl)piperazine (149).** A stirred suspension of ethyl triphenylphosphonium bromide (2.73 g, 7.34 mmol) in dry THF (15 mL) was cooled at 0° C and then treated with *n*-BuLi (2.9 mL, 7.28 mmol) giving an orange-red suspension. The mixture was stirred for one hour at 0° C. 1,4-dibenzyl-piperazine-2-carbaldehyde **44** (1.06 g, 3.64 mmol) in dry THF (4 mL) was added dropwise to the ylide solution. The reaction was allowed to warm to RT° C and stirred for 18 h. The reaction was quenched with water (20 mL). The solvent (THF) was removed *in vacuo*, and then treated with sat. NaHCO<sub>3</sub> (20 mL). The aqueous phase was extracted with CH<sub>2</sub>Cl<sub>2</sub> (4 x 15 mL), the organic portions were combined, dried (K<sub>2</sub>CO<sub>3</sub>) and concentrated *in vacuo* to give a white/tan semi-solid (3.5 g). The crude material was purified by column chromatography over silica gel (80 g) loaded with CHCl<sub>3</sub> and eluting with 2:3 EtOAc/hexanes followed by 3:2 EtOAc/hexanes, concentration *in vacuo* gave **149** as a light tan oil (0.78 g, 71%, 2 steps overall): TLC  $R_f$  = 0.57 (3:2 EtOAc/Hexanes); <sup>1</sup>H NMR (CDCl<sub>3</sub>, 400 MHz) δ 1.68 (dd, J = 1.8 and 7.0 Hz, 3H), 1.98-2.25 (m, 3H), 2.60-2.78 (m, 3H), 3.08 and 4.06 (2d, J = 13.2 Hz, 2H), 3.27 (dt, J = 2.9 and 9.5 Hz, 1H), 3.50 (dd, J = 13.2 and 38.5, 2H), 5.43 (bt, J = 9.5 Hz, 1H), 5.58-5.70 (m, 1H), 7.12-7.38 (m, 10H); <sup>13</sup>C NMR (CDCl<sub>3</sub>, 100 MHz) δ 13.6, 51.2, 52.8, 58.1, 58.3, 58.8, 62.9, 126.7, 126.9, 127.2, 128.0, 128.1, 129.1, 129.2, 131.4, 137.9, 138.8.

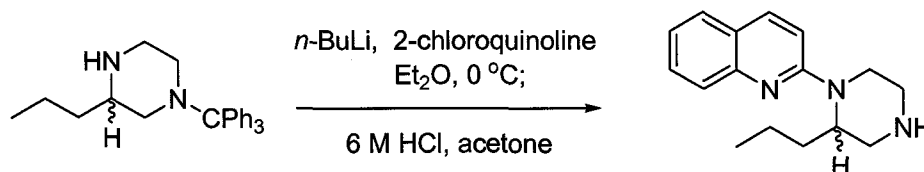


**2-Propylpiperazine dihydrochloride (150).** 5% Pd/C (1.2 g) was added to a stirred solution of 1,4-dibenzyl-2-(prop-1-enyl)piperazine **149** (0.78 g, 2.6 mmol) in MeOH (25 mL) and HCl (0.45 mL, 12 M, 5.4 mmol) with stirring. The flask was sealed with a septum and hydrogen gas was bubbled through the solution at atmospheric pressure. The reaction mixture was filtered over a pad of Celite. The pad was rinsed with MeOH and concentrated *in vacuo* to give **150** (0.48 g, 92%) as a white solid:  $^1\text{H}$  NMR ( $\text{D}_2\text{O}$ , 400 MHz)  $\delta$  0.76 (t,  $J = 7.3$ , 3H), 1.18-1.32 (m, 2H), 1.46-1.60 (m, 2H), 3.02 (dd,  $J = 12.1$  Hz, 1H), 3.18-3.30 (m, 2H), 3.39-3.49 (m, 1H), 3.51-3.61 (m, 3H);  $^{13}\text{C}$  NMR ( $\text{D}_2\text{O}$ , 100 MHz)  $\delta$  12.8, 17.5, 32.0, 40.1, 40.5, 44.5, 52.6.



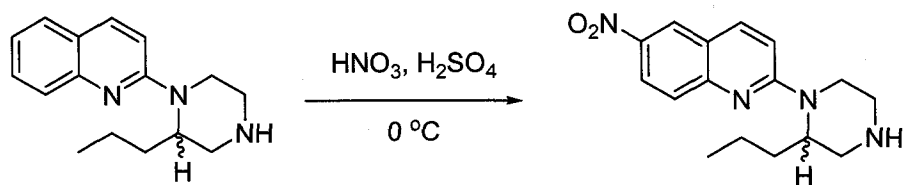
**3-Propyl-1-tritylpiperazine (151).** To a stirred solution of 2-propylpiperazine dihydrochloride **150** (0.48 g, 2.4 mmol) in dry  $\text{CH}_2\text{Cl}_2$  (12 mL) under argon was added dry  $\text{Et}_3\text{N}$  (1.3 mL, 9.5 mmol). The solution was cooled at  $0^\circ\text{C}$ , and trityl chloride (0.64 g, 2.28 mmol) in dry  $\text{CH}_2\text{Cl}_2$  (5 mL) was added drop-wise. Once the addition was complete the ice bath was removed and the reaction stirred overnight at room temperature. The reaction mixture was washed with saturated  $\text{NaHCO}_3$  (75 mL), water (75 mL), and then brine (75 mL). The organic portions

were combined, dried ( $K_2CO_3$ ), and concentrated *in vacuo* to give **151** (0.84 g, 99% yield) as a white amorphous foam. The crude material was used without further purification or spectroscopic characterization: TLC  $R_f = 0.15$  (1:9 MeOH/ $CH_2Cl_2$ ).



**2-(2-Propylpiperazin-1-yl)quinoline (152).** A solution of 3-propyl-1-tritylpiperazine **151** (0.85 g, 2.28 mmol) in dry Et<sub>2</sub>O (30 mL) cooled at 0 °C, was treated with *n*-BuLi (dropwise)(0.93 mL, 2.45 M in hexanes), generating a light orange solution. The solution was allowed to stir for 20 min. A solution of 2-chloroquinoline (0.25 g, 1.52 mmol) in dry Et<sub>2</sub>O (5 mL) was added drop-wise to the lithium amide. The resulting mixture was allowed to stir for 1 h at 0 °C then the ice bath was removed. The reaction was allowed to warm to RT °C and stir for 4 h, giving a brown colored solution. The reaction was quenched with saturated NaHCO<sub>3</sub> (30 mL). The organic layer was separated, and then washed with water (20 mL) and brine (20 mL). The organic portion was dried ( $K_2CO_3$ ), filtered, and concentrated *in vacuo* to give a white foam. The foam was purified by column chromatography over silica gel (45 g) loaded with CHCl<sub>3</sub> and eluted with 1:9 EtOAc/hexanes to give the N-trityl protected product as a clear yellow oil (0.54 g, 71% yield). The oil was dissolved in Acetone (8 mL) and HCl (6 M, 2.5 mL), the mixture was allowed to stir 20 min. The reaction mixture was diluted with 1 M HCl (20 mL) and extracted with CH<sub>2</sub>Cl<sub>2</sub> (4 x15 mL), the aqueous layer

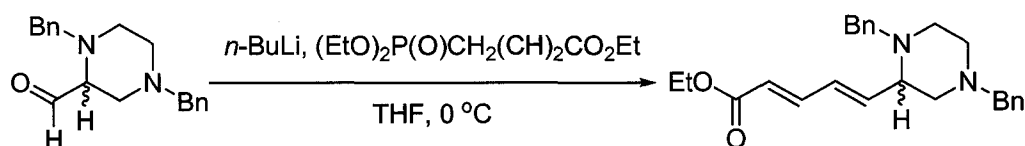
was basified to pH 12 with 4 M NaOH and then buffered to pH 10 with saturated NaHCO<sub>3</sub>. The aqueous layer was then extracted with CH<sub>2</sub>Cl<sub>2</sub> (4 x 15 mL), dried with K<sub>2</sub>CO<sub>3</sub>, and concentrated *in vacuo* to give **152** (0.18 g, 64%) as a light yellow oil: <sup>1</sup>H NMR (CDCl<sub>3</sub>, 400 MHz) δ 0.93 (t, J = 7.3 Hz, 3H), 1.20-1.46 (m, 2H), 1.60-1.72 (m, 1H), 1.76-1.90 (m, 2H), 2.81-2.91 (m, 1H), 2.96-3.22 (m, 4H), 4.34-4.46 (bm, 2H), 6.93 (d, J = 9.2 Hz, 1H), 7.2 (m, 1H), 7.5 (m, 1H), 7.57 (d, J = 8.1 Hz, 1H), 7.66 (d, J = 8.4 Hz, 1H), 7.85 (d, J = 9.2 Hz, 1H).



**2-(2-propylpiperazin-1-yl)-6-nitroquinoline (52).** A stirred solution of 2-(2-propylpiperazin-1-yl)quinoline **152** (0.16 g, 0.64 mmol) in H<sub>2</sub>SO<sub>4</sub> (16 M, 4 mL) was cooled at 0° C. To the cooled solution was added HNO<sub>3</sub> (15.4 M, 0.17 mL) (dropwise). The reaction was stirred for 20 min, then quenched pouring onto ice. The acid was neutralized with 4 M NaOH to give a bright yellow solution, and the resulting solution was buffered to pH 10 with sat NaHCO<sub>3</sub>. The aqueous solution was extracted with CH<sub>2</sub>Cl<sub>2</sub> until minimal yellow color persisted in the aqueous layer. The organic portions were combined, dried (K<sub>2</sub>CO<sub>3</sub>), and concentrated *in vacuo* to give a bright yellow oil **52** (0.20 g, quantitative yield): TLC *R<sub>f</sub>* = 0.11 (1:9 MeOH/CH<sub>2</sub>Cl<sub>2</sub>); <sup>1</sup>H NMR (CDCl<sub>3</sub>, 400 MHz) δ 0.94 (t, J = 7.3 Hz, 3H), 1.20-1.42 (m, 2H), 1.63-1.91 (2m, 3H), 2.83 (dt, J = 3.3 and 12.1 Hz, 1H), 3.00-3.24 (m, 4H), 4.50 (bs, 2H), 7.00 (d, J = 9.5 Hz, 1H), 7.57 (d, J = 9.2 Hz, 1H), 7.89 (d, J =

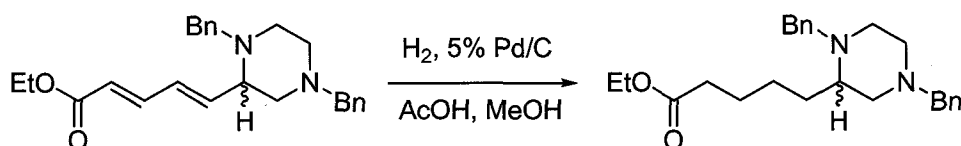
9.2 Hz, 1H), 8.24 (dd, J = 2.6 and 9.2 Hz, 1H), 8.47 (d, J = 2.6 Hz, 1H);  $^{13}\text{C}$  NMR ( $\text{CDCl}_3$ , 100 MHz)  $\delta$  14.0, 19.7, 30.7, 40.3, 46.2, 48.2, 51.8, 110.8, 120.7, 123.5, 124.1, 126.8, 138.4, 141.5, 151.6, 158.4; HRMS (ESI-TOF)  $m/z$  ( $\text{M} + \text{H}$ ) $^+$  calcd. for  $\text{C}_{16}\text{H}_{21}\text{N}_4\text{O}_2$  301.1665 found 301.1655.

## 6.6 Racemic Pent-NQP Series.



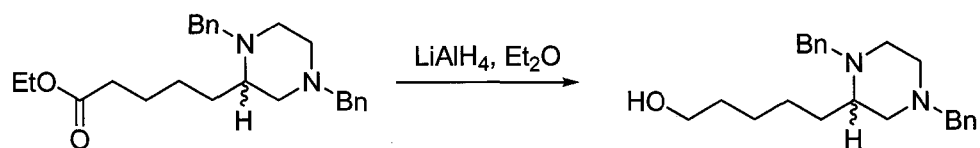
**Ethyl 5-(1,4-dibenzylpiperazin-2-yl)penta-2,4-dienoate (76).** A stirred solution of  $n\text{-BuLi}$  (2.45 M, 5.6 mL in hexanes, 13.6 mmol) in dry THF (20 mL) was treated with triethylphosphonocrotonate (2.8 g, 13.6 mmol) at  $0\text{ }^\circ\text{C}$  under argon, to give a yellow solution. After 30 min a solution of the 1,4-dibenzyl-piperazine-2-carbaldehyde **44** (2.0 g, 13.6 mmol) in dry THF (10 mL) was added dropwise to the cooled ylide solution, and stirring was maintained for 45 min. The reaction mixture was allowed to warm to room temperature, stir for 20 h. The reaction was quenched by the addition of water (15 mL) and concentrated *in vacuo* to remove THF. The resulting aqueous layer was treated with 20 mL of sat.  $\text{NaHCO}_3$  and extracted with  $\text{Et}_2\text{O}$  (3 x 30 mL). The combined organic extracts were washed with brine (20 mL), dried ( $\text{K}_2\text{CO}_3$ ) and concentrated *in vacuo*, to give an orange oil. The crude oil was purified by column chromatography over silica gel (70 g) loaded with  $\text{CHCl}_3$  and eluting with 1:3  $\text{EtOAc}$ /hexanes followed

by 2:3 EtOAc/hexanes to give **76** as a light tan oil (1.8 g, 66% 2 steps overall): TLC  $R_f$  = 0.36 (4:6 EtOAc/Hexanes);  $^1\text{H}$  NMR ( $\text{CDCl}_3$ , 400 MHz)  $\delta$  1.29 (t,  $J$  = 7.1 Hz, 3H), 2.08-2.32 (2m, 3H), 2.60-2.80 (m, 3H), 3.00-3.18 (2m, 2H, overlapped doublet at 3.11,  $J$  = 13.6 Hz, 1H,  $\text{CH}_{2\text{-Ar}}$ ), 3.49 (s, 2H,  $\text{CH}_2\text{Ar}$ ), 3.94 (d,  $J$  = 13.6 Hz, 2H,  $\text{CH}_2\text{Ar}$ ), 4.20 (q,  $J$  = 7.1 Hz, 2H), 5.85 (d,  $J$  = 15.2 Hz, 1H), 6.08-6.24 (m, 1H), 6.37 (dd,  $J$  = 11.0 and 15.2 Hz, 1H), 7.18-7.48 (m, 11H, overlapped, 10H Ar);  $^{13}\text{C}$  NMR ( $\text{CDCl}_3$ , 100 MHz)  $\delta$  14.3, 50.7, 52.9, 58.5, 59.5, 60.3, 62.8, 63.6, 121.1, 126.9, 127.0, 128.1, 128.2, 128.9, 129.1, 130.7, 137.8, 138.4, 143.5, 143.8, 166.9.



**Ethyl 5-(1,4-dibenzylpiperazin-2-yl)pentanoate (77).** To a solution of ethyl 5-(1,4-dibenzylpiperazin-2-yl)penta-2,4-dienoate **76** (1.6 g, 4.1 mmol) in HPLC grade MeOH (20 mL) and acetic acid (1.2 g, 20.5 mmol) was added 5% Pd/C (0.32 g). The reaction flask was sealed with a septum, fitted with hydrogen balloon and a bleed needle. One balloon of hydrogen was bubbled through the stirred solution; the bleed needle was removed and a second balloon was attached and the reaction was stirred overnight. The reaction was filtered over a pad of Celite, the pad was rinsed with MeOH and the filtrate was concentrated *in vacuo*. The resulting oil was dissolved in  $\text{CH}_2\text{Cl}_2$ , basified with 4 M NaOH and then buffered to pH 10 with sat.  $\text{NaHCO}_3$ . The organic layer was separated and the aqueous layer was extracted with  $\text{CH}_2\text{Cl}_2$  (3 x 10 mL). The organic portions

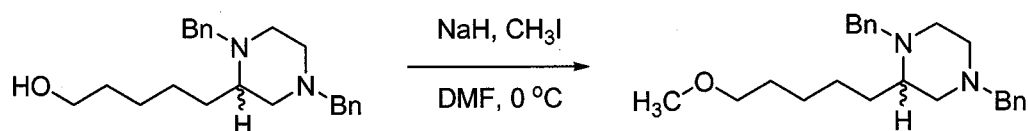
were combined, dried ( $K_2CO_3$ ) and concentrated *in vacuo*. The crude oil was purified by column chromatography over silica gel (60 g) loaded with  $CHCl_3$  and eluted 1.5 column lengths with 1:3 EtOAc/hexanes followed by 2:3 EtOAc/hexanes to give the product **77** after concentration as clear oil (3.5 g, 78%): product was visualized in two different TLC solvent systems;  $R_f = 0.27$  (2:3 EtOAc/Hexanes) and  $R_f = 0.6$  (1:9 MeOH/ $CH_2Cl_2$ );  $^1H$  NMR ( $CDCl_3$ , 400 MHz)  $\delta$  1.16-1.50 (m, 5H, overlapped triplet at 1.25,  $J = 7.1$  Hz, 3H,  $CO_2CH_2CH_3$ ), 1.52-1.76 (m, 4H), 2.10-2.80 (m, 9H), 3.20 (d,  $J = 13.2$  Hz, 1H,  $CH_{2-AX}Ar$ ), 3.49 (dd,  $J = 13.2$  and 41.7 Hz, 2H,  $CH_{2-AM}Ar$ ), 4.00 (d,  $J = 13.2$  Hz, 1H,  $CH_{2-AX}Ar$ ), 4.12 (q,  $J = 7.1$  Hz, 2H,  $CO_2CH_2CH_3$ ), 7.18-7.45 (m, 10H);  $^{13}C$  NMR ( $CDCl_3$ , 100 MHz)  $\delta$  14.2, 25.0, 25.4, 29.3, 34.2, 50.7, 52.8, 57.5, 57.6, 59.4, 60.1, 63.0, 126.7, 126.8, 128.1, 128.8, 128.9, 138.2, 139.0, 173.5.



**5-(1,4-Dibenzylpiperazin-2-yl)pentan-1-ol (78).** A solution ethyl 5-(1,4-dibenzylpiperazin-2-yl)pentanoate **77** (1.0 g, 2.5 mmol) in dry ether (20 mL) was treated at 0 °C with portions  $LiAlH_4$  powder (0.12 g, 3.0 mmol), then placed under an atmosphere of argon. The ice bath was removed and the reaction was allowed to stir for 35 min at 25 °C. The reaction was quenched by the consecutive addition of  $H_2O$  (0.12 mL), NaOH (0.24 mL 4 M), and  $H_2O$  (0.12 mL). The inorganic salts were filtered over a pad of Celite and the pad was rinsed with EtOAc. The filtrate was concentrated *in vacuo* to give **78** (2.8 g, 95%): TLC  $R_f =$

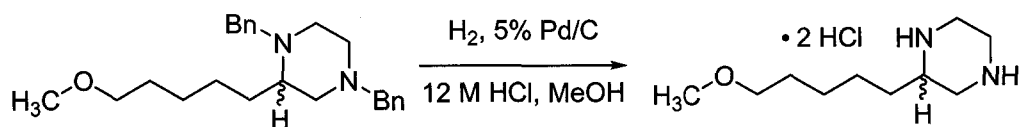


0.06 (2:3 EtOAc/Hexanes);  $^1\text{H}$  NMR ( $\text{CDCl}_3$ , 400 MHz)  $\delta$  1.20-1.45 (m, 4H), 1.48-1.68 (m, 5H), 2.10-2.28 (m, 3H), 2.40-2.76 (m, 4H), 3.20 (d,  $J = 13.2$  Hz, 1H,  $\text{CH}_{2\text{-AXAr}}$ ), 3.49 (dd,  $J = 13.2$  and 44.0 Hz, 2H,  $\text{CH}_{2\text{-AMAr}}$ ), 3.58-3.64 (bm, 2H), 4.00 (d,  $J = 13.2$  Hz, 1H,  $\text{CH}_{2\text{-AXAr}}$ ), 7.20-7.35 (m, 10H);  $^{13}\text{C}$  NMR ( $\text{CDCl}_3$ , 100 MHz)  $\delta$  25.3, 26.2, 29.6, 32.6, 50.8, 52.7, 57.5, 59.5, 62.5, 63.0, 126.7, 126.9, 128.0, 128.9, 129.0, 137.9, 138.9 (1 unresolved peak).

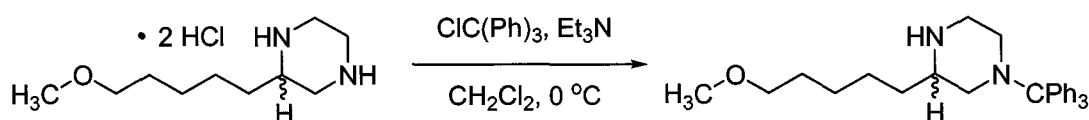


**1,4-Dibenzyl-2-(5-methoxypentyl)piperazine (79).** A stirred solution of 5-(1,4-dibenzylpiperazin-2-yl)pentan-1-ol **78** (0.69 g, 2.0 mmol) in dry DMF (10 mL) at 0 °C was treated with NaH powder (0.14 g, 5.9 mmol) to give a turbid white suspension. The flask was placed under argon and stirring was continued for 30 min. Iodomethane (0.30 g, 2.1 mmol) was added dropwise to the cooled solution. The reaction was allowed to stir on ice for 30 min, followed by stirring at room temperature for 3.5 h. The reaction was quenched by the addition of water (20 mL) followed by sat.  $\text{NaHCO}_3$  (20 mL). The aqueous layer was extracted with  $\text{Et}_2\text{O}$  (4 x 10 mL). The organic portions were combined, dried ( $\text{K}_2\text{CO}_3$ ), and concentrated *in vacuo* to give a tan oil. The oil was purified by column chromatography over silica gel (30 g) loaded with  $\text{CHCl}_3$  and eluted with 2:3 EtOAc/hexanes to give **79** after concentration as a clear oil (0.44 g, 60%): TLC  $R_f = 0.39$  (2:3 EtOAc/Hexanes);  $^1\text{H}$  NMR ( $\text{CDCl}_3$ , 400 MHz)  $\delta$  1.22-1.48 (m, 4H), 1.52-1.70 (m, 4H), 2.08-2.32 (m, 3H), 2.40-2.78 (3m, 4H), 3.20 (d,  $J = 13.2$  Hz,

1H,  $CH_{2-AX}Ar$ ), 3.32-3.40 (m, 5H, overlapped singlet, 3.33, 3H,  $OCH_3$ ), 3.49 (dd,  $J = 13.2$  and  $43.6$  Hz, 2H,  $CH_{2-AM}Ar$ ), 4.02 (d,  $J = 13.2$  Hz, 1H,  $CH_{2-AX}Ar$ ), 7.20-7.40 (m, 10H);  $^{13}C$  NMR ( $CDCl_3$ , 100 MHz)  $\delta$  25.4, 26.6, 29.0, 29.5, 50.8, 52.8, 57.6, 58.5, 59.6, 63.0, 72.0, 72.7, 126.6, 126.8, 128.0, 128.9, 129.0, 138.2, 139.0.

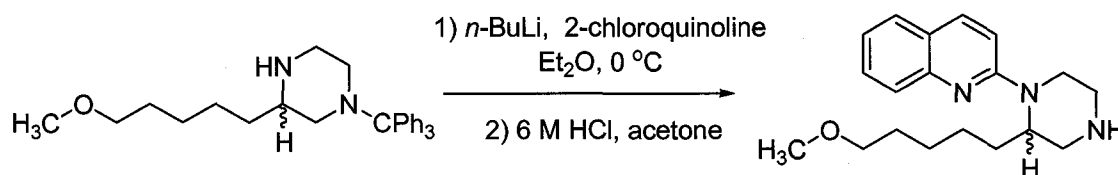


**2-(5-Methoxypentyl)piperazine dihydrochloride (80).** A solution of 1,4-dibenzyl-2-(5-methoxypentyl)piperazine **79** (0.23 g, 0.64 mmol) in HPLC grade MeOH (14 mL) and HCl (12 M, 1.92 mmol, 0.16 mL) was treated with 5% Pd/C (0.07 g). The flask was sealed with a septum and a balloon of hydrogen was bubbled through the stirred solution. The reaction mixture was filtered over a pad of Celite rinsing with MeOH and concentrated *in vacuo* to give a white solid **80** (0.17 g, quantitative).



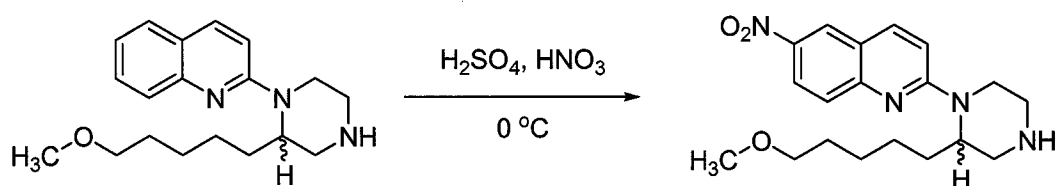
**3-(5-Methoxypentyl)-1-tritylpiperazine (81).** A solution of 2-(5-methoxypentyl)piperazine dihydrochloride **80** (0.38 g, 1.5 mmol) in dry  $CH_2Cl_2$  (10 mL) and dry  $Et_3N$  (0.59 g, 0.81 mL, 5.8 mmol) at  $0\text{ }^\circ C$ , was treated dropwise with a solution of trityl chloride (0.41 g, 1.5 mmol) in dry  $CH_2Cl_2$  (5 mL). The ice bath was removed and the reaction stirred for 20 h at room temperature. The reaction mixture was transferred to a separatory funnel and diluted to 15 mL with

CH<sub>2</sub>Cl<sub>2</sub>. The organic portion was washed with saturated NaHCO<sub>3</sub> (25 mL), brine (25 mL). The organic portion was dried (K<sub>2</sub>CO<sub>3</sub>), filtered, and concentrated *in vacuo* to give an amorphous white foam **81** (0.62 g, 99% yield): TLC 0.34 (1:9 MeOH/CH<sub>2</sub>Cl<sub>2</sub>); 3-(5-Methoxypentyl)-1-tritylpiperazine **81** was used without further purification, or spectroscopic characterization.



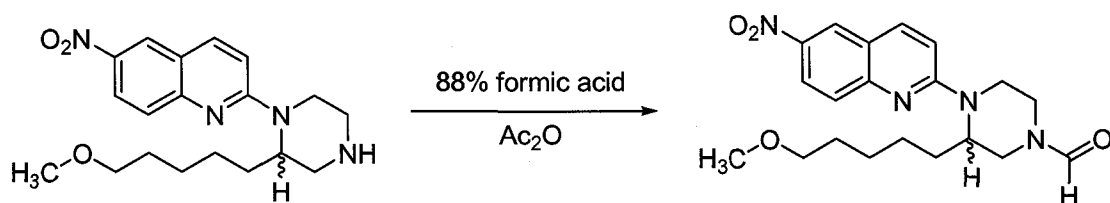
**2-(2-(5-Methoxypentyl)piperazin-1-yl)quinoline (82).** A stirred solution of 3-(5-methoxypentyl)-1-tritylpiperazine **81** (0.40 g, 0.93 mmol) in dry Et<sub>2</sub>O (25 mL) at 0 °C was treated with *n*-BuLi (0.38 mL, 2.45M in hexanes, 0.93 mmol) giving a pale orange-white suspension. The solution was allowed to stir at 0 °C for 20 min, then treated with a solution of 2-chloroquinoline (0.10 g, 0.62 mmol) in Et<sub>2</sub>O (4 mL) to give an orange-white suspension. The mixture was allowed to stir for 30 min, then warmed to RT °C and stirred overnight. The reaction was quenched by the addition water (10 mL). The organic portion was separated and washed with sat. NaHCO<sub>3</sub> (10 mL) and brine (10 mL). Then the organic layer was dried (K<sub>2</sub>CO<sub>3</sub>), filtered, and concentrated *in vacuo*. The crude material was purified by column chromatography over silica gel (30 g) loaded with CHCl<sub>3</sub> and eluted with 1:9 EtOAc/hexanes to give the N-trityl protected product as a light yellow oil (0.23 g, 66%). TLC *R<sub>f</sub>* = 0.57 (2:3 EtOAc/Hexanes). The product oil was dissolved in acetone (8 mL) and HCl (6 M, 4 mL) and allowed to stir (20 min). The reaction was diluted with 1 M HCl (20 mL) and extracted with CH<sub>2</sub>Cl<sub>2</sub> (4 x15 mL). The

aqueous layer was brought to pH 12 with 4 M NaOH and then buffered to pH 10 with saturated NaHCO<sub>3</sub>. The aqueous layer was extracted with CH<sub>2</sub>Cl<sub>2</sub> (4 x 15 mL), dried with K<sub>2</sub>CO<sub>3</sub>, and concentrated *in vacuo* to give **82** as a light yellow oil (0.11 g, 88%, 58% 2 steps overall): <sup>1</sup>H NMR (CDCl<sub>3</sub>, 400 MHz) δ 1.18-1.42 (m, 4H), 1.44-1.58 (m, 2H), 1.60-1.72 (m, 1H), 1.76-1.90 (m, 1H), 2.11 (bs, 1H), 2.84 (m, 1H), 2.94-3.18 (m, 4H), 3.24-3.34 (m, 5H, overlapped singlet, 3.28, 3H, OCH<sub>3</sub>), 4.38 (bd, 2H), 6.90 (d, J = 9.5 Hz, 1H), 7.18 (t, J = 8.06 Hz, 1H), 7.50 (t, J = 8.4 Hz, 1H), 7.56 (d, J = 8.1 Hz, 1H), 7.65 (d, J = 8.4 Hz, 1H), 7.84 (d, J = 9.2 Hz, 1H); <sup>13</sup>C NMR (CDCl<sub>3</sub>, 100 MHz) δ 26.0, 26.4, 27.7, 29.4, 40.1, 46.0, 47.8, 51.7, 58.4, 72.6, 109.3, 121.9, 122.7, 126.3, 127.0, 129.3, 137.2, 147.9, 157.0.

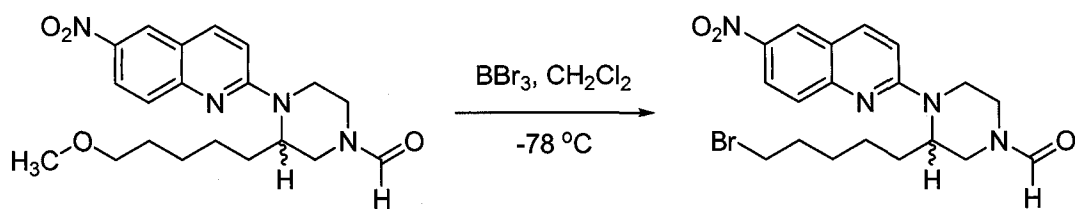


**2-(2-(5-Methoxypentyl)piperazin-1-yl)-6-nitroquinoline ((±)-83).** A stirred solution of 2-(2-(5-methoxypentyl)piperazin-1-yl)quinoline **82** (0.11 g, 0.36 mmol) in H<sub>2</sub>SO<sub>4</sub> (16 M, 4 mL) was cooled at 0° C. HNO<sub>3</sub> (15.4 M, 0.09 mL) was added drop-wise, and the reaction stirred for 20 min at 0 °C. The reaction was quenched by pouring onto ice, the acid was neutralized with 4 M NaOH to give a bright yellow solution, and the resulting solution was buffered to pH 10 with sat. NaHCO<sub>3</sub>. The yellow aqueous solution was extracted with CH<sub>2</sub>Cl<sub>2</sub> until no yellow color was extracted into the organic layer. The organics were dried (K<sub>2</sub>CO<sub>3</sub>), filtered and concentrated *in vacuo* to give a bright yellow oil ((±)-**83**) (0.13 g,

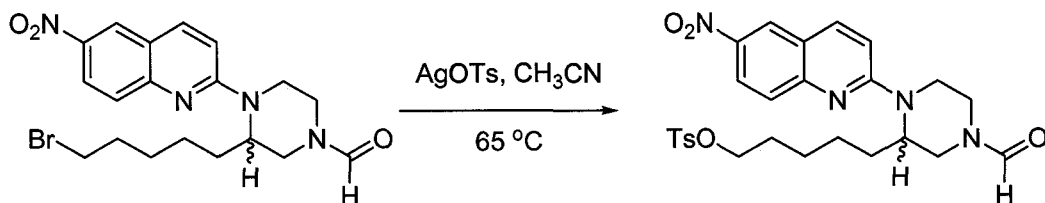
quantitative yield): TLC  $R_f$  = 0.16 (1:9 MeOH/CH<sub>2</sub>Cl<sub>2</sub>); <sup>1</sup>H NMR (CDCl<sub>3</sub>, 400 MHz)  $\delta$  1.26-1.46 (m, 4H), 1.50-1.60 (m, 2H), 1.71-1.96 (m, 2H), 2.06 (bs, 1H), 2.85 (dt, J = 3.6 and 12.3 Hz, 1H), 2.98 (dd, J = 3.6 and 12.3 Hz, 1H), 3.06-3.26 (m, 3H), 3.29 (s, 3H), 3.33 (m, 2H), 4.52 (bs, 2H), 7.01 (d, J = 9.1 Hz, 1H), 7.61 (d, J = 9.4 Hz, 1H), 7.93 (d, J = 9.4 Hz, 1H), 8.27 (dd, J = 2.6 and 9.4 Hz, 1H), 8.51 (d, J = 2.6 Hz, 1H); <sup>13</sup>C NMR (CDCl<sub>3</sub>, 100 MHz)  $\delta$  26.0, 26.2, 28.2, 29.4, 40.3, 46.1, 48.0, 51.8 58.4, 72.5, 110.7, 120.7, 123.4, 124.1, 126.8, 138.4, 141.4, 151.6, 158.3; HRMS (ESI-TOF)  $m/z$  (M + H)<sup>+</sup> calcd. for C<sub>19</sub>H<sub>27</sub>N<sub>4</sub>O<sub>3</sub> 359.2083 found 359.2086.



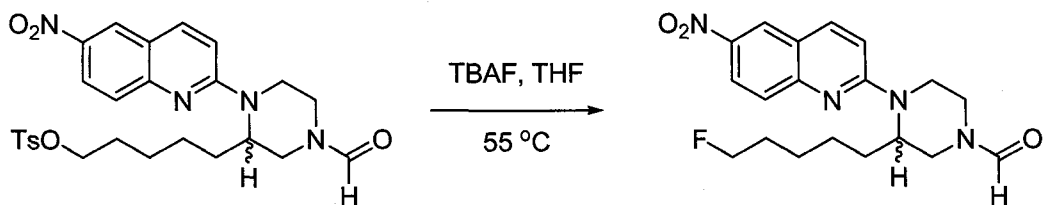
**N-Formyl-3-(5-methoxypentyl)-4-(6-nitroquinolin-2-yl)piperazine (84).** A stirred solution of 2-(2-(5-methoxypentyl)piperazin-1-yl)-6-nitroquinoline (**±**)-**83** (0.049 g, 0.14 mmol) in 88% formic acid (0.35 mL) was treated with Ac<sub>2</sub>O (0.13 g, 0.12 mL, 1.23 mmol) and the reaction was stirred for 30 min. The reaction was quenched by pouring onto ice, then brought to basic pH with 4 M NaOH, buffered to pH 10 with sat. NaHCO<sub>3</sub>, and then extracted with CH<sub>2</sub>Cl<sub>2</sub> (3 x 10 mL). The organic portions were combined, dried (K<sub>2</sub>CO<sub>3</sub>), and concentrated *in vacuo* to give **84** as a yellow oil (0.053 g, 97%): TLC  $R_f$  = 0.55 (1:9 MeOH/CH<sub>2</sub>Cl<sub>2</sub>).



**N-Formyl-3-(5-bromopentyl)-4-(6-nitroquinolin-2-yl)piperazine (85).** A solution of N-formyl-3-(5-methoxypentyl)-4-(6-nitroquinolin-2-yl)piperazine **84** (0.038 g, 0.098 mmol) in dry CH<sub>2</sub>Cl<sub>2</sub> (8 mL) was cooled at -78 °C in a dry ice, acetone bath. A solution of BBr<sub>3</sub> (0.59 mL, 1M in CH<sub>2</sub>Cl<sub>2</sub>, 0.59 mmol) was added dropwise under argon giving a deep purple suspension. The reaction was allowed to warm to RT °C while stirring overnight, giving a tan suspension. The reaction was quenched by the addition of sat. NaHCO<sub>3</sub> (20 mL). The organic layer was separated and the aqueous was extracted with CH<sub>2</sub>Cl<sub>2</sub> (3 x 20 mL). The organic portions were combined, dried (K<sub>2</sub>CO<sub>3</sub>), filtered and concentrated *in vacuo*. The crude material was purified by column chromatography over silica gel (3 g) eluting with 4:1 EtOAc/CHCl<sub>3</sub> to give **85** as a yellow oil (0.40 g, 93% yield): TLC *R<sub>f</sub>* = 0.48 (1:9 MeOH/CH<sub>2</sub>Cl<sub>2</sub>); <sup>1</sup>H NMR (CDCl<sub>3</sub>, 400 MHz) (mixture of amide rotamers) δ 1.25-1.90 (m, 8H), 2.86-2.95 (m, 0.5H), 2.99 (dd, *J* = 4.2 and 13.3 Hz, 0.5H), 3.16-3.39 (m, 4H), 3.44-3.60 (m, 1H), 3.68-3.75 (bm, 0.5H), 4.40-4.52 (m, 1.5H), 4.70 (bs, 0.5H), 4.91 (bs, 0.5H), 7.06 (dd, *J* = 3.2 and 9.4 Hz, 1H), 7.66 (d, *J* = 9.1 Hz, 1H), 8.01 (d, *J* = 9.4 Hz, 1H), 8.10 (s, 0.5H), 8.24 (s, 1H), 8.30 (dd, *J* = 2.6 and 9.1 Hz, 1H), 8.54 (d, *J* = 2.6 Hz, 1H); <sup>13</sup>C NMR (CDCl<sub>3</sub>, 100 MHz) (mixture of amide rotamers) δ 25.0, 25.2, 27.8, 28.0, 28.2, 32.3, 33.6, 33.7, 38.6, 39.6, 39.7, 42.3, 45.1, 47.9, 50.9, 51.5, 110.7, 121.2, 123.8, 124.2, 127.2, 139.1, 142.1, 151.1, 158.0, 161.3.

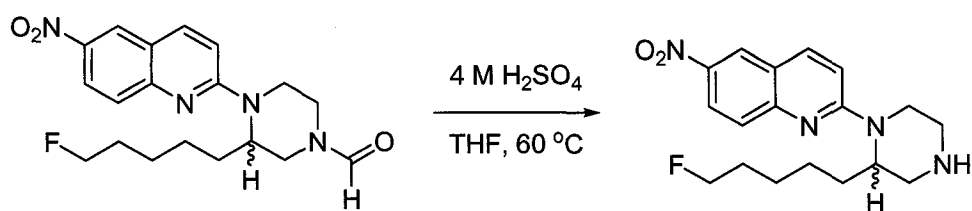


**5-(4-Formyl-1-(6-nitroquinolin-2-yl)piperazin-2-yl)pentyl 4-methylbenzenesulfonate (86).** A cooled (0 °C) stirred solution of N-formyl-3-(5-bromopentyl)-4-(6-nitroquinolin-2-yl)piperazine **85** (0.040 g, 0.092 mmol) in dry acetonitrile (ACN) (0.5 mL) was treated with silver tosylate (AgOTs) (0.051 g, 0.18 mmol) giving a clear solution. The solution was stirred for 5 min at 0 °C, 4 h at 25 °C, and 4 h at 65 °C, forming a silvery-black precipitate. The reaction was cooled and filtered over cotton, rinsing with ACN and concentrating *in vacuo*. The crude material was purified over silica gel (4 g) loading with CHCl<sub>3</sub> and eluting with 2:3 EtOAc/hexanes followed by 4:1 EtOAc/CHCl<sub>3</sub>, concentration *in vacuo* gave **86** as a yellow oil (0.042 g, 88%): <sup>1</sup>H NMR (CDCl<sub>3</sub>, 400 MHz) δ 1.21-1.49 (m, 4H), 1.51-1.80 (m, 4H), 2.43 (s, 3H), 2.84-3.02 (m, 1H), 3.12-3.26 (bm, 1H), 3.27-3.39 (m, 0.5H), 3.42-3.60 (m, 1H), 3.65-3.77 (m, 0.5H), 3.91-4.02 (m, 2H), 3.36-4.51 (m, 1.5H), 4.69 (bs, 0.5H), 4.86 (bs, 0.5H), 7.00-7.10 (m, 1H), 7.31 (d, J = 8.1 Hz, 2H), 7.61-7.68 (bm, 1H), 7.74 (d, J = 8.1 Hz, 2H), 7.96-8.04 (m, 1H), 8.08 (s, 0.5H), 8.23 (s, 0.5H), 8.25-8.32 (m, 1H), 8.52 (bs, 1H).



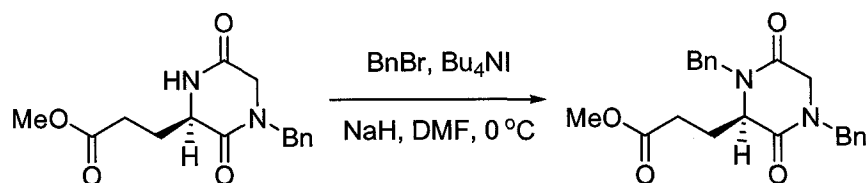
**N-Formyl-3-(5-fluoropentyl)-4-(6-nitroquinolin-2-yl)piperazine (87).** In an 8 mL vial a solution of 5-(4-formyl-1-(6-nitroquinolin-2-yl)piperazin-2-yl)pentyl 4-methylbenzene-sulfonate **86** (0.042 g, 0.080 mmol) in dry THF (0.4 mL) was treated with TBAF (0.12 mL, 1 M in THF, 0.12 mmol) to give a dark orange solution. The vial was capped and heated at 55 °C for 3.5 h. The reaction was cooled then concentrated *in vacuo* and dissolved in CHCl<sub>3</sub>. The solution was purified by column chromatography over silica gel (4 g) eluting with 3:2 EtOAc/hexanes followed by 4:1 EtOAc/CHCl<sub>3</sub>, concentration *in vacuo* gave **87** as a yellow oil (0.025 g, 84%): <sup>1</sup>H NMR (CDCl<sub>3</sub>, 400 MHz) (mixture of amide rotamers) δ 1.26-1.82 (m, 8H), 2.85-3.04 (2m, 1H), 3.15-3.39 (m, 1.5H), 3.43-3.63 (m, 1H), 3.67-3.77 (m, 0.5H), 4.06-4.18 (m, 1H), 4.30-4.37 (m, 0.5H), 4.40-4.54 (m, 2H), 4.71 (bs, 0.5H), 4.90 (bs, 0.5H), 7.00-7.10 (m, 1H), 7.66 (d, J = 9.1 Hz, 1H), 8.01 (d, J = 9.1 Hz, 1H), 8.10 (s, 0.5H), 8.25 (s, 0.5H), 8.31 (dd, J = 2.6 and 9.1 Hz, 1H), 8.54 (d, J = 2.6 Hz, 1H); <sup>13</sup>C NMR (CDCl<sub>3</sub>, 100 MHz) (mixture of amide rotamers) δ 24.9, 25.06, 25.12, 25.6, 25.7, 28.1, 28.2, 28.3, 30.0, 30.2, 38.6, 39.5, 39.6, 39.8, 42.4, 45.2, 47.9, 51.0, 51.6, 83.0, 84.6, 110.7, 123.8, 124.2, 127.3, 139.1, 142.2, 151.2, 158.1, 161.4.





**2-(2-(5-Fluoropentyl)piperazin-1-yl)-6-nitroquinoline (88).** A solution of N-formyl-3-(5-fluoropentyl)-4-(6-nitroquinolin-2-yl)piperazine **87** (0.025 g, 0.067 mmol) in THF (0.25 mL) was treated with H<sub>2</sub>SO<sub>4</sub> (16 M, 0.75 mL) and heated at 60 °C for 2 h. The reaction was quenched by pouring onto ice, the solution was brought to a basic pH with 4 M NaOH, and buffered to pH 10 with sat. NaHCO<sub>3</sub>. The aqueous layer was extracted with CH<sub>2</sub>Cl<sub>2</sub> (3 x 10 mL), the organic portions were combined, dried (K<sub>2</sub>CO<sub>3</sub>), filtered and concentrated *in vacuo* to give **88** as yellow oil (0.021 g, 91%): <sup>1</sup>H NMR (CDCl<sub>3</sub>, 400 MHz) δ 1.25-2.04 (m, 9H), 2.85 (dt, J = 3.6 and 12.0 Hz, 1H), 2.98 (dd, J = 3.9 and 12.3 Hz, 1H), 3.06-3.28 (m, 3H), 3.4703.64 (m, 1H), 4.35 (m, 0.5H), 4.42-4.66 (m, 2.5H), 7.01 (d, J = 9.4 Hz, 1H), 7.61 (d, J = 9.4 Hz, 1H), 7.93 (d, J = 9.4 Hz, 1H), 8.27 (dd, J = 2.6 and 9.4 Hz, 1H), 8.51 (d, J = 2.6 Hz, 1H).

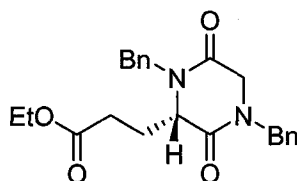
## 6.7 Chiral Pent-NQP Series.



**Methyl (R)-3-(1,4-dibenzyl-3,6-dioxopiperazin-2-yl)propanoate ((R)-145).** A stirred solution of methyl (R)-3-(4-benzyl-3,6-dioxopiperazin-2-yl)propanoate (R)-

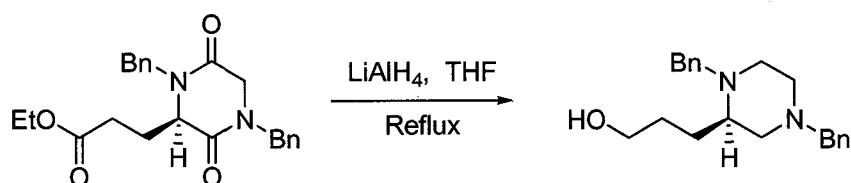
**134** (1.3 g, 4.6 mmol) in dry DMF (50 mL) at 0 °C was treated consecutively with Bu<sub>4</sub>Ni (0.68 g, 1.9 mmol), benzyl bromide (0.83 g, 4.9 mmol), and NaH (0.12 g, 4.9 mmol). The flask was sealed with a septum and placed under an atmosphere of argon. The reaction was allowed to stir for 1 hour at 0 °C, then at 25 °C overnight. The reaction was quenched by the cautious addition of water (50 mL), then buffered to pH 10 using sat. NaHCO<sub>3</sub> (30 mL). The aqueous layer was extracted with Et<sub>2</sub>O (3 x 30 mL) and EtOAc (2 x 30 mL). The organic portions were combined, washed with water (30 mL) followed by brine (30 mL), dried (K<sub>2</sub>CO<sub>3</sub>), filtered, and concentrated *in vacuo*. The oil was purified by column chromatography over silica gel (90 g) loaded with CHCl<sub>3</sub> and eluted with 0.4:19.6 MeOH/CHCl<sub>3</sub> to give a clear oil **(R)-145** (1.57 g, 89%): Product was visualized by two separate TLC solvent systems; *R<sub>f</sub>* = 0.29 (6:4 EtOAc/Hexanes) or *R<sub>f</sub>* = 0.73 (1:9 MeOH/CHCl<sub>3</sub>); <sup>1</sup>H NMR (CDCl<sub>3</sub>, 400 MHz) δ 1.98-2.10 (m, 1H), 2.16-2.28 (m, 1H), 2.32-2.50 (m, 2H), 3.66 (s, 3H), 3.84 (d, *J* = 17.5 Hz, 1H, CH<sub>2-AJ</sub>Ar), 3.92-4.02 (m, 3H), 4.42 (d, *J* = 14.6, 1H, CH<sub>2-AM</sub>Ar), 4.69 (d, *J* = 14.6 Hz, 1H, CH<sub>2-AM</sub>Ar), 5.26 (d, *J* = 14.9 Hz, 1H, CH<sub>2-AX</sub>), 7.18-7.40 (m, 10H); <sup>13</sup>C NMR (CDCl<sub>3</sub>, 100 MHz) δ 26.5, 29.0, 46.9, 48.9, 49.4, 51.9, 58.2, 128.0, 128.1, 128.2, 128.8, 128.9, 135.1, 135.4, 163.9, 165.5, 172.6.

The opposing enantiomer was similarly prepared:



**Methyl (S)-3-(1,4-dibenzyl-3,6-dioxopiperazin-2-yl)propanoate ((S)-145).**

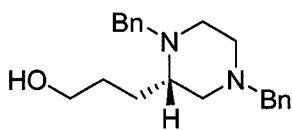
Clear oil; (1.62 g, 93%).



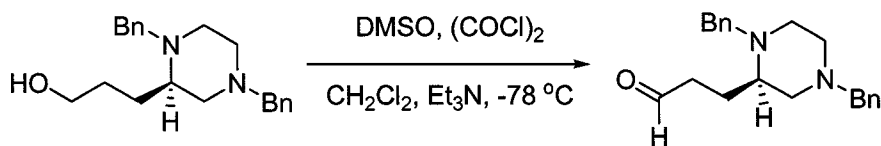
**(R)-3-(1,4-Dibenzylpiperazin-2-yl)propan-1-ol ((R)-56).** A stirred suspension of  $\text{LiAlH}_4$  (0.86 g, 22.6 mmol) in dry THF (90 mL) at  $0^\circ\text{C}$  was treated with a solution of methyl (*R*)-3-(1,4-dibenzyl-3,6-dioxopiperazin-2-yl)propanoate (**(R)-145**) (1.57 g, 4.1 mmol) in THF (20 mL) by syringe under argon maintaining a gentle effervescence. The reaction flask was fitted with a water-cooled condenser and the reaction was heated at reflux for 2 h. The solution was allowed to cool to room temperature and stir overnight. The reaction was quenched by consecutive addition of water (0.84 mL), NaOH (1.7 mL 4 M), and then water (0.84 mL). The inorganic solids were filtered off with a pad of Celite and the pad was rinsed with EtOAc. The filtrate was concentrated *in vacuo*, giving a clear oil (**(R)-56**) (1.2 g, 98% crude). The oil was purified by column chromatography over silica gel (50 g) loaded with  $\text{CHCl}_3$  and eluted one column length with 0.4:19.6 MeOH/ $\text{CHCl}_3$  followed by 1:19 MeOH/ $\text{CHCl}_3$ , concentrated to give a clear oil (**(R)-56**) (1.2 g,

92%): TLC  $R_f$  = 0.3 (1:9 MeOH/CHCl<sub>3</sub>); <sup>1</sup>H NMR (CDCl<sub>3</sub>, 400 MHz) δ 1.52-1.95 (3m, 4H), 2.12-2.37 (2m, 3H), 2.48-2.80 (3m, 4H), 3.20 and 4.19 (2d, J = 12.8, 2H), 3.48 (dd, J = 17.9 and 13.2 Hz), 3.66 (m, 2H), 7.20-7.40 (m, 10H); <sup>13</sup>C NMR (CDCl<sub>3</sub>, 100 MHz) δ 27.6, 28.6, 50.5, 52.2, 56.4, 57.8, 59.4, 62.8, 63.0, 126.9, 127.1, 128.1, 128.3, 129.0, 129.3, 137.8, 138.0.

The opposing enantiomer was similarly prepared:



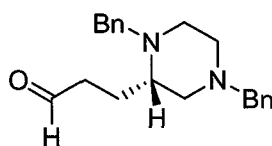
**(S)-3-(1,4-Dibenzylpiperazin-2-yl)propan-1-ol ((S)-56).** Clear oil; (1.16 g, 90%).



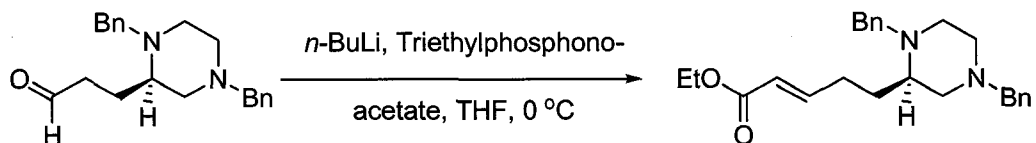
**(R)-3-(1,4-Dibenzylpiperazin-2-yl)propanal ((R)-89).** A solution of DMSO (0.33 g, 4.3 mmol) and dry CH<sub>2</sub>Cl<sub>2</sub> (1 mL) was added dropwise to a solution of oxalyl chloride (2 M in CH<sub>2</sub>Cl<sub>2</sub>, 1.1 mL, 2.1 mmol) in dry CH<sub>2</sub>Cl<sub>2</sub> (5 mL) at -78 °C (dry ice, acetone bath). After 5 min, a solution of (R)-3-(1,4-dibenzylpiperazin-2-yl)propan-1-ol (**(R)-56**) (0.63 g, 1.9 mmol) in dry CH<sub>2</sub>Cl<sub>2</sub> (3 mL) was added dropwise. The mixture was allowed to stir for an additional 20 min. The reaction was treated with Et<sub>3</sub>N (0.98 g, 9.7 mmol), forming a tan precipitate. The suspension was allowed to stir for 5 min, then the reaction was warmed to room temperature and stirred for 1 hour. The reaction was quenched by the addition of

water (25 mL). The organic layer was separated and the aqueous layer was extracted with an additional 15 mL of CH<sub>2</sub>Cl<sub>2</sub>. The organic portions were combined, washed with saturated NaHCO<sub>3</sub> (20 mL), dried (K<sub>2</sub>CO<sub>3</sub>) and concentrated *in vacuo*. The aldehyde (**R**)-**89** was used in the next step without further purification: TLC  $R_f = 0.54$  (2:3 EtOAc/hexanes).

The opposing enantiomer was similarly prepared:



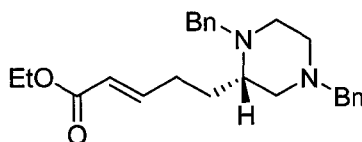
**(S)-3-(1,4-Dibenzylpiperazin-2-yl)propanal ((S)-89)**. Used directly in the subsequent Horner-Emmons olefination.



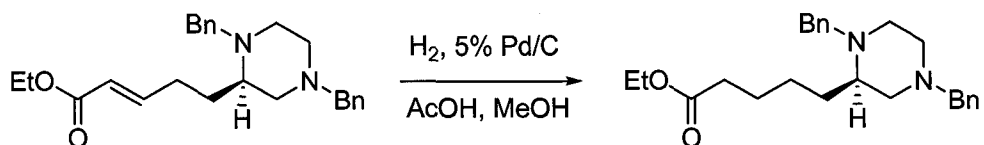
**Ethyl (R)-5-(1,4-dibenzylpiperazin-2-yl)pent-2-enoate ((R)-146)**. A stirred solution of *n*-BuLi (2.25 M in hexanes, 2.6 mL, 5.9 mmol) in dry THF (10 mL) at 0 °C was treated with triethylphosphonoacetate (1.3 g, 5.9 mmol) under argon, to give a light yellow solution. After 30 min, a solution of (**R**)-3-(1,4-dibenzylpiperazin-2-yl)propanal (**R**)-**89** (0.6 g, 2.0 mmol) in dry THF (3 mL) was added dropwise to the original solution. The reaction mixture was allowed to warm to room temperature and was stirred for 20 h. The reaction was quenched by the addition of water (25 mL) and concentrated *in vacuo* to remove the THF.

The aqueous layer was treated with 20 mL of sat.  $\text{NaHCO}_3$  and extracted with  $\text{Et}_2\text{O}$  (3 x 15 mL) and  $\text{EtOAc}$  (1 x 15 mL). The organic fractions were combined, washed with brine (20 mL), dried ( $\text{K}_2\text{CO}_3$ ), filtered and concentrated *in vacuo*. The resulting orange oil was purified by column chromatography over silica gel (30 g) loaded with  $\text{CHCl}_3$  and eluted with 3:2  $\text{EtOAc}$ /hexanes and concentration *in vacuo* to give (**R**)-**146** as a light tan oil (0.46 g, 60% 2 steps overall): TLC  $R_f$  = 0.33 (3:2  $\text{EtOAc}$ /Hexanes);  $^1\text{H}$  NMR ( $\text{CDCl}_3$ , 400 MHz)  $\delta$  1.29 (t,  $J$  = 7.1 Hz, 3H), 1.62-1.88 (bm, 2H), 2.06-2.34 (bm, 5H), 2.44-2.76 (bm, 4H), 3.26 (d,  $J$  = 13.3 Hz, 1H,  $\text{CH}_{2\text{-AXAr}}$ ), 3.49 (dd,  $J$  = 12.6 and 34.3 Hz, 2H,  $\text{CH}_{2\text{-AMAr}}$ ), 4.18 (q,  $J$  = 7.1 Hz, 2H), 5.78 (m, 1H), 6.88-6.98 (m, 1H), 7.18-7.36 (m, 10H);  $^{13}\text{C}$  NMR ( $\text{CDCl}_3$ , 100 MHz)  $\delta$  14.3, 27.5, 28.2, 50.2, 52.8, 56.7, 57.6, 58.7, 60.2, 63.0, 121.3, 126.9, 127.0, 128.2, 128.8, 129.0, 148.9, 166.6, 183.8.

The opposing enantiomer was similarly prepared:



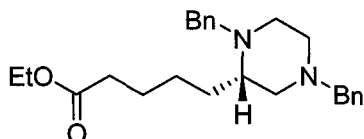
**Ethyl (S)-5-(1,4-dibenzylpiperazin-2-yl)pent-2-enoate ((S)-146).** Light tan oil; (0.47 g, 66% 2 steps overall).



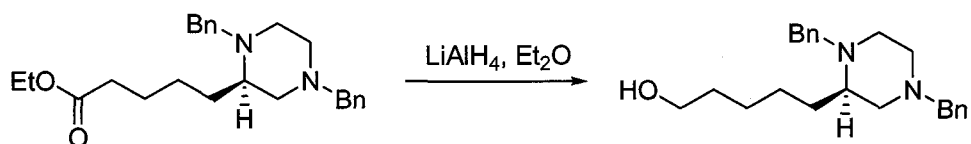
**Ethyl (R)-5-(1,4-dibenzylpiperazin-2-yl)pentanoate ((R)-77).** To a solution of ethyl (R)-5-(1,4-dibenzylpiperazin-2-yl)pent-2-enoate (**(R)-146**) (0.46 g, 1.2 mmol) in HPLC grade MeOH (10 mL) and acetic acid (0.35 g, 5.9 mmol) was added 5% Pd/C (0.9 g). The reaction flask was sealed with a septum, fitted with hydrogen balloon and a bleed needle. One balloon of hydrogen was bubbled through the stirred solution, the needle was removed a second balloon was attached and the mixture was stirred overnight. The reaction was filtered over a pad of Celite. The pad was rinsed with MeOH and concentrated *in vacuo*. The resulting oil was dissolved in CH<sub>2</sub>Cl<sub>2</sub>, free based with 4 M NaOH to a basic pH then buffered to pH 10 with sat. NaHCO<sub>3</sub>. The organic layer was separated and the aqueous layer was extracted with CH<sub>2</sub>Cl<sub>2</sub> (2 x 30 mL). The organic portions were combined, dried (K<sub>2</sub>CO<sub>3</sub>) and concentrated *in vacuo* to give an tan oil. The crude oil was purified by column chromatography over silica gel (15 g) loaded with CHCl<sub>3</sub> and eluted with 1:3 EtOAc/hexanes followed by 2:3 EtOAc/hexanes, concentration *in vacuo* gave (**(R)-77**) as clear oil (0.28 g, 60%): The product was visualized by two separate TLC solvent systems; TLC  $R_f = 0.27$  (2:3 EtOAc/Hexanes),  $R_f = 0.6$  (1:9 MeOH/CH<sub>2</sub>Cl<sub>2</sub>); <sup>1</sup>H NMR (CDCl<sub>3</sub>, 400 MHz)  $\delta$  1.16-1.50 (m, 5H, overlapped triplet at 1.25, J = 7.1 Hz, 3H, CO<sub>2</sub>CH<sub>2</sub>CH<sub>3</sub>), 1.52-1.76 (m, 4H), 2.10-2.80 (m, 9H), 3.20 (d, J = 13.2 Hz, 1H, CH<sub>2-AX</sub>Ar), 3.49 (dd, J = 13.2 and 41.7 Hz, 2H, CH<sub>2-AM</sub>Ar), 4.00 (d, J = 13.2 Hz, 1H, CH<sub>2-AX</sub>Ar), 4.12 (q, J = 7.1 Hz, 2H, CO<sub>2</sub>CH<sub>2</sub>CH<sub>3</sub>), 7.18-7.45 (m, 10H); <sup>13</sup>C NMR (CDCl<sub>3</sub>, 100 MHz)  $\delta$  14.2, 25.0,

25.4, 29.3, 34.2, 50.7, 52.8, 57.5, 57.6, 59.4, 60.1, 63.0, 126.7, 126.8, 128.1, 128.8, 128.9, 138.2, 139.0, 173.5.

The opposing enantiomer was similarly prepared:



**Ethyl (S)-5-(1,4-dibenzylpiperazin-2-yl)pentanoate ((S)-77).** Clear oil; (0.27 g, 57%).

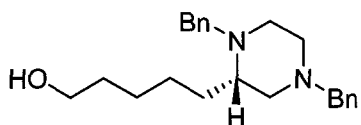


**(R)-5-(1,4-Dibenzylpiperazin-2-yl)pentan-1-ol ((R)-78).** A solution of ethyl (*R*)-5-(1,4-dibenzylpiperazin-2-yl)pentanoate (**(R)-77**) (0.28 g, 0.7 mmol) in dry ether (10 mL) was treated with LiAlH<sub>4</sub> powder (0.03 g, 0.8 mmol) at 0 °C, then placed under an atmosphere of argon. The ice bath was removed and the reaction was allowed to stir overnight at 25 °C. The reaction was quenched by consecutive addition of H<sub>2</sub>O (0.03 mL), NaOH (0.06 mL 4 M) and then H<sub>2</sub>O (0.03 mL). The inorganic salts were filtered over a pad of Celite and the pad was rinsed with EtOAc. The filtrate was concentrated *in vacuo* to give **(R)-78** (0.24 g, 99%): TLC  $R_f$  = 0.10 (2:3 EtOAc/Hexanes); <sup>1</sup>H NMR (CDCl<sub>3</sub>, 400 MHz) δ 1.20-1.45 (m, 4H), 1.48-1.68 (m, 5H), 2.10-2.28 (m, 3H), 2.40-2.76 (m, 4H), 3.20 (d, J = 13.2 Hz, 1H, CH<sub>2-AX</sub>Ar), 3.49 (dd, J = 13.2 and 44.0 Hz, 2H, CH<sub>2-AM</sub>Ar), 3.58-3.64 (bm,

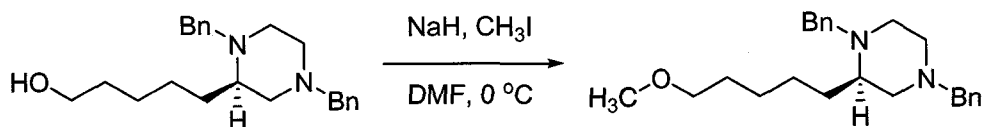


2H), 4.00 (d,  $J = 13.2$  Hz, 1H,  $\text{CH}_2\text{-Ar}$ ), 7.20-7.35 (m, 10H);  $^{13}\text{C}$  NMR ( $\text{CDCl}_3$ , 100 MHz)  $\delta$  25.3, 26.2, 29.6, 32.6, 50.8, 52.7, 57.5, 59.5, 62.5, 63.0, 126.7, 126.9, 128.0, 128.9, 129.0, 137.9, 138.9 (1 overlapped peak).

The opposing enantiomer was similarly prepared:



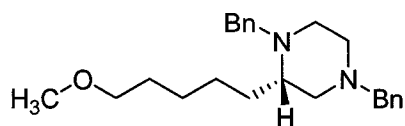
**5-((S)-1,4-Dibenzylpiperazin-2-yl)pentan-1-ol ((S)-78).** Clear oil; (0.24 g, quantitative).



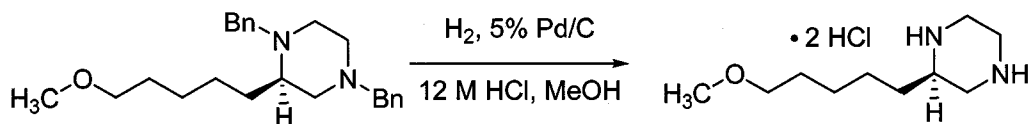
**(R)-1,4-Dibenzyl-2-(5-methoxypentyl)piperazine ((R)-79).** A stirred solution of (*R*)-5-(1,4-dibenzylpiperazin-2-yl)pentan-1-ol (**(R)-78**) (0.24 g, 0.69 mmol) in dry DMF (5 mL) at 0 °C was treated with NaH powder (0.05 g, 2.1 mmol) to give a turbid white suspension. The reaction was placed under argon and stirring was continued for 20 min. Iodomethane (0.10 g, 0.69 mmol) was added dropwise to the cooled solution and the reaction was allowed to stir on ice for 30 min followed by room temperature overnight. The reaction was quenched by the addition of water (10 mL) followed by sat.  $\text{NaHCO}_3$  (10 mL). The aqueous layer was extracted with  $\text{Et}_2\text{O}$  (4 x 20 mL). The organic portions were combined, dried ( $\text{K}_2\text{CO}_3$ ), and concentrated *in vacuo* to give a tan oil. The oil was purified by column chromatography over silica gel (9 g) loaded with  $\text{CHCl}_3$  and eluted with

2:3 EtOAc/hexanes followed by 3:2 EtOAc/hexanes, concentration of the product fractions gave (*R*)-79 as a clear oil (0.14 g, 56%): TLC  $R_f$  = 0.39 (4:6 EtOAc/Hexanes);  $^1\text{H}$  NMR ( $\text{CDCl}_3$ , 400 MHz)  $\delta$  1.22-1.48 (m, 4H), 1.52-1.70 (m, 4H), 2.08-2.32 (m, 3H), 2.40-2.78 (3m, 4H), 3.20 (d,  $J$  = 13.2 Hz, 1H,  $\text{CH}_{2\text{-AXAr}}$ ), 3.32-3.40 (m, 5H, overlapped singlet, 3.33, 3H,  $\text{OCH}_3$ ), 3.49 (dd,  $J$  = 13.2 and 43.6 Hz, 2H,  $\text{CH}_{2\text{-AMAr}}$ ), 4.02 (d,  $J$  = 13.2 Hz, 1H,  $\text{CH}_{2\text{-AXAr}}$ ), 7.20-7.40 (m, 10H);  $^{13}\text{C}$  NMR ( $\text{CDCl}_3$ , 100 MHz)  $\delta$  25.4, 26.6, 29.0, 29.5, 50.8, 52.8, 57.6, 58.5, 59.6, 63.0, 72.0, 72.7, 126.6, 126.8, 128.0, 128.9, 129.0, 138.2, 139.0.

The opposing enantiomer was similarly prepared:



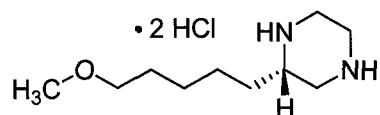
**(*S*)-1,4-Dibenzyl-2-(5-methoxypentyl)piperazine ((*S*)-79).** Clear oil; (0.14 g, 57%).



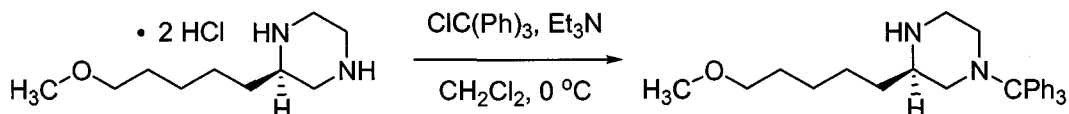
**(*R*)-2-(5-Methoxypentyl)piperazine dihydrochloride ((*R*)-80).** A solution of (*R*)-1,4-dibenzyl-2-(5-methoxypentyl)piperazine (**(*R*)-79**) (0.14 g, 0.39 mmol) in HPLC grade MeOH (8 mL) and HCl (12 M, 0.77 mmol, 0.06 mL) was treated with 5% Pd/C (0.021 g). The flask was sealed with a septum and three balloons of hydrogen were bubbled through the stirred solution. The reaction mixture was filtered over a pad of Celite, the pad was rinsed with MeOH and the combined

organic portions were concentrated *in vacuo* to give a white solid (**R**)-**80** (0.083 g, 83%).

The opposing enantiomer was similarly prepared:

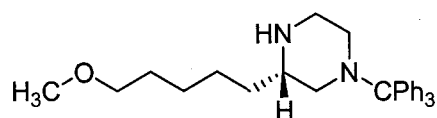


**(S)-2-(5-Methoxypentyl)piperazine dihydrochloride ((S)-80)**. Clear oil; (0.10 g, 98%).

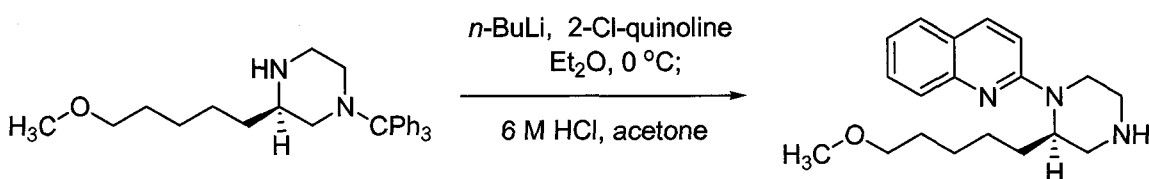


**(R)-3-(5-Methoxypentyl)-1-tritylpiperazine ((R)-81)**. A solution of hydrochloride (**R**)-**80** (0.082 g, 0.32 mmol) in dry  $\text{CH}_2\text{Cl}_2$  (5 mL) and dry  $\text{Et}_3\text{N}$  (0.13 g, 0.18 mL, 1.3 mmol) at 0 °C, was treated with a solution of trityl chloride (0.089 g, .32 mmol) in dry  $\text{CH}_2\text{Cl}_2$  (2 mL) by dropwise addition. The ice bath was removed after one hour and the reaction stirred for 20 h at room temperature. The reaction mixture was transferred to a separatory funnel and diluted to 20 mL with  $\text{CH}_2\text{Cl}_2$ . The organic portion was washed with saturated  $\text{NaHCO}_3$  (10 mL), water (10 mL), brine (10 mL), dried ( $\text{K}_2\text{CO}_3$ ) and concentrated *in vacuo* to give an amorphous white foam (**R**)-**81** (0.14 g, 99% yield): TLC 0.34 (1:9 MeOH/ $\text{CH}_2\text{Cl}_2$ ). The product was used directly without further purification, or spectroscopic characterization.

The opposing enantiomer was similarly prepared:



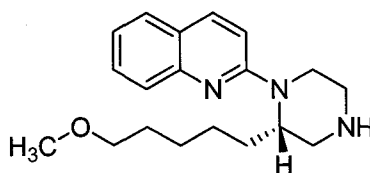
**(S)-3-(5-Methoxypentyl)-1-tritylpiperazine ((S)-81).** White foam; (0.16 g, 97%).



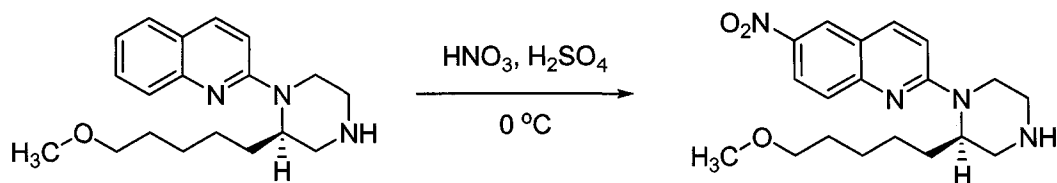
**(R)-2-(2-(5-Methoxypentyl)piperazin-1-yl)quinoline ((R)-82).** A solution of (*R*)-3-(5-methoxypentyl)-1-tritylpiperazine (**(R)-81**) (0.14 g, 0.32 mmol) in dry Et<sub>2</sub>O (8 mL) under argon at 0° C, was treated dropwise with *n*-BuLi (0.93 mL, 2.45 M in hexanes) generating an off-white suspension. The suspension was allowed to stir for 20 min. A solution of 2-chloroquinoline (0.034 g, 0.21 mmol) in dry Et<sub>2</sub>O (2 mL) was added drop-wise, the mixture was allowed to stir for 1 h and then the ice bath was removed. The reaction was allowed to stir for a total of 4 h giving a red-brown colored suspension. The reaction was quenched with saturated NaHCO<sub>3</sub> (20 mL), diluted to 40 mL with Et<sub>2</sub>O and the organic layer was separated. The organic layer was washed with water (20 mL), brine (20 mL), dried (K<sub>2</sub>CO<sub>3</sub>), and concentrated *in vacuo* to give a white foam. The foam was purified by column chromatography over silica gel (9 g) loaded with CHCl<sub>3</sub> and eluted with 1:9 EtOAc/hexanes followed by 1:3 EtOAc/Hexanes to give the N-trityl protected product (0.099 g, 85% yield) as a clear yellow oil. R<sub>f</sub> = 0.3 (4:6

EtOAc/Hexanes). The purified oil was dissolved in acetone (1.5 mL) and HCl (6 M, 0.5 mL) and allowed to stir for 15 min. The reaction was diluted with 1 M HCl (10 mL) and extracted with CH<sub>2</sub>Cl<sub>2</sub> (3 x 15 mL), the aqueous layer was basified to pH 12 with 4 M NaOH and then buffered to pH 10 with saturated NaHCO<sub>3</sub>. The aqueous layer was extracted with CH<sub>2</sub>Cl<sub>2</sub> (3 x 15 mL), the organic portions were combined, dried (K<sub>2</sub>CO<sub>3</sub>), and concentrated *in vacuo* to give **(R)-82** (0.035 g, 53% 2 steps) as a light yellow oil:  $[\alpha]_D^{25} = -39^\circ$  (c = 0.001, CH<sub>2</sub>Cl<sub>2</sub>); <sup>1</sup>H NMR (CDCl<sub>3</sub>, 400 MHz)  $\delta$  1.18-1.42 (m, 4H), 1.44-1.58 (m, 2H), 1.60-1.72 (m, 1H), 1.76-1.90 (m, 1H), 2.11 (bs, 1H), 2.84 (m, 1H), 2.94-3.18 (m, 4H), 3.24-3.34 (m, 5H, overlapped singlet, 3.28, 3H, OCH<sub>3</sub>), 4.38 (bd, 2H), 6.90 (d, J = 9.5 Hz, 1H), 7.18 (t, J = 8.06 Hz, 1H), 7.50 (t, J = 8.4 Hz, 1H), 7.56 (d, J = 8.1 Hz, 1H), 7.65 (d, J = 8.4 Hz, 1H), 7.84 (d, J = 9.2 Hz, 1H); <sup>13</sup>C NMR (CDCl<sub>3</sub>, 100 MHz)  $\delta$  26.0, 26.4, 27.7, 29.4, 40.1, 46.0, 47.8, 51.7, 58.4, 72.6, 109.3, 121.9, 122.7, 126.3, 127.0, 129.3, 137.2, 147.9, 157.0.

The opposing enantiomer was similarly prepared:

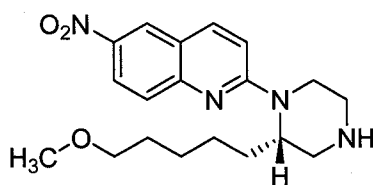


**(S)-2-(2-(5-Methoxypentyl)piperazin-1-yl)quinoline ((S)-82)**. Light yellow oil; (0.022 g, 29% 2 steps overall).



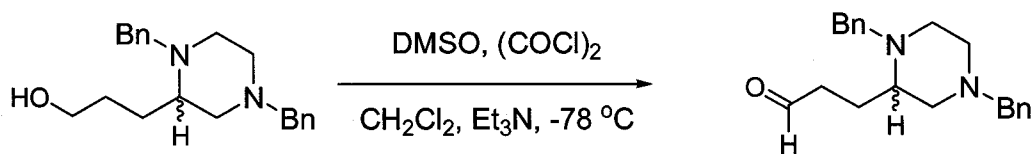
**(R)-2-(2-(5-Methoxypentyl)piperazin-1-yl)-6-nitroquinoline ((R)-83).** A stirred solution of (*R*)-2-(2-(5-methoxypentyl)piperazin-1-yl)quinoline (**(R)-82**) (0.035 g, 0.11 mmol) in H<sub>2</sub>SO<sub>4</sub> (16 M, 2 mL) was cooled at 0° C. HNO<sub>3</sub> (15.4 M, 0.03 mL, 0.45 mmol) was added drop-wise, and the reaction stirred for 20 min at 0 °C. The reaction was quenched by pouring into ice water. The acid was neutralized with 4 M NaOH to give a bright yellow solution, and the resulting mixture was buffered to pH 10 with sat. NaHCO<sub>3</sub>. The yellow aqueous solution was extracted with CH<sub>2</sub>Cl<sub>2</sub> until no yellow color was extracted into the organic layer. The organic portions were combined, dried (K<sub>2</sub>CO<sub>3</sub>), and concentrated *in vacuo* to give a bright yellow oil (**(R)-83**) (0.041 g, quantitative yield): TLC *R<sub>f</sub>* = 0.16 (1:9 MeOH/CH<sub>2</sub>Cl<sub>2</sub>); [α]<sup>25</sup><sub>D</sub> = -105° (c = 0.0008, CH<sub>2</sub>Cl<sub>2</sub>); <sup>1</sup>H NMR (CDCl<sub>3</sub>, 400 MHz) δ 1.26-1.46 (m, 4H), 1.50-1.60 (m, 2H), 1.71-1.96 (m, 2H), 2.06 (bs, 1H), 2.85 (dt, J = 3.6 and 12.3 Hz, 1H), 2.98 (dd, J = 3.6 and 12.3 Hz, 1H), 3.06-3.26 (m, 3H), 3.29 (s, 3H), 3.33 (m, 2H), 4.52 (bs, 2H), 7.01 (d, J = 9.1 Hz, 1H), 7.61 (d, J = 9.4 Hz, 1H), 7.93 (d, J = 9.4 Hz, 1H), 8.27 (dd, J = 2.6 and 9.4 Hz, 1H), 8.51 (d, J = 2.6 Hz, 1H); <sup>13</sup>C NMR (CDCl<sub>3</sub>, 100 MHz) δ 26.0, 26.2, 28.2, 29.4, 40.3, 46.1, 48.0, 51.8, 58.4, 72.5, 110.7, 120.7, 123.4, 124.1, 126.8, 138.4, 141.4, 151.6, 158.3.

The opposing enantiomer was similarly prepared:



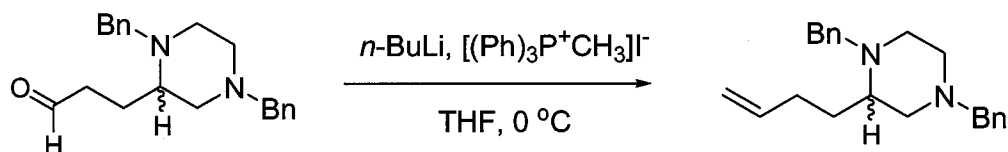
**(R)-2-(2-(5-Methoxypentyl)piperazin-1-yl)-6-nitroquinoline ((R)-83).** Bright yellow oil; (0.024 g, 95%);  $[\alpha]_D = +86^\circ$  ( $c = 0.0005$ ,  $\text{CH}_2\text{Cl}_2$ ).

### 6.8 Racemic BuM-NQP Series.



**3-(1,4-Dibenzylpiperazin-2-yl)propanal (89).** A solution of DMSO (0.55 g, 7.0 mmol) in dry  $\text{CH}_2\text{Cl}_2$  (2.5 mL) was added dropwise to a solution of oxalyl chloride (2 M in  $\text{CH}_2\text{Cl}_2$ , 1.75 mL, 3.5 mmol) in dry  $\text{CH}_2\text{Cl}_2$  (8 mL) at  $-78^\circ\text{C}$  (dry ice, acetone bath). After 5 min, a solution of 1,4-dibenzyl-2-(3-hydroxypropyl)piperazine **56** (0.94 g, 2.9 mmol) in dry  $\text{CH}_2\text{Cl}_2$  (5 mL) was added dropwise. The combined mixture was allowed to stir for an additional 20 min at  $-78^\circ\text{C}$ . The reaction was treated with  $\text{Et}_3\text{N}$  (1.6 g, 16 mmol) forming a tan precipitate. The suspension was allowed to stir for 5 min then warmed to room temperature and stirred for 1 hour. The reaction was quenched by the addition of water (25 mL). The organic layer was separated and the aqueous layer was extracted with 15 mL of  $\text{CH}_2\text{Cl}_2$ . The organic portions were combined, washed with saturated

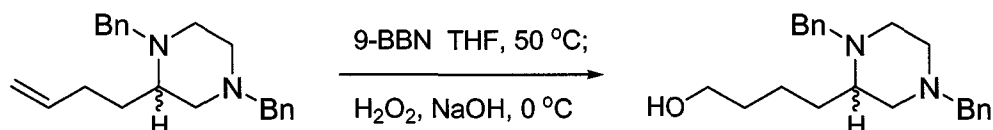
NaHCO<sub>3</sub> (20 mL), dried (K<sub>2</sub>CO<sub>3</sub>), filtered, and concentrated *in vacuo*. The aldehyde **89** was used in the next step without further purification: TLC *R<sub>f</sub>* = 0.54 (2:3 EtOAc/hexanes).



**1,4-Dibenzyl-2-(but-3-enyl)piperazine (90).** A stirred suspension of methyl triphenylphosphonium iodide (2.4 g, 5.9 mmol) in dry THF (15 mL) cooled at 0° C, was treated with *n*-BuLi (2.4 mL, 2.45 M in hexanes, 5.8 mmol) giving an yellow-orange suspension. The suspension was stirred for an additional hour at 0° C. A solution of 3-(1,4-dibenzylpiperazin-2-yl)propanal **89** (0.94 g, 2.9 mmol) in dry THF (5 mL) was added dropwise to the ylide. After 1 h, the reaction was allowed to warm to RT° C and stir for 18 h. The reaction was quenched with water (15 mL). The THF was removed *in vacuo*, and aqueous layer was treated with sat. NaHCO<sub>3</sub> (20 mL). The aqueous phase was extracted with CH<sub>2</sub>Cl<sub>2</sub> (3 x 30 mL), the organic portions were combined, dried (K<sub>2</sub>CO<sub>3</sub>) and concentrated *in vacuo* to give a white/tan semi-solid (3.25 g). The crude material was purified by column chromatography over silica gel (60 g) loaded with CHCl<sub>3</sub>, eluting with 1:3 EtOAc/hexanes followed by 2:3 EtOAc/hexanes, after concentration *in vacuo* gave (**R**)-**90** as a light tan oil (0.69 g, 74%, 2 steps overall): TLC *R<sub>f</sub>* = 0.54 (2:3 EtOAc/hexanes); <sup>1</sup>H NMR (CDCl<sub>3</sub>, 400 MHz) δ 1.68-1.79 (m, 2H), 1.93-2.34 (m, 5H), 2.45-2.79 (m, 4H), 3.24 (d, *J* = 13.3 Hz, 1H, CH<sub>2-AM</sub>Ar), 3.51 (dd, *J* = 12.9 and 34.9 Hz, 2H, CH<sub>2-AB</sub>Ar), 4.02 (d, *J* = 13.3 Hz, 1H, CH<sub>2-AM</sub>Ar), 4.91-5.03 (m,

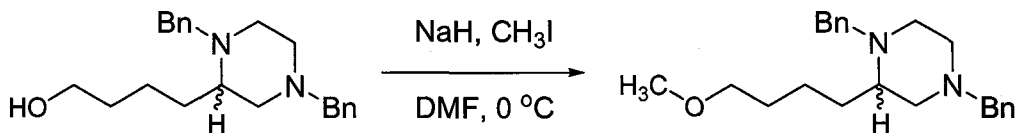


1H), 5.74-5.87 (m, 1H), 7.20-7.38 (m, 10H); <sup>13</sup>C NMR (CDCl<sub>3</sub>, 100 MHz) δ 28.7, 29.8, 50.6, 52.9, 57.2, 57.6, 59.1, 63.1, 114.4, 126.7, 126.9, 128.1, 128.9, 129.0, 138.2, 138.7, 139.1.



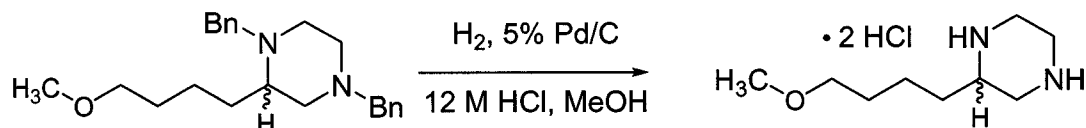
**4-(1,4-Dibenzylpiperazin-2-yl)butan-1-ol (91).** A cooled (0 °C) stirred solution of 1,4-dibenzyl-2-(but-3-enyl)piperazine **90** (0.58 g, 1.8 mmol) in dry THF (15 mL) was treated (dropwise) with a solution of 9-BBN (7.2 mL, 0.5 M in THF, 3.6 mmol), and then heated at 55 °C for 1.5 h. The reaction was cooled to 0 °C and treated (dropwise) with a solution of NaOH (5.4 mL, 1 M), followed by 30% H<sub>2</sub>O<sub>2</sub> (5.4 mL). The reaction was concentrated *in vacuo* to remove the THF, then diluted with 1 M HCl (10 mL) and extracted with CH<sub>2</sub>Cl<sub>2</sub> (3 x 20 mL). The resulting aqueous layer was brought to basic pH with 4 M NaOH, buffered to pH 10 with sat. NaHCO<sub>3</sub>, and extracted with CH<sub>2</sub>Cl<sub>2</sub> (4 x 15 mL). The combined organic portions were, dried (K<sub>2</sub>CO<sub>3</sub>), and concentrated *in vacuo*. The crude oil was purified by column chromatography over silica gel (37 g) loaded with CHCl<sub>3</sub> and eluted with 3:2 EtOAc/hexanes to give a clear oil **91** (0.45 g, 73%): The product was visualized using two separate TLC solvent systems; *R<sub>f</sub>* = 0.06 (4:6 EtOAc/Hexanes) and *R<sub>f</sub>* = 0.42 (1:9 MeOH/CH<sub>2</sub>Cl<sub>2</sub>); <sup>1</sup>H NMR (CDCl<sub>3</sub>, 400 MHz) δ 1.25-1.70 (m, 6H), 2.12-2.32 (m, 3H), 2.41-2.76 (m, 5H), 3.22 (d, *J* = 13.3 Hz, 1H, CH<sub>2-AM</sub>Ar), 3.49 (dd, *J* = 12.9 and 42.7 Hz, 2H, CH<sub>2-AB</sub>Ar), 3.62 (m, 2H, CH<sub>2</sub>OH), 4.01 (d, *J* = 13.3 Hz, 1H, CH<sub>2-AM</sub>Ar), 7.20-7.36 (m, 10H); <sup>13</sup>C NMR

(CDCl<sub>3</sub>, 100 MHz)  $\delta$  21.8, 29.4, 33.1, 50.7, 52.7, 57.4, 57.6, 59.6, 62.5, 63.0, 126.7, 126.9, 128.1, 128.9, 129.1, 138.0, 138.9.

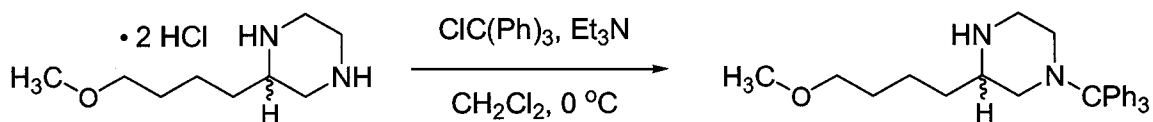


**1,4-Dibenzyl-2-(4-methoxybutyl)piperazine (92).** A stirred solution of 4-(1,4-dibenzylpiperazin-2-yl)butan-1-ol **91** (1.6 g, 4.73 mmol) in dry DMF (40 mL) at 0 °C was treated with NaH powder (0.34 g, 14.2 mmol) to give a white suspension. The flask was placed under argon and stirring was continued for 20 min. Iodomethane (0.71 g, 4.97 mmol) was added (dropwise) to the cooled solution. The reaction was allowed to stir on ice for 30 min, followed by room temperature overnight. The reaction was quenched by the addition of water (40 mL) followed by sat. NaHCO<sub>3</sub> (40 mL). The aqueous layer was extracted with Et<sub>2</sub>O (4 x 15 mL), the organic portions were combined, washed with ether, dried (K<sub>2</sub>CO<sub>3</sub>), filtered and concentrated *in vacuo* to give a tan oil. The oil was purified by column chromatography over silica gel (56 g) loaded with CHCl<sub>3</sub> and eluted with 2:3 EtOAc/hexanes, concentration *in vacuo* gave **92** as a clear oil (1.02 g, 61%): TLC  $R_f$  = 0.35 (2:3 EtOAc/Hexanes),  $R_f$  = 0.48 (1:9 MeOH/CH<sub>2</sub>Cl<sub>2</sub>); <sup>1</sup>H NMR (CDCl<sub>3</sub>, 400 MHz)  $\delta$  1.24-1.70 (m, 6H), 2.12-2.30 (m, 3H), 2.41-2.50 (bm, 1H), 2.52-2.60 (bm, 1H), 2.66-2.76 (m, 2H), 3.20 (d, J = 13.2 Hz, 1H, CH<sub>2</sub>Ar), 3.33 (s, 3H), 3.36 (m, 2H), 3.49 (dd, J = 13.2 and 41.8, 2H, CH<sub>2-AB</sub>Ar), 4.02 (d, J = 13.2 Hz, 1H, CH<sub>2</sub>Ar), 7.20-7.40 (m, 10H); <sup>13</sup>C NMR (CDCl<sub>3</sub>, 100 MHz)  $\delta$  22.2, 29.6,

30.1, 50.8, 52.8, 57.6, 58.5, 59.6, 63.1, 72.6, 126.7, 126.8, 128.1, 128.9, 129.0, 138.2, 139.1.

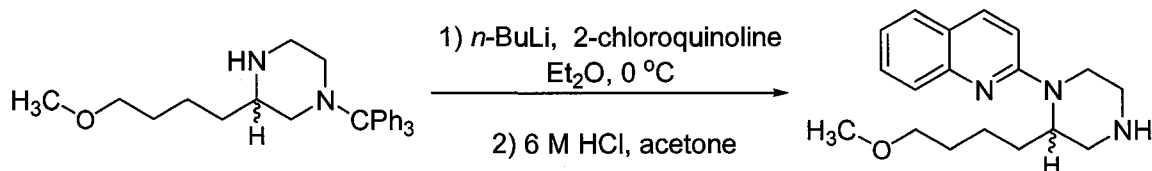


**2-(4-Methoxybutyl)piperazine dihydrochloride (93).** A solution of 1,4-dibenzyl-2-(4-methoxybutyl)piperazine **92** (1.0 g, 2.9 mmol) in HPLC grade MeOH (50 mL) and HCl (12 M, 6.1 mmol, 0.5 mL) was treated with 5% Pd/C (0.15 g). The flask was sealed with a septum and a balloon of hydrogen was bubbled through the stirred solution. The reaction mixture was filtered over a pad of Celite; the pad was rinsed with MeOH and concentrated *in vacuo* to give a white solid **93** (0.70 g, 98%):  $^1\text{H NMR}$  ( $\text{D}_2\text{O}$ , 400 MHz)  $\delta$  1.40-1.52 (m, 2H), 1.56-1.68 (m, 2H), 1.70-1.84 (m, 2H), 3.21 (m, 1H), 3.34 (s, 3H), 3.41 (m, 1H), 3.49 (m, 2H), 3.56-3.80 (bm, 4H).



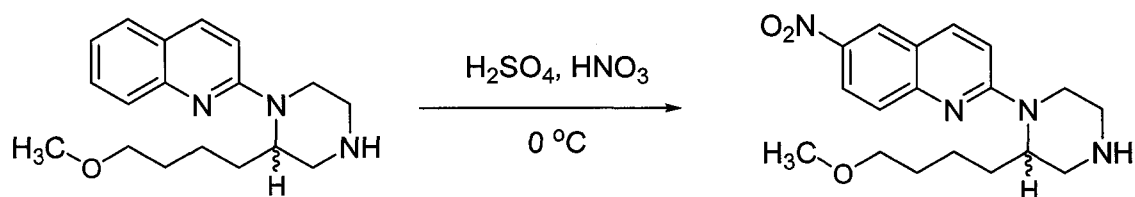
**3-(4-methoxybutyl)-1-tritylpiperazine (94).** A solution of 2-(4-methoxybutyl)piperazine dihydrochloride **93** (0.70 g, 2.8 mmol) in dry  $\text{CH}_2\text{Cl}_2$  (20 mL) and dry  $\text{Et}_3\text{N}$  (1.15 g, 1.6 mL, 11.4 mmol) at 0 °C, was treated (dropwise) with a solution of trityl chloride (0.79 g, 2.8 mmol) in dry  $\text{CH}_2\text{Cl}_2$  (10 mL). The ice bath was removed after one hour and the reaction stirred for 20 h at room temperature. The reaction mixture was transferred to a separatory funnel, diluted

to 20 mL with  $\text{CH}_2\text{Cl}_2$ . The organic fraction was washed with saturated  $\text{NaHCO}_3$  (20 mL), water (20 mL), brine (20 mL), dried ( $\text{K}_2\text{CO}_3$ ) and concentrated *in vacuo* to give an amorphous white foam **94** (1.11 g, 94% yield). The product was directly used without further purification or characterization.



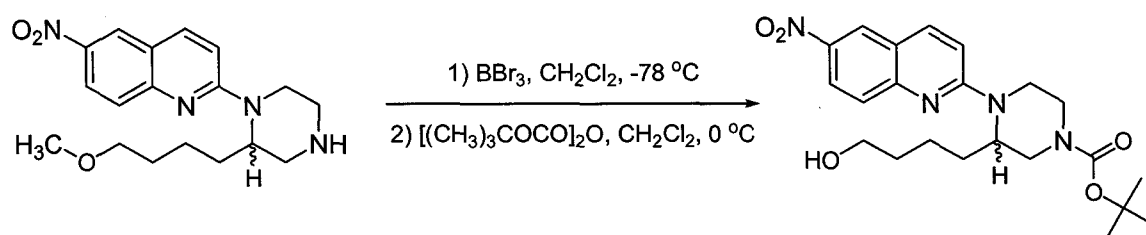
**2-(2-(4-Methoxybutyl)piperazin-1-yl)quinoline (95).** A solution of 3-(4-methoxybutyl)-1-tritylpiperazine **94** (0.54 g, 1.30 mmol) in dry  $\text{Et}_2\text{O}$  (20 mL) under argon at  $0^\circ\text{C}$ , was treated (dropwise) with *n*-BuLi (0.6 mL, 2.2 M in hexanes, 1.30 mmol) generating a creamy white suspension. The suspension was allowed to stir for 20 min. A solution of 2-chloroquinoline (0.14 g, 0.86 mmol) in dry  $\text{Et}_2\text{O}$  (5 mL) was added dropwise to the lithium amide and the reaction was allowed to stir for 1 h and the ice bath was removed. The reaction was allowed to stir for a total of 4 h giving a purple colored suspension. The reaction was quenched with saturated  $\text{NaHCO}_3$  (20 mL), diluted to 40 mL with  $\text{Et}_2\text{O}$  and the organic layer was separated. The organic layer was washed with water (20 mL), brine (20 mL), dried ( $\text{K}_2\text{CO}_3$ ), and concentrated *in vacuo* to give a white foam. The foam was purified by column chromatography over silica gel (9 g) loaded with  $\text{CHCl}_3$  and eluted with 1:9 EtOAc/hexanes followed by 1:3 EtOAc/Hexanes to give the N-trityl protected product (0.099 g, 85% yield) as a clear yellow oil.  $R_f = 0.3$  (4:6 EtOAc/Hexanes). The purified oil was dissolved in acetone (1.5 mL) and HCl (6 M, 0.5 mL) and the mixture was allowed to stir for 15 min. The reaction was

diluted with 1 M HCl (10 mL) and extracted with CH<sub>2</sub>Cl<sub>2</sub> (3 x 15 mL). The aqueous layer was basified to pH 12 with 4 M NaOH and then buffered to pH 10 with saturated NaHCO<sub>3</sub>. The aqueous layer was extracted with CH<sub>2</sub>Cl<sub>2</sub> (3 x 15 mL), the organic portions were combined, dried (K<sub>2</sub>CO<sub>3</sub>), and concentrated *in vacuo* to give **95** (0.035 g, 63%) as a light yellow oil: <sup>1</sup>H NMR (CDCl<sub>3</sub>, 400 MHz) δ 1.28-1.46 (m, 2H), 1.54-1.76 (2m, 3H), 1.81-1.94 (m, 1H), 2.18 (bs, 1H), 2.86 (m, 1H), 2.99 (dd, J = 4.0 and 12.5 Hz, 1H), 3.05-3.21 (m, 3H), 3.28 (s, 3H), 3.33 (m, 2H), 4.36-4.44 (bm, 2H), 6.91 (d, J = 9.2 Hz, 1H), 7.18 (m, 1H), 7.50 (m, 1H), 7.56 (m, 1H), 7.65 (d, J = 8.4 Hz, 1H), 7.85 (d, J = 9.2 Hz, 1H); <sup>13</sup>C NMR (CDCl<sub>3</sub>, 100 MHz) δ 23.3, 27.6, 29.5, 40.1, 46.0, 47.7, 51.7, 58.5, 72.6, 109.3, 122.0, 122.8, 126.4, 127.1, 129.4, 137.3, 148.0, 156.9.



**2-(2-(4-Methoxybutyl)piperazin-1-yl)-6-nitroquinoline ((±)-96).** A stirred solution of 2-(2-(4-methoxybutyl)piperazin-1-yl)quinoline **95** (0.21 g, 0.70 mmol) in H<sub>2</sub>SO<sub>4</sub> (16 M, 5 mL) was cooled at 0 °C. Dropwise addition of HNO<sub>3</sub> (15.4 M, 0.18 mL) to the solution was followed by stirring for 20 min at 0 °C. The reaction was quenched by pouring into ice water, the acid was neutralized with 4 M NaOH to give a bright yellow solution and the resulting solution was buffered to pH 10 with sat. NaHCO<sub>3</sub>. The aqueous solution was extracted with CH<sub>2</sub>Cl<sub>2</sub> until no yellow color was extracted into the organic layer. The organic portions were

combined, dried ( $K_2CO_3$ ), and concentrated *in vacuo* to give a bright yellow oil (**(±)-96**) (0.21 g, 88%): TLC  $R_f$  = 0.22 (1:9 MeOH/ $CH_2Cl_2$ );  $^1H$  NMR ( $CDCl_3$ , 400 MHz)  $\delta$  1.24-1.42 (m, 2H), 1.52-1.62 (m, 2H), 1.65-1.95 (2m, 3H), 2.79 (dt,  $J$  = 2.9 and 12.1 Hz, 1H), 2.88-2.96 (m, 1H), 3.00-3.20 (m, 3H), 3.23 (s, 3H), 3.26-3.32 (m, 2H), 4.46 (bs, 2H), 6.97 (d,  $J$  = 9.5 Hz, 1H), 7.54 (d,  $J$  = 9.2 Hz, 1H), 7.86 (d,  $J$  = 9.5 Hz, 1H), 8.2 (dd,  $J$  = 2.6 and 9.5 Hz, 1H), 8.43 (d,  $J$  = 2.6 Hz, 1H);  $^{13}C$  NMR ( $CDCl_3$ , 100 MHz)  $\delta$  23.0, 28.1, 29.4, 40.3, 46.0, 47.9, 51.8, 58.4, 72.4, 110.7, 120.7, 123.5, 124.1, 126.7, 138.3, 141.3, 151.5, 158.3; HRMS (ESI-TOF)  $m/z$  ( $M + H$ ) $^+$  calcd. for  $C_{18}H_{25}N_4O_3$  345.1927 found 345.1938.



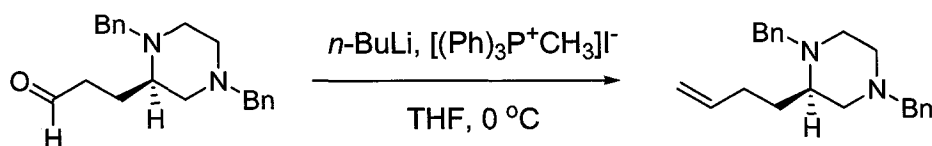
**tert-Butyl-3-(4-hydroxybutyl)-4-(6-nitroquinolin-2-yl)piperazine-1-**

**carboxylate (97).**

A solution of 2-(2-(4-methoxybutyl)piperazin-1-yl)-6-nitroquinoline (**(±)-96**) (0.11g, 0.33 mmol) in dry  $CH_2Cl_2$  (33 mL) was cooled at  $-78\text{ }^\circ C$  in a dry ice, acetone bath. A solution of  $BBr_3$  (2.4 mL, 1M in  $CH_2Cl_2$ , 2.4 mmol) was added dropwise under argon giving a dark purple suspension. The suspension was warmed to RT  $^\circ C$  and stirred overnight giving a yellow-orange suspension. The reaction was quenched by the addition of sat.  $NaHCO_3$  (25 mL). The organic layer was separated and the aqueous layer was extracted with  $CH_2Cl_2$  (3 x 20 mL). The organic portions were combined, dried ( $K_2CO_3$ ), filtered and concentrated *in vacuo*. The resulting yellow semi-solid was transferred to a

50 mL flask with CH<sub>2</sub>Cl<sub>2</sub> and concentrated. The residue was treated with CH<sub>2</sub>Cl<sub>2</sub> (15 mL) sonicated to suspend all the material, then cooled to 0 °C, and treated with di-*tert*-butyl dicarbonate (0.07 g, 0.33 mmol). After 2.5 h, the reaction was warmed to RT °C. The solution was concentrated *in vacuo* (25 °C) and dissolved in CHCl<sub>3</sub>. The crude solution was purified by column chromatography over silica gel (8 g) eluting with 3:2 EtOAc/hexanes to give **97** as a yellow foam (0.088 g, 44% yield 2 steps): <sup>1</sup>H NMR (CDCl<sub>3</sub>, 400 MHz) δ 1.30-1.85 (m, 15H), 2.80-3.43 (2bm, 4H), 3.63 (bs, 2H), 4.00-4.78 (3bm, 4H), 7.02 (d, J = 9.5 Hz, 1H), 7.63 (d, J = 9.2 Hz, 1H), 7.97 (d, J = 9.2 Hz, 1H), 8.28 (dd, J = 2.6 and 9.2 Hz, 1H), 8.52 (d, J = 2.6 Hz, 1H).

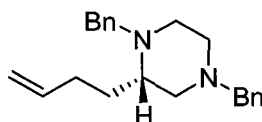
## 6.9 Chiral BuM-NQP Series.



**(R)-1,4-Dibenzyl-2-(but-3-enyl)piperazine ((R)-90).** A stirred suspension of methyl triphenylphosphonium iodide (3.0 g, 7.4 mmol) in dry THF (20 mL), cooled at 0° C, was treated with *n*-BuLi (3.3 mL, 2.2 M in hexanes, 7.3 mmol) giving an yellow-orange suspension. The mixture was stirred for 1 h at 0° C. A solution of 3-(1,4-dibenzylpiperazin-2-yl)propanal **(R)-89** (1.2 g, 3.7 mmol) in dry THF (5 mL) was added dropwise to the ylide. After 1 hour, the reaction was allowed to warm to RT° C and stir for 18 h. The reaction was quenched with water (15 mL). The

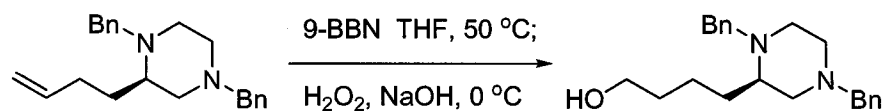
THF was removed *in vacuo*, and the resulting aqueous solution was treated with sat. NaHCO<sub>3</sub> (20 mL). The aqueous phase was extracted with CH<sub>2</sub>Cl<sub>2</sub> (3 x 30 mL), the organic portions were combined, dried (K<sub>2</sub>CO<sub>3</sub>) and concentrated *in vacuo* to give a white-tan semi-solid. The crude material was purified by column chromatography over silica gel (60 g) loaded with CHCl<sub>3</sub> and eluted with 1:3 EtOAc/hexanes followed by 2:3 EtOAc/hexanes to give (**R**)-**90** as a light tan oil (0.57 g, 49%, 2 steps): TLC *R<sub>f</sub>* = 0.54 (4:6 EtOAc/hexanes); <sup>1</sup>H NMR (CDCl<sub>3</sub>, 400 MHz) δ 1.68-1.79 (m, 2H), 1.93-2.34 (m, 5H), 2.45-2.79 (m, 4H), 3.24 (d, *J* = 13.3 Hz, 1H, CH<sub>2-AM</sub>Ar), 3.51 (dd, *J* = 12.9 and 34.9 Hz, 2H, CH<sub>2-AB</sub>Ar), 4.02 (d, *J* = 13.3 Hz, 1H, CH<sub>2-AM</sub>Ar), 4.91-5.03 (m, 1H), 5.74-5.87 (m, 1H), 7.20-7.38 (m, 10H); <sup>13</sup>C NMR (CDCl<sub>3</sub>, 100 MHz) δ 28.7, 29.8, 50.6, 52.9, 57.2, 57.6, 59.1, 63.1, 114.4, 126.7, 126.9, 128.1, 128.9, 129.0, 138.2, 138.7, 139.1.

The opposing enantiomer was similarly prepared:



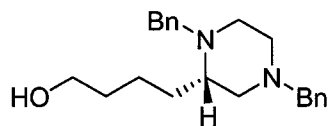
**(S)-1,4-Dibenzyl-2-(but-3-enyl)piperazine ((S)-90)**. Light tan oil; (0.56 g, 55% 2 steps).





**(R)-4-(1,4-Dibenzylpiperazin-2-yl)butan-1-ol ((R)-91).** A cooled (0 °C) stirred solution of (R)-1,4-dibenzyl-2-(but-3-enyl)piperazine (**(R)-90**) (0.57 g, 1.8 mmol) in dry THF (15 mL) was treated (dropwise) with a solution of 9-BBN (5.4 mL, 0.5 M in THF, 2.7 mmol), then heated at 55 °C for 1.5 h. The reaction was cooled to 0 °C and treated (dropwise) with a solution of NaOH (4.5 mL, 1 M), followed by 30% H<sub>2</sub>O<sub>2</sub> (4.5 mL). The reaction was then concentrated *in vacuo* to remove the THF. The solution was subsequently diluted with 1 M HCl (10 mL) and extracted with CH<sub>2</sub>Cl<sub>2</sub> (3 x 20 mL). The resulting aqueous layer was brought to basic pH with 4 M NaOH, buffered to pH 10 with sat. NaHCO<sub>3</sub>, extracted with CH<sub>2</sub>Cl<sub>2</sub> (4 x 15 mL). The organic portions were combined, dried (K<sub>2</sub>CO<sub>3</sub>), filtered and concentrated *in vacuo* to give a tan oil. The resultant crude oil was purified by column chromatography over silica gel (34 g) loaded with CHCl<sub>3</sub> and eluted with 0.4:9.6 MeOH/CHCl<sub>3</sub> followed by 1:19 MeOH/CHCl<sub>3</sub> to give a clear oil (**(R)-91**) (0.58 g, 94%): TLC *R<sub>f</sub>* = 0.06 (2:3 EtOAc/Hexanes); <sup>1</sup>H NMR (CDCl<sub>3</sub>, 400 MHz) δ 1.20-1.45 (m, 4H), 1.48-1.68 (m, 5H), 2.10-2.28 (m, 3H), 2.40-2.76 (m, 4H), 3.20 (d, J = 13.2 Hz, 1H, CH<sub>2-AX</sub>Ar), 3.49 (dd, J = 13.2 and 44.0 Hz, 2H, CH<sub>2-AM</sub>Ar), 3.58-3.64 (bm, 2H), 4.00 (d, J = 13.2 Hz, 1H, CH<sub>2-AX</sub>Ar), 7.20-7.35 (m, 10H); <sup>13</sup>C NMR (CDCl<sub>3</sub>, 100 MHz) δ 25.3, 26.2, 29.6, 32.6, 50.8, 52.7, 57.5, 59.5, 62.5, 63.0, 126.7, 126.9, 128.0, 128.9, 129.0, 137.9, 138.9 (1 overlapped peak).

The opposing enantiomer was similarly prepared:

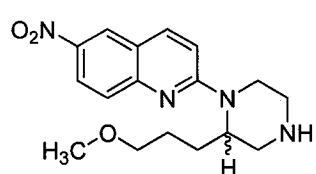


**4-((S)-1,4-dibenzylpiperazin-2-yl)butan-1-ol ((S)-91).** Clear oil; (0.58 g, 99%).

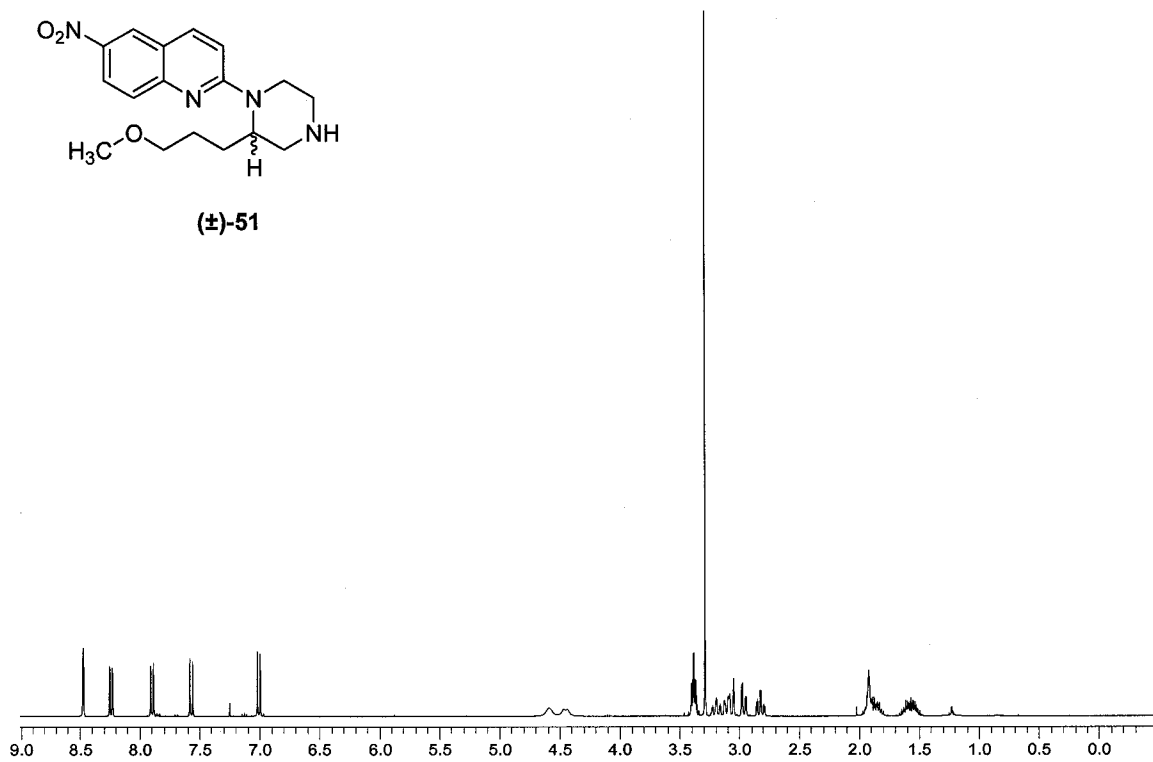
## Appendix

### Select NMR Spectra

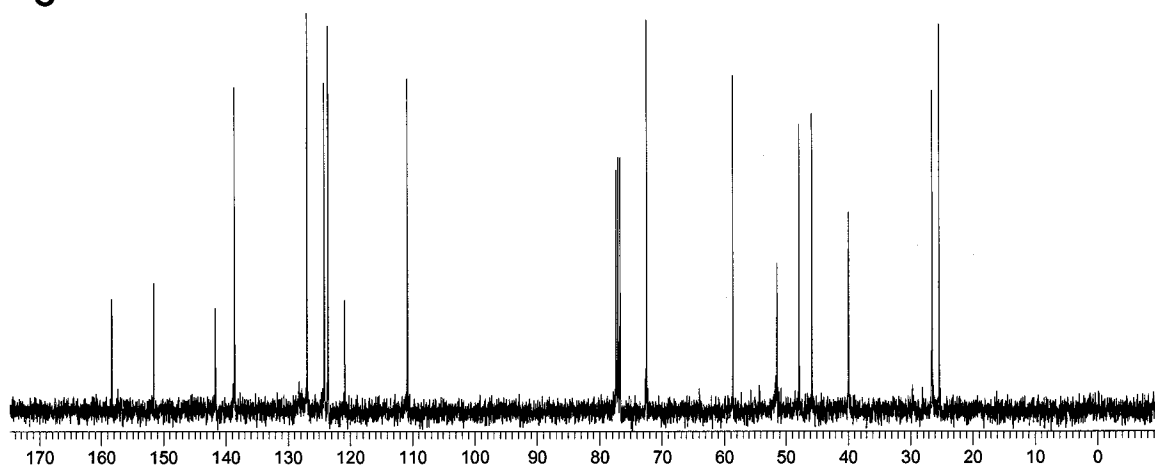
$^1\text{H}$



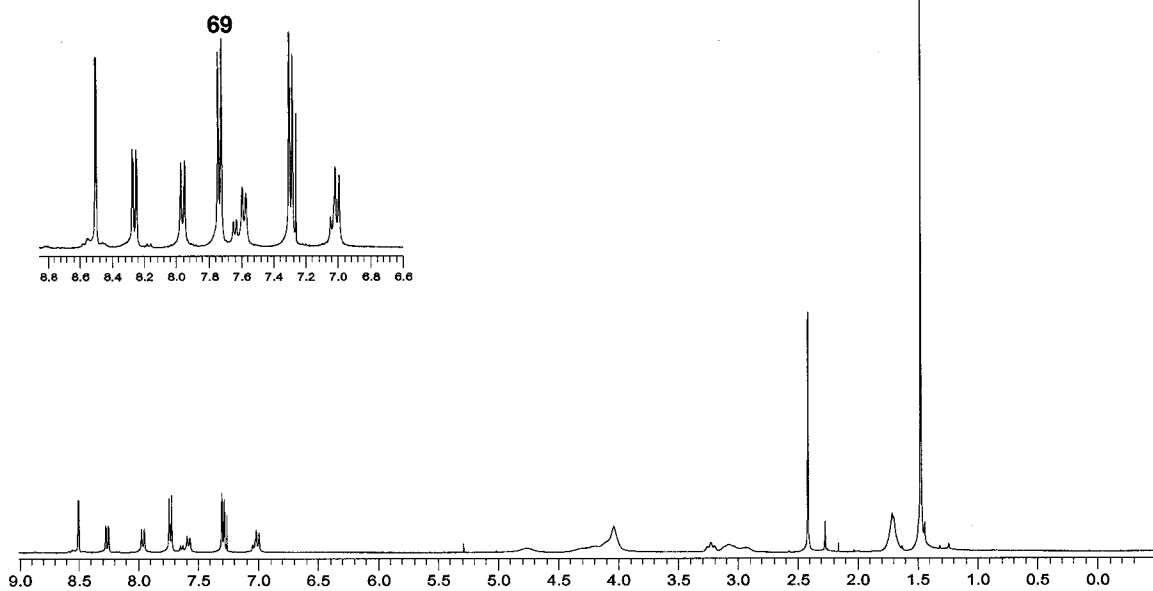
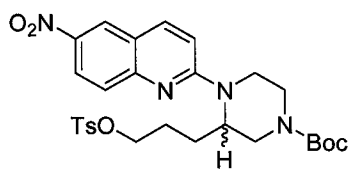
(±)-51



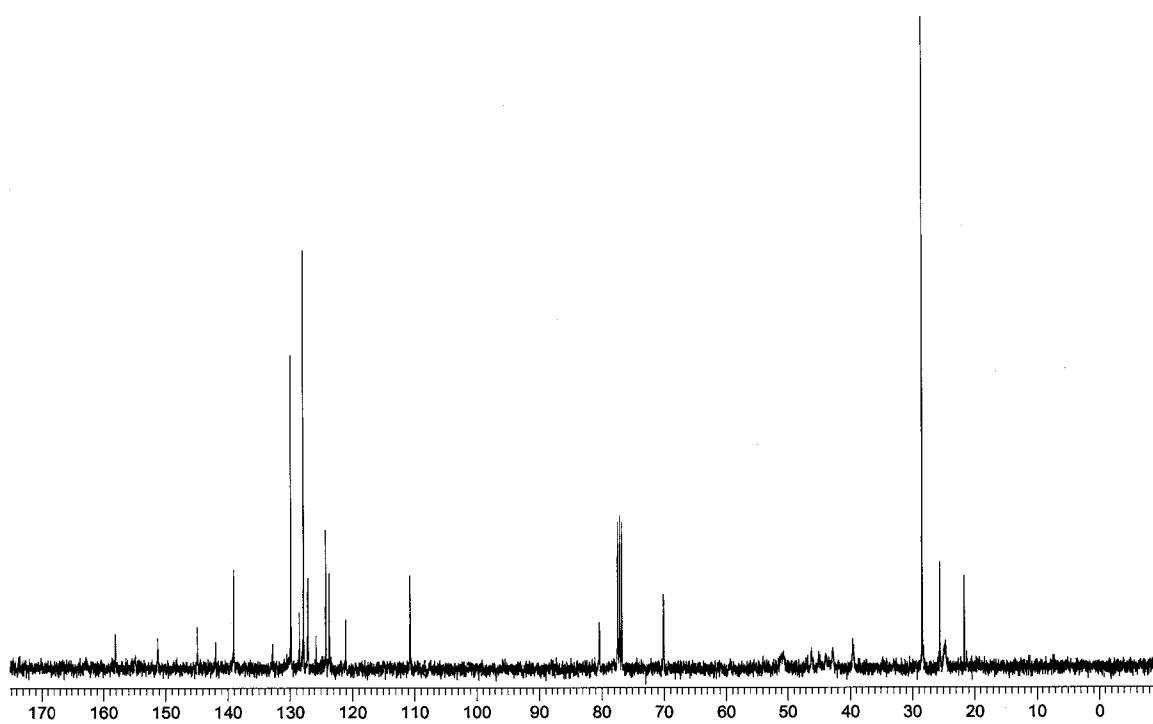
$^{13}\text{C}$



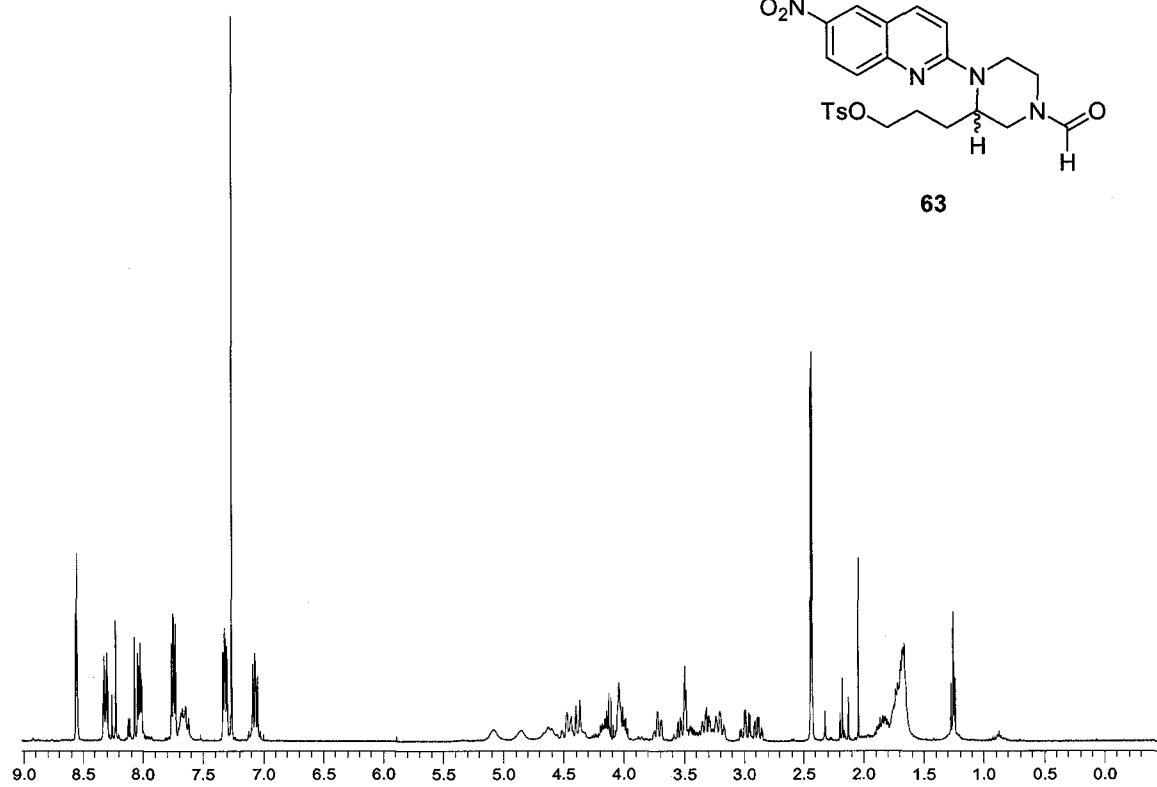
<sup>1</sup>H



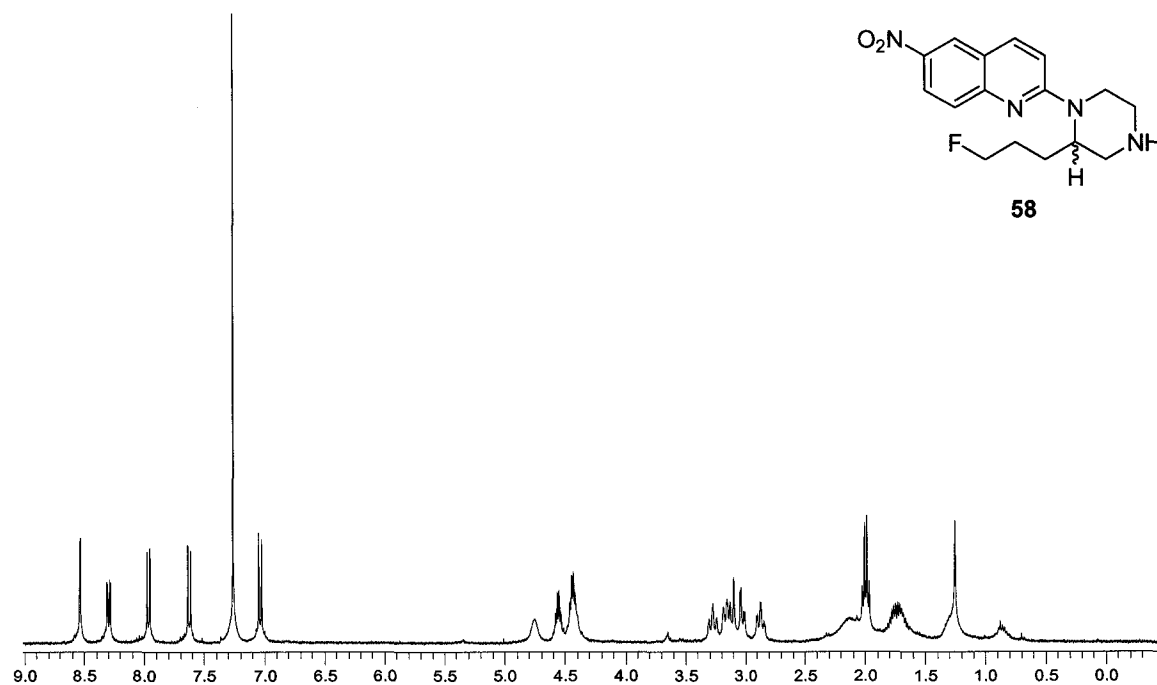
<sup>13</sup>C



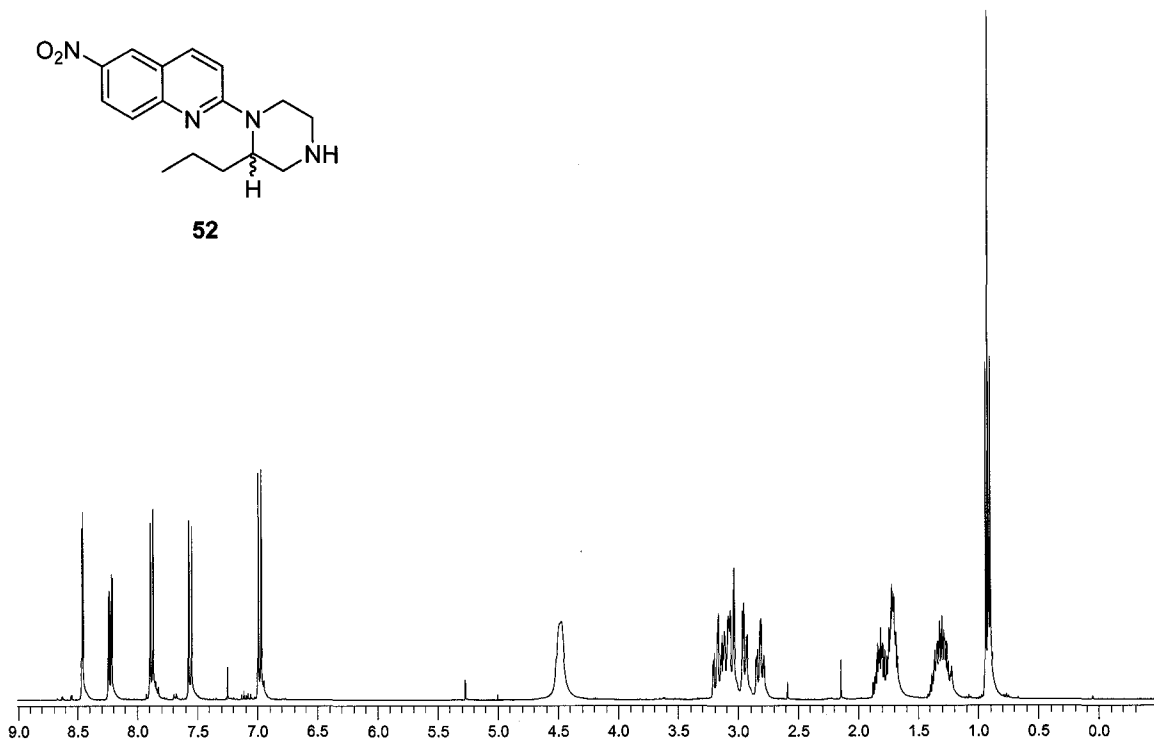
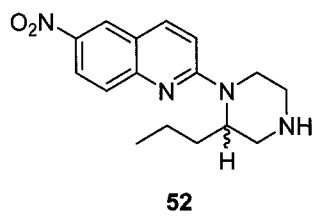
<sup>1</sup>H



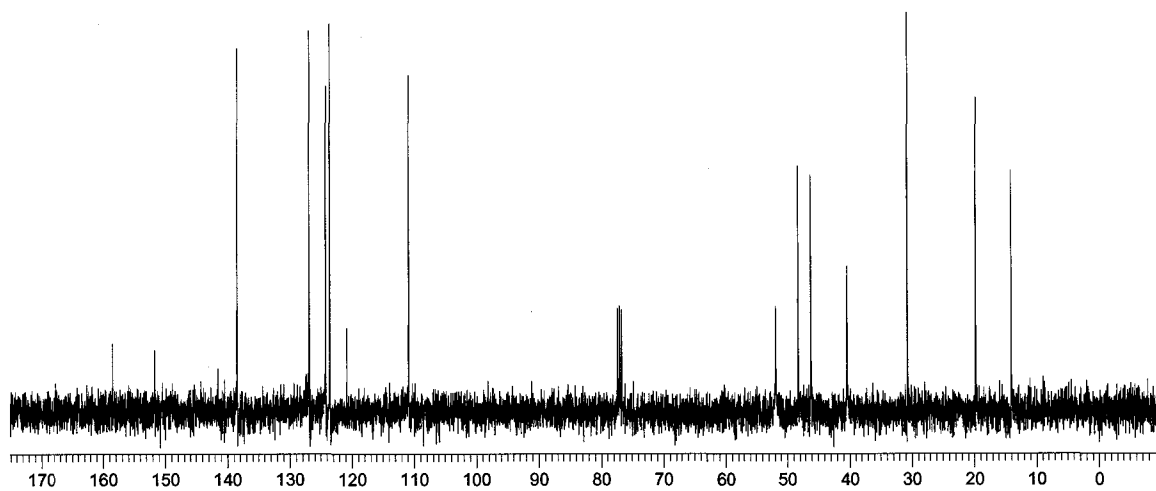
<sup>1</sup>H



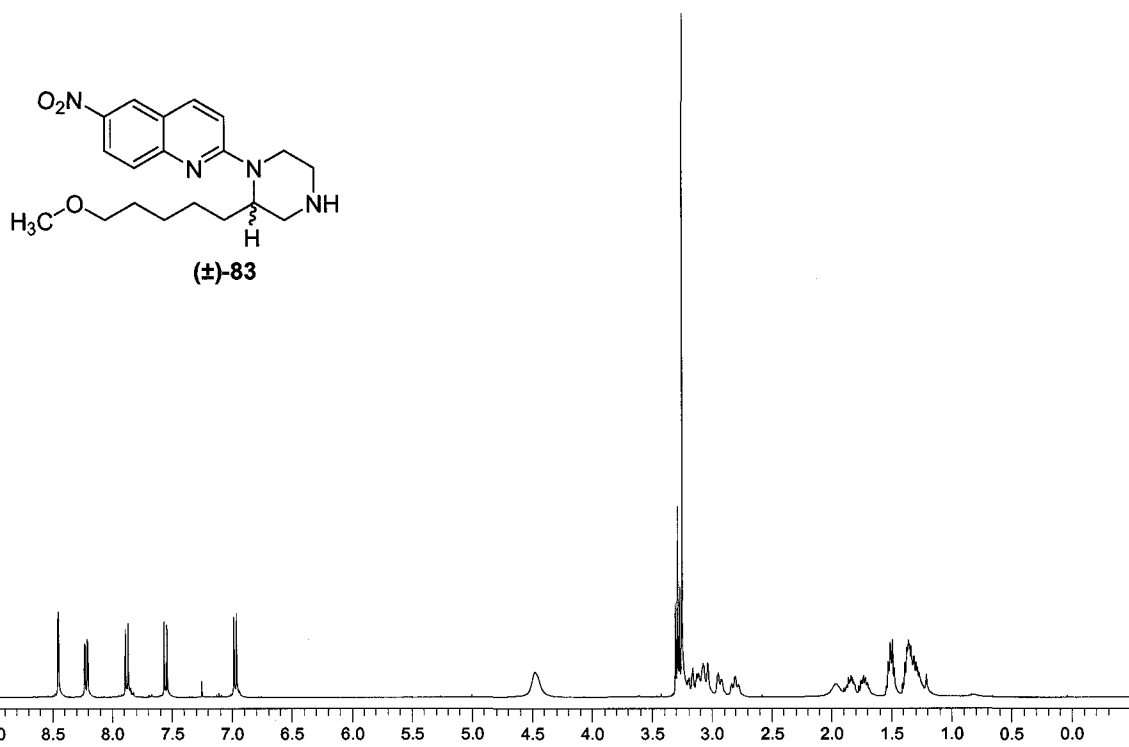
<sup>1</sup>H



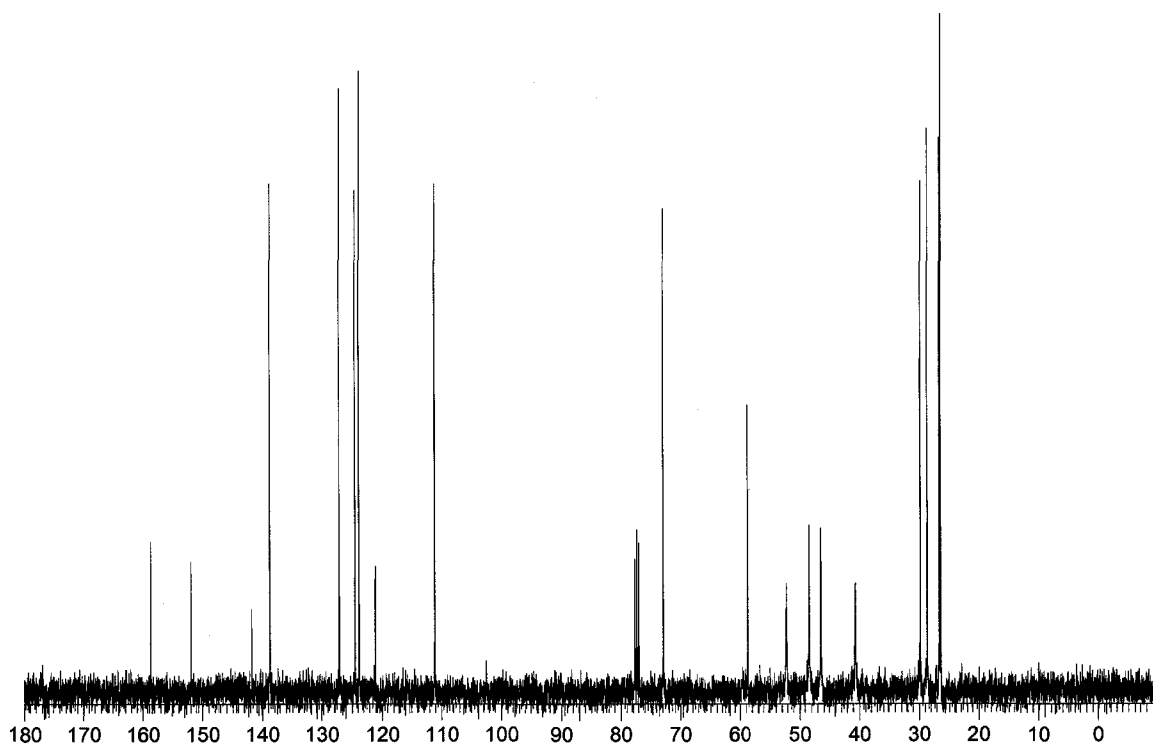
<sup>13</sup>C



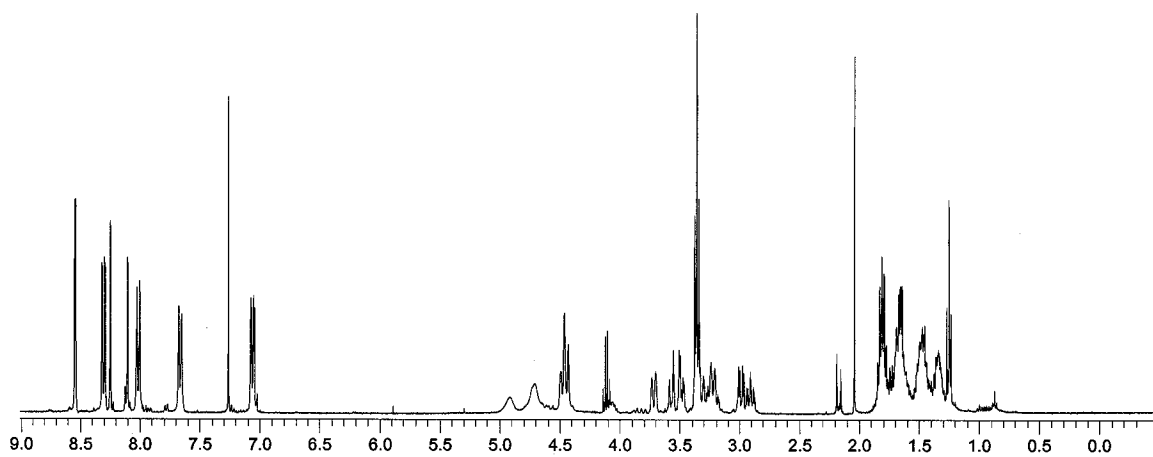
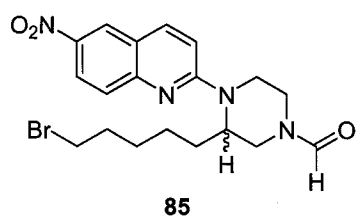
<sup>1</sup>H



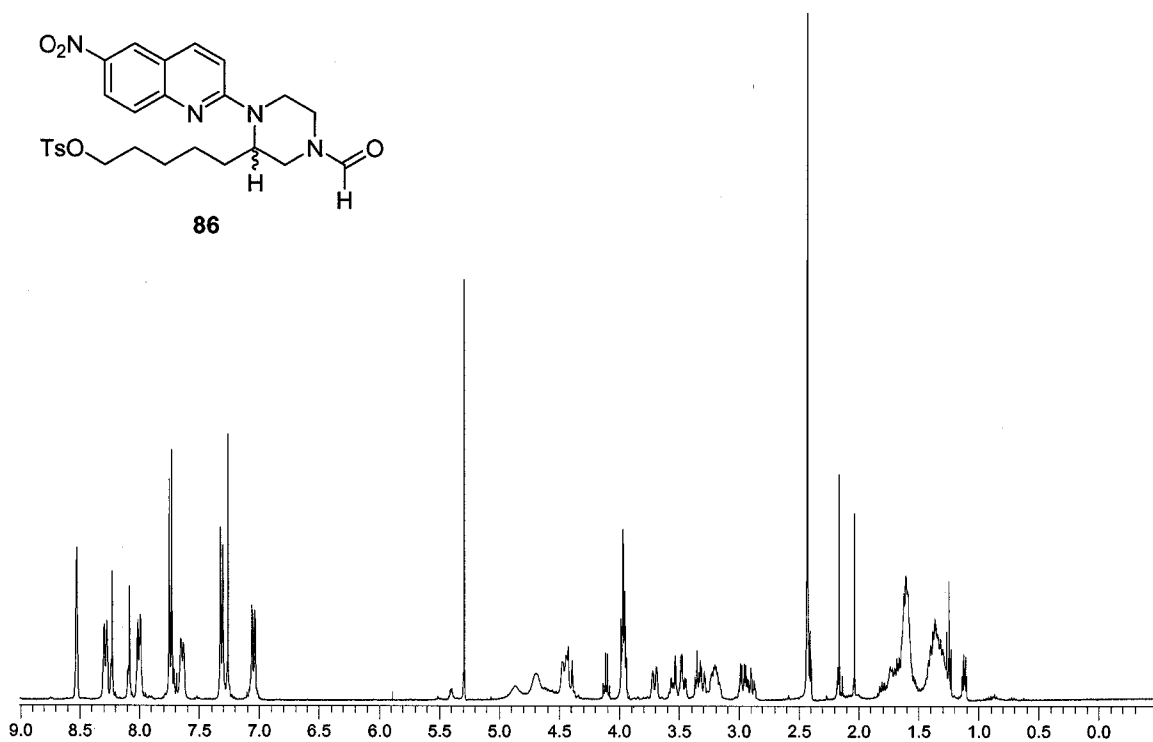
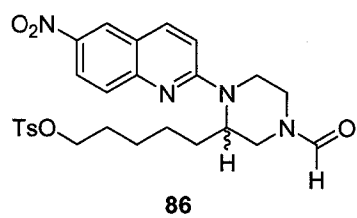
<sup>13</sup>C



<sup>1</sup>H

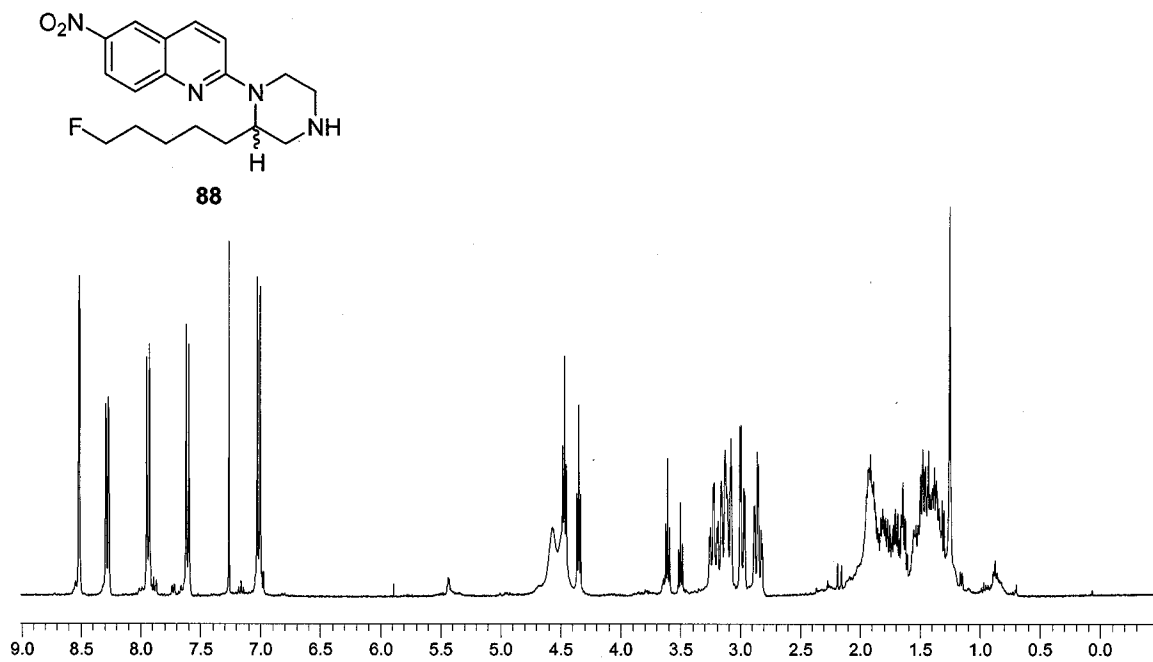


<sup>1</sup>H

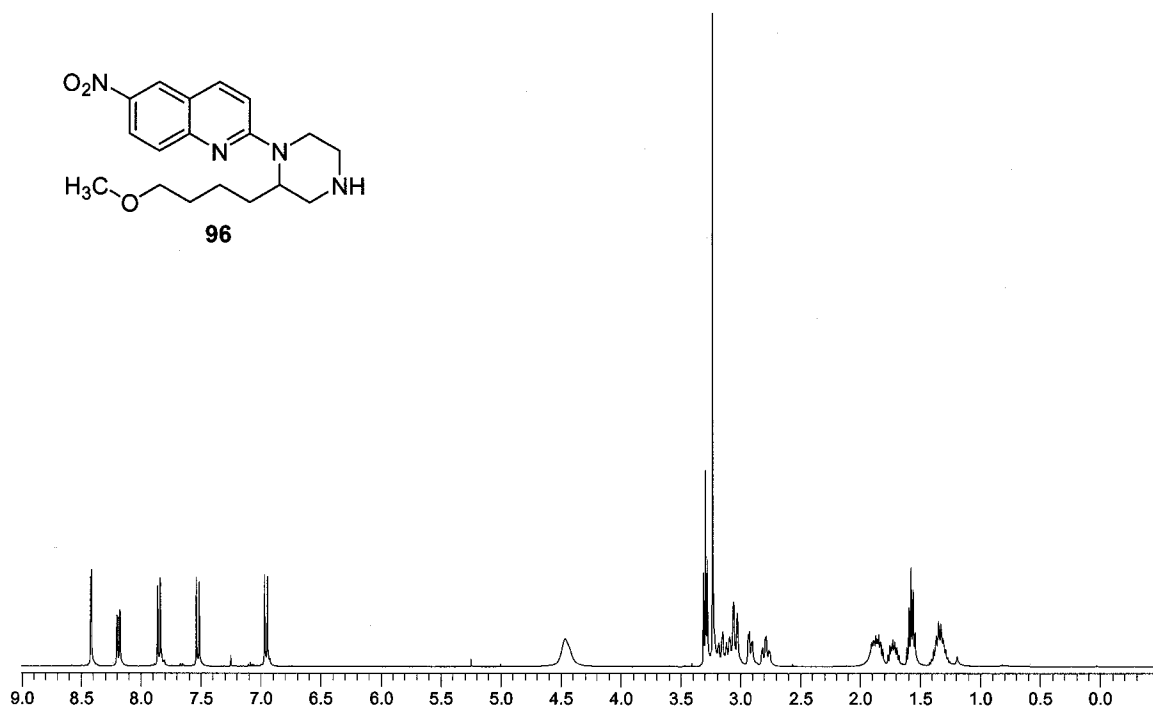




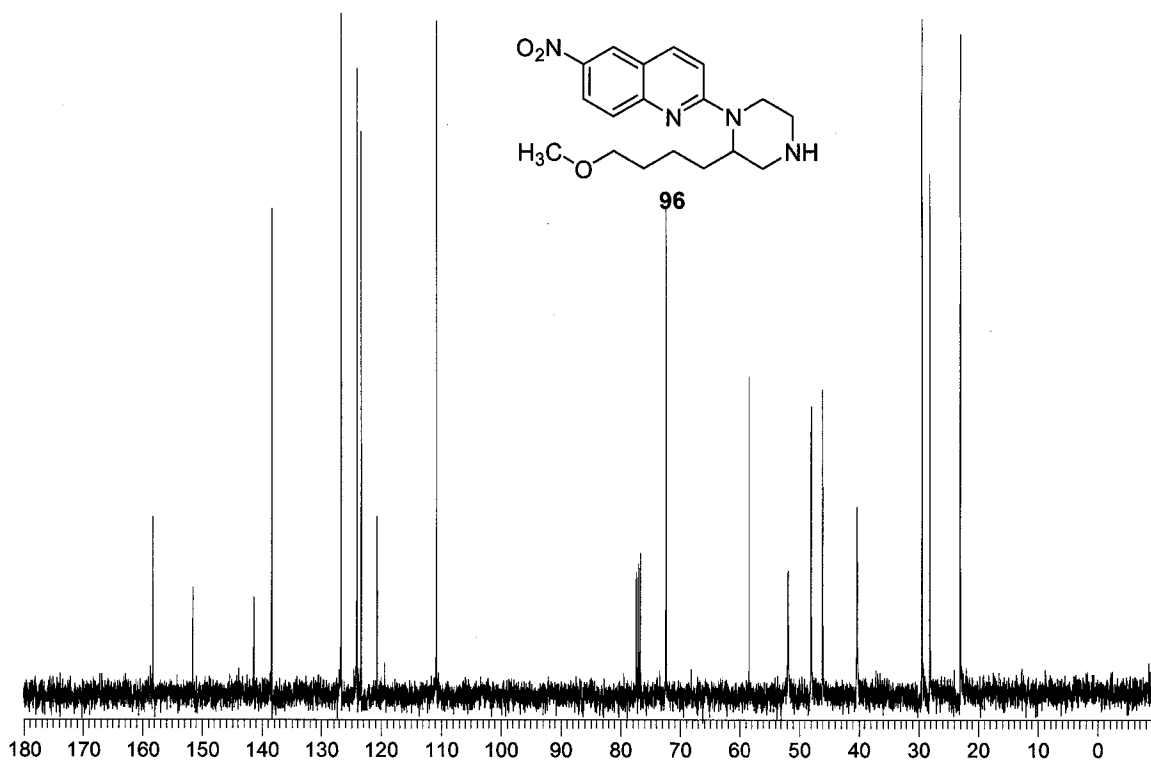
<sup>1</sup>H



<sup>1</sup>H



<sup>13</sup>C



## Bibliography

- (1) Emond, P.; Vercouillie, J.; Innis, R.; Chalon, S.; Mavel, S. et al. Substituted diphenyl sulfides as selective serotonin transporter ligands: synthesis and in vitro evaluation. *J Med Chem* **2002**, *45*, 1253-1258.
- (2) Oya, S.; Choi, S. R.; Hou, C.; Mu, M.; Kung, M. P. et al. 2-((2-((dimethylamino)methyl)phenyl)thio)-5-iodophenylamine (ADAM): an improved serotonin transporter ligand. *Nucl Med Biol* **2000**, *27*, 249-254.
- (3) Huang, Y.; Hwang, D. R.; Narendran, R.; Sudo, Y.; Chatterjee, R. et al. Comparative evaluation in nonhuman primates of five PET radiotracers for imaging the serotonin transporters: [<sup>11</sup>C]McN 5652, [<sup>11</sup>C]ADAM, [<sup>11</sup>C]DASB, [<sup>11</sup>C]DAPA, and [<sup>11</sup>C]AFM. *J Cereb Blood Flow Metab* **2002**, *22*, 1377-1398.
- (4) Rapport, M. M.; Green, A. A.; Page, I. H. Partial purification of the vasoconstrictor in beef serum. *J Biol Chem* **1948**, *174*, 735-741.
- (5) Rapport, M. M.; Green, A. A.; Page, I. H. Serum vasoconstrictor (serotonin). IV. Isolation and characterization. *J Biol Chem* **1948**, *176*, 1243-1251.
- (6) Hamlin, K. E.; Fischer, F. E. The synthesis of 5-hydroxytryptamine. *J Am Chem Soc* **1951**, *73*, 5007-5008.
- (7) Zifa, E.; Fillion, G. 5-Hydroxytryptamine receptors. *Pharmacological Reviews* **1992**, *44*, 401-458.
- (8) Gaddum, J. H.; Picarelli, Z. P. Two kinds of tryptamine receptor. *Br J Pharmacol Chemother* **1957**, *12*, 323-328.
- (9) Peroutka, S. J.; Snyder, S. H. Multiple serotonin receptors: differential binding of [<sup>3</sup>H]5-hydroxytryptamine, [<sup>3</sup>H]lysergic acid diethylamide and [<sup>3</sup>H]spiroperidol. *Mol Pharmacol* **1979**, *16*, 687-699.
- (10) Childers, W. E., Jr.; Robichaud, A. J. Recent Advances in Selective Serotonergic Agents. *Annual Reports in Medicinal Chemistry*; Elsevier: San Diego, 2005; pp 17-33.
- (11) Inoue, T.; Kusumi, I.; Yoshioka, M. Serotonin transporters. *Curr Drug Targets CNS Neurol Disord* **2002**, *1*, 519-529.
- (12) Nelson, N. The family of Na<sup>+</sup>/Cl<sup>-</sup> neurotransmitter transporters. *J Neurochem* **1998**, *71*, 1785-1803.

- (13) Elfving, B.; Bjornholm, B.; Ebert, B.; Knudsen, G. M. Binding characteristics of selective serotonin reuptake inhibitors with relation to emission tomography studies. *Synapse* **2001**, *41*, 203-211.
- (14) Blakely, R. D.; Moore, K. R.; Qian, Y. Tails of serotonin and norepinephrine transporters: deletions and chimeras retain function. *Soc Gen Physiol Ser* **1993**, *48*, 283-300.
- (15) Cortes, R.; Soriano, E.; Pazos, A.; Probst, A.; Palacios, J. M. Autoradiography of antidepressant binding sites in the human brain: localization using [<sup>3</sup>H]imipramine and [<sup>3</sup>H]paroxetine. *Neuroscience* **1988**, *27*, 473-496.
- (16) Laruelle, M.; Vanisberg, M. A.; Maloteaux, J. M. Regional and subcellular localization in human brain of [<sup>3</sup>H]paroxetine binding, a marker of serotonin uptake sites. *Biol Psychiatry* **1988**, *24*, 299-309.
- (17) Backstrom, I.; Bergstrom, M.; Marcusson, J. High affinity [<sup>3</sup>H]paroxetine binding to serotonin uptake sites in human brain tissue. *Brain Res* **1989**, *486*, 261-268.
- (18) Frankle, W. G.; Huang, Y.; Hwang, D. R.; Talbot, P. S.; Slifstein, M. et al. Comparative evaluation of serotonin transporter radioligands <sup>11</sup>C-DASB and <sup>11</sup>C-McN 5652 in healthy humans. *J Nucl Med* **2004**, *45*, 682-694.
- (19) Marjamaki, P.; Zessin, J.; Eskola, O.; Gronroos, T.; Haaparanta, M. et al. S-[<sup>18</sup>F]fluoromethyl-(+)-McN5652, a PET tracer for the serotonin transporter: evaluation in rats. *Synapse* **2003**, *47*, 45-53.
- (20) Purselle, D. C.; Nemeroff, C. B. Serotonin transporter: a potential substrate in the biology of suicide. *Neuropsychopharmacology* **2003**, *28*, 613-619.
- (21) Arango, V.; Underwood, M. D.; Mann, J. J. Serotonin brain circuits involved in major depression and suicide. *Prog Brain Res* **2002**, *136*, 443-453.
- (22) Mann, J. J.; Huang, Y. Y.; Underwood, M. D.; Kassir, S. A.; Oppenheim, S. et al. A serotonin transporter gene promoter polymorphism (5-HTTLPR) and prefrontal cortical binding in major depression and suicide. *Arch Gen Psychiatry* **2000**, *57*, 729-738.
- (23) Reivich, M.; Amsterdam, J. D.; Brunswick, D. J.; Shiue, C. Y. PET brain imaging with [<sup>11</sup>C](+)McN5652 shows increased serotonin transporter availability in major depression. *J Affect Disord* **2004**, *82*, 321-327.

- (24) Stein, M. B.; Seedat, S.; Gelernter, J. Serotonin transporter gene promoter polymorphism predicts SSRI response in generalized social anxiety disorder. *Psychopharmacology (Berl)* **2006**.
- (25) Helbecque, N.; Sparks, D. L.; Hunsaker, J. C., 3rd; Amouyel, P. The serotonin transporter promoter polymorphism and suicide. *Neurosci Lett* **2006**, *400*, 13-15.
- (26) Arato, M.; Tekes, K.; Tothfalusi, L.; Magyar, K.; Palkovits, M. et al. Serotonergic split brain and suicide. *Psychiatry Res* **1987**, *21*, 355-356.
- (27) Naylor, L.; Dean, B.; Opeskin, K.; Pavey, G.; Hill, C. et al. Changes in the serotonin transporter in the hippocampus of subjects with schizophrenia identified using [<sup>3</sup>H]paroxetine. *J Neural Transm* **1996**, *103*, 749-757.
- (28) Joyce, J. N. The dopamine hypothesis of schizophrenia: limbic interactions with serotonin and norepinephrine. *Psychopharmacology (Berl)* **1993**, *112*, S16-34.
- (29) Laruelle, M.; Abi-Dargham, A.; Casanova, M. F.; Toti, R.; Weinberger, D. R. et al. Selective abnormalities of prefrontal serotonergic receptors in schizophrenia. A postmortem study. *Arch Gen Psychiatry* **1993**, *50*, 810-818.
- (30) Frankie, W. G.; Narendran, R.; Huang, Y.; Hwang, D. R.; Lombardo, I. et al. Serotonin transporter availability in patients with schizophrenia: a positron emission tomography imaging study with [<sup>11</sup>C]DASB. *Biol Psychiatry* **2005**, *57*, 1510-1516.
- (31) Gorwood, P. Eating disorders, serotonin transporter polymorphisms and potential treatment response. *Am J Pharmacogenomics* **2004**, *4*, 9-17.
- (32) Tammela, L. I.; Rissanen, A.; Kuikka, J. T.; Karhunen, L. J.; Bergstrom, K. A. et al. Treatment improves serotonin transporter binding and reduces binge eating. *Psychopharmacology (Berl)* **2003**, *170*, 89-93.
- (33) Lundquist, P.; Wilking, H.; Hoglund, A. U.; Sandell, J.; Bergstrom, M. et al. Potential of [<sup>11</sup>C]DASB for measuring endogenous serotonin with PET: binding studies. *Nucl Med Biol* **2005**, *32*, 129-136.
- (34) Brust, P.; Zessin, J.; Kuwabara, H.; Pawelke, B.; Kretschmar, M. et al. Positron emission tomography imaging of the serotonin transporter in the pig brain using [<sup>11</sup>C](+)-McN5652 and S-([<sup>18</sup>F]fluoromethyl)-(+)-McN5652. *Synapse* **2003**, *47*, 143-151.
- (35) Davidson, R. J.; Pizzagalli, D.; Nitschke, J. B.; Putnam, K. Depression: perspectives from affective neuroscience. *Annu Rev Psychol* **2002**, *53*, 545-574.

- (36) Gurevich, E. V.; Joyce, J. N. Comparison of [<sup>3</sup>H]paroxetine and [3H]cyanoimipramine for quantitative measurement of serotonin transporter sites in human brain. *Neuropsychopharmacology* **1996**, *14*, 309-323.
- (37) Talbot, P. S.; Laruelle, M. The role of in vivo molecular imaging with PET and SPECT in the elucidation of psychiatric drug action and new drug development. *European Neuropsychopharmacology* **2002**, *12*, 503-511.
- (38) Halldin, C.; Gulyas, B.; Langer, O.; Farde, L. Brain radioligands--state of the art and new trends. *Q J Nucl Med* **2001**, *45*, 139-152.
- (39) Laruelle, M.; Slifstein, M.; Huang, Y. Relationships between radiotracer properties and image quality in molecular imaging of the brain with positron emission tomography. *Mol Imaging Biol* **2003**, *5*, 363-375.
- (40) Huang, Y.; Narendran, R.; Bae, S. A.; Erritzoe, D.; Guo, N. et al. A PET imaging agent with fast kinetics: synthesis and in vivo evaluation of the serotonin transporter ligand [<sup>11</sup>C]2-[2-dimethylaminomethylphenylthio]-5-fluorophenylamine ([<sup>11</sup>C]AFA). *Nucl Med Biol* **2004**, *31*, 727-738.
- (41) Madsen, J.; Merachtsaki, P.; Davoodpour, P.; Bergstrom, M.; Langstrom, B. et al. Synthesis and biological evaluation of novel carbon-11-labelled analogues of citalopram as potential radioligands for the serotonin transporter. *Bioorg Med Chem* **2003**, *11*, 3447-3456.
- (42) Hume, S. P.; Lammertsma, A. A.; Bench, C. J.; Pike, V. W.; Pascali, C. et al. Evaluation of S-[<sup>11</sup>C]citalopram as a radioligand for in vivo labelling of 5-hydroxytryptamine uptake sites. *Int J Rad Appl Instrum B* **1992**, *19*, 851-855.
- (43) Hume, S. P.; Pascali, C.; Pike, V. W.; Turton, D. R.; Ahier, R. G. et al. Citalopram: labelling with carbon-11 and evaluation in rat as a potential radioligand for in vivo PET studies of 5-HT re-uptake sites. *Int J Rad Appl Instrum B* **1991**, *18*, 339-351.
- (44) Suehiro, M.; Wilson, A. A.; Scheffel, U.; Dannals, R. F.; Ravert, H. T. et al. Radiosynthesis and evaluation of N-(3-[<sup>18</sup>F]fluoropropyl)paroxetine as a radiotracer for in vivo labeling of serotonin uptake sites by PET. *Int J Rad Appl Instrum B* **1991**, *18*, 791-796.
- (45) Szabo, Z.; Kao, P. F.; Scheffel, U.; Suehiro, M.; Mathews, W. B. et al. Positron emission tomography imaging of serotonin transporters in the human brain using [<sup>11</sup>C](+)McN5652. *Synapse* **1995**, *20*, 37-43.
- (46) Szabo, Z.; Scheffel, U.; Suehiro, M.; Dannals, R. F.; Kim, S. E. et al. Positron emission tomography of 5-HT transporter sites in the baboon brain with [<sup>11</sup>C]McN5652. *J Cereb Blood Flow Metab* **1995**, *15*, 798-805.

- (47) Suehiro, M.; Greenberg, J. H.; Shiue, C. Y.; Gonzalez, C.; Dembowski, B. et al. Radiosynthesis and biodistribution of the S-[<sup>18</sup>F]fluoroethyl analog of McN5652. *Nucl Med Biol* **1996**, *23*, 407-412.
- (48) Kung, M. P.; Hou, C.; Oya, S.; Mu, M.; Acton, P. D. et al. Characterization of [(<sup>123</sup>I)]IDAM as a novel single-photon emission tomography tracer for serotonin transporters. *Eur J Nucl Med* **1999**, *26*, 844-853.
- (49) Acton, P. D.; Kung, M. P.; Mu, M.; Plossl, K.; Hou, C. et al. Single-photon emission tomography imaging of serotonin transporters in the non-human primate brain with the selective radioligand [(<sup>123</sup>I)]IDAM. *Eur J Nucl Med* **1999**, *26*, 854-861.
- (50) Choi, S. R.; Hou, C.; Oya, S.; Mu, M.; Kung, M. P. et al. Selective in vitro and in vivo binding of [(<sup>125</sup>I)]ADAM to serotonin transporters in rat brain. *Synapse* **2000**, *38*, 403-412.
- (51) Huang, Y.; Bae, S.-A.; Zhu, Z.; Guo, N.; Roth, B. L. et al. Fluorinated Diaryl Sulfides as Serotonin Transporter Ligands: Synthesis, Structure-Activity Relationship Study, and in Vivo Evaluation of Fluorine-18-Labeled Compounds as PET Imaging Agents. *J Med Chem* **2005**, *48*, 2559-2570.
- (52) Lee, B. S.; Chu, S.; Lee, B. C.; Chi, D. Y.; Choe, Y. S. et al. Syntheses and binding affinities of 6-nitroquipazine analogues for serotonin transporter. Part 1. *Bioorg Med Chem Lett* **2000**, *10*, 1559-1562.
- (53) Se Lee, B.; Chu, S.; Lee, B. S.; Yoon Chi, D.; Song, Y. S. et al. Syntheses and binding affinities of 6-nitroquipazine analogues for serotonin transporter. Part 2: 4-substituted 6-nitroquipazines. *Bioorg Med Chem Lett* **2002**, *12*, 811-815.
- (54) Jagust, W. J.; Eberling, J. L.; Roberts, J. A.; Brennan, K. M.; Hanrahan, S. M. et al. In vivo imaging of the 5-hydroxytryptamine reuptake site in primate brain using single photon emission computed tomography and [<sup>123</sup>I]5-iodo-6-nitroquipazine. *Eur J Pharmacol* **1993**, *242*, 189-193.
- (55) Jagust, W. J.; Eberling, J. L.; Biegon, A.; Taylor, S. E.; VanBrocklin, H. F. et al. Iodine-123-5-iodo-6-nitroquipazine: SPECT radiotracer to image the serotonin transporter. *J Nucl Med* **1996**, *37*, 1207-1214.
- (56) Lundkvist, C.; Loc'h, C.; Halldin, C.; Bottlaender, M.; Ottaviani, M. et al. Characterization of bromine-76-labelled 5-bromo-6-nitroquipazine for PET studies of the serotonin transporter. *Nucl Med Biol* **1999**, *26*, 501-507.
- (57) Karamkam, M.; Dolle, F.; Valette, H.; Besret, L.; Bramoulle, Y. et al. Synthesis of a fluorine-18-labelled derivative of 6-nitroquipazine, as a radioligand for the in vivo serotonin transporter imaging with PET. *Bioorg Med Chem* **2002**, *10*, 2611-2623.

- (58) Sandell, J.; Halldin, C.; Sovago, J.; Chou, Y. H.; Gulyas, B. et al. PET examination of [<sup>11</sup>C]5-methyl-6-nitroquipazine, a radioligand for visualization of the serotonin transporter. *Nucl Med Biol* **2002**, *29*, 651-656.
- (59) Sandell, J.; Yu, M.; Emond, P.; Garreau, L.; Chalon, S. et al. Synthesis, radiolabeling and preliminary biological evaluation of radiolabeled 5-methyl-6-nitroquipazine, a potential radioligand for the serotonin transporter. *Bioorg Med Chem Lett* **2002**, *12*, 3611-3613.
- (60) Griffin, L. D.; Mellon, S. H. Selective serotonin reuptake inhibitors directly alter activity of neurosteroidogenic enzymes. *Proc Natl Acad Sci U S A* **1999**, *96*, 13512-13517.
- (61) Oh, S. J.; Ha, H. J.; Chi, D. Y.; Lee, H. K. Serotonin receptor and transporter ligands - current status. *Curr Med Chem* **2001**, *8*, 999-1034.
- (62) Rosen, R. C.; Lane, R. M.; Menza, M. Effects of SSRIs on sexual function: a critical review. *J Clin Psychopharmacol* **1999**, *19*, 67-85.
- (63) Banov, M. D. Improved outcome in fluvoxamine-treated patients with SSRI-induced sexual dysfunction. *J Clin Psychiatry* **1999**, *60*, 866-868.
- (64) Waldinger, M. D.; van De Plas, A.; Pattij, T.; van Oorschot, R.; Coolen, L. M. et al. The selective serotonin re-uptake inhibitors fluvoxamine and paroxetine differ in sexual inhibitory effects after chronic treatment. *Psychopharmacology (Berl)* **2002**, *160*, 283-289.
- (65) Wilson, P. A. A Simple Methodology for the Production of Three-Dimensional Models: Serotonin Transporter as an Example; Doctor of Philosophy, Chemistry; The University of Montana: Missoula, 2004.
- (66) Davis, E. S. Comparative analysis of serotonin and norepinephrine reuptake inhibitor pharmacophore constructs for ligand designs; Doctor of Philosophy, Chemistry; The University of Montana: Missoula, 2006.
- (67) Gerdes, J. M.; DeFina, S. C.; Wilson, P. A.; Taylor, S. E. Serotonin transporter inhibitors: synthesis and binding potency of 2'-methyl- and 3'-methyl-6-nitroquipazine. *Bioorg Med Chem Lett* **2000**, *10*, 2643-2646.
- (68) Rondou, F.; Le Bihan, G.; Wang, X.; Lamouri, A.; Touboul, E. et al. Design and Synthesis of Imidazoline Derivatives Active on Glucose Homeostasis in a Rat Model of Type II Diabetes. 1. Synthesis and Biological Activities of N-Benzyl-N'-(arylalkyl)-2-(4',5'-dihydro-1'H-imidazol-2'-yl)piperazines. *J. Med. Chem.* **1997**, *40*, 3793-3803.



- (69) Walker, M. A. Serotonin Transporter Inhibitors: Studies of 2'-Substituted-6-nitroquipzine agents; Master of Science, Chemistry; Central Washington University: Ellensburg, 2001.
- (70) Le Bihan, G.; Rondu, F.; Pele-Tounian, A.; Wang, X.; Lidy, S. et al. Design and Synthesis of Imidazoline Derivatives Active on Glucose Homeostasis in a Rat Model of Type II Diabetes. 2. Syntheses and Biological Activities of 1,4-Dialkyl-, 1,4-Dibenzyl, and 1-Benzyl-4-alkyl-2-(4',5'-dihydro-1'H-imidazol-2'-yl)piperazines and Isosteric Analogues of Imidazoline. *J Med Chem* **1999**, *42*, 1587-1603.
- (71) Gilman, H.; Crouse, N. N.; Massie, S. P.; Benkeser, R. A. J.; Spatz, S. M. Rearrangement in the Reaction of alpha-Halogenonaphthalenes with Lithium Diethylamide. *J Am Chem Soc* **1945**, *67*, 2106-2108.
- (72) Bolstad, D. B.; Chandler-Ferguson, D.; Davis, E. S.; DeFina, S. C.; Gerdes, J. M. et al. Serotonin Transporter Inhibitor Ligands: Synthesis and Biochemical Studies of 2'-Methoxymethyl-6-nitroquipazine. *American Chemical Society 221 National Meeting*: Chicago, IL, 2001.
- (73) Davis, E. S.; Gerdes, J. M.; Walker, M. A.; Weller, M. L.; Wilson, P. A. et al. Studies of the Serotonin Transporter: Synthetic, Pharmacological and Whole Animal Investigations of Inhibitor 2'-Methyl-6-nitroquipazine. *American Chemical Society 221 National Meeting*: Chicago, IL, 1999.
- (74) Bolstad, D. B. Synthesis of Novel 6-Nitroquipazine Analogs for Imaging the Serotonin Transporter by Positron Emission Tomography; Doctor of Philosophy, Chemistry; The University of Montana: Missoula, 2006.
- (75) O'Neil, J. P.; VanBrocklin, H. F.; Bolstad, D. B.; Gerdes, J. M.; Kusche, B. K. Serotonin Transporter Ligands: Synthesis of (+/-)-[<sup>11</sup>C]2'-Methoxymethyl-6-nitroquipazine. *J Label Compd Radiopharm* **2003**, *46*, S1-S403.
- (76) Thompson, S. K.; Heathcock, C. H. Effect of Cation, Temperature, and Solvent on the Stereoselectivity of the Horner-Emmons Reaction of Trimethyl Phosphonoacetate with Aldehydes. *J Org Chem* **1990**, *55*, 3386-3388.
- (77) Mancuso, A. J.; Brownfain, D. S.; Swern, D. Structure of the dimethyl sulfoxide-oxalyl chloride reaction product. Oxidation of heteroaromatic and diverse alcohols to carbonyl compounds. *J Org Chem* **1979**, *44*, 4148-4150.
- (78) Mancuso, A. J.; Huang, S.-L.; Swern, D. Oxidation of long-chain and related alcohols to carbonyls by dimethyl sulfoxide "activated" by oxalyl chloride. *J Org Chem* **1978**, *43*, 2480-2482.

- (79) Epstein, W. W.; Sweat, F. W. Dimethyl sulfoxide oxidations. *Chemical Reviews (Washington, DC, United States)* **1967**, *67*, 247-260.
- (80) Fadel, A.; Vandromme, L. Total synthesis of (-)-sporochinol A, the fish deterrent, from a chiral malonate. *Tetrahedron: Asymmetry* **1999**, *10*, 1153-1162.
- (81) Hudlicky, T.; Sinai-Zingde, G.; Natchus, M. G. Selective reduction of  $\alpha,\beta$ -unsaturated esters in the presence of olefins. *Tet Lett* **1987**, *28*, 5287-5290.
- (82) Angelovski, G.; Costisella, B.; Kolaric, B.; Engelhard, M.; Eilbracht, P. Complexation of Metals with Piperazine-Containing Azamacrocyclic Fluorophores. *J Org Chem* **2004**, *69*, 5290-5294.
- (83) Sheehan, J. C.; Yang, D. D. H. The Use of N-Formylamino Acids in Peptide Synthesis. *J Am Chem Soc* **1958**, *80*, 1154-1158.
- (84) Kuduk, S. D.; DiPardo, R. M.; Bock, M. G. Tetrabutylammonium Salt Induced Denitration of Nitropyridines: Synthesis of Fluoro-, Hydroxy-, and Methoxypyridines. *Org Lett* **2005**, *7*, 577-579.
- (85) Frédéric Dolle, H. V., Michel Bottlaender, Françoise Hinnen, Françoise Vaufrey, Ilonka Guenther, Christian Crouzel, Synthesis of 2-[ $^{18}\text{F}$ ]fluoro-3-[2(S)-2-azetidylmethoxy]pyridine, a highly potent radioligand for in vivo imaging central nicotinic acetylcholine receptors. *J Label Compd Radiopharm* **1998**, *41*, 451-463.
- (86) Shozo Furumoto, R. I., Tatsuo Ido, Synthesis of 1-O-(8-[ $^{18}\text{F}$ ]fluorooctanoyl)-2-O-palmitoyl-*rac*-glycerol for imaging intracellular signal transduction. *J Label Compd Radiopharm* **2000**, *43*, 1159-1172.
- (87) Agranat, I.; Caner, H.; Caldwell, J. Putting chirality to work: the strategy of chiral switches. *Nat Rev Drug Discov* **2002**, *1*, 753-768.
- (88) Eichelbaum, M.; Evert, B. Influence of pharmacogenetics on drug disposition and response. *Clin Exp Pharmacol Physiol* **1996**, *23*, 983-985.
- (89) Agranat, I. I.; Caner, H. Intellectual property and chirality of drugs. *Drug Discov Today* **1999**, *4*, 313-321.
- (90) Owens, M. J.; Knight, D. L.; Nemeroff, C. B. Second-generation SSRIs: human monoamine transporter binding profile of escitalopram and R-fluoxetine. *Biol Psychiatry* **2001**, *50*, 345-350.
- (91) Sanchez, C.; Bergqvist, P. B.; Brennum, L. T.; Gupta, S.; Hogg, S. et al. Escitalopram, the S-(+)-enantiomer of citalopram, is a selective serotonin reuptake inhibitor with potent effects in animal models predictive of

- antidepressant and anxiolytic activities. *Psychopharmacology (Berl)* **2003**, *167*, 353-362.
- (92) Bedurftig, S.; Wunsch, B. Chiral, nonracemic (piperazin-2-yl)methanol derivatives with [sigma]-receptor affinity. *Bioorganic & Medicinal Chemistry* **2004**, *12*, 3299-3311.
- (93) Naylor, A.; Judd, D. B.; Lloyd, J. E.; Scopes, D. I. C.; Hayes, A. G. et al. A Potent New Class of kappa-Receptor Agonist: 4-Substituted 1-(Arylacetyl)-2-[(dialkylamino)methyl]piperazines. *J Med Chem* **1993**, *36*, 2075-2083.
- (94) Dinsmore, C. J.; Bergman, J. M.; Bogusky, M. J.; Culberson, J. C.; Hamilton, K. A. et al. 3,8-Diazabicyclo[3.2.1]octan-2-one Peptide Mimetics: Synthesis of a Conformationally Restricted Inhibitor of Farnesyltransferase. *Org Lett* **2001**, *3*, 865-868.
- (95) Tillement, J. P.; Testa, B.; Bree, F. Compared pharmacological characteristics in humans of racemic cetirizine and levocetirizine, two histamine H1-receptor antagonists. *Biochem Pharmacol* **2003**, *66*, 1123-1126.
- (96) Kawachi, J.; Matsubara, H.; Nakahara, Y. Optical resolution of 2-methylpiperazine using dibasic acids: Japan, 2002, JP 2002080459.
- (97) Yamazaki, H.; Kiyohara, M. Preparation of optically active 2-methylpiperazines: Japan, 2001, JP 2001131157.
- (98) Weigl, M.; Wunsch, B. Synthesis of chiral non-racemic 3-(dioxopiperazin-2-yl)propionic acid derivatives. *Tetrahedron* **2002**, *58*, 1173-1183.
- (99) Kukula, P.; Prins, R. Diastereoselective Hydrogenation of Pyrazine Derivatives: An Alternative Method of Preparing Piperazine-(2S)-Carboxylic Acid. *Journal of Catalysis* **2002**, *208*, 404-411.
- (100) Eichhorn, E.; Roduit, J.-P.; Shaw, N.; Heinzmann, K.; Kiener, A. Preparation of (S)-piperazine-2-carboxylic acid, (R)-piperazine-2-carboxylic acid, and (S)-piperidine-2-carboxylic acid by kinetic resolution of the corresponding racemic carboxamides with stereoselective amidases in whole bacterial cells. *Tetrahedron: Asymmetry* **1997**, *8*, 2533-2536.
- (101) Guosheng, W.; Zhao, H.; Luo, R. G.; Wei, D.; Malhotra, S. V. Chiral Synthesis and Enzymatic Resolution of (S)-(-)Piperazine-2-Carboxylic Acid Using Enzyme Alcalase. *Enantiomer* **2001**, *6*, 343-345.
- (102) Velluz, L.; Anatol, J.; Amiard, G. Use of N-benzyl intermediates in peptide synthesis. II. Transition through mixed ethyl carbonic anhydrides of N,N-

- dibenzyl- $\alpha$ -amino acids. *Bulletin de la Societe Chimique de France* **1954**, 1449-1454.
- (103) Le Bail, M.; Aitken, D. J.; Vergne, F.; Husson, H. P. Alkylation of Chiral 2-(aminomethyl)oxazolines. *J. Chem. Soc., Perkins Trans. 1* **1997**, 1681-1689.
- (104) Nefkens, G. H. L.; Zwanenburg, B. Boroxazolidones as simultaneous protection of the amino and carboxyl group in  $\alpha$ -amino acids. *Tetrahedron* **1983**, 39, 2995-2998.
- (105) Gong, B.; Lynn, D. G. Regioselective Reductions of Diacids: Aspartic Acid to Homoserine. *J Org Chem* **1990**, 55, 4763-4765.
- (106) Garcia, M.; Serra, A.; Rubiralta, M.; Diez, A.; Segarra, V. et al. Efficient method for the preparation of (S)-5-hydroxynorvaline. *Tetrahedron: Asymmetry* **2000**, 11, 991-994.
- (107) Graham, S. L. Inhibitors of farnesyl protein transferase: USA, 1992, 92202923.6.
- (108) Greene, T. W.; Wuts, P. G. M. *Protective Groups in Organic Synthesis*; Third ed.; John Wiley & Sons, Inc.: New York, 1999.
- (109) Ishida, Y.; Aida, T. Homochiral Supramolecular Polymerization of an S-Shaped Chiral Monomer: Translation of Optical Purity into Molecular Weight Distribution. *J Am Chem Soc* **2002**, 124, 14017-14019.
- (110) Mathis, C. A.; Taylor, S. E.; Biegon, A.; Enas, J. D. [<sup>125</sup>I]5-iodo-6-nitroquipazine: a potent and selective ligand for the 5-hydroxytryptamine uptake complex. I. In vitro studies. *Brain Res* **1993**, 619, 229-235.
- (111) Habert, E.; Graham, D.; Tahraoui, L.; Claustre, Y.; Langer, S. Z. Characterization of [<sup>3</sup>H]paroxetine binding to rat cortical membranes. *Eur J Pharmacol* **1985**, 118, 107-114.
- (112) Cheng, Y.; Prusoff, W. H. Relationship between the inhibition constant (K<sub>1</sub>) and the concentration of inhibitor which causes 50 per cent inhibition (I<sub>50</sub>) of an enzymatic reaction. *Biochem Pharmacol* **1973**, 22, 3099-3108.
- (113) <http://www.daylight.com/daycgi/clogp>.
- (114) Gatley, S. J.; Ding, Y. S.; Brady, D.; Gifford, A. N.; Dewey, S. L. et al. In vitro and ex vivo autoradiographic studies of nicotinic acetylcholine receptors using [<sup>18</sup>F]fluoronochloroepibatidine in rodent and human brain. *Nucl Med Biol* **1998**, 25, 449-454.

- (115) Matthews, J. C. *Fundamentals of Receptor, Enzyme, and Transport Kinetics*; CRC Press, Inc.: Boca Raton, 1993.
- (116) McCortney, B. A.; Jacobsen, B. M.; Vreeke, M.; Lewis, E. S. Methyl Transfers. 14. Nucleophilic Catalysis of Nucleophilic Substitution. *J Am Chem Soc* **1990**, *112*, 3554-3559.
- (117) Armarego, W. L. F.; Perrin, D. D. *Purification of Laboratory Chemicals*; Fourth ed.; Butterworth-Heinemann: Oxford, 1997.
- (118) Kofron, W. G. A Convenient Method for Estimation of Alkyl lithium Concentrations. *J Org Chem* **1976**, *41*, 1879-1880.